Author/s:
Lee, Ariane Renita

Title:
The role of microbiota-derived short chain fatty acids in T cell differentiation and function

Date:
2023-05

Persistent Link:
https://hdl.handle.net/11343/337578

The role of microbiota-derived short chain fatty acids in T cell differentiation and function

Ariane Renita Lee

ORCID ID:
0000-0002-4454-5366

Submitted in total fulfilment of the requirements of the degree of
Doctor of Philosophy

The Department of Microbiology and Immunology
The Peter Doherty Institute for Infection and Immunity
The University of Melbourne
VIC, Australia

Table of contents

Abbreviations

2-DG	2-deoxy-glucose
2-ME	2-mercaptoethanol
Ac-H3	Acetyl-histone H3
ACC1	Acetyl-CoA carboxylase
Acetyl-CoA	Acetyl-coenzyme A
ACSS2	Acetyl-CoA synthetase 2
AP-1	Activator protein 1
APC	Antigen presenting cell
ATCC	American Type Culture Collection
ATP	Adenosine triphosphate
Bcl-6	B-cell lymphoma 6
BFA	Brefeldin A
Blimp-1	B-lymphocyte-induced maturation protein 1
bLN	Brachial lymph node
BM	Bone marrow
BRE	Butyrate response element
BSA	Bovine serum albumin
CAR	Chimeric antigen receptor
Cat.	Catalogue
cDC	Conventional DC
cDNA	Complementary DNA
ChIP-seq	Chromatin immunoprecipitation-sequencing
CMV	Cytomegalovirus
CPT1a	Carnitine palmitoyltransferase 1a
CTLA-4	Cytotoxic T-lymphocyte-associated protein 4
CTL	Cytotoxic lymphocyte
cTregs	Colonic regulatory T cell

Ctrl	Control
d	Day
DAMP	Danger associated molecular pattern
DAPI	4',6-diamidino-2-phenylindole
DC	Dendritic cell
DMSO	Dimethyl sulfoxide
DNA	Deoxyribonucleic acid
DNase	Deoxyribonuclease
DPBS	Dulbecco’s phosphate buffered saline
E:T	Effector cell to target cell
e.c.	Epicutaneous
EC_{50}	Half maximal effective concentration
ECAR	Extracellular acidification rates
EEC	Early effector cell
eGFP	Enhanced green fluorescent protein
Eomes	Eomesodermin
FACS	Fluorescence activated cell sorting
$FADH_2$	Dihydroflavine-adenine dinucleotide
FAO	Fatty acid oxidation
FasL	Fas ligand
FCCP	Carbonyl cyanide-4 (trifluoromethoxy) phenylhydrazone
FCS	Fetal calf serum
FMO	Fluorescence minus one
FMT	Fecal microbiota transplant
FoxO1	Forkhead box O 1
FoxO1i	Forkhead box O 1 inhibitor
Foxp3	Forkhead box P3
GAPDH	Glyceraldehyde 3-phosphate dehydrogenase
GATA3	GATA binding protein 3
gB	Herpes simplex virus glycoprotein B

gD	Herpes simplex virus glycoprotein D
GFP	Green fluorescent protein
GLUT1	Glucose transporter 1
GLUT4	Glucose transporter 4
GPR	G protein-coupled receptor
GzmB	Granzyme B
H3K27ac	Histone H3 lysine 27 acetylation
H3K4me3	Histone H3 lysine 4 trimethylation
H3K9ac	Histone 3 lysine 9 acetylation
H4ac5	Penta-acetylated histone H4
HAT	Histone acetyltransferase
HBSS	Hank’s balanced salt solution
HDAC	Histone deacetylase
HEPES	N-2-hydroxyethylpiperazine-N’-2-ethane sulfonic acid
HSV-1	Herpes simplex virus type 1
i.p.	Intraperitoneal
i.v.	Intravenous
ICB	Immune checkpoint blockade
IFN-γ	Interferon gamma
IL	Interleukin
IL-2Rα	Interleukin-2 receptor alpha
iNOS	Inducible nitric oxide synthase
KLRG1	Killer cell lectin-like receptor G1
LCFA	Long chain fatty acid
LCMV	Lymphocytic choriomeningitis virus
LeY	Lewis Y antigen
MEM	Minimal essential medium
MFP	Mammary fat pad
MCT1	Monocarboxylate transporter 1

MFI	Mean fluorescence intensity
MHC-I	Major histocompatibility complex class I
MHC-II	Major histocompatibility complex class II
MoMLV	Moloney murine leukemia virus
MPEC	Memory precursor effector cell
mRNA	Messenger ribonucleic acid
mTOR	Mammalian target of rapamycin
NAD	Nicotinamide adenine dinucleotide
NADH	Reduced nicotinamide adenine dinucleotide
NF-κB	Nuclear factor kappa-light-chain-enhancer of activated B cells
NSCLC	Non-small cell lung cancer
NSG	NOD SCID gamma
OCR	Oxygen consumption rate
Olfr78	Olfactory receptor 78
Oligo	Oligomycin
OR51E2	Olfactory Receptor Family 51 Subfamily E Member 2
OXPHOS	Oxidative phosphorylation
p70-S6	70-kDa ribosomal protein S6 kinase
PAMP	Pathogen associated molecular pattern
PBS	Phosphate buffered saline
PGC-1α	Peroxisome proliferator-activated receptor-gamma coactivator 1-alpha
PDI	The Peter Doherty Institute for Infection and Immunity
PD-1	Programmed cell death protein 1
PFU	Plaque-forming unit
pH	Potential hydrogen
PI	Propidium iodide
PMA	Phorbol 12-myristate 13-acetate
PMCC	Peter MacCallum Cancer Centre
RBC	Red blood cell
RE	Relative expression

RNA	Ribonucleic acid
RORγt	Retinoic-acid-receptor-related orphan receptor gamma t
Rot/AA	Rotenone and antimycin A
rRNA	Ribosomal RNA
rpS6	Ribosomal protein S6
RT-qPCR	Real-time quantitative polymerase chain reaction
SDS	Sodium dodecyl sulphate
Seq	Sequencing
SLC5a8	Solute carrier family 5 member 8
SLEC	Short-lived effector cell
SPF	Specific pathogen-free
T-bet	T-box protein expressed in T cells
TBS	Tris-buffered saline
Tc17	Type 17 $CD8^+$ T cell
TCA	Tricarboxylic acid
TCF-1	T cell factor-1
TCR	T cell receptor
Tfh	T follicular helper
TGF-β	Transforming growth factor beta
Th	T helper
TIL	Tumour infiltrating lymphocyte
TME	Tumour microenvironment
TMRM	Tetramethylrhodamine methyl ester
TNF-α	Tumor necrosis factor alpha
TRAIL	Tumor necrosis factor-related apoptosis inducing factor
Tregs	Regulatory T cells
TSA	Trichostatin A
U	Unit
VSV	Vesicular stomatitis virus
v/v	Volume per volume

WEHI	The Walter and Eliza Hall Institute of Medical Research
WT	Wildtype
w/v	Weight per volume

List of tables

List of figures

Abstract

CD4$^+$ and CD8$^+$ T cells are crucial orchestrators and effectors in immune responses against diseases such as cancer and infections. T cell differentiation into distinct subsets allows for specialised responses and the formation of immunological memory. A multitude of factors influence T cell differentiation and functionality, including metabolite availability in the microenvironment. Microbiota-derived short chain fatty acids (SCFAs) are metabolites that can modulate cellular metabolism and epigenetic changes, and signal through the G protein-coupled receptors 41 and 43 (GPR41 and GPR43). While SCFAs can promote CD4$^+$ regulatory T cell differentiation, their effects on T helper 1 (Th1) cells and CD8$^+$ T cells are not as well characterised. In this thesis, we investigated how SCFAs influence CD4$^+$ and CD8$^+$ T cell differentiation and functionality.

To understand whether SCFA sensing contributes to CD8$^+$ T cell priming, we measured the CD8$^+$ T cell responses of GPR41/GPR43-deficient mice that had been infected with herpes simplex virus type 1. We demonstrated that GPR41 and GPR43 were required for optimal memory precursor effector cell (MPEC) differentiation, TNF-α production, and viral control. Together, these findings showed that these receptors influence CD8$^+$ T cell priming and anti-viral responses. Next, to explore how SCFAs affected CD4$^+$ T cells, we exposed *in vitro*-activated CD4$^+$ T cells to the SCFA butyrate. Butyrate enhanced the expression of Th1-associated effector molecules and the master transcription factor T-bet. However, the metabolic profile and killing capacity of butyrate-treated cells was distinct from classical Th1 cells. Importantly, butyrate enhanced direct killing of melanoma cells by CD4$^+$ T cells, primarily through Fas ligand interactions. This indicated that butyrate induced the development of non-classical Th1-like cells with proficient anti-tumour cytotoxicity. We therefore assessed if butyrate could alter the efficacy of CD4$^+$ and CD8$^+$ chimeric antigen receptor (CAR) T cells. CAR T cells cultured with butyrate displayed enhanced effector molecule expression and *in vitro* killing of tumour cells. Using an animal model of breast cancer, we revealed that butyrate-treated CAR T cell monotherapy was as effective as combination therapy consisting of CAR T cells and immune checkpoint blockade. Butyrate hence improved the anti-tumour function of CAR T cells.

In summary, butyrate skewed $CD4^+$ and $CD8^+$ T cell differentiation in favour of highly functional cytotoxic Th1-like cells and MPECs respectively. These findings underline the importance of metabolite availability, such as butyrate, in the microenvironment for immune responses against cancer. A deeper understanding of how butyrate skews T cell stemness and effector function might provide novel targets for CAR T cell therapy.

Declaration

The work presented in this thesis was conducted at The University of Melbourne, in the laboratory of Prof Sammy Bedoui. This work was funded by the National Health and Medical Research Council, German Research Foundation and Merck KGaA. Ariane Lee was supported by an Australian Government Research Training Program Scholarship from The University of Melbourne.

This is to certify that,
(i) the thesis comprises only my original work towards the PhD except where indicated in the preface;
(ii) due acknowledgement has been made in the text to all other material used;
(iii) the thesis is less than 100,000 word limit in length, exclusive of tables, maps, bibliographies and appendices.

12th May 2023 Ariane Lee

Preface

My contribution to the experiments within each chapter was as follows:

Chapter 3: 90%
Chapter 4: 95%
Chapter 5: 75%

I acknowledge the important contributions of others to the experiments presented herein:

Chapter 3: Experiments using an intravenous route of HSV-1 infection were performed by Dr Annabell Bachem, Bedoui laboratory, The University of Melbourne.

Chapter 4: Seahorse metabolic assays were performed in collaboration with Mrs Michele Clarke, Bedoui laboratory, The University of Melbourne.

Chapter 5: *In vivo* murine CAR T cell experiments were performed by Dr Lai Junyun, Darcy laboratory, Peter MacCallum Cancer Centre (PMCC) and human CAR T cell generation was performed in collaboration with Dr Kevin Sek, Darcy laboratory, PMCC.

Acknowledgements

I would firstly like to express my deepest appreciation for my primary supervisor, Sammy Bedoui. This endeavour would not have been possible without your knowledge, guidance, and optimism even in the face of challenges. Your enthusiasm towards this project and science in general has been infectious. A huge thank you to my co-supervisor, Annabell Bachem, for your invaluable insight as well as supporting me in the development of my technical skills and independence in the lab. I have appreciated your encouragement through the highs and lows of this project. Sammy and Annabell, you have been fantastic mentors. The many opportunities that you have provided for me to sharpen my critical thinking skills and build my confidence have been instrumental in my improvement as a researcher. I am extremely lucky to have had your unwavering support. Thank you for believing in me.

I would like to acknowledge my PhD committee, Tim Stinear, Sarah Londrigan and Malcom McConville for their feedback and insightful discussions. Thank you to our collaborators Phil Darcy, Lai Junyun and Kevin Sek from the Peter MacCallum Cancer Centre for welcoming me into their lab and teaching me about CAR T cells.

Thank you to all past and present members of the Bedoui and Gebhardt laboratories for providing an incredibly healthy and supportive environment. Your friendship and willingness to provide technical help has been a major reason why my PhD journey has been so enjoyable. I would especially like to extend my appreciation to Sven for being my lab bestie from the start. You have always been there to lend a listening ear and provide emotional support. It has been great to laugh and cry with you throughout the PhD. You made this journey much more enjoyable. Thank you to Emma for being my $CD4^+$ T cell mentor and teaching me so much. To Michele and Lindsay, a big thank you for working on experiments with me – you have both been a great help! Elise, Lewis and Sharon, thanks for being wonderful companions during late night experiments and writing sessions.

To my lovely friends, Mitchell, Gordon, Isabelle, Calvin, Rebecca, Ashleigh, Kevin, Jessie, So Young, Meghana and Sharanya, a huge thank you for enriching my life. I have immensely enjoyed the time we spent together, both inside and outside of the institute. Coincidentally meeting you in the animal house and FACS facility made time fly. Our catch ups, be it meals, ice cream, pottery classes or hikes, always brought me joy and peace. There were moments when I wished I could hold onto those feelings forever. I am extremely grateful for your support and empathy. Knowing that we were all in it together was one of the best parts of this journey. Last but not least, a huge thank you to my family for your love and support. Thank you to my sister, Karina, for being my rock – from making sure that I was eating well enough and being understanding when I was busy or tired, to celebrating my wins and being happy for me. Thanks to my parents for providing me with opportunities, encouraging me to work hard since young and for being supportive of my PhD journey.

Research outputs

Publication

Engel, S., Doerflinger, M., **Lee, A.R.**, Strasser, A., Herold, M.J., Bedoui, S., Bachem, A. (2021). Caspase-2 does not play a critical role in cell death induction and bacterial clearance during Salmonella infection. *Cell death and differentiation*, 28(12), 3371–3373.

Conference presentations

2022 – 50th ASI Annual Meeting. *Participant (Talk).*

2022 – PDI/Postgraduate Student Society for Infection and Immunity (POSSIIM) Conference. *Participant (Talk).*

2022 – Immunology Group of Victoria (IgV) Student Roadshow. *Participant (Talk).*

2021 – 49th ASI Annual Meeting. *Participant (Talk).*

2021 – Melbourne Immunotherapy Network (MIN) Conference. *Participant (Poster).*

2021 – 11th Lorne Infection & Immunity Conference. *Participant (Talk).*

2020 – VIIN Young Investigator Symposium 2020. *Participant (Talk).*

2019 – Biomed Link. *Participant (Poster).*

2019 – 11th PDI Postgraduate Student Society Biennial Scientific Conference. *Participant (Talk).*

Awards

2023 – Major Bartlett Travel Scholarship – The University of Melbourne

2022 – ASI 2022 bursary

2021 – ASI 2021 bursary

2021 – Best Student Poster – Melbourne Immunotherapy Network (MIN)

2021 – Major Bartlett Travel Scholarship – The University of Melbourne

2021 – Best Science Bite – 11th Lorne Infection & Immunity Conference

2020 – Best Student Science Bite – VIIN Young Investigator Symposium

2020 – People's Choice Award for Science Bite – VIIN Young Investigator Symposium

2019 – Best Elevator Pitch – 11th PDI Biennial Scientific Conference

2019 – Research Training Program (RTP) Scholarship – The University of Melbourne

Chapter 1:

Introduction

Chapter 1 Introduction

1.1 The immune system

The immune system is a complex network of cells and organs that collaborate to defend the host against pathogens and maintain tissue homeostasis. The potentiation of appropriate responses hinge on the ability of the immune system to discriminate between self and non- or altered-self. This can include neoplastic cells and can range to exogenous threats posed by viruses or bacteria. These perturbations can trigger signalling cascades that culminate in specific immune responses. The responses aim to limit the immune threat, subsequently resolving the perturbation.

The immune system can be categorised into innate and adaptive immunity. The innate immune system provides the first line of defence. It acts fast and typically responds non-specifically to evolutionarily conserved factors from pathogens called pathogen-associated molecular patterns (PAMPs) or damaged cells that release danger-associated molecular patterns (DAMPs). The innate immune system comprises of surface barriers, soluble mediators and immune cells, such as monocytes, macrophages, granulocytes, innate lymphoid cells, natural killer cells and dendritic cells. Professional antigen presenting cells (APCs), such as dendritic cells (DCs) and macrophages, are particularly proficient at phagocytosing and processing antigens from pathogens or tumour cells. Their capacity to present antigens bridges the innate and adaptive immune systems.

Adaptive immunity consists of humoral immunity in the form of antibodies that are produced by B cells and cell-mediated immunity which is mediated by T cells. A distinguishing feature between the innate and adaptive immune systems is that the latter has evolved extraordinary diverse repertoires of highly specifc and unique antigen receptors. Another important characteristic of adaptive immunity is its generation of immunological memory that gives rise to faster and efficient responses when the same antigen is re-encountered. These sophisticated pathways are tightly regulated and tuned according to the immunological context. A myriad of genetic and environmental factors shape the immune system, further adding to the substantial diversity between individuals. Recently, there has been a growing appreciation of the

role of the gut microbiota and its derivatives in modulating responses of immune cells including T cells in both a localised and distant fashion [1-3].

1.2 T cells in health and disease

T cells are critical players of the adaptive immune system that serve two broad purposes: firstly, they drive pro-inflammatory responses towards pathogens, tumours, and allergens. Secondly, they maintain self-tolerance and homeostasis by regulating these responses. The major T cell subsets are namely $CD4^+$ and $CD8^+$ T cells. Both subsets develop and mature in the thymus, where recombination of T cell receptor (TCR) gene segments results in the generation of up to 10^{18} unique TCRs, allowing for the specific recognition of millions of different antigen epitopes [4].

1.2.1 T cell activation and subsets

Upon egress from the thymus into the blood for continuous recirculation, naïve T cells pass through lymphoid organs where they survey the environment for their cognate antigen. Naïve T cells are maintained in a state of quiescence where homeostatic proliferation is tightly regulated to promote long-term survival [5]. This is key in the homeostatic maintenance of a large pool of naïve T cells, which is available to respond under the appropriate conditions to as many epitopes as possible. Effective T cell activation requires three signals provided by APCs. The TCR binds to its cognate antigen presented in the context of major histocompatibility complex class I (MHC-I) or class II (MHC-II) molecules of APCs, triggering the activation of the T cell. The co-receptors CD4 and CD8 stabilise the TCR/MHC-peptide interactions. The binding of co-stimulatory molecules of the T cell such as CD28 to CD80/86 on the APC results in induction of clonal expansion. Finally, the production of specific cytokines by the APCs including interleukin (IL)-2 and IL-12 induces T cell expansion and differentiation in a context-dependent manner. For example, IL-12 production results in the differentiation of $CD4^+$ T cells into a subset known as T helper 1 (Th1) cells [6]. Activated T cells migrate out of the lymphoid organ to distribute around the body, concentrating at sites of infection or inflammation where they contribute to the control and elimination of the immune threat.

T cell proliferation serves to generate large pools of activated T cells against a specific antigen and their acquisition of effector functions. The level of terminal T cell differentiation is inversely related to stemness, which refers to the multipotency or the differentiation potential of the cell [7, 8]. Increasingly differentiated T cells possess poorer features of stemness, such as a lower capacity for survival, as well as a limited self-renewal and proliferative potential [9, 10]. The effector response is typically mediated by a heterogenous pool of T cells with different functional and survival capacities. These qualities depend on the quality and quantity of signals received during activation such as strength of antigen stimulation, cytokine exposure and metabolite availability [11-14]. T cell subsets are distinguished by their phenotype, including effector molecule and transcription factor expression, and their metabolic profile [15].

The majority of effector T cells are short-lived and undergo activation-induced cell death following elimination of the threat [16]. However, some cells survive to form long-lived memory T cells that are capable of self-renewal and remaining quiescent until re-activation upon secondary antigen exposure. These memory cells are faster in responding to re-stimulation with their cognate antigen compared to naive T cells, which together with increased precursor frequencies provides the foundation for long-term protective immunity [17].

1.2.2 $CD8^+$ T cells

$CD8^+$ T cells, also known as cytotoxic lymphocytes (CTLs), recognise MHC-I-restricted antigens. They can directly lyse target cells, which makes them an important mediator for the control of intracellular pathogens and tumours. Key $CD8^+$ T cell cytokines that mediate these responses are interferon gamma (IFN-γ) and tumour necrosis factor alpha (TNF-α), which alert and activate various innate and adaptive immune cell types. IFN-γ can upregulate MHC expression on APCs and tumour cells [18, 19], induce a pro-inflammatory phenotype in macrophages [20] and enhance anti-tumour and anti-viral effects of $CD8^+$ T cells themselves [21]. TNF-α is a pleiotropic cytokine that regulates cell proliferation, differentiation and possesses cytolytic potential [22, 23]. Additionally, cytotoxic mediators including granzyme B, perforin, Fas

ligand (FasL) and TNF-related apoptosis-inducing ligand (TRAIL) result in programmed cell death of target cells [24-26].

The acquisition of these effector functions occurs when naïve $CD8^+$ T cells are activated and differentiate into effector cells. Multiple models of differentiation have been suggested in the case of acute infections that are characterised by sudden disease onset and rapid antigen clearance or death of the host [27, 28]. One similarity between models is the ability of a less differentiated cell to form effector cells that range in plasticity. For example, $CD8^+$ T cells can progressively differentiate from early effector cells (EECs) to short-lived effector cells (SLECs) or memory precursor effector cells (MPECs). The presence of these subsets has been demonstrated in various models of acute infection, including lymphocytic choriomeningitis virus (LCMV), vesicular stomatitis virus (VSV), *Listeria monocytogenes* and herpes simplex virus type 1 (HSV-1) [16, 29-31]. The proportion of each subset is influenced by antigenic stimulation, cytokines, $CD4^+$ T cell help and metabolites in the microenvironment [31-34]. EECs, SLECs and MPECs can be distinguished by their expression of the killer cell lectin-like receptor G1 (KLRG1) and interleukin-7 receptor alpha chain (CD127).

Before the peak of an acute infection, $KLRG1^-CD127^-$ EECs are the most prevalent effector subset [16]. EECs differentiate into $KLRG1^+CD127^-$ SLECs and $KLRG1^-CD127^+$ MPECs [29, 30]. SLECs are terminally differentiated T cells that undergo apoptosis during the contraction phase. In contrast, MPECs possess stem-like qualities and metabolic adaptations that give them a survival advantage [29]. As such, MPECs make up the majority of cells that mature into memory T cells [29]. $CD8^+$ T cell subsets can furthermore be distinguished through their transcription factor profiles. T-box protein expressed in T cells (T-bet), a key regulator of effector function, is highly expressed by SLECs cells while high Forkhead box O 1 (FoxO1), T cell factor-1 (TCF-1) and Eomesodermin (Eomes) expression define MPECs and memory T cells [35, 36].

1.2.3 $CD4^+$ T cells

$CD4^+$ T cells respond to MHC-II-restricted antigens. They orchestrate immune responses by influencing $CD8^+$ T cell and B cell priming, as well as directly

counteracting a variety of immune threats and maintaining tolerance. Upon activation, they can differentiate into heterogenous lineages depending on the TCR signal strength, co-stimulatory molecules and cytokines, for example IL-12, IL-4 and transforming growth factor beta (TGF-β). $CD4^+$ lineages that participate in pro-inflammatory responses are T follicular helper (Tfh), Th1, Th2 and Th17 cells, as well as newer subgroups including Th9 and Th22 cells [37, 38]. In contrast, regulatory T (Treg) cells play vital roles in regulating immune responses. Each subset is specialised for a particular role, and consistent with this has a distinct master transcription factor and cytokine profile. Tfh cells express the master transcription factor B-cell lymphoma 6 (Bcl-6), and produce cytokine such as IL-21 to facilitate B cell differentiation and antibody responses [39, 40]. Th1 cells, defined by their expression of the transcription factor T-bet, potentiate pro-inflammatory responses against intracellular pathogens and tumours mainly through the production of IFN-γ and TNF-α [41, 42]. Th2 cells express the transcription factor GATA Binding Protein 3 (GATA3) [43]. They target helminths but also mediate allergic responses through IL-4 and IL-5 [42]. Th17 cells are controlled by the transcription factor retinoic-acid-receptor-related orphan receptor gamma t (RORγt) and mediate responses towards extracellular pathogens via IL-17 and IL-22 [44, 45]. Another subset of emerging importance is cytotoxic $CD4^+$ T cells which is under the control of the transcription factors Eomes and runt-related transcription factor 3 (Runx3) [46]. Like $CD8^+$ T cells, cytotoxic $CD4^+$ T cells can directly kill target cells via granzyme B, perforin and FasL [47]. Their development is not as well understood – they may form a separate lineage or belong to other subsets. They can arise from Th1, Th2, Th17 and Treg cells, or even unpolarised Th0 cells under particular conditions such as IL-2 [47-49], but are thought to be most closely related to Th1 cells [46].

Tregs are defined by the expression of the transcription factor forkhead box P3 (Foxp3) and can suppress Th1, Th2 and Th17 cells through TGF-β, IL-10 and other mediators, which keeps in check potentially harmful pro-inflammatory responses [50, 51]. This is vital in the maintenance of tolerance, defined as unresponsiveness to self and non-self antigens, and homeostasis to prevent the development of autoimmunity and pathological immune responses. Successful clearance of the immune threat and resolution of the immune response both hinge on the fine balance between pro-inflammatory and anti-inflammatory T cell subsets.

$CD4^+$ T cell stemness and longevity is maintained by the transcription factor FoxO1 [52] and involves metabolic and epigenetic modifications [53], which will be discussed in greater detail in the following section. $CD4^+$ memory T cells cells are important in infection and cancer settings, although they have been proven difficult to study due to their low frequencies [54-56].

1.2.4 Activation-induced molecular changes in T cells

1.2.4.1 Gene expression

Stimulation through the TCR results in the activation of canonical transcription factors such as activator protein 1 (AP-1) and nuclear factor kappa-light-chain-enhancer of activated B cells (NF-κB), and subset-determining transcription factors such as T-bet, FoxO1 and Eomes. These transcription factors regulate the expression of downstream molecules including cytokines and metabolic enzymes, which are closely associated with differentiation and functional outcomes. For example, IFN-γ and TNF-α are under the transcriptional control of T-bet in both $CD4^+$ and $CD8^+$ T cells, leading to an effector phenotype in T-bet expressing T cells [57, 58]. FoxO1 can regulate mitochondrial biogenesis by inducing peroxisome proliferator-activated receptor-gamma coactivator 1-alpha (PGC-1α) expression [59], and may also localise to the mitochondria for binding to mitochondrial deoxyribonucleic acid (DNA) [60]. This has implications on differentiation due to the preferential reliance of memory T cell on mitochondrial respiration [61]. Furthermore, the activation markers CD25 and CD69, and programmed cell death protein 1 (PD-1) are upregulated; while CD62L is downregulated [62, 63]. Such markers have been shown to regulate T cell survival and functionality [64, 65]. These changes in expression are in part determined by epigenetic modifications.

1.2.4.2 Epigenetic remodelling

Histone modifications refer to the covalent addition or removal of functional groups to histones. These chemical changes in the chromatin structure are preserved throughout T cell division and immunological memory development [66, 67], serving as inheritable traits without requiring changes in the DNA sequence itself. Several types of histone modifications exist that include but are not limited to methylation,

phosphorylation and acetylation. Histone acetylation is an active process by which histone acetyltransferases (HATs) add an acetyl group from acetyl-coenzyme A (acetyl-CoA) to lysine residues of histones. This acetylation is generally believed to 'open' the structure of chromatin, thereby allowing chromatin accessibility, transcription factor binding and increased gene expression [68, 69]. Conversely, histone deacetylases (HDACs) are enzymes that remove these acetyl groups resulting in a 'closed' chromatin conformation and repression of transcription [70]. Inhibitors of deacetylases block this process, leading to greater acetylation.

T cells adopt unique chromatin states during the naïve, effector, and memory phase, which is required for significant changes in transcriptional profiles during differentiation [71, 72]. Similarly, during $CD4^+$ T cell lineage commitment, epigenetic silencing and activation dictate subset-specific gene expression [73, 74]. Changes in histone acetylation shape T cell differentiation and functionality. Histone remodelling during differentiation has been clearly demonstrated in genes encoding cytokines and cytotoxic mediators. Total histone H3 acetylation of *Ifng* in naïve $CD4^+$ and $CD8^+$ T cells is low and this correlates with little IFN-γ protein expression [75, 76]. Several studies have shown that the acetylation of lysine residue 9 of histone H3 (H3K9ac) at the *Ifng*, *Tnfa* and *Gzma* promoters were associated with the acquisition of effector function following $CD4^+$ and $CD8^+$ T cell activation [77-80]. Greater H3K9ac was also detected at *EOMES*, *PRF1* and *GZMB* promoters in human $CD8^+$ memory T cells than naïve T cells [81]. Moreover, this particular chromatin remodelling in $CD8^+$ T cells was maintained from the effector to memory T cell phase, and was associated with a more robust recall response [80]. Retention of epigenetic imprinting likely allows rapid induction of memory T cells recall responses, importantly distinguishing memory T cells from naïve T cells [82].

1.2.4.3 T cell metabolism

The T cell differentiation program is intimately linked to changes in metabolism to provide energy and biomolecule precursors required for their proliferation, migration and functional state. T cells can utilise different pathways to produce energy in the form of adenosine triphosphate (ATP) and provide precursor metabolites required for many differentiation steps, for example lipid synthesis for membrane forming [13].

These energy generating pathways are very diverse in terms of their end products but are tightly linked because of a reliance on products from one pathway to feed into another as biosynthetic precursors. This section will focus on four main metabolic pathways that T cells heavily rely on: glycolysis, fatty acid oxidation (FAO), mitochondrial tricarboxylic acid (TCA) cycle, and oxidative phosphorylation (OXPHOS).

Glycolysis occurs in the cytoplasm. It requires the uptake and processing of extracellular glucose to yield pyruvate along with numerous other biosynthetic products, reduced nicotinamide adenine dinucleotide (NADH) and adenosine triphosphate (ATP). Pyruvate can be introduced into the TCA cycle during aerobic glycolysis which occurs in the presence of oxygen. Alternatively, pyruvate can be reduced to lactate, which is termed ‘anaerobic’ glycolysis. FAO, a metabolic pathway that takes place in the mitochondrial matrix, breaks down fatty acids into numerous products that the T cell can use for energy generation including acetyl-CoA, NADH and dihydroflavine-adenine dinucleotide ($FADH_2$). The TCA cycle occurs in the mitochondrial matrix. It can catabolise precursor molecules, such as pyruvate from glycolysis and acetyl-CoA from FAO, to generate NADH, $FADH_2$ and metabolic intermediates. OXPHOS is performed in the inner mitochondrial membrane. It describes the pathway by which electrons are transferred from electron donors, such as NADH and $FADH_2$, to oxygen in a series of redox reactions to produce ATP along the inner mitochondrial membrane. These pathways are regulated by signalling pathways – for example, TCR engagement and cytokine signalling [83, 84].

For most T cell subsets, preferential use of certain metabolic pathways has been described [61, 85, 86]. Naïve T cells are metabolically ‘quiescent’ meaning that they maintain a low metabolic activity and preferentially perform FAO and OXPHOS to promote their survival and persistence [87, 88]. Once activated, proliferation and acquisition of effector function alter the bioenergetic needs of the T cell, so it is not surprising that their activation is coupled to profound changes in metabolism. Effector T cells increase anaerobic glycolysis [14, 89]. Although this energy pathway produces fewer units of ATP per glucose molecule than OXPHOS, glycolysis has the advantage of generating ATP approximately 100 times faster [90] and allows for the provision of additional metabolic intermediates for the biosynthesis of macromolecules [91]. This

pathway enables effectors to undergo rapid cell growth, proliferation, and effector molecule biosynthesis – which is collectively known as anabolism [14]. When extrinsic signals that support glycolysis are removed following clearance of the immune threat, the cell is unable to maintain sufficient glucose uptake to sustain itself [92]. At the same time, the relatively low mitochondrial mass of effector T cells results in insufficient OXPHOS for the conversion of glycolysis-derived NADH to nicotinamide adenine dinucleotide (NAD^+), leading to a build-up of electrons in the mitochondria and ATP reduction – this can induce apoptosis [61, 93]. Although effector T cells mainly rely on glycolysis, MPECs in this heterogenous pool of effectors have a relatively higher capacity for mitochondrial respiration than SLECs [94].

The metabolism of memory T cells is somewhat similar to that of naïve T cells, where catabolic metabolism, which involves breaking down metabolic substrates, supports long-term survival and steady homeostatic proliferation until re-activation. Memory T cells have a greater reliance on FAO and OXPHOS than glycolysis [61, 95]. FAO in memory T cells fuel a higher mitochondria spare respiratory capacity, which is the capacity to produce extra energy under stress, increasing resistance to apoptosis [61, 96]. Enhanced OXPHOS and FAO improve cell survival and recall responses, boosting the immune response to re-infection [97]. As OXPHOS and FAO are major metabolic pathways for memory T cells, enhancement of these processes promotes Memory T cell generation and characteristics, thereby boosting long-term protective immunity [95, 98].

Overall, cellular metabolism is an essential determinant of T cell survival and function. Alterations in metabolism are crucial for increasing cell size and supporting proliferation, and in the synthesis of effector molecules following activation. Metabolic adaptations are therefore important in T cell differentiation (Figure 1.1). Each environmental niche in the body provides different levels of metabolites such as glucose or fatty acids, and understanding the utilisation of these metabolites will increase our knowledge on T cell immunity.

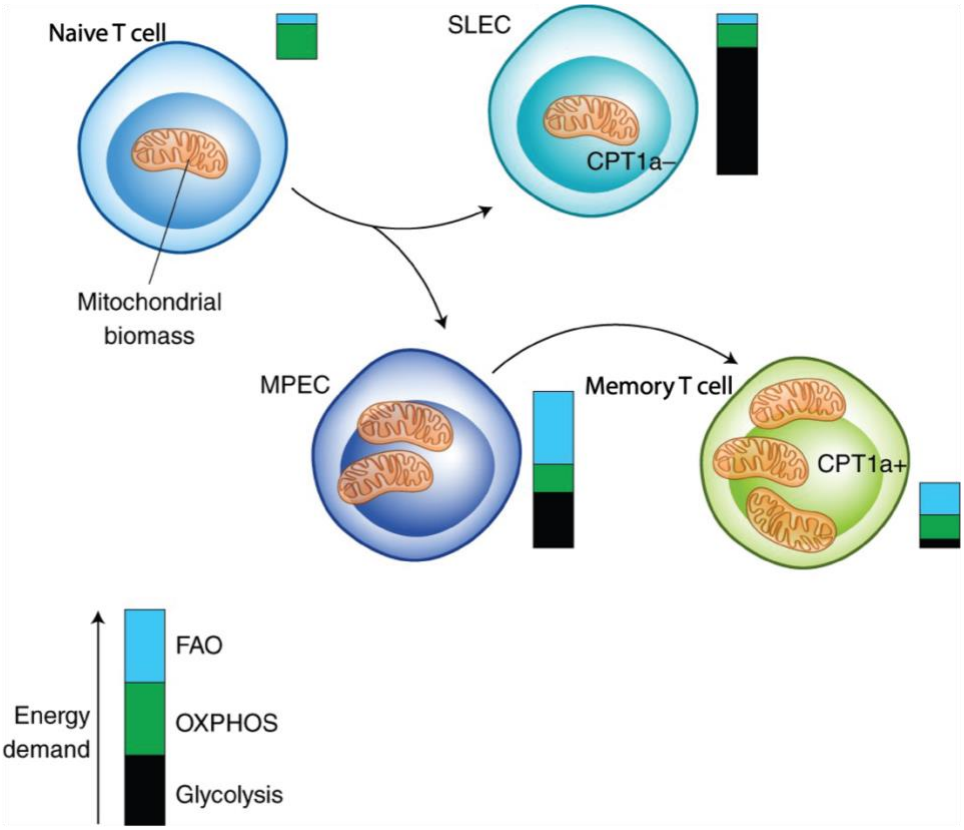

Figure 1.1 Metabolic adaptations during T cell differentiation.

Naïve T cells mainly rely on oxidative phosphorylation (OXPHOS). Differentiation into short-lived effector cells (SLECs) and memory precursor effector cells (MPECs) leads to a greater energy demand and a corresponding change in metabolic profile. Glycolysis is the preferred energy producing pathway in SLECs, while fatty acid oxidation (FAO) and glycolysis dominate in MPECs. MPECs mature into memory T cells, which are equipped with a greater mitochondrial biomass and carnitine palmitoyltransferase 1A (CPT1a) that aid in long-term survival. Adapted from McKinney E. F. and Smith, K. G. C. *Nature Immunology*. 2018. [94]

1.2.5 The importance of T cells in cancer control

T cells are crucial in the control of pathological conditions including cancer, where their differentiation heavily influences patient outcomes. For example, memory T cells cells have been identified to be important in anti-cancer responses [99-101]. High levels of $CD8^+$ memory T cells significantly correlated to greater progression-free survival and overall survival of cancer patients receiving immune checkpoint blockade (ICB) immunotherapy that aims to reduce T cell exhaustion [102, 103]. Tumour tissue with enriched cytotoxic $CD4^+$ T cell and Th1 cell-associated gene expression was found in colorectal cancer patients who experienced improved disease-free survival [104]. Head and neck squamous cell carcinoma patients with better OS possessed a greater memory $CD4^+$ T cell infiltration [105]. In contrast, terminally differentiated or exhausted $CD4^+$ and $CD8^+$ T cells with compromised functionality and survival were associated with more advanced disease states and poorer progression-free survival [54]. However, ICB such as anti-PD-1 induced transcriptional and metabolic alterations which reversed dysfunction, restoring anti-tumour T cell responses [106].

The ability of T cells to elicit long-term control of cancer has led to the development of a powerful immunotherapeutic tool known as chimeric antigen receptor (CAR) T cells. These T cells are genetically engineered to express a tumour-specific T cell receptor before being transfused into patients. Their notable success, such as response rates of up to 90% in clinical trials [107, 108], has led to their approval by the U.S. Food and Drug Administration (FDA) for use against various forms of blood cancers. The efficacy of CAR T cells is influenced by both their functionality and stemness. Memory CAR T cells are reportedly more effective than effector CAR T cells due to improved persistence of the former [109, 110]. In particular, cytotoxic memory CAR T cells denoted by CD161 upregulation exhibited better killing of tumour cells than their $CD161^-$ counterparts [111]. A better understanding of the factors that determine T cell differentiation and function therefore has therapeutic relevance. Determining the role of extrinsic factors, such as the gut microbiome and their metabolic derivatives, requires further exploration.

1.3 Microbiota and their metabolic products

The gut microbiota are a collection of microorganisms inhabiting the gastrointestinal tract that due to co-evolution have developed a mutually beneficial relationship with the host. The collective genomes of this community of microorganisms are referred to as the microbiome. The colon is the most densely populated site and its commensals collectively produce a large variety of metabolites from otherwise indigestible food [112, 113]. For example, metagenomic approaches, such as 16S ribosomal RNA (rRNA) community profiling and functional gene-targeted sequencing have shown that the gut microbiome encodes multiple biosynthetic pathways that allow for the fermentation of dietary fibre and other complex polysaccharides to short chain fatty acids (SCFA) [114-118]. SCFAs are carboxylic acids defined by the presence of an aliphatic tail less than six carbons long. The immunological impact of microbiota diversity within and between individuals has led to a growing interest in characterising how microbiota-dependent differences, particularly their capacity to produce metabolites, influence the host immune responses [119-121]. Gut microbiota-derived metabolites include trimethylamine N-oxide, branched amino acids and highly abundant SCFAs that can be used as metabolic substrates by various cells in the body such as hepatocytes and colonocytes [122]. SCFAs are particularly interesting in the context of T cell immunity as various studies have shown that they alter T cell metabolic and epigenetic reprogramming [31, 123, 124].

1.3.1 SCFA-producing bacteria

SCFAs include acetic acid (C2), propionic acid (C3), butyric acid (C4) and pentanoic acid (C5). SCFAs can be synthesised by various sources including the liver [125], but are most commonly known to be gut microbiota-derived. Acetate, propionate and butyrate make up more than 95% of SCFAs in the intestine, with localised concentrations reaching up to 140 mM and an approximate 60:20:20 molar ratio [126]. The bulk of SCFAs produced by the microbiota are subsequently absorbed and metabolised by enterocytes. The remaining SCFAs are transported via the portal vein to the liver and other organs (Figure 1.2). In the peripheral blood, the concentrations of acetate, propionate and butyrate has been estimated to be 70 μM, 5 μM and 4 μM respectively [127]. SCFAs can be used as backbones for the *de novo* synthesis of

lipids and glucose in the intestinal tract and liver and thereby serve as energy source for the host [128].

SCFA concentrations depend on various factors including gut transit time, the potential hydrogen (pH) level of the colonic content, source of the substrate, quantity and composition of gut microbiota. Bacteroidetes and Firmicutes are the dominant phyla in the gut microbiota, with the former capable of synthesising acetate and propionate, and the majority of the latter being butyrate producers [129-131]. However, other phyla are also capable of SCFA biosynthesis. Specific acetate-producing species belong to the genera *Escherichia*, *Enterobacter*, *Streptococcu*s, *Akkermansia muciniphila*, *Ruminococcus*, *Prevotella* and *Bacteroides* [132-134]. Propionate and butyrate production has been detected in relatively fewer bacterial genera [135]. Propionate producers include *Bacteroides thetaiotaomicron*, *Bacteroides vulgatus*, *Lactobacillus plantarum*, and *Akkermansia muciniphila* [136, 137]. In contrast, butyrate is primarily produced by *Eubacterium rectale*, *Eubacterium hallii*, *Roseburia faecis*, and *Faecalibacterium prausnitzii* [126, 138, 139]. Interestingly, specific forms of dietary fibre have been associated with increased SCFA production by gut microbes, for example *Akkermansia muciniphilia* was mainly responsible for mucin fermentation into propionate [140] whereas *Ruminococcus bromii* converted resistant starch into butyrate [141]. SCFA availability in the body is therefore dependent on diet and gut microbiota composition.

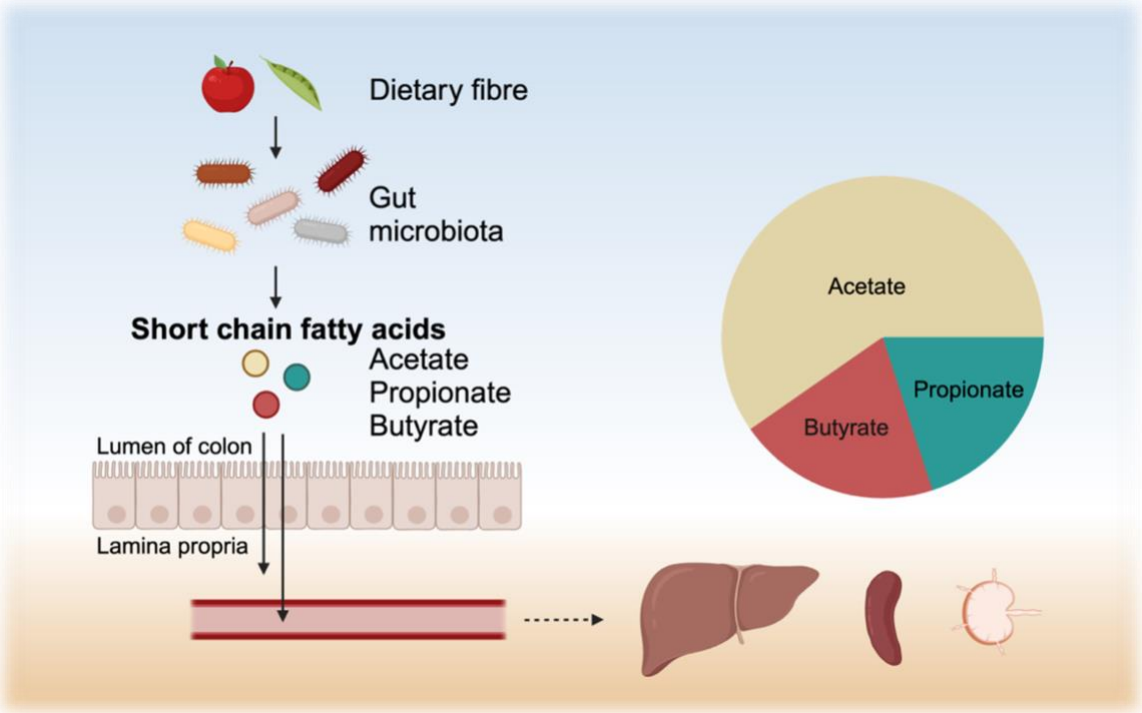

Figure 1.2 Gut microbiota-derived short chain fatty acids circulate to organs.

Short chain fatty acids (SCFAs) are generated by the fermentation of dietary fibre by the gut microbiota. A large majority of SCFAs in the intestine are acetate, propionate and butyrate, which are present in a molar ratio of approximately 60:20:20. While most of the SCFAs are absorbed by enterocytes, the remaining SCFAs enter the circulatory system through the portal vein and are transported to organs such as the liver, spleen and lymph nodes. (This figure was made using Biorender.)

1.3.2 SCFAs in health and disease

SCFAs can be utilised by cells as metabolic substrates that feed into mitochondrial metabolic pathways. In recent years an increasing number of studies have demonstrated physiological roles of SCFAs in organs, tissues and cells beyond the intestine. This also extends to pathological conditions, with low SCFAs levels correlating with diseases such as inflammatory bowel syndrome [142], diabetes [143], and colorectal cancer [144]. Alterations of SCFA concentrations have shown promise in reverting important aspects of such diseases in pre-clinical mouse models [145-150]. One way in which SCFAs have been implicated in influencing disease status is through their impact on T cells. Recent work from our group and others has implicated the incorporation of signals from SCFAs and their metabolism in T cell differentiation and function [31, 151, 152]. The ability to regulate T cell responses via SCFA has the potential to be harnessed for CAR T cell therapy [123, 153, 154]. Indeed, $CD8^+$ CAR T cells pre-treated with pentanoate were found to significantly reduce the rate of Panc02 pancreatic tumour growth in mice, compared to untreated CAR T cells [123].

1.3.3 SCFAs influence host cell responses

SCFA can act on cells by different means. They can passively diffuse through the cell and mitochondrial membranes [155] or enter the cell via carrier-mediated transportation through Solute carrier family 5 member 8 (SLC5a8) and monocarboxylate transporter 1 (MCT1) [156-159]. In doing so, SCFAs become available as metabolic substrates for FAO. They are converted into acetyl-CoA for integration into the TCA cycle and OXPHOS, ultimately leading to energy production in form of ATP and the provision of precursor metabolites. Furthermore, although SCFAs are not direct metabolic substrates for glycolysis, FAO generates acetyl-CoA that is able to promote glycolysis. Acetyl-CoA can firstly activate the glycolytic enzyme glyceraldehyde 3-phosphate dehydrogenase (GAPDH) by inducing post-translational modifications [160]. Secondly, acetyl-CoA can be used to generate ATP, resulting in the reversal of AMP-mediated suppression of mammalian target of rapamycin (mTOR), a positive regulator of cell growth, effector function, and glycolysis [161].

SCFAs can additionally diffuse through nuclear membranes to induce epigenetic modifications. Certain SCFAs can promote histone acetylation in various

cell types, such as T cells, B cells, and macrophages [162-164]. Butyrate in particular, has been found to be a stronger agent of histone acetylation than acetate and propionate [165, 166]. SCFAs can mediate histone acetylation by acting as HDAC inhibitors directly or via the provision of acetyl-CoA for histone acetylation [123, 167, 168]. At physiological concentrations, they are more likely to promote histone acetylation through the latter [166], although HDAC inhibition can additionally be induced by administering higher concentrations of SCFAs [123].

SCFAs are also cognate ligands of the G protein-coupled receptor (GPR) 41, GPR43, GPR109a, and olfactory receptor 78 (Olfr78; mice)/Olfactory Receptor Family 51 Subfamily E Member 2 (OR51E2; humans) found on the cell surface [169-172]. Of greater interest in this study are GPR41 (encoded by the gene *Ffar3*) which is relatively highly expressed on adipocytes and granulocytes, and GPR43 (*Ffar2*) that has been found on intestinal epithelial cells and immune cells [164, 173, 174]. The affinity of binding to GPR41 is butyrate ≈ propionate > acetate, while that of GPR43 is acetate ≈ propionate > butyrate [175-177]. GPR41 and GPR43 signalling can modulate processes in colonic epithelial cells including apoptosis, and cytokine and chemokine production [173, 178]. Additionally, they can induce chemotaxis of neutrophils through GPR43-dependent signalling [3, 170, 179, 180]. The half maximal effective concentration (EC_{50}) values are estimated to be in the high micromolar to low millimolar range, indicating a low affinity of SCFAs to these receptors [169-171]. However, these values were derived from transfected cell lines and yeast cells, and hence may not accurately reflect that of T cells. The expression of these SCFA receptors on T cells is controversial, with some studies finding low levels of expression [174, 181-183], and others reporting non-detectable levels [124, 184, 185], as recently summarised by Kim and colleagues [186]. GPR41 and GPR43 expression have indeed been shown to be dependent on T cell subsets and tissue localisation [124, 174, 184].

In summary, the most thoroughly-investigated mechanisms of SCFAs involve metabolic adaptations, epigenetic modifications and receptor-mediated signalling. An overview of these mechanisms is depicted in Figure 1.3. Studying these effects can

better inform us about how SCFAs may alter T cell differentiation and functional outcomes.

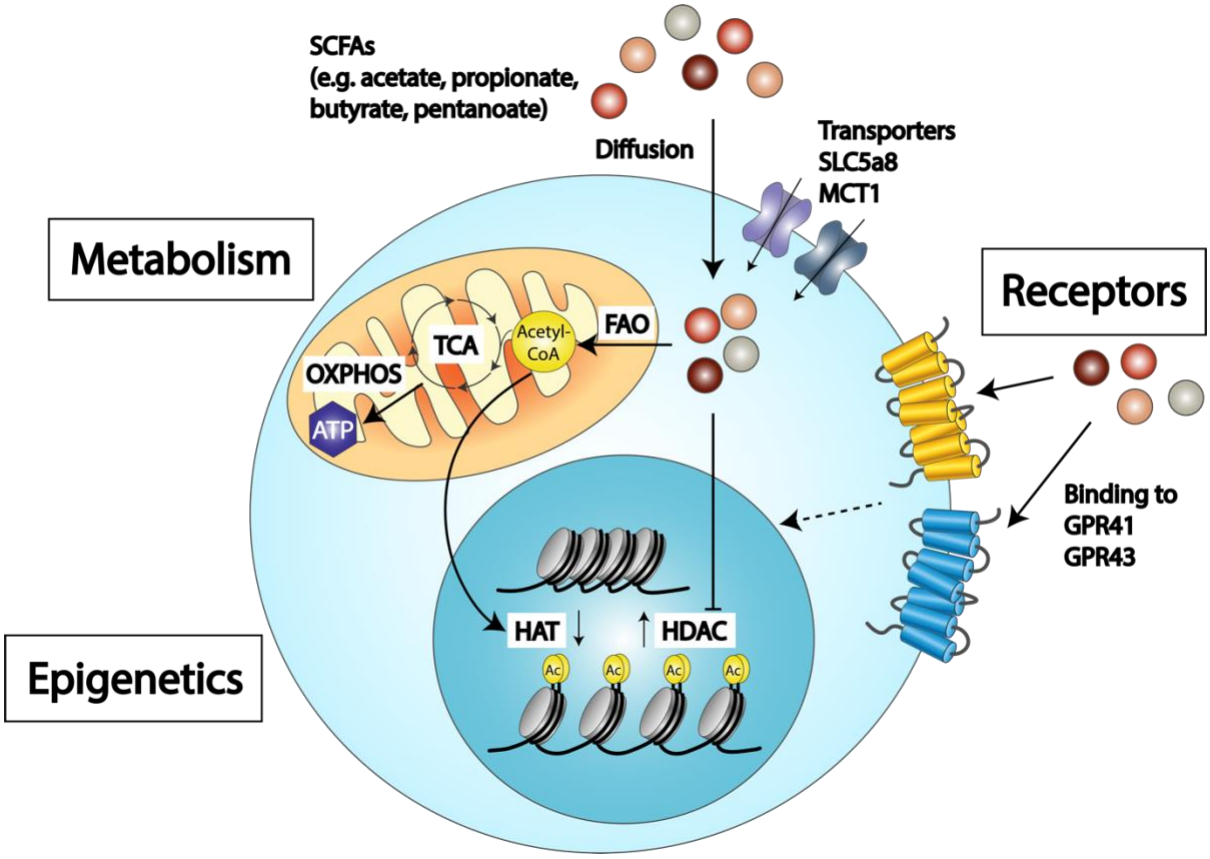

Figure 1.3 SCFAs act through metabolic, epigenetic, and receptor-mediated mechanisms in T cells.

Short chain fatty acids (SCFAs) such as acetate, propionate, butyrate, and pentanoate can either diffuse into the cell passively or via the transporters solute carrier family 5 member 8 (SLC5a8) and monocarboxylate transporter 1 (MCT1). Once in the cell, the SCFAs can be metabolised through fatty acid oxidation (FAO), by which they are converted into the metabolic intermediate acetyl coenzyme A (acetyl-CoA) for incorporation into the tricarboxylic acid (TCA) cycle. Through oxidative phosphorylation (OXPHOS), ATP is produced. SCFAs also have the ability to induce epigenetic modifications. They can directly inhibit histone deacetylase (HDAC) activity or indirectly promote histone acetylase (HAT) activity via its co-factor acetyl-CoA. The addition or maintenance of acetyl (Ac) groups on histone groups promotes gene expression. Finally, SCFAs can bind to G protein-coupled receptors 41 and 43 (GPR41 and GPR43). Downstream signalling cascades result in regulation in expression of select genes.

1.4 The influence of SCFAs on CD8$^+$ T cell immunity

The main pathways that SCFAs can alter CD8$^+$ T cell immunity include metabolic, epigenetic, and receptor-mediated mechanisms. Within the CD8$^+$ T cell compartment, more is known about how SCFAs influence effector function rather than differentiation. It is clear that SCFAs can promote CD8$^+$ T cell cytokine production, albeit to extents varying between different SCFAs [123, 151, 181, 187]. Apart from influencing effector responses, a few studies have uncovered how SCFAs can additionally impact re-activation and secondary immune response generated by memory T cells [31, 160, 188]. This section describes the mechanisms by which SCFAs can induce these effects, as summarised in Figure 1.4.

1.4.1 Metabolic effects on CD8$^+$ T cells

It has been suggested that SCFAs can enhance the function of effector CD8$^+$ T cells through metabolic rewiring. Several studies have shown that SCFAs can increase the expression of effector molecules such as IFN-γ and TNF-α, and degranulation markers of effector T cells [123, 151, 181, 187], with some of them linking these vital features of CD8$^+$ T cells to metabolic adaptations [123, 181]. For example, pentanoate promoted glycolysis in activated CD8$^+$ T cells, inducing IFN-γ expression [123]. This study showed that IFN-γ upregulation was partially reversed by blocking glycolysis with the mTOR inhibitor rapamycin, indicating that SCFAs can improve cytokine production to an extent by altering metabolism. In a key study, Trompette and colleagues observed that butyrate supplemented during *in vitro* T cell activation increased CD8$^+$ T cell mitochondrial biomass and expression of the degranulation marker CD107α in a FAO-dependent manner, indicating that butyrate could improve cytotoxicity through metabolic effects [181]. These butyrate-mediated changes were ameliorated by FAO inhibitor etomoxir that transports long chain fatty acids (LCFAs) from the cytoplasm to mitochondria for LCFA FAO. This indicated a role for butyrate in LCFA metabolism.

Various studies have demonstrated the importance of fatty acid metabolism in memory T cells to support their survival and re-activation [95, 96, 189, 190]. Van der Windt *et al.* reported that OXPHOS of memory T cells mainly relies on non-glucose derived inputs such as fatty acids, supporting the potency of the recall response [97].

FAO contributed significantly to the rapid re-activation and proliferation of *in vitro*-generated memory T cells, as shown through the inhibition of the FAO rate-limiting enzyme carnitine palmitoyltransferase 1a (CPT1a) [97]. Importantly, SCFAs and their precursors resulted in enhanced mitochondrial respiration in $CD8^+$ T cells. Activated $CD8^+$ T cells from mice fed a high fibre diet possessed a higher maximal mitochondrial respiration and spare respiratory capacity than mice on a control diet [181]. This hints that SCFA metabolism may induce an effector $CD8^+$ T cell metabolic phenotype that resembles that of $CD8^+$ memory T cell precursors. Indeed, we showed that butyrate promoted OXPHOS which correlated with increased MPEC formation [31].

Mechanistically, $CD8^+$ T cells directly catabolised butyrate in the TCA cycle, and this correlated with greater FoxO1 expression and responsiveness to IL-15 [31]. Upon adoptive transfer of these cells and rechallenge, butyrate-treated $CD8^+$ T cells preferentially differentiated into MPECs, which also occurred *in vivo* following high fibre feeding [31]. The ability of butyrate to act as a metabolic substrate was thus positively associated with significant skewing of $CD8^+$ T cell fate decisions towards MPECs. In terms of metabolic effects induced by specific SCFAs at a memory phase, a separate study found that acetate treatment of memory T cells promoted basal mitochondrial respiration and spare respiratory capacity by directly feeding into FAO, increasing acetyl-CoA input into the TCA cycle [160]. Interestingly, acetate also significantly increased memory T cell glycolysis through acetyl-CoA-induced post-translational activation of the glycolytic enzyme GAPDH. A better recall response and IFN-γ production were accompanied by this glycolytic switch, indicating greater differentiation into highly functional secondary effector cells [160]. This expands the role of SCFA from solely acting as direct metabolites to influencing metabolism by changing the activation status of key metabolic transcriptions factors and enzymes such as mTOR and GAPDH. Taken together, these studies have established that SCFAs can promote metabolic adaptations that skew $CD8^+$ T cell fate decisions towards greater effector capacity and a memory phenotype.

1.4.2 Epigenetic modifications in $CD8^+$ T cells

T cell functionality and plasticity are tightly regulated by epigenetic modifications that can be modulated by SCFAs. Direct treatment of $CD8^+$ T cells with

butyrate induced histone H4 acetylation of *Tbx21* and *Ifng* promoter sites [151]. This promoted a CTL effector phenotype, even in Type 17 $CD8^+$ T (Tc17) cells that are known to typically produce low levels of IFN-γ [151]. SCFA-induced histone acetylation thus appeared to promote a CTL effector phenotype. SCFAs may also impact differentiation through epigenetic modifications which regulate the cell cycle. Various studies have suggested that rapid expansion is linked to preferential differentiation into short-lived, terminally differentiated subsets, while effector T cells that undergo less proliferation retain stem-like qualities and become memory T cells [191-193]. HDAC inhibition by butyrate and propionate reduced human $CD8^+$ T cell proliferation [168]. The ability of SCFAs to reduce proliferation via histone acetylation may hence contribute towards maintaining stemness. This would not be surprising as histone modifications heavily influence lineage determination of $CD8^+$ T cells through the silencing and activation of crucial genes [80, 194].

Importantly, SCFA-derived acetyl-CoA can act as a co-factor for enzymes involved in histone modifications. For example, acetate does not possess HDAC inhibitor activity but can form the metabolic intermediate acetyl-CoA that is a co-factor for histone acetylases [160, 187]. In murine $CD8^+$ T cells, carbon derived from exogenous acetate was found to be incorporated in histones H3 and H4 through acetyl-CoA synthetase 2 (ACSS2)-dependent generation of acetyl-CoA [187]. This drove greater IFN-γ expression in tumour infiltrating lymphocytes (TILs) and antigen-specific $CD8^+$ T cells under glucose-restricted conditions. Acetate can hence promote effector responses in glucose-deficient microenvironments. Altogether, SCFAs can mediate epigenetic modifications, thereby altering the expression of genes involved in $CD8^+$ T cell proliferation, lineage decisions, and effector function.

1.4.3 SCFA receptor-mediated effects on $CD8^+$ T cells

Multiple groups have shown that the development and severity of disorders such as human colorectal cancer, asthma and inflammatory bowel disease are impacted by the expression of SCFA receptors on various cell types, including T cells [178, 184, 195, 196]. However, a role for these SCFA receptors in regulating $CD8^+$ T cell immunity is controversial. Oral administration of butyrate to both naïve GPR41/GPR43-deficient and wildtype (WT) mice similarly increased the proportion of

IFN-γ$^+$ CD8$^+$ T cells from the mesenteric lymph nodes compared to untreated mice upon phorbol 12-myristate 13-acetate (PMA)/ionomycin re-stimulation [151]. In the same study, re-stimulation of GPR41/GPR43-deficient and WT CD8$^+$ T cells following direct butyrate exposure *in vitro* resulted in comparable increases in IFN-γ expression upon re-stimulation [151]. A similar trend between GPR41/GPR43-deficient and WT CD8$^+$ T cells was observed after *in vitro* activation and pentanoate treatment [123]. This indicated that the SCFA-mediated increase in cytokine expression is dependent on factors other than GPR41 and GPR43. This is in line with other studies demonstrating that these receptors were not required for optimal effector function *in vitro* [31, 181].

Another way in which these receptors may impact disease outcome is by influencing CD8$^+$ T cell differentiation. We have shown that secondary viral antigen exposure of memory T cells in mixed bone marrow chimeric mice resulted in less expansion and IFN-γ expression in GPR41/GPR43-deficient CD8$^+$ T cells compared to WT CD8$^+$ T cells [31]. One of the many distinguishing factors between our study and others was the experimental model used and the timepoint examined. For example, the analysis of bulk CD8$^+$ T cells at an effector phase *in vitro* by others yielded no differences [151]. Similarly, we found that comparable frequencies of WT and GPR41/GPR43-deficient CD8$^+$ T cells were present in the blood of mice before secondary antigen challenge [31]. Only after re-activation at a memory timepoint *in vivo* did we observe a clear effect of GPR41 and GPR43 on the CD8$^+$ T cell frequency and IFN-γ expression [31]. The mechanism of how these receptors improve CD8$^+$ T cell recall responses is still unresolved. Interestingly, certain members of the GPRs play a role in cell cycle arrest [197], leading to the possibility that GPR41 and GPR43 may improve cell survival and hence differentiation into memory T cells [198-200]. As relatively few studies have investigated how SCFA receptor signalling influences T cell differentiation and function, further interrogation of the topic is required. This includes possible effects of GPR41/GPR43 in MPEC and SLEC development, given that memory T cell responses are affected.

It is important to note that the effects of SCFAs on T cell immunometabolism, epigenetic modifications and SCFA receptor signalling are complex and not mutually

exclusive. In summary, SCFAs have the potential to improve $CD8^+$ T cell functionality and promote stemness.

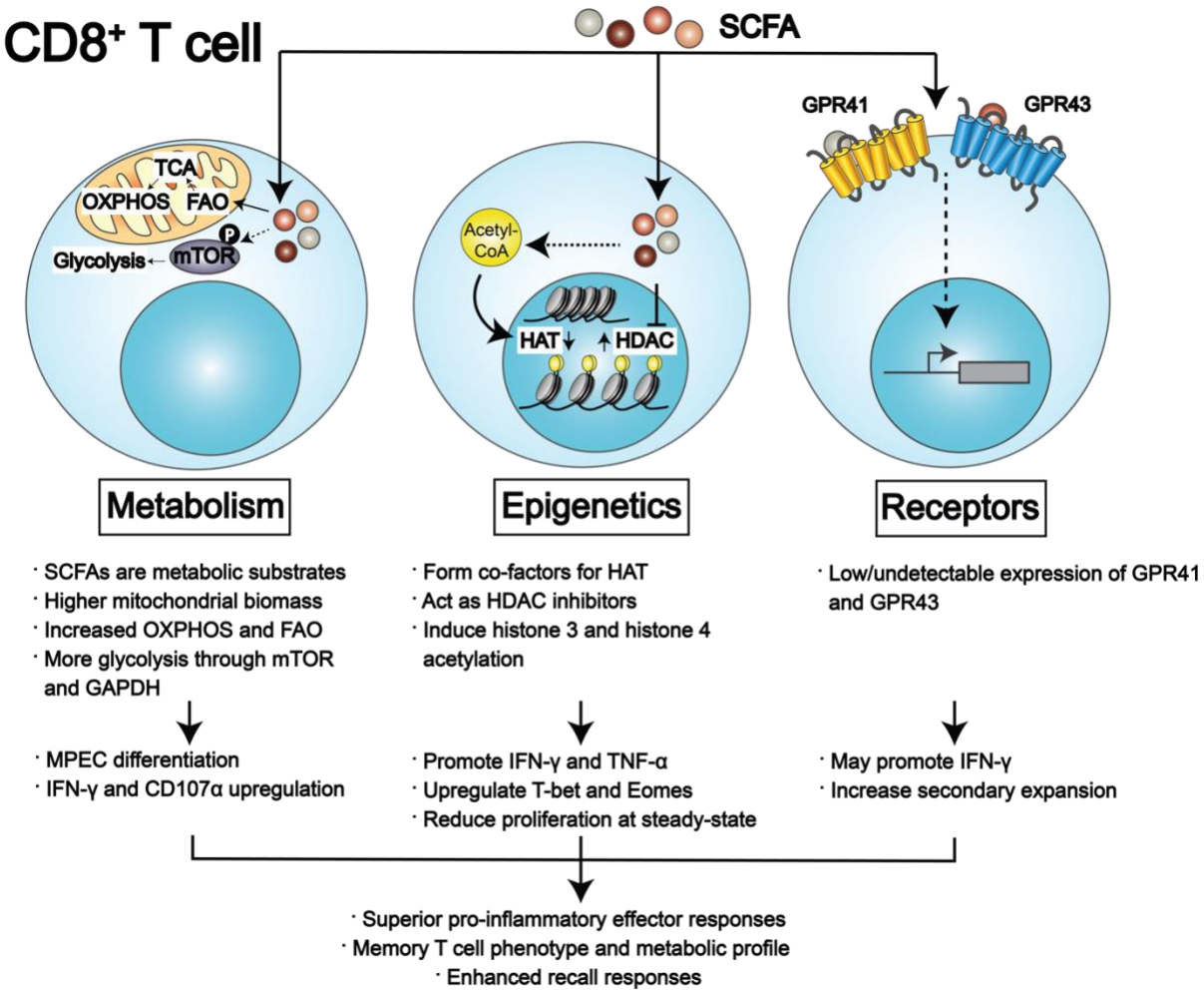

Figure 1.4 SCFAs promote CD8⁺ T cell immune responses.

Short chain fatty acids (SCFAs) can be converted to acetyl-coenzyme A (acetyl-CoA), which feeds into the metabolic pathways fatty acid oxidation (FAO), tricarboxylic acid (TCA) cycle and oxidative phosphorylation (OXPHOS) to be utilised by CD8⁺ T cells as substrates for energy production. This coincides with a higher mitochondrial biomass in cells that have been treated with SCFAs such as butyrate. As memory T cells rely heavily on mitochondrial respiration, the metabolic effects of SCFAs are likely a key factor for enhanced memory precursor effector cell (MPEC) differentiation. SCFA-induced increases in glycolysis via mammalian target of rapamycin (mTOR) and glyceraldehyde 3-phosphate dehydrogenase (GAPDH) contribute to enhanced effector molecule expression. SCFAs can also mediate epigenetic modifications by supporting histone acetyltransferase (HAT) activity via the provision of the co-factor acetyl-CoA and inhibiting histone deacetylases (HDACs), which upregulate the expression of the cytokines interferon-gamma (IFN-γ) and tumor necrosis factor-alpha (TNF-α), the transcription factors T-box expressed in T cells (T-bet) and Eomesodermin (Eomes), and reduce proliferation. Expression of the G protein-coupled receptors 41 and 43 (GPR41 and GPR43) on CD8⁺ T cells is controversial. Despite this, SCFA sensing by CD8⁺ T cells promotes IFN-γ expression and T cell

expansion upon secondary antigen exposure. Altogether, SCFAs promote $CD8^+$ T cell effector responses, differentiation into memory T cells and superior recall responses.

1.5 The influence of SCFAs on CD4$^+$ T cell immunity

Like CD8$^+$ T cells, SCFAs can alter CD4$^+$ T cell immunity through metabolic, epigenetic, and receptor-mediated effects. The importance of fatty acids in CD4$^+$ T cell differentiation was first defined for Tregs, where SCFAs support their immunomodulatory function [183, 201]. While the effect of SCFAs on memory CD4$^+$ T cell development has not been well characterised, they have been shown to skew effector subset differentiation and function [155]. This section focuses on Treg and Th1 cell subsets, although Th2- and Th17-type responses can also be influenced by SCFAs [202-204]. The SCFA-induced mechanisms behind these effects are summarised in Figure 1.5.

1.5.1 Metabolic effects on CD4$^+$ T cells

Similar to CD8$^+$ T cells, SCFA skew CD4$^+$ T cell differentiation and function, and hence play an important role in determining the nature and degree of immune responses [50, 205, 206]. Individual CD4$^+$ T cell lineages undergo distinct metabolic adaptations during differentiation that support their distinct bioenergetic requirements.

Tregs rely mainly on FAO and OXPHOS [13, 207] evident by their higher mitochondrial biomass compared to other CD4$^+$ T cell subsets [208]. Many reports have indicated that SCFAs promote Foxp3$^+$ Treg formation both *in vitro* and *in vivo* [165, 183, 201, 209]. Hao *et al.* demonstrated that butyrate metabolism possessed a dual role in promoting FAO for the differentiation into inducible Tregs [210]. Butyrate firstly increased FAO by acting as a carbon source, and was additionally metabolised into butyryl-CoA which antagonised the endogenous CPT1a inhibitor malonyl-CoA and thus maintained CPT1a activity. Butyrate therefore regulates FAO directly and indirectly in CD4$^+$ T cells [210].

Conventional CD4$^+$ T cell subsets were found to be more reliant on glycolysis than FAO [206]. Upon recognition of their cognate antigen, Th1, Th2 and Th17 subsets activated mTOR which promoted aerobic glycolysis resulting in T cell differentiation and effector function such as cytokine synthesis [124, 211-214]. The SCFA acetate, propionate and butyrate influenced mTOR activation thereby skewing T cell differentiation into Th1 cells and upregulating IFN-γ expression [124]. Administration

of the mTOR pathway inhibitors rapamycin and metformin completely blocked the SCFA-induced Th1 skewing, demonstrating that glycolysis mediated by SCFAs was crucial for subset specification [215]. Improved glucose uptake may have been another contributor as SCFAs have been shown to upregulate glucose transporter 1 and 4 (GLUT1 and GLUT4) in other cell types [216, 217]. Nevertheless, further studies are needed to clarify how SCFAs influence Th1, Th2, and Th17 differentiation and function from a metabolic perspective.

The aforementioned studies illustrated that SCFAs can influence $CD4^+$ T cell lineage specification and cytokine production through metabolic means. SCFAs are not only metabolic substrates but can also indirectly alter metabolic enzyme activity. As a result, glycolysis, FAO, and OXPHOS can all be upregulated by SCFAs. As $CD4^+$ T cell metabolism is closely tied to pro- or anti-inflammatory subset differentiation, SCFA may modulate this homeostatic balance. To date, there is limited knowledge on the metabolic effects of SCFAs on $CD4^+$ T cell stemness. A study on acetyl-CoA carboxylase (ACC1)-deficient cells that cannot perform fatty acid synthesis, has revealed that FAO of extracellular fatty acids was required for generating memory Th1 cells [205]. It would be interesting to understand whether SCFAs may promote $CD4^+$ T cell differentiation into memory T cells because memory Th1 cells have been associated with a greater protection against pathogen infections [218, 219] and better prognosis in patients with cancer, such as non-small cell lung cancer (NSCLC) [220].

1.5.2 Epigenetic modifications in $CD4^+$ T cells

Epigenetic modifications mediated by SCFAs can also alter $CD4^+$ T cell differentiation and effector molecule expression. Various groups have demonstrated that the pro-inflammatory and anti-inflammatory functions of $CD4^+$ T cells are affected by histone modifications [124, 149, 152, 201, 203, 221, 222]. HDAC activity in activated $CD4^+$ T cells was found to be diminished by acetate, propionate, and butyrate [124]. Treatment of unpolarised $CD4^+$ T cells with high SCFA concentrations of 10 mM lowered the HDAC activity, similar to the HDAC inhibitor Trichostatin A (TSA). Interestingly, these measurements were observed after a mere 2 hours of SCFA treatment, indicating that HDAC inhibition by SCFAs was fast-acting.

In line with findings in $CD8^+$ T cells, suppression in HDAC activity is mediated most strongly by butyrate, followed by propionate, then acetate [124, 152]. Multiple studies have substantiated that HDAC inhibitor properties of butyrate promote Th1 effector responses through large increases in IFN-γ expression [124, 152, 203, 221, 222]. The strong Th1-polarising effect of butyrate was evident from H3 and H4 hyperacetylation even in Treg-polarised $CD4^+$ T cells, where Tregs showed elevated expression of Th1-associated molecules IFN-γ and T-bet *in vitro* [152]. Similar trends were observed *in vivo* with oral butyrate administration [152]. As different groups have shown through flow cytometry, real-time quantitative PCR (RT-qPCR), and RNA sequencing, butyrate-mediated upregulation may not be specific to Th1 cytokines, as they also promote Th17 effector molecule expression [124, 221]. Likewise, acetate and propionate were found to increase both IFN-γ and IL-17 expression in Th1 and Th17 cells respectively, possibly through HDAC inhibition as TSA showed similar outcomes [124]. Interestingly, HDAC activity has been shown to be a critical determinant for $CD4^+$ T cell polarisation into cytotoxic $CD4^+$ T cells [222]. Butyrate, pentanoate, and to a smaller extent propionate treatment led to T-bet and granzyme B upregulation, which resembled that of HDAC1 and HDAC2-deficient $CD4^+$ T cells [222].

Butyrate has also been shown to induce other epigenetic modifications in addition to acetylation. With regards to $CD4^+$ T cells, butyrate induced greater H3K9ac and reduced lysine 4 trimethylation on histone H3 (H3K4me3) of the *Il22* promoter to increase the expression of the pro-inflammatory cytokine IL-22 in Th1 cells [221]. Whether butyrate regulates $CD4^+$ T cell gene expression through epigenetic modifications apart from acetylation and methylation is not well understood but important in deciphering the mechanisms of butyrate. As the central factors involved in metabolism also act as co-factors for methylation, it is likely that the ability of SCFAs to alter metabolism also directly impacts histone modifications [223]. Indeed, a crosslink between metabolism and epigenetic alterations has been shown in $CD4^+$ T cells. Sustained activation of the mTOR pathway and subsequently glycolysis was promoted through acetate and propionate-mediated acetylation of the 70-kDa ribosomal protein S6 (p70-S6) kinase and phosphorylation of ribosomal protein S6 (rpS6), likely through HDAC inhibition [124].

The suppression of HDAC activity by SCFAs is not limited to pro-inflammatory effects, but can also promote anti-inflammatory gene expression. Butyrate promoted histone 3 and histone 4 hyperacetylation of *Foxp3*, improving Treg phenotypic stability and function [149, 201]. Various modifications at *Foxp3* have been identified, such as H3K27ac, H3K9ac, and penta-acetylated histone H4 (H4ac5) – all of which were mediated by butyrate, but not acetate [149]. In the same study, an acetate-rich diet induced a similar amount of histone acetylation and penta-acetylation at *Foxp3* in Tregs as the control diet [149]. These modifications in T cells of the acetate-fed group were up to 100 times less abundant compared to those on a butyrate-rich diet. Acetate may not possess HDAC inhibitor activity and was therefore unlikely to induce the same level of modifications that butyrate could. Furusawa *et al.* determined that histone H3 acetylation of Tregs was found at *Foxp3* but not *Tbx21* or *Gata3*, implying that butyrate-induced epigenetic modifications were gene-specific under these settings. Various epigenetic changes at multiple sites of histones can be induced by a single condition [224, 225]. These findings altogether indicate a dual role of SCFAs in inflammation and immunosuppression through histone acetylation of various subset-specific genes.

1.5.3 SCFA receptor-mediated effects on $CD4^+$ T cells

SCFA receptor-mediated mechanisms have mostly been shown to confer anti-inflammatory implications on $CD4^+$ T cells due to their impact on Tregs. The tolerogenic function of colonic Tregs (cTregs) has been suggested to be GPR43-dependent, with GPR43 being required for propionate to upregulate the Treg-associated factors Foxp3 and IL-10 [183]. Consistent with the aforementioned study, Tanoue *et al*. found that the combined effects of GPR43 and HDAC inhibition regulated the induction of cTregs but not Tregs in other organs that expressed lower levels of these GPRs [226]. Provision of an acetate-rich diet resulted in a higher prevalence of type 1 diabetes in mice lacking GPR43 compared to control mice, with the former possessing fewer splenic and peripheral lymph node Tregs [149]. This effect was specific to the SCFA acetate and did not occur after butyrate feeding [149]. In line with this, another study reported that Tregs generated from spleens of WT and GPR41/43-deficient mice reacted similarly in terms of Foxp3 upregulation after butyrate

administration [152]. These studies collectively show that SCFA signalling can affect Treg differentiation but this seems to be model-dependent.

Of note, there is little evidence for effects upon engagement of SCFA receptor in other $CD4^+$ T cell subsets. Yang *et al*. showed that butyrate functions as a GPR41 agonist to promote *Hif1α* and *Ahr* gene expression in $CD4^+$ T cells, upregulating IL-22 production [221]. However, butyrate-mediated cytokine upregulation in Th1 cells is GPR43-independent [203]. Acetate had no effect on Th1 differentiation of mice deficient in GPR41 or GPR43 [124, 215]. In line with this, IFN-γ expression was similar between WT, GPR41-deficient, and GPR43-deficient $CD4^+$ T cells, regardless of acetate treatment [124, 215]. Like for the aforementioned Treg studies, the involvement of SCFA receptors in Th1 immunity may be model-dependent. Given that few studies have investigated the role of these receptors in pro-inflammatory $CD4^+$ T cell subsets, more work is required to better understand their contribution.

Similar to $CD8^+$ T cells, inter-dependence between SCFA-mediated mechanisms has been shown in $CD4^+$ T cells. At least 2 studies have demonstrated that SCFA receptor signalling supports histone hyperacetylation. Upon acetate, propionate, or butyrate treatment, Park *et al*. measured a reduction in HDAC activity in WT $CD4^+$ T cells, but not their GPR41/GPR43-deficient counterparts [124]. Propionate treatment reduced the expression of HDAC6 and HDAC9 in cTregs of WT mice, while GPR43-deficient mice expressed similar levels as the untreated group [183]. Also, propionate induced histone H3 acetylation in WT cTregs, but not in GPR43-deficient cells [183]. This highlights a certain degree of dependency of epigenetic modifications on SCFA receptor signalling. The mechanism of this requires further investigation considering HDAC inhibition requires entry of SCFAs into the cell while SCFA-binding occurs on the cell surface without any known uptake. Altogether, various aspects of $CD4^+$ T cell differentiation and function are altered by receptor-mediated, metabolic, and epigenetic effects of SCFAs but many details are not well understood.

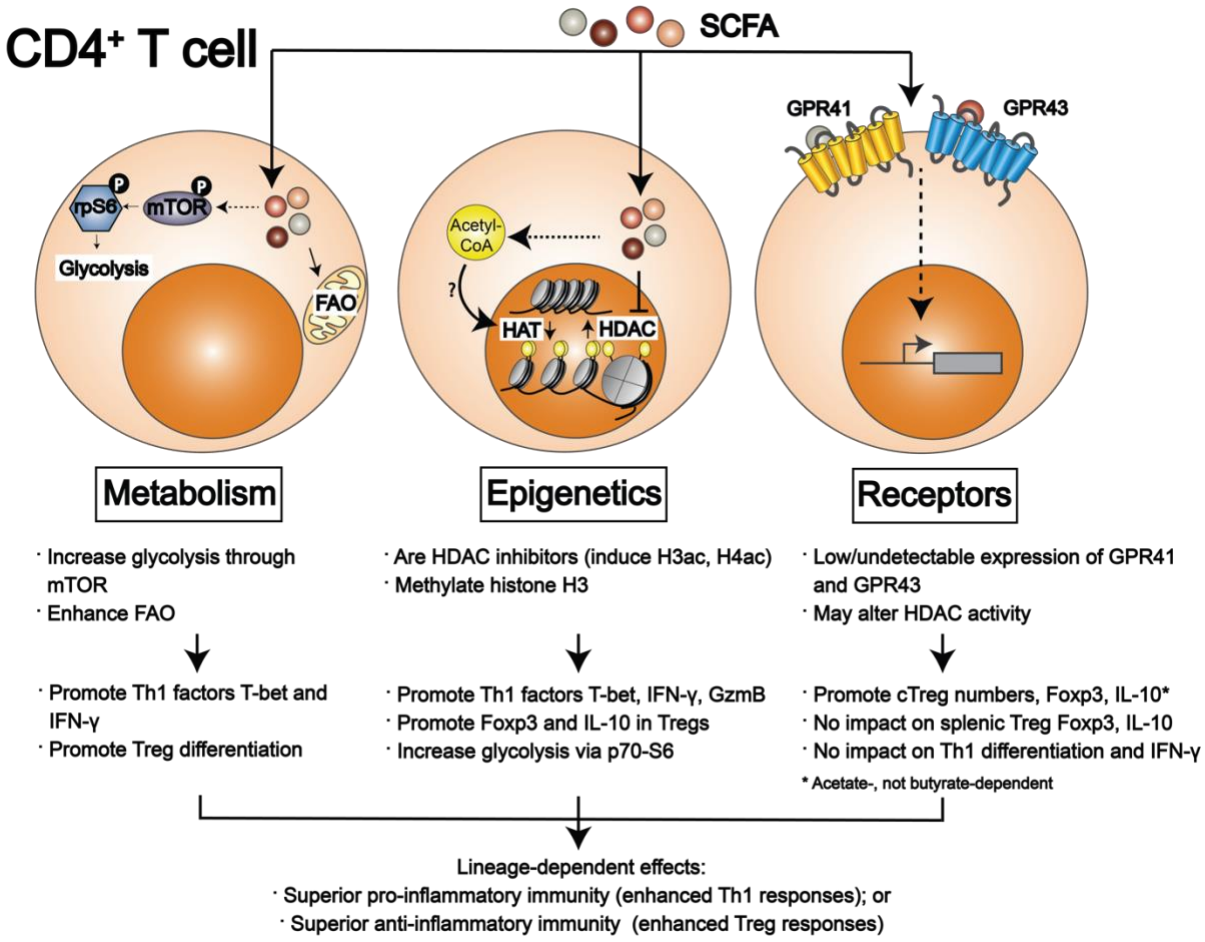

Figure 1.5 SCFAs alter CD4⁺ T cell immune responses.

The effect that short chain fatty acids (SCFAs) have on CD4⁺ T cells is highly context-dependent. SCFAs can promote glycolysis through phospho-mammalian target of rapamycin (mTOR) and phospho-ribosomal protein S6 (rpS6). Additionally, they can enhance fatty acid oxidation (FAO) by acting as metabolic substrates. This promotes the expression of the T helper 1 (Th1)-associated factors T-box expressed in T cells (T-bet) and interferon-gamma (IFN-γ), as well as regulatory T (Treg) cell differentiation. SCFAs induce epigenetic effects. They act as inhibitors of histone deacetylases (HDAC), resulting in histone H3 and H4 acetylation (H3ac and H4ac respectively). Other epigenetic modifications include histone H3 methylation. SCFAs are also likely to increase the availability of acetyl-coenzyme A (acetyl-CoA) for histone acetyltransferase (HAT) activity. As a result, the expression of Th1-associated molecules T-bet, IFN-γ and granzyme B (GzmB), as well as Treg-associated forkhead box P3 (Fox3) and interleukin-10 (IL-10) are promoted. HDAC inhibition has also been reported to enhance glycolysis through acetylation of the 70-kDa ribosomal protein S6 (p70-S6). The expression of the G protein-coupled receptors 41 and 43 (GPR41 and GPR43) on CD4⁺ T cells is reportedly low or undetectable. However, HDAC activity is possibly altered through receptor-mediated mechanisms. Acetate enhances Foxp3

and IL-10 expression in colonic Tregs (cTregs) but not those found in the spleen. Th1 cell differentiation and IFN-γ are also not affected.

1.6 Indirect effects of SCFAs on T cells

Apart from acting on T cells directly, microbiota-derived SCFAs can impact T cells indirectly by influencing other cell types and tissues that affect T cell priming, differentiation or memory development. This includes DCs which are central in initiating and coordinating both $CD4^+$ and $CD8^+$ T cell responses [227, 228]. The main subsets of DCs are conventional DCs (cDCs) and plasmacytoid DCs (pDCs). cDCs can be subdivided into type-1 cDCs (cDC1s) and type-2 cDCs (cDC2s). cDC1s perform antigen cross-presentation to MHC-I molecules and prime $CD8^+$ T cells [229]. This subset consists of resident $CD8^+$ DCs in lymphoid tissues and migratory $CD103^+$ DCs from peripheral organs including the lungs and skin [230, 231]. cDC2s are a phenotypically and functionally heterogeneous subset that preferentially initiates conventional $CD4^+$ T cell responses [232, 233].

In contrast to T cells where GPR43 expression is controversial, DCs are known to express high levels of GPR43 [184, 185]. This might explain some of the discrepancies between studies as SCFA-influenced DCs might have induced changes in T cell immunity rather than direct effects of SCFAs. Although the association between SCFAs and Th1 cells through DC-dependent effects is largely unresolved, the topic has been investigated in the context of Th2 cells and Tregs. A hallmark study by Trompette *et al*. demonstrated that SCFA levels altered bone marrow haematopoiesis and DC-mediated priming of Th2 cells [204]. In this house dust mite allergy model, low SCFA levels led to increased activation of lung cDC2s, whereas increased propionate concentrations led to a less activated phenotype. Propionate reduced the capacity of DCs to prompt Th2 responses, thereby protecting against allergic airway inflammation [204]. This was dependent on the expression of GPR41 but not GPR43. As mentioned above, SCFAs were not detected in the lung itself. This demonstrated that peripheral SCFA levels altered $CD4^+$ T cells indirectly by acting on DCs.

Similar effects of SCFA have been observed in another DC subset, with results demonstrating that SCFA levels influence the proportion of $CD103^+$ DCs in the gut draining lymph nodes [234]. Increased SCFA levels led to higher expression of key tolerogenic genes which correlated with an increased ability to convert naïve $CD4^+$ T

cells into Tregs, resulting in reduced clinical symptoms after peanut allergy induction. In contrast, *Ffar2*$^{-/-}$ mice also showed exacerbated clinical symptoms. Together, these findings suggest that SCFAs can alter CD4$^+$ T cell immunity through DC responses.

SCFAs may also influence CD8$^+$ T cell responses through DCs. A translational study by Coutzac and colleagues analysed SCFA levels in metastatic melanoma patients treated with anti-cytotoxic T-lymphocyte-associated protein 4 (CTLA-4) immunotherapy, a form of ICB [235]. Experiments in mice demonstrated that butyrate reduced the efficacy of CTLA-4 blockade, which correlated with lower DC maturation and CD8$^+$ T cell priming. This hypothesis is in line with findings that butyrate blocks DC activation *in vitro* [236, 237]. Together, these data show that SCFAs can regulate CD4$^+$ and CD8$^+$ T cell immunity through T cell extrinsic effects.

1.7 Harnessing SCFAs for cancer immunotherapies

T cells play a major role in the pathogenesis and resolution of various conditions, including cancer. Through influencing T cell responses, SCFAs can skew disease outcomes. Although the ability of dietary fibre and SCFAs to alter disease outcomes has largely been autoimmune disease-focused [152, 162, 183, 201, 203, 215, 221, 238], their effects have also been demonstrated in cancer. CD8$^+$ T cells and Th1 cells are key effectors in tumour control [239, 240], with clinical studies highlighting their prognostic importance [241, 242]. Importantly, T cell-based immunotherapies such as ICB and CAR T cells show variable success between patients [243, 244]. As such, there is a need to understand the factors that may influence treatment outcomes. This section will focus on how SCFAs can modify anti-tumour T cell responses.

1.7.1 Altering gut microbiota composition

The availability of SCFAs in the body is heavily reliant on the gut microbiome composition and diversity. A variety of studies have utilised techniques such as faecal transplants, antibiotic treatments, and specialised diets to investigate the diverse physiological effects of gut microbiota on cancer [121, 133, 245]. The intimate link between a fibre consumption, gut microbiome composition, SCFA availability, and immune control of cancer has been demonstrated in a small number of studies, as

summarised by Mirzaei *et al.* and Helmink *et al*. [246, 247]. However, the extent of T cell involvement is not well understood.

A clear role of gut microbiota in shaping responses to cancer immunotherapy has been described by multiple groups. In a study assessing the association of microbiota species and melanoma patient responses to anti-PD-1 and anti-CTLA-4 treatment, a greater abundance of *Akkermansia muciniphila* and *Faecalibacterium prausnitzii* was detected in responders than non-responders [248-251]. As these bacterial strains are butyrate producers [252, 253], it is possible that SCFA production influences anti-cancer responses. Frankel and colleagues additionally noted an enrichment in *Bacteroides thetaiotamicron* which supports the growth of butyrate-producing bacterial strains through cross-feeding, the process of lactose fermentation that produces glucose and galactose for breakdown by SCFA producers [254]. A recent study of anti-PD-1 and anti-CTLA-4 ICB treatment responses in melanoma patients showed that higher fibre consumption was significantly associated with the abundance of Ruminococcacae, a family of SCFA producers [255]. Patients with Ruminococcacae-dominated gut microbiomes were more likely to respond to ICB, compared to those with Bacteroidaceae-dominated gut microbiomes [255]. Interestingly, patients with Bacteroidaceae-dominated gut microbiomes were less likely to encounter immune-related adverse events if they also possessed a high Ruminococcacae abundance [255]. This suggested a regulatory role of microbiota in responses induced by ICB. Similar to the previous study, melanoma patients with a comparably higher fibre consumption responded better to anti-PD-1 and possessed a significantly greater abundance of Ruminococcacae compared to non-responders [256]. The association between fibre intake and survival was recapitulated in pre-clinical mouse models, where T cell receptor signalling pathways and T cell activation gene sets were enriched in high-fibre diet mice compared to their low-fibre diet counterparts [256].

It could be argued that an enrichment of these commensals increases SCFA availability for T cells. Indeed, the abundance of Clostridiales, Ruminococcaceae or *Faecalibacterium* in patients receiving anti-PD-1 was positively correlated with cytokine-producing $CD4^+$ and $CD8^+$ T cells [248]. Mice colonised with fecal microbiota transplants (FMTs) from ICB non-responders were further supplemented with

Akkermansia muciniphila, increasing $CD4^+$ T cell recruitment into tumours and overcoming ICB resistance [249]. Synergy between SCFA-producer *Bifidobacterium bifidum* K57 and anti-PD-1 treatment increased IL-2 expression by $CD4^+$ TILs and favoured the formation of effector $CD4^+$ T cells over Tregs [257, 258]. Transferring faecal contents containing elevated *Bifidobacteriaceae* operational taxonomic units (OTU) or a defined consortium of gut bacteria consisting of *Faecalibacterium*, *Bacteroidetes* and *Fusobacterium* promoted $CD8^+$ T cell IFN-γ expression and, induced improved ICB responses in mice [245, 257, 259]. Interestingly, the majority of the beneficial bacteria strains identified were known producers of SCFAs [132, 133, 260]. In a clinical study, *Faecalibacterium* was additionally positively correlated to better antigen presentation in the tumour microenvironment, suggesting that indirect effects on T cells may be another mechanism by which microbiota regulates host responses to cancer [248].

The gut microbiome has been shown to be highly variable from day-to-day and between individuals [261]. While dietary changes can cause alterations in gut microbiome composition, it is unknown whether these changes are permanent due to a lack of long-term human studies [262]. FMTs can alter microbiota composition, but their success is in part dependent on antibiotic treatments that are required to create a niche. A few caveats of antibiotic treatment include the selection of antibiotic-resistant organisms [263, 264] and an altered gut metabolome such as arginine and secondary bile acid availability which have immunomodulatory effects [265, 266]. As such, direct administration of SCFAs may be a better alternative to alter the availability of these metabolites.

1.7.2 Direct SCFA treatment

SCFAs have been a subject of study in several pre-clinical cancer models, where they improved anti-tumour T cell responses [123, 187, 267]. Intraperitoneal injection of acetate into EL4 tumour inoculated mice improved IFN-γ production by $CD8^+$ T cells and tumour control, partially through ACSS2, an enzyme that converts acetate to acetyl-CoA [187]. Additionally, the use of SCFAs has been tested in CAR T cell therapy. Both butyrate and pentanoate-treated CAR T cells produced more IFN-γ and TNF-α in pre-clinical melanoma and pancreatic cancer models [123]. Improved

proliferation and/or survival were indicated by higher frequencies of pentanoate-treated cells, likely through greater IL-2 autocrine signalling and *in vivo* proliferation [123]. This suggests that incorporating SCFAs such as pentanoate into the CAR T cell manufacturing process may improve current treatment regimens [123].

Contrary to the beneficial application of SCFAs in immunotherapy, the immunosuppressive ability of certain SCFAs has been shown to hinder anti-tumour therapy. As described in detail above, Coutzac and colleagues showed that oral butyrate administration reduced the efficacy of anti-CTLA-4 ICB in a murine CT26 colon carcinoma model by limiting DC maturation and memory $CD4^+$ T cell formation [235]. The discordance in SCFA efficacy in improving T cell responses may rest in differences in administration routes, tumour models and type of immunotherapy tested. Great potential exists for SCFAs to be introduced into therapeutic treatment regimes, but rigorous testing and optimisation is required to ensure that possible tolerogenic effects are minimised in therapies aimed at improving pro-inflammatory effector T cell responses.

Immunotherapies, such as ICB and CAR T cell therapy, have shown major successes in controlling cancer even in patients at advanced disease stages [244, 268]. However, there remains a critical medical need to optimise these therapies in order to improve response rates. The direct and indirect influences of SCFAs on T cell differentiation and function could serve as a potential avenue to optimise these therapies. For example, SCFAs administered as a supplement in existing treatments. Notably, there is a lack of data studying causative relationships between SCFAs and T cells in the context of cancer. This presents the potential for further exploration into therapeutic uses of SCFAs for $CD4^+$ and $CD8^+$ T cell anti-tumour immunity.

1.8 Thesis aims

T cell fate decisions are underpinned by widescale differences in transcriptional, epigenetic and metabolic profiles which determine the effector function and longevity of cells. Importantly, SCFAs can directly alter $CD8^+$ and $CD4^+$ T cell responses through the complex interplay between epigenetic, metabolic and receptor-mediated mechanisms. While various groups have shown that SCFAs improved $CD8^+$

T cell cytokine production [151, 181], a study by our team has indicated that their differentiation was also skewed [31]. Interestingly, GPR41 and GPR43 signalling was required for optimal memory T cell recall responses, which calls into question if SCFA receptor signalling influences $CD8^+$ T cell priming. Furthermore, SCFAs can modify anti-inflammatory Treg and pro-inflammatory helper $CD4^+$ T cell responses [124, 173, 183]. Considerable attention has been placed on Tregs to date, but SCFA mechanisms in cytotoxic $CD4^+$ T cell and Th1 immunity are not as well characterised. Understanding how SCFAs skew T cell stemness and functionality is key in their therapeutic application. While SCFAs have been rigorously studied in the context of autoimmunity, their role in improving T cell-mediated anti-cancer responses is still relatively unexplored. Given the multi-faceted effects of SCFAs in Th1 and $CD8^+$ T cells, their application in cancer immunotherapies such as CAR T cell therapy may hold great potential.

The aims of this project are the following:

1. Characterise the role of the SCFA receptors GPR41 and GPR43 in $CD8^+$ T cell priming to understand their effects on T cell differentiation and function upon viral infection (Chapter 3).
2. Establish the role of the SCFA butyrate in $CD4^+$ T cell differentiation and function by studying the contributions of SCFA-mediated mechanisms including SCFA receptors and SCFA-induced metabolic and epigenetic modifications (Chapter 4).
3. Explore the therapeutic application of butyrate in improving $CD4^+$ and $CD8^+$ T cell stemness and anti-tumour effector function in CAR T cell therapy (Chapter 5).

Chapter 2:
Materials and Methods

Chapter 2 Materials and Methods

2.1 Materials

2.1.1 Mice

Table 2.1 Experimental mouse strains.

Strain	Description	Source	Publication
C57BL/6J (B6)	Mice that express MHC-I H-2b and MHC-II I-Ab and the congenic marker Ly5.2.	The Jackson Laboratory	[269]
gDT-II × Ly5.1 (gDT-II.Ly5.1)	Mice generated on a B6 background that express the congenic marker Ly5.1 and a I-Ab-restricted T cell receptor (Va3.2 Ja16/Vb2 Db2.1Jb2.1) specific for HSV-1-derived glycoprotein D peptide ($gD_{315\text{-}327}$, IPPNWHIPSIQDA).	Heath Laboratory, PDI	[231]
gDT-II × B6.*Prf1*$^{-/-}$ (gDT-II.*Prf1*$^{-/-}$)	gDT-II mice that lack expression of perforin due to gene deletion.	Gebhardt Laboratory, PDI	
gBT-I × Ly5.1 (gBT-I.Ly5.1)	Mice generated on a B6 background that express the congenic marker Ly5.1 and a H-2Kb restricted transgenic TCR specific for the HSV-1 glycoprotein B peptide ($gB_{498\text{-}505}$, SSIEFARL)	PDI	[270]
B6.*Ffar2*$^{-/-}$; *Ffar3*$^{-/-}$ (*Ffar2*$^{-/-}$; *Ffar3*$^{-/-}$)	Mice generated on a B6 background that lack expression of GPR41 and GPR43.	Provided by S. Offermanns	[271]

B6.Cg-Pds5b$^{Tg(Wap-ERBB2)229Wzw}$/J (C57BL/6 hHER2)	Transgenic mice generated on a B6 background, which express the human ERBB2 (HER2) gene in mammary gland and brain, are tolerant to the ERBB2 antigen.	The Jackson Laboratory	[272]

All mice listed above were bred and maintained in specific pathogen-free conditions in the Bioresources Facility in the Department of Microbiology and Immunology at the University of Melbourne, with the exception of B6.Cg-Pds5b$^{Tg(Wap-ERBB2)229Wzw}$/J mice and B6 mice used in CAR T cell experiments that were bred at the PMCC. Mice were housed in ventilated cages, in 12-hour light/dark cycles, and received sterile food and water *ad libitum*. All mice were female and aged between 6 and 13 weeks of age at the beginning of experiments, unless otherwise stated. All animal experiments were approved by the University of Melbourne Animal Ethics Committee (animal ethics numbers 1814545 and 24625) and PMCC Animal Experimentation Ethics Committee (animal ethics number E671), and complied with the Prevention of Cruelty to Animal Act (1986) and the National Health and Medical Research Council (NHMRC) Australian Code of Practice for the Care and Use of Animals for Scientific Purposes (1997).

2.1.2 Cell lines

Table 2.2 Cell lines for tumour and infection models.

Cell line	Origin	Description	Source/Publication
B16F10.gD.eGFP (B16.gD)	Mouse melanoma	B16F10 melanoma cell line retrovirally transduced with a construct containing HSV-1-derived gD and enhanced green fluorescent protein (eGFP). Gene products	Waithman laboratory, Telethon Kids Institute, University of Western Australia

		are expressed independently.	
B16F1.gB.GFP (B16.gB)	Mouse melanoma	B16 melanoma cell line expressing full length membrane bound gB and green fluorescent protein (GFP) under control of the early cytomegalovirus (CMV) promoter.	Waithman laboratory, Telethon Kids Institute, University of Western Australia [101]
E0771.HER2	Murine mammary cancer	E0771 cell line expressing a truncated form of the human HER2 protein [273].	Prof. Robin Anderson, Olivia-Newton John Cancer Centre Heidelberg, Victoria, Australia [274]
Vero cells	African green monkey kidney epithelial cells	A cell line that is susceptible to HSV-1 infection, resulting in apoptosis.	CSL, Parkville, Australia [275]
GP+E-86-LXSN	Mouse fibroblast	A cell line that was transformed with Moloney murine leukemia virus (MoMLV) *gag*, *pol*, and *env*. The retroviral GP+E-86 cell line was used to package LXSN-mouse CAR plasmids encoding the anti-HER2 scFv-CD28-CD3ζ CAR T construct.	American Type Culture Collection (ATCC) [276]

PG13	Mouse fibroblast	A cell line that was transformed with MoMLV *gag-pol* and Gibbon ape leukemia virus *env*. The retroviral PG13 cell line was used to package the pSAMEN retroviral vector containing humanized anti-Lewis Y antigen (LeY) scFv-CD28-CD3ζ receptor as described by [277].	ATCC [278]

B16.gB and B16.gD cells were generated by transduction of parental B16 cell lines with retroviral vectors containing a full-length membrane bound form of HSV gB and eGFP or full-length membrane bound form of HSV gD and eGFP respectively, as previously described [279]. E0771.HER2 was generated through retroviral transduction of the parental E0771 cell line, to express the human-HER2 antigen under the control of the mouse stem cell virus LTR promoter.

2.1.3 Virus

Table 2.3 Viral strain for mouse infections.

Virus	Description	Source	Publication
HSV-1 KOS	HSV-1 strain possessing a reduced virulence	F.R. Carbone, University of Melbourne	[280]

2.1.4 Peptides and recombinant proteins

Table 2.4 Peptides and recombinant proteins for T cell cultures.

Peptide and recombinant proteins	Source
HSV-1-derived $gB_{498-505}$ (Sequence: SSIEFARL)	Auspep, Australia
HSV-1-derived $gD_{315-327}$ (Sequence: IPPNWHIPSIQDA)	Auspep, Australia
Recombinant human IL-2	Peprotech Inc., USA
Recombinant murine IL-7	Peprotech Inc., USA
Recombinant murine IL-12 p70	Peprotech Inc., USA

2.1.5 Enzymes

Table 2.5 Enzymes for organ digestions.

Enzyme	Source
Trypsin/EDTA (10 X; 0.5% trypsin, 0.2% EDTA)	Sigma Aldrich, USA
Collagenase Type III	Worthington, USA
Deoxyribonuclease (DNase) I	Roche, Germany
Liberase™ TL Research Grade	Sigma-Aldrich, USA
Dispase II (neutral protease, grade II)	Roche, Switzerland

2.1.6 Reagents for RT-qPCR

Table 2.6 Reagents for RT-qPCR.

Reagent	Source
Direct-zol™ RNA MicroPrep kit	Zymo Research, USA
Taqman Universal PCR Master Mix	Life Technologies, USA
Omniscript RT kit	Qiagen, Germany
Oligo-dT primers	Promega, USA
RNaseOUT™ Recombinant Ribonuclease Inhibitor	Thermo Fisher Scientific, USA

Table 2.7 Primers for Taqman RT-qPCR.

Gene target	Assay ID	Source
Ffar2	Mm02620654_s1	Life Technologies, USA
Ffar3	Mm02621638_s1	Life Technologies, USA
Hcar2	Mm01199527_s1	Thermo Fisher Scientific, USA
Gapdh	Mm99999915_g1	Life Technologies, USA
B2m	Mm00437762_m1	Life Technologies, USA

2.1.7 Reagents for western blotting

Table 2.8 Reagents for western blotting.

Reagent	Source
RIPA lysis buffer	Merck, USA
PhosSTOP	Merck, USA
Complete protease inhibitor cocktail	Roche, Switzerland
NuPAGE MOPS SDS running buffer	Invitrogen, USA
Tween-20	Sigma-Aldrich, USA
Precision Plus protein dual color standards	Bio-Rad, USA
Invitrogen novex ECL Chemiluminescent Substrate Reagent Kit	Thermo Scientific, USA

2.1.8 Antibodies, tetramers and dyes

Table 2.9 Antibodies for naïve $CD4^+$ T cell enrichment.

Purified rabbit anti-mouse	Clone
Anti-erythrocyte	Ter119
Anti-I-A/E	M5114

Anti-CD8	53-6.7
Anti-GR-1	RB6-8C5
Anti-Mac-1	M1/70
Anti-F4/80	F4/80

All antibodies for $CD4^+$ T cell enrichment were made by the Walter and Eliza Hall Institute of Medical Research (WEHI) Antibody Facility, Australia.

Table 2.10 Antibodies for *in vitro* stimulation and polarisation of T cells.

Antibody	Clone	Supplier
Anti-human CD3 functional grade	OKT3	Thermo Fisher Scientific, USA
Anti-mouse CD3ε functional grade	17A2	Thermo Fisher Scientific, USA
Anti-mouse CD28 functional grade	37.51	Thermo Fisher Scientific, USA
Anti-mouse IL-4	S4B6	WEHI Antibody Facility, Australia

Table 2.11 Antibodies for western blotting.

Antibody	Clone	Source
Anti-acetyl-histone H3	Polyclonal	Sigma-Aldrich, USA
Anti-acetyl-histone H4 (acetyl K5 + K8 + K12 + K16)	EPR16606	Abcam, UK
Anti-histone H3	D1H2	Cell Signalling Technology, USA
Anti-β-actin	13E5	Cell Signalling Technology, USA
Anti-Sp1	Polyclonal	Thermo Fisher Scientific, USA

Table 2.12 Antibodies for immune checkpoint blockade therapy.

Antibody	Clone	Source
Anti-PD-1	RMP1-14	Thermo Fisher Scientific, USA
Rat IgG2a Isotype Control	2A3	Thermo Fisher Scientific, USA

Table 2.13 Antibodies and dyes for flow cytometry.

Name	Conjugate	Clone	Source	Cat. #	Dilution
Bcl-6	FITC	7D1	BioLegend, USA	358513	1:100
CD103	PacB	2E7	BioLegend, USA	121418	1:100
CD11b	BV711	M1/70	BioLegend, USA	101242	1:100
CD11c	PE-Cy7	N418	eBioscience, USA	25-0114-82	1:400
CD127	APC	A7R34	eBioscience, USA	17-1271-82	1:100
CD127	PE-Cy7	A7R34	BioLegend, USA	135014	1:200
CD178 (FasL)	BV421	MFL3	BD OptiBuild, USA	740054	1:100
CD19	PerCP-Cy5.5	1D3	BD Pharmingen, USA	551001	1:100
CD24	PE	M1/69	BD Pharmingen, USA	553262	1:200
CD25	APC-Cy7	PC61	BD Pharmingen, USA	557658	1:100
CD25	eFluor450	PC61.5	eBioscience	48-0251-82	1:100
CD279 (PD-1)	APC	RMP1-30	BioLegend, USA	109112	1:100
CD279 (PD-1)	PE-Cy7	J43	eBioscience, USA	25-9985-82	1:200
CD326	APC-eFluor780	G8.8	BioLegend, USA	118218	1:200

CD3ε	PerCP-Cy5.5	145-2C11	Life Research, Australia	45-0031-82	1:100
CD4	AF700	RM4-5	BD Pharmingen, USA	557956	1:100
CD4	APC	RM4-5	BD Pharmingen, USA	553051	1:100
CD4	BUV805	GK1.5	BD Horizon, USA	20-0041-U025	1:200
CD40	FITC	HM40-3	BD Pharmingen, USA	553723	1:100
CD44	AF700	IM7	eBioscience, USA	56-0441-82	1:100
CD44	BV510	IM7	BD Horizon, USA	563114	1:100
CD44	PerCP-Cy5.5	IM7	eBioscience, USA	45-0441-82	1:400
CD45.1	APC	A20	eBioscience, USA	17-0453-82	1:100
CD45.1	BV711	A20	BD Horizon, USA	563982	1:100
CD45.1	FITC	A20	BD Pharmingen, USA	553775	1:200
CD45.2	APC-eFluor 780	104	eBioscience	47-0454-82	1:100
CD45.2	BUV737	104	BD Horizon	612778	1:200
CD45.2	FITC	104	BD Pharmingen	553772	1:100
CD45.2	PacB	104.2	WEHI, Australia	104.2-1	1:200
CD45R (B220)	PerCP-Cy5.5	RA3-6B2	eBioscience, USA	45-0452-82	1:200
CD62L	FITC	MEL-14	BD Pharmingen	553150	1:200
CD62L	PE-Cy7	MEL-14	eBioscience, USA	25-0621-82	1:500
CD69	BV421	H1.2F3	BioLegend, USA	104528	1:100
CD83	PE	Michel-17	eBioscience, USA	12-0831-80	1:100

CD86	BV510	GL1	BD Horizon, USA	563077	1:100
CD8a	APC	53-6.7	eBioscience, USA	17-0081-82	1:100
CD8a	BUV805	53-6.7	BD Biosciences, USA	612898	1:200
CD8a	BV711	53-6.7	BioLegend, USA	100748	1:200
CD8a	PacB	53-6.7	BD Pharmingen	558106	1:200
CXCR3	BV510	CXCR3-173	BioLegend, USA	126527	1:100
CXCR5	APC	L138D7	BioLegend, USA	145506	1:100
Eomes	PercP-eFluor710	Dan11mag	eBioscience, USA	46-4875-82	1:100
Fc block (CD16/32)	-	2.4G2	BD Biosciences, USA	553141	1:200
FoxO1	PE	C29H4	Cell Signalling Technology, USA	14262	1:200
Foxp3	eFluor450	FJK-16s	eBioscience, USA	48-5773-82	1:200
GATA-3	PE-Cy7	TWAJ	eBioscience, USA	25-9966-41	1:200
Granzyme B	FITC	GB11	BioLegend, USA	515403	1:100
IFN-γ	PE-Cy7	XMG1.2	BD Pharmingen, USA	557649	1:200
KLRG1	APC	2F1	eBioscience, USA	17-5893-82	1:100
KLRG1	BB700	2F1	BD OptiBuild, USA	742199	1:100
KLRG1	BV711	2F1	BioLegend, USA	138427	1:100
KLRG1	FITC	2F1	eBioscience, USA	11-5893-82	1:100

LIVE/ DEAD Fixable Near-IR Dead Cell Stain Kit for 633 or 635 nm excitation	-	-	Life Technologies, Australia	L10119	1:600
Ly6C	AF700	HK1.4	BioLegend, USA	128024	1:100
MHC-II	AF700	M5/114.15.2	eBioscience, USA	56-5321-82	1:100
NK1.1	PerCP-Cy5.5	PK136	BD Pharmingen, USA	551114	1:200
Normal mouse serum	-	-	eBioscience, USA	24-5544-94	1:50 or 1:200
Normal rat serum	-	-	ThermoFisher Scientific, USA	31888	1:50 or 1:200
Perforin	PE	S16009A	BioLegend, USA	154306	1:200
T-bet	APC	REA102	Miltenyi Biotec, Germany	130-119-783	1:100
TCF-1	AF488	C63D9	Cell Signalling Technology, USA	6444S	1:100
TCRb	BV510	H57-597	BD Horizon, USA	563221	1:100
TNF-α	APC	MP6-XT22	BD Pharmingen, USA	554420	1:100
Va2	AF700	B20.1	BD Pharmingen, USA	561239	1:100
Va2	BV421	B20.1	BD Horizon, USA	562944	1:100
Va2	PE-Cy7	B20.1	BD Pharmingen, USA	560624	1:400
Va3.2	FITC	RR3-16	BioLegend, USA	135406	1:100

Va3.2	PE	RR3-16	BioLegend, USA	135403	1:400
XCR1	AF647	ZET	BioLegend, USA	148214	1:100

2.1.9 Tetramer

Table 2.14 Tetramer for flow cytometric analyses.

Tetramer	Fluorochrome	Source
H2-K^b-gB SSIEFARL	PE	Dr Jie Lin, University of Melbourne, Australia

2.1.10 Metabolic probes

Table 2.15 Metabolic probes for flow cytometric analyses.

Probe	Colour/Fluorescence	Dilution	Source
Mitotracker	Deep Red	1:25000	Thermo Fisher Scientific, USA
Tetramethylrhodamine methyl ester (TMRM)	Orange	1:500	Life Technologies, Australia

Table 2.16 Blocking antibodies for real-time propidium iodide incorporation assays.

Antibody	Clone	Source
Anti-IFN-γ	AN-18	Thermo Fisher Scientific, USA
Anti-FasL	MLF3	BioLegend, USA

2.1.11 Chemicals and reagents

Table 2.17 Chemicals and reagents.

Chemicals	Source
2-mercaptoethanol (2-ME)	Life Technologies, USA

Agarose	Sigma-Aldrich, USA
Benzylpenicillin	CSL, Australia
BioMag goat anti-rat IgG beads	Qiagen, Germany
Bovine serum albumin (BSA)	Sigma-Aldrich, USA
Brefeldin A (BFA)	Sigma-Aldrich, USA
DAPI (4′,6-diamidino-2-phenylindole)	BioLegend/Australian Biosearch, USA
Dimethyl sulfoxide (DMSO)	Sigma-Aldrich, USA
E. coli lipopolysaccharide (LPS)	Sigma-Aldrich, USA
Ethylenediaminetetraacetic acid (EDTA)	Sigma-Aldrich, USA
Ficoll-plaque plus	GE Healthcare, USA
Fetal calf serum (FCS) (heat-inactivated)	CSL, Australia
Formaldehyde solution	Science Supply Australia Pty Ltd., Australia
FoxO1 inhibitor, AS1842856	Calbiochem, USA
N-2-hydroxyethylpiperazine-N'-2-ethane sulfonic acid (HEPES)	Sigma-Aldrich, USA
Ionomycin	Sigma-Aldrich, USA
Isoflurane	Cenvet, Australia
Ketamine	Parnell Laboratories, Australia
L-glutamine	Thermo Fisher Scientific, USA
Matrigel basement membrane matrix	Corning, USA
Phorbol 12-myristate 13-acetate (PMA)	Sigma-Aldrich, USA
Propidium iodide (PI)	Sigma-Aldrich, USA
Red blood cell (RBC) lysis buffer	Sigma-Aldrich, USA
RetroNectin	Takara Bio Inc., Japan
Sodium acetate	Sigma-Aldrich, USA
Sodium butyrate	Sigma-Aldrich, USA
Sodium dodecyl sulphate (SDS)	Sigma-Aldrich, USA
Sodium propionate	Sigma-Aldrich, USA
Sphero blank calibration beads (6.0 – 6.4 µM)	BD Bioscience, USA
Streptomycin	Sigma-Aldrich, USA
Toluidine blue	Sigma-Aldrich, USA

Trichostatin A (TSA)	Sigma-Aldrich, USA
Triton X-100	Sigma-Aldrich, USA
TRIzol	Life Technologies, USA
Trypan Blue	Sigma-Aldrich, USA

2.1.12 Media and solutions

Table 2.18 Composition of media and solutions.

Media/solution	Composition
CD4 isolation buffer	Phosphate buffered saline (PBS) supplemented with 2% FCS and 2 mM EDTA.
Dulbecco's Phosphate Buffered Saline (DPBS)	A balanced salt solution lacking calcium and magnesium.
KDS-RPMI – 2% FCS (KDS-RPMI-2)	Roswell Park Memorial Institute Buffer (RPMI)-1640 powder dissolved to 1X strength in MilliQ water supplemented with 2% FCS.
MEM – 2% FCS (MEM-2)	Minimal essential medium (MEM) supplemented with 2% FCS.
MEM – 10% FCS (MEM-10)	MEM supplemented with 10% FCS and 5% supplementum completum (SC).
PBS-EDTA – 10% BSA (Fluorescence activated cell sorting buffer; FACS buffer)	PBS supplemented with 10% w/v BSA and 5 mM EDTA.
RIPA buffer mix	RIPA buffer with 10% 1X PhosSTOP and 4% 1X Complete Protease Inhibitor Cocktail.
RPMI-1640 – 10% FCS (RP-10)	RPMI-1640 supplemented with 5% SC and 10% heat-inactivated FCS.
SC	23.83 g/L HEPES; 2×10^6 units (U)/L benzylpenicillin; 2 g/L streptomycin; 6 g/L L-glutamine; 1 mM 2-ME.

Western blot blocking solution	Tris-buffered saline (TBS) or PBS with 50 g/L BSA and 0.1% Tween-20.
Western blot sample buffer	350 mM Tris (pH 6.8) with 10.3% v/v SDS, 36% v/v glycerol, 5% 2-ME and 0.0012% bromophenol blue.

KDS-RPMI, PBS, MEM, RPMI-1640 and TBS were prepared by the Media Preparation Unit, Department of Microbiology and Immunology, The University of Melbourne, Australia. DPBS was obtained from Thermo Fisher Scientific, USA.

2.1.13 Commercially available kits

Table 2.19 Commercially available kits.

Kit	Source
Cytofix/Cytoperm Fixation/Permeabilization Solution Kit	BD Biosciences, USA
Dynabeads Flowcomp Mouse CD4	Invitrogen, USA
Foxp3/Transcription Factor Staining Buffer Set	eBioscience, USA
RNeasy MicroKit	Qiagen, Germany

2.1.14 Consumables

Table 2.20 Laboratory consumables and materials.

Reagents and materials	Supplier
1 mL syringe	Terumo, Australia
10 mL syringe	Terumo, Australia
18G needle	Terumo, Australia
24 well flat bottom tissue culture plate	Corning, USA
26G needle	Terumo, Australia
3 mL syringe	Terumo, Australia
48 well flat bottom tissue culture plate	Corning, USA
6 well flat bottom tissue culture plate	Corning, USA

96 well flat bottom black polystyrene microplate	Corning, USA
96 well U bottom clear polystyrene microplate	Corning, USA
96 well V bottom clear polystyrene microplate	Corning, USA
Cell strainer, 70 µm	Miltenyi Biotec, Germany
Cotton tip applicator	Livingstone, Australia
Goat anti-rat IgG magnetic beads	Qiagen, Germany
Lacri-lube lubricating eye gel	Allergen Australia, Australia
Micropore surgical tape	3M, USA
Op-Site Flexigrid	Smith and Nephew, UK
Polypropylene round-bottom FACS tubes (5 ml)	BD Bioscience, USA
Tissue culture flask, T150	Corning, USA
Tissue culture flask, T25	Corning, USA
Tissue culture flask, T75	Corning, USA
Tissue culture petri dish (90 mm)	Greiner Bio-One, Germany
Trans-Blot Turbo Mini 0.2 µm nitrocellulose transfer membrane	Bio-Rad, USA
Transpore surgical tape	3M, USA
Veet	Reckitt Benckiser, UK

2.1.15 Laboratory equipment

Table 2.21 Equipment

Equipment	Supplier
Allegra X-12R Centrifuge	Beckman Coulter, USA
Amersham Imager 600	GE Healthcare Life Sciences, USA
Centrifuge 5424R	Eppendorf, Germany
Dremel (grindstone attachment)	Demel, USA
DynaMag-5 magnet	Thermo Fisher Scientific, USA
EasySep magnet	STEMCELL Technologies, Canada

Electric shaver	Wahl, USA
Finnpipette	Thermo Fisher Scientific, USA
Force Mini Microcentrifuge	Fisher Biotec, Australia
Forceps	Australian Entomological Supplies, Australia
Homogeniser (PT 1200 E)	Polytron, Australia
Inverted microscope CKX31	Olympus Lifescience, Japan
LSRFortessa cell analyser	BD Bioscience, USA
NanoDrop 2000 Spectrophotometer	Thermo Fisher Scientific, USA
Neubauer Improved Brightline haemocytometer	Optik Labor, UK
S@fegrow 188 CO_2 Incubator	EuroCloneBioair, Italy
S@femate 1.2 Vision Class II Biological Safety Cabinet	Laftech, Australia
Scalpel	Livingstone, Australia
Sissors	Australian Entomological Supplies, Australia
SWB24D Digital Water Bath	Stuart
Upright microscope CX23	Olympus Lifescience, Japan
Vortex mixer VM1	Ratek Instruments, Australia
Wallac Wizard 1470	PerkinElmer, USA

2.2 Methods

2.2.1 Cell preparation and tissue culturing

2.2.1.1 Enrichment of gDT-II cells and polyclonal CD4$^+$ T cells

Spleens and lymph nodes from naïve gDT-II, GPR41/GPR43-deficient (*Ffar2*$^{-/-}$; *Ffar3*$^{-/-}$) or B6 mice were harvested into ice cold RP-10 and single cell suspensions were produced by meshing the organs through 70 µm cell strainers. Cells were washed in PBS and resuspended in RBC lysis buffer for 3 minutes. Cells were washed again in PBS supplemented with 2% FCS and 2 mM EDTA (CD4 isolation buffer), then enriched for CD4$^+$ T cells using magnetic beads. Negative enrichment was first performed by incubating the cells on ice for 30 minutes in CD4$^+$ T cell enrichment cocktail consisting of purified rat mAbs anti-F4/80, anti-Mac-1 (M1/70), anti-I-A/E (M5114), anti-GR-1 (RB6-8C5), anti-erythrocyte (TER-119) and anti-CD8 (53-6.7). After washing in isolation buffer, cells were incubated for 20 minutes on a roller at 4 °C with 6 mL pre-washed goat anti-rat IgG-coupled magnetic beads (approximately 8 beads per cell). Bead-bound cells were removed using a magnetic column and the supernatant containing CD4$^+$ T cells was collected for positive enrichment. For positive enrichment, cells were incubated with anti-CD4 (Dynabeads Flowcomp mouse CD4 kit) for 15 minutes on ice. Dynabeads were added and the mixture was incubated for 20 minutes on a roller at 4 °C. Bead-bound cells were collected using a magnetic column and resuspended in release buffer for incubation on a roller for 20 minutes at room temperature. The suspension was placed on a magnetic column, and the supernatant containing the released cells was collected according to the manufacturer's instructions.

2.2.1.2 Activation of gDT-II cells

For activation with peptide-pulsed splenocytes, naïve B6 splenocytes were pulsed with 5 µM $gD_{315\text{-}327}$ peptide for 45 minutes in a 37 °C water bath. gDT-II cells were enriched from lymph nodes and the spleen as described previously, and co-cultured with pulsed B6 splenocytes in RPMI-1640 media supplemented with 10% FCS, 5 mM HEPES, 2 mM L-glutamine, 50 U/ml penicillin, 100 mg/mL streptomycin and 0.05 mM 2-ME (RP-10) with 0.15 mg/mL LPS. In certain experiments, gDT-II cells were polarised into Th1 cells by the addition of 20 ng/mL IL-12 and 10 µg/mL IL-4 blocking antibody into culture media on the day of activation.

gDT-II cells were cultured in RP-10. Cells in T75 flasks were split daily with 20 mL RP-10 and supplemented with 12.5 U/mL human recombinant IL-2, starting from day 2 post-activation. Cells were maintained for 6 days in an incubator at 37 °C, 6.5% CO_2.

2.2.1.3 Activation of polyclonal $CD4^+$ T cells

For the polyclonal activation of $CD4^+$ T cells, 0.5 mL PBS containing anti-CD3ε (5 mg/mL) and anti-CD28 (5 mg/mL) was incubated in 24 well plates overnight at 4 °C, protected from light. Wells were washed twice with PBS. $CD4^+$ T cells were enriched for, as described in Section 2.2.1.2. Enriched cells were seeded into wells with plate-bound anti-CD3ε and anti-CD28 at a concentration of $1 – 2 \times 10^6$ cells/mL RP-10. $CD4^+$ T cells were split daily with 1 mL RP-10 and supplemented with 12.5 U/mL human recombinant IL-2, starting from day 2 post-activation. Cells were kept in a 6.5% CO_2 incubator at 37 °C.

2.2.1.4 Activation of gBT-I cells

Spleens from naïve gBT-I mice were harvested to and meshed through 70 µm cell strainers to produce single cell suspensions. Naïve B6 splenocytes were pulsed with $gB_{498-505}$ peptide for 45 minutes in a 37 °C water bath. For activation with peptide-pulsed splenocytes, gBT-I cells were co-cultured with pulsed splenocytes at an approximate ratio of 1:1 in RP-10 with 0.15 mg/mL LPS. Cells in T75 flasks were split daily with 20 mL RP-10 and supplemented with 12.5 U/mL human recombinant IL-2, starting from day 2 post-activation. Cells were kept in a 6.5% CO_2 incubator at 37 °C.

2.2.1.5 B16 cell passaging

B16.gB and B16.gD melanoma cell lines were cultured in RP-10. Every 2 to 3 days, supernatant was aspirated and cells were washed gently with 5 mL PBS. Cells were dislodged from the T175 flask using 1X trypsin and split in RP-10. Flasks were placed lying down in a 6.5% CO_2 incubator at 37 °C.

2.2.1.6 SCFA treatment of T cells

Sodium butyrate, sodium propionate, and sodium acetate were dissolved in PBS and filter-sterilised. T cells were treated with 0.5 mM SCFAs or at the concentrations

otherwise stated, starting on day 2 (for adoptive transfer experiments) or day 3 (for *in vitro* analysis) post-activation.

2.2.1.7 Trichostatin A treatment of T cells

In certain experiments, $CD4^+$ T cells were treated with pan-histone deacetylase inhibitor TSA. TSA was prepared as per manufacturer's instructions, and further diluted in PBS for a final concentration of 5 nM to 15 nM.

2.2.1.8 FoxO1 inhibitor treatment of T cells

In certain experiments, the transcription factor FoxO1 was inhibited in $CD4^+$ T cells using AS1842856. AS1842856 was prepared according to the manufacturer's instructions and further diluted in PBS for a final concentration of 0.1 to 1 µM.

2.2.2 Generation of CAR T cells

2.2.2.1 Murine anti-HER2 CAR T cells

For activation, naïve splenocytes from B6 mice were treated with red cell lysis buffer and resuspended in RP-10 containing anti-CD3ε (0.5 mg/mL), anti-CD28 (0.5 mg/mL), IL-2 (100 U/mL) and IL-7 (200 pg/mL). Cells were cultured at a concentration of 5×10^6 cells/mL in 6 well flat bottom tissue culture plates at 37 °C, 5% CO_2 for 24 hours.

T cells were harvested from plates and centrifuged once in PBS. The cells were resuspended in 20 – 30 mL RP-10 and gently laid over 15 mL Ficoll-plaque Plus, followed by centrifugation at 1400 RPM for 10 minutes with acceleration 3, deceleration 3. T cells suspended in the interface were collected. To remove any remaining Ficoll-plaque, the collected cells were centrifuged twice in media. RetroNectin (10 µg/ml) was prepared by plating 1.5 mL RetroNectin (10 µg/mL) diluted in PBS in 6 well non-tissue culture treated plates, followed by overnight incubation at 4 °C.

To prepare for viral transduction, the GP+E-86-LXSN/anti-HER2 scFv-CD28-CD3ζ packaging line was seeded in T75 flasks at $5 – 6 \times 10^6$ cells/mL in RP-10 for an overnight incubation at 37 °C, 5% CO_2. Viral supernatant was collected. To adhere

the virus to RetroNectin-treated plates, unbound RetroNectin was removed from wells and replaced with 4 mL of filtered viral supernatant. Plates were centrifuged at 1200 x g for 30 mins at room temperature with acceleration 4, deceleration 3. T cells were resuspended at 7 – 10 $\times$ 10^6 cells/mL in remaining viral supernatant. 100 U/mL IL-2 and 200 pg/mL IL-7 were added to the cell suspension. An additional 1 mL viral supernatant containing T cells was added to each RetroNectin well, and plates were again centrifuged at 1200 x g for 90 minutes at room temperature with acceleration 4, deceleration 3. Cells were incubated overnight at 37°C, 5% CO_2.

The transduction process was repeated by collecting T cells from RetroNectin plates and centrifuging the plates with 4 mL fresh viral supernatant per well. T cells were centrifuged separately and resuspended in fresh viral supernatant containing IL-2 and IL-7. 1 mL cell suspension per well was transferred into RetroNectin plates, which were centrifuged and incubated at 37°C, 5% CO_2 for a minimum of 3 hours. T cells were collected and centrifuged in PBS. Cells were resuspended in RP-10 containing IL-2 and IL-7 to be incubated in 6 well tissue culture-treated plates at 37 °C, 5% CO_2. CAR T cells were treated with 0.5 mM butyrate on the following 2 days (day 3 and day 4 post-activation). On day 4, cells were split 1:2 with IL-2 and IL-7 added to fresh RP-10. CAR T cells were harvested on day 5.

2.2.2.2 Human anti-LeY CAR T cells

This study was approved by the PMCC Ethics Committee (ethics number E671). Peripheral blood from healthy donors was diluted with an equal volume of PBS. 30 mL of diluted blood was slowly pipetted into a Falcon tube containing 15 minutes of Ficoll-plaque Plus. Samples were centrifuged for 10 minutes at 1000 x g. PBMCs were collected into PBS and centrifuged at 1800 RPM for 7 minutes. Cells were treated with 10 mL ACK lysis buffer, then washed once with RPMI and twice with PBS, followed by enumeration. 50 $\times$ 10^6 cells were cultured in RP-10 containing 600 U/mL IL-2 and 30 ng/mL anti-CD3 (OKT3). Cells were incubated for 2 days at 37 °C, 5% CO_2.

RetroNectin was prepared by plating 1.5 mL RetroNectin (10 µg/mL) diluted in PBS in 6 well non-tissue culture treated plates, followed by overnight incubation at

4 °C. 2 days after T cell activation, RetroNectin was removed from plates, wells were washed with PBS. The packaging line PG13/anti-LeY scFv-CD28-CD3ζ was seeded 2 days prior in T75 flasks at 1.5 × 10^6 cells/mL in RP-10 and incubated at 37 °C, 5% CO_2. Viral supernatant was collected, and 4 mL of retroviral supernatant was added per well. The plates were centrifuged at 1000 x g for 1 hour at room temperature with acceleration 5, deceleration 5. T cells were washed and resuspended in viral supernatant at a concentration of 2.5 x 10^6 T cells/mL, supplemented with IL-2. 1 mL of cells resuspended in viral supernatant was added to each well. The final concentration of IL-2 was 600 U/mL. The plates were centrifuged at 1000 x g for 1 hour at room temperature with acceleration 5, deceleration 5, followed by an overnight incubation at 37 °C, 5% CO_2. This process was repeated the next day, with 300 U/mL IL-2 supplemented. Cells were treated with 0.5 mM butyrate on the following 2 days (day 4 to 6 post-activation). Cells were split 1:2 and supplemented with a final concentration of 150 U/mL IL-2 on days 5 and 6 post-activation. Analysis was performed 7 days after activation.

2.2.3 Manipulation of mice

2.2.3.1 HSV-1 infections

2×10^5 plaque-forming units (PFU) of HSV-1 KOS in 200 µL PBS were injected intravenously (i.v.) into the lateral tail vein. Alternatively, for epicutaneous (e.c.) infection with HSV-1 KOS, mice were anesthetised with a mixture of ketamine (100 mg/kg bodyweight) and xylazine (15 mg/kg bodyweight) via intraperitoneal (i.p.) injection. Lubricating eye gel was applied to prevent eyes from drying. The left flank of the mouse was shaved, followed by depilation for 2 to 3 minutes using Veet hair removal cream. The skin was wiped with a tissue moistened with water to remove Veet. A dremel rotary tool with grindstone attachment was used to lightly abrade the skin for 5 seconds on setting 2. The abrasion site was cleaned firstly with a cotton topped applicator soaked in sterile PBS, then a dry cotton topped applicator. 1 × 10^6 PFU HSV-1 in 10 µL PBS was applied to the abrasion site. A transparent waterproof film (Op-Site Flexigrid) was used to cover the infected flank, and mice were bandaged with Micropore and Transpore surgical tape. Films and bandages were removed after 2 days. In experiments assessing DC maturation, e.c. infections on both the left and right flank of mice were performed.

2.2.3.2 Mammary fat pad inoculations of E0771-HER2 cells

An orthotopic model of breast cancer was used, where 1×10^5 E0771-HER2 cells resuspended in 20 µL PBS was injected into the fourth mammary fat pad of female C57BL/6 hHER2 mice. Tumours were measured with a digital calliper. Tumour volume was calculated as the following: (width × length)/2. Mice were culled when the tumour area exceeded 150 mm^2.

2.2.3.3 Adoptive gDT-II cell transfers

On day 6 post-activation, viable activated gDT-II cells were enumerated using a haemocytometer with trypan blue exclusion. FACS analysis was performed to ensure that purity of gDT-II cells ($Va3.2^+CD45.1^+CD4^+$) was at least 85% and cells were activated ($CD44^+$). 1×10^6 gDT-II cells were adoptively transferred into recipients in 200 µL PBS via i.v. injection into the lateral tail vein.

2.2.3.4 Adoptive gBT-I cell transfers

Skin-draining lymph nodes were harvested, and single cell suspensions were prepared by meshing the lymph nodes through a 70 µm cell strainer. Cells were washed in PBS and centrifuged at 1600 RPM for 5 minutes. For the transfer of naïve gBT-I cells, viable gBT-I cells were resuspended in PBS and enumerated using a haemocytometer with trypan blue exclusion. FACS analysis was performed to ensure that the purity of cells ($Va2^+CD8^+$) from lymph nodes was at least 60% and cells were naïve ($CD44^-$). 5×10^4 naïve gBT-I cells were adoptively transferred into naïve recipients. In the case of co-transfers, 2.5×10^5 of each type of gBT-I cells was transferred in 200 µL PBS via i.v. injection into the lateral tail vein.

2.2.3.5 CAR T cell transfers

7 days after E0771-HER2 tumour inoculation, mice were subjected to full-body irradiation (5 Gy) for pre-conditioning. 2 doses of 1×10^7 anti-HER2 CAR T cells were transferred into the lateral tail vein of mice via i.v. infection, 5 and 6 days after inoculation. On days 0 to 5 post-T cell transfer, 5×10^4 IU IL-2 was injected (i.v.) into the lateral tail vein to support CAR T cell maintenance.

2.2.3.6 Immune checkpoint blockade therapy

For immune checkpoint blockade therapy, E0771-HER2 tumour-bearing mice were treated with either 200 µg anti-PD-1 (RMP1-14) or an isotype control (2A3; i.p.) on days 0 and 4 post-CAR T cell transfer.

2.2.4 Preparation of mouse tissues for flow cytometric analyses

2.2.4.1 Blood

The submandibular vein of the restrained mouse was punctured with a 21G needle. Approximately 50 µL blood from the vein was passed through a heparinised capillary tube to prevent clotting. Blood was treated with 1 mL RBCL buffer twice for 5 minutes and washed once with FACS buffer. The full sample was stained for FACS analysis as described in Section 2.2.5.

2.2.4.2 Spleens, axillary and brachial lymph nodes

For T cell analysis, organs were harvested into cold RP-10 and single cell suspensions were generated by pressing the organs through a 70 µm filter, followed by washing in PBS. Approximately 2.5% of the spleen or 50% of the lymph node was stained for FACS analysis as described in Section 2.2.5.

In experiments analysing *ex vivo* dendritic cells, the draining axillary and brachial lymph nodes of mice that were infected with HSV-1 via e.c. route were harvested separately into 6 mL sterile KDS-RPMI supplemented with 2% FCS (KDS-RPMI-2). Lymph nodes were vigorously dissociated with a scalpel in a petri dish, then the emulsified tissue was returned to their original tube. 1 mL of digestion solution (containing 7 mg/mL Collagenase III and 1 mg/mL DNase I in KDS-RPMI-2) was added to each tube. Tissues were resuspended using a Pasteur pipette for 20 minutes. 700 µL EDTA (0.1 M) was added before resuspending for 5 minutes. Samples were filtered through 30 µm nylon meshes, then enumerated. Approximately 5×10^6 cells were stained per sample.

2.2.4.3 Skins

For endogenous T cell analysis, 2 cm $\times$ 0.5 cm skin was harvested directly into 1.5 mL of liberase solution (0.5 mg/mL Liberase TL Research Grade and 10 µg/mL

DNase I in HBSS), followed by incubation in a 37 °C water bath for 30 minutes. The epidermal and dermal layer were separated using forceps, then returned to the liberase solution that they were originally in. Skins were finely cut for 2 minutes and incubated in a 37 °C water bath for 60 minutes. After digestion, samples were then transferred into RP-10, homogenised by resuspending 20 times with a transfer pipette, then filtered using 70 µm nylon meshes. Samples were stained as described in Section 2.2.5. Samples were filtered through 30 µm nylon meshes before flow cytometric analysis.

For analysis of adoptively transferred T cells, 2 cm x 0.5 cm skin was harvested directly into dispase solution (2.5 mg/mL Dispase II in PBS) and incubated for 90 minutes in a 37 °C water bath. The epidermal and dermal layer were separated using forceps, then the epidermal layer was transferred into 1 mL collagenase solution (3 mg/mL Collagenase Type III in RPMI media containing 2% FCS and 5% SC) and dermal layer into 1 mL trypsin solution (0.5% trypsin with 0.2% EDTA and 2 mg/mL DNase in PBS). The epidermal layer was finely cut for 2 minutes and both layers were incubated in a 37°C water bath for 30 minutes. After digestion, both the epidermal and dermal layers were transferred together into RP-10, homogenised by resuspending 20 times with a transfer pipette, then filtered using 70 µm nylon meshes. Samples were either divided into half or stained whole as described in Section 2.2.5. Samples were filtered through 30 µm nylon meshes before flow cytometric analysis.

2.2.5 Flow cytometry

2.2.5.1 Staining of surface markers

Single cell suspensions were stained with antibodies against specific markers diluted in 50 – 100 µL FACS buffer or PBS (in cases when fixable viability dyes were included). 50 µL or 100 µL of antibody cocktail was used for samples containing fewer or greater than 5×10^6 cells respectively. Samples were incubated on ice for at least 20 minutes. Chemokine receptors were stained for at least 1 hour on ice. Staining with tetramers was performed for 45 minutes in a 37 °C incubator. Cells were washed in FACS buffer. Cells derived from skins were filtered through 30 µm nylon meshes, while 70 µm nylon meshes were used for cells from other organs. Live dead discrimination was performed using LIVE/DEAD Fixable Near-IR stain during staining with antibodies

or by the addition of 1 µg/mL PI to cells immediately before acquisition. For cell enumeration, a known number of SPHERO Blank Calibration Particles was added to samples before analysis. Samples were run on an LSRFortessa (BD Biosciences) and analysed using FlowJo 10 software.

2.2.5.2 Intracellular and intranuclear marker staining

Cells were stained for surface markers, as detailed above, followed by fixation and permeabilisation using a Fixation/Permeabilization kit for intracellular cytokine analysis or Foxp3/Transcription Factor Staining kit for intranuclear marker analysis, according to the manufacturer's instructions. Blocking with anti-rat and anti-mouse serum was performed in permeabilization buffer prior to intranuclear staining for at least 1 hour on ice, or simultaneously with intracellular staining. Samples were incubated with antibodies against intracellular/intranuclear markers overnight in the dark. For anti-histone antibodies, the incubation was performed for 20 minutes at room temperature. Cells were washed in FACS buffer, filtered through 70 µm nylon meshes, and analysed.

2.2.5.3 Metabolic analyses

$0.4 – 1 \times 10^6$ cells were resuspended in PBS containing antibodies to surface markers, as well as the metabolic probes TMRM and Mitotracker. Samples were incubated in a 37 °C incubator for 15 – 30 minutes. Cells were washed twice in FACS buffer, filtered through 70 µm nylon meshes, and stained with either 1 µg/mL PI or 5 µg/mL DAPI. Flow cytometric analysis was performed within 40 minutes of staining.

2.2.5.4 Fluorescence activated cell sorting

Thymi from 6 week-old naïve B6 and GPR41/GPR43-deficient mice were harvested into ice cold RP-10. Single cell suspensions were generated by meshing the thymi through 70 µm filters. Cells were stained for CD3, CD4, and CD8, washed twice, and filtered through 70 µm nylon meshes. Cell sorting was performed using a FACS Aria III. Dead cells were excluded using staining with 1 µg/mL PI. $CD4^-CD8^-$, $CD4^+CD8^+$, and $CD4^-CD8^+$ and $CD8^+CD4^-$ single positive populations were collected into sterile FCS.

2.2.6 Functional assays

2.2.6.1 Assessment of cytokine and cytotoxic mediator expression

Cytokine and cytotoxic mediator expression was measured after *ex vivo* re-stimulation. Cells were resuspended in 200 µL RP-10 containing 10 µg/mL BFA. gBT-I cells were restimulated with 1 µg/mL $gB_{498-505}$ peptide, while gDT-II cells and polyclonal $CD4^+$ T cells were restimulated with either 5 µM $gD_{290-302}$ peptide or 0.5 µg/mL PMA and 1 mg/mL ionomycin for 5 hours in a 37 °C incubator. Cytotoxic molecules were measured after re-stimulation as newly synthesised molecules have been shown to contribute to killing [281].

2.2.6.2 Chromium-51 release assays

Effector:target cell ratios of 40:1 to 0.31:1 were prepared in triplicates in a 96 well V bottom plate by performing serial dilutions to arrive at 4×10^5 to 3.125×10^3 CAR T cells (effector cells) in 100 µL RP-10 per well. The supernatant of a cell pellet containing 3×10^6 E0771-HER2 (target cells) was aspirated, and target cells were labelled with 100 µCi Chromium-51 for 1 hour at 37 °C in an incubator with lead shield, then washed thrice with 10 mL RPMI without additives. 1×10^4 labelled E0771-HER2 cells in 100 µL RP-10 were seeded into each well containing effector cells. As controls, some wells lacked effector cells and consisted of only untreated target cells or target cells lysed with 100 µL SDS. The plate was pulsed at 1400 RPM for 1 minute, then incubated at 37 °C for 4 hours.

To analyse Chrominum-51 release into the supernatant, the plate was centrifuged at 1400 RPM for 4 minutes. 100 µL supernatant was transferred into FACS tubes for chromium release analysis using the Wallac Wizard 1470. Spontaneous release and maximum release were calculated from wells containing untreated target cells and SDS-lysed target cells respectively. Percentage of specific lysis was calculated as follows: [(Experimental Release – Spontaneous Release)/(Maximum Release – Spontaneous Release)] × 100%.

2.2.6.3 Real-time PI incorporation assays

B16.gD cells were resuspended in RP-10 at 5×10^4 cells/mL, and divided into 2 samples, with only the first containing 100 U/mL recombinant IFN-γ for MHC-II

upregulation. 200 µL cells/well were carefully seeded into a 96 well flat bottom black polystyrene microplate and incubated for 2.5 days at 37 °C, 5% CO_2.

gDT-II cells were resuspended at 1.25 × 10^6 cells/mL in RP-10 containing 6.02 µg/mL PI. In certain experiments, gDT-II cells were resuspended in media containing 10 µg/mL anti-IFN-γ or 2 µg/mL anti-FasL blocking antibodies, and incubated at 37 °C for 30 minutes prior to co-culture. B16.gD cells were gently washed twice with warmed RP-10. For an effector cell to target cell (E:T) ratio of 12:1, 2.5 × 10^5 gDT-II cells in a volume of 200 uL were seeded into each well. Positive controls containing B16.gD cells resuspended in 0.5% Triton X-100 and PI, and negative control containing either B16.gD only or gDT-II cells only in RP-10/PI mix were prepared. To monitor cell death, PI signal of the co-culture was measured on the CLARIOstar Plus for 24 hours at 37 °C, 5.6% CO_2, using the 'Florescence' setting. Cell death was calculated by deducting the fluorescence of co-cultured samples containing B16.gD cells that lacked IFN-γ pre-treatment from matched samples with IFN-γ pre-treated B16.gD cells. Cell dealth was normalised to co-cultures containing tumour cells and untreated gDT-II cells.

2.2.6.4 HSV-1 PFU assays

Vero cells were cultured in 5 mL MEM-10 in petri dishes and passaged every 1 to 5 days. When passaging, supernatant was aspirated and cells were washed gently with 5 mL PBS. Cells were incubated with 1X trypsin for 3 minutes in an incubator at 37 °C. The reaction was quenched by the addition of 9 mL MEM-10. Cells were split by transferring an appropriate volume to a fresh petri dish, and made up to 5 mL with MEM-10. Vero cells were kept in a 6.5% CO_2 incubator at 37 °C. 3 to 4 days before the PFU assay, the cells were dislodged and transferred from the petri dish sterile 6 well flat-bottomed plates.

2 cm × 0.5 cm skin from mice infected with HSV-1 (e.c.) was collected into 1 mL sterile PBS. Skins were stored at -80 °C until further use. Thawed samples were homogenised for 30 seconds using a homogeniser to liberate the virus from the skin. Between samples, the aggregate was cleaned by running it in sodium hypochlorite, ethanol, and 2 tubes of sterile PBS.

Viral dilutions (½, 10^{-1}, 10^{-2}, 10^{-3}, 10^{-4} and 10^{-5}) were prepared in serum-free MEM and 900 µL of each dilution was transferred into a well of a 6 well plate containing a confluent monolayer of Vero cells that had been pre-washed with MEM to remove FCS. Plates were incubated for 1 hour at room temperature with occasional shaking to increase the probability of virus attaching to cells. 1% agarose in MEM supplemented with 2% FCS was prepared and maintained at 37 °C in a water bath. 3 mL of 1% agarose solution was added to each well and allowed to set at room temperature. Plates were incubated in a 37 °C incubator for 4 days.

Each well was incubated with 4 mL of 10% formalin for 1 hour at room temperature to fix the Vero cells and virus. 2 mL of 0.1% Toluidine blue in water was added to each well and incubated for 1 minute. The Toluidine blue solution was poured off and wells were rinsed with tap water. Plaques resulting from lytic infection by HSV-1 were enumerated.

2.2.7 Molecular biology methods

2.2.7.1 RT-qPCR

To extract RNA for the analysis of the expression of *Ffar2*, *Ffar3*, and *Hcar2*, 2×10^6 cells were lysed with 400 µL TRIzol for 5 minutes at room temperature. Samples were stored at -80 °C until use. For RT-qPCR, RNA extraction was performed with the Direct-zol RNA MicroPrep kit according to the manufacturer's instructions. Briefly, RNA from cells lysed in TRIzol was precipitated with 100% ethanol and centrifuged in Zymo-Spin columns at 14000 x g, 10 °C for 1.5 minutes. Columns were washed with 400 µL RNA wash buffer and centrifuged. DNA was digested by incubating 40 µL DNase I cocktail (5 U DNase I in DNA digestion buffer) in each column for 15 minutes at 35 °C, then centrifuging for 1.5 minutes. Columns were washed twice with 400 µL pre-wash buffer and once with 700 µL RNA wash buffer. Remaining buffer was removed by centrifugating twice. For RNA elution, 15 µL DNase/RNase-free water was incubated in the columns for 7 minutes at room temperature, followed by centrifugation. This step was performed twice. RNA quantification was performed using the NanoDrop 2000.

Complementary DNA (cDNA) was synthesised from extracted RNA using the Omniscript RT kit. A maximum of 2 µg of each sample was resuspended in 8.5 µL of cDNA synthesis mix (Table 2.22), and incubated for 90 minutes at 37 °C. cDNA was diluted in RNase/DNase-free water to derive a final concentration of 2.5 ng/µL.

Table 2.22 Components of cDNA synthesis mix.

Reagent in cDNA synthesis mix	Volume
Reverse transcription 10X Buffer	3.5 µL
dNTP mix (5 mM per dNTP)	2 µL
Oligo(dT)15 primers	1 µL (Final concentration = 0.5 µg/µL)
RNase-OUT Recombinant Ribonuclease Inhibitor	1 µL (Final concentration = 10 U/µL)
Omniscript Reverse Transcriptase	1 µL (Final concentration = 4 U/µL)
Total volume	15 µL

Taqman Universal PCR Master Mix and primers for genes of interest were added to the template cDNA. To obtain a final volume of 10 µL, water was added. The components and volumes in the qPCR mix are listed in Table 2.23.

Table 2.23 Components of qPCR mix.

Reagent	Volume
Taqman Universal PCR Master Mix	5 µL
Template cDNA	2 µL (Final concentration = 2.5 µg/mL)
Primer	0.5 µL/primer (Final concentration = 10 µM)
H_2O	Remaining volume
Total volume	10 µL

RT-qPCR was performed on the QuantStudio Real-Time PCR machine with the following cycle conditions: 95 °C for 2 minutes, 40 cycles at 95 °C for 15 seconds, and 60 °C for 1 minute. Messenger ribonucleic acid (mRNA) expression was normalised to the housekeeping genes *β2m* and *Gapdh*. The relative expression of genes was calculated using the following formula: $2^{-(CT_{sample} - CT_{average\ of\ housekeeping\ genes})}$.

2.2.7.2 Western blotting

For protein extraction, 1 × 10^6 activated gDT-II cells were washed twice in DPBS. Cells were resuspended in 50 µL RIPA buffer mix containing RIPA buffer, PhosSTOP and Complete Protease Inhibitor Cocktail. The cell suspension was incubated for 30 minutes under constant rotation at 4 °C, mixed briefly by vortexing, then centrifuged at 8000 x g for 10 minutes. Supernatants containing proteins were collected and stored at -80 °C until further use.

50 µL of sample lysates were mixed with 10 µL of 6X sample buffer and boiled at 90 °C for 5 minutes. 35 µL cooled sample lysates and 10 µL protein ladder were loaded onto NuPAGE gel that was immersed in running buffer. A 150 V current was applied for approximately 1 hour. Proteins were transferred onto a Trans-Blot Turbo Mini 0.2 µm nitrocellulose transfer membrane using the Trans-Blot Turbo Transfer System. The membrane was placed in a Falcon tube of 20 mL blocking solution (containing TBS if acetylation was probed for, or otherwise PBS). Blocking was performed by incubating the membrane on a roller at room temperature for 30 minutes. The blocking solution was replaced with 6 mL of blocking solution containing primary antibodies, and incubated rolling overnight at 4 °C. Samples were washed rolling four times in 20 mL of 0.1% Tween-20 PBS/TBS for 5 minutes. The final wash was performed in 1X PBS/TBS. The membrane was incubated with 3 mL developing solution consisting of a 1:1 ratio of developer and substrate from Invitrogen novex ECL Chemiluminescent Substrate Reagent Kit for 1 minute. Analysis was performed with the Amersham Imager 600.

2.2.8 Statistical analysis

Statistical analysis was performed using Graphpad Prism 9. P values were calculated using Student's *t*-tests, ANOVA tests or log-rank (Mantel-Cox) tests, as indicated in figure legends. Statistical significance was achieved when p values were less than 0.05. Significance values were denoted as * $p < 0.05$, ** $p < 0.01$, *** $p < 0.001$, **** $p < 0.0001$. Statistical analysis was performed only when data was collected from at least 2 independent experiments and $n \geq 2$.

Chapter 3:

Characterising the role of GPR41 and GPR43 in $CD8^+$ T cell priming

Chapter 3 Characterising the role of GPR41 and GPR43 expression in $CD8^+$ T cell priming

3.1 Introduction

$CD8^+$ T cells play central roles in the control of intracellular infections and tumour surveillance by contributing to the elimination of infected or malignant cells. To gain effector functions, which includes the capacity to kill altered cells, naïve $CD8^+$ T cells require priming by DCs. This is facilitated upon TCR-mediated recognition of specific antigens displayed as MHC-peptide complexes (signal 1), co-stimulatory molecule binding (signal 2), and cytokine signalling (signal 3). Such T cell priming prompts substantial phenotypic and metabolic changes that shape the effector T cell response.

In recent years, it has become apparent that T cell priming can furthermore be influenced by the microbiota and their metabolic derivatives [204, 234, 235, 282]. Interestingly, changes in T cell function induced by the gut microbiota extend beyond the gut microbiota-host interface to more distal compartments [245, 248], suggesting that some of the effects are likely induced via microbiota-derived molecules that can distribute throughout the body. A significant group of such metabolites are SCFAs which have been shown to promote $CD8^+$ T cell cytokine production [31, 181]. SCFAs have not only been implicated as metabolic substrates and epigenetic regulators of T cells, but also as ligands of the G-protein coupled receptors GPR41 and GPR43. To date, GPR41 and GPR43 have been suggested to regulate the immune response in several diseases and disorders, such as intracellular infections, inflammation, obesity and autoimmunity [31, 181, 283-286]. However, the influence of SCFAs through GPR41/43 interactions on specific immune cell types, such as $CD8^+$ T cells, is less well understood. Hence, in this chapter we analysed the role of GPR41 and GPR43 in $CD8^+$ T cell priming.

We chose an epicutanous HSV-1 infection model, due to the fact that $CD8^+$ T cells play a crucial role in the immune response against HSV-1 infection [287-289]. T

cell priming following HSV-1 is not only characterised by clonal expansion and the resulting quantitative changes in cell numbers, but also induces significant qualitive adaptations that are often referred to as differentiation. In the case of $CD8^+$ T cells, this typically involves the activation of naïve T cells into EECs, which subsequently differentiate into MPECs and SLECs [29]. Both MPECs and SLECs are subsets of effector cells that are formed upon primary antigen encounter. Importantly, it is mainly the MPECs that survive the contraction phase of the response and form memory cells [290].

Our previous work explored the link between microbiota-derived SCFAs and secondary $CD8^+$ T cell responses following HSV-1 challenge [31]. In this setting, GPR41/GPR43-deficient $CD8^+$ T cells were impaired in their expansion and exhibited reduced IFN-γ production relative to their WT counterparts shown in mixed-bone marrow (BM) chimeric mice [31]. In line with this, microbiota and SCFAs enhanced secondary T cell responses and skewed T cell differentiation towards MPECs. As GPR41 and GPR43 ensured optimal secondary responses, and microbiota and SCFAs promoted MPECs, we hypothesised that these receptors potentially influenced $CD8^+$ T cell priming *in vivo*. The role of GPR41 and GPR43 in $CD8^+$ T cell priming has only been described in a study that did not examine T cell differentiation [181]. It would thus be interesting to consider the dependency of $CD8^+$ T cell differentiation and function on SCFA signalling by GPR41 and GPR43 during primary HSV-1 infection.

In this chapter, we aimed to investigate if GPR41 and GPR43 signalling mediated changes in $CD8^+$ T cell differentiation and function during priming upon HSV-1 infection, as well as their effect on viral control. As T cell priming is influenced by signals from other cells, we further analysed whether receptor signalling mediated changes in a $CD8^+$ T cell intrinsic or extrinsic manner.

3.2 Results

3.2.1 T cells express low levels of *Ffar2* and *Ffar3*

To analyse if GPR41 (*Ffar3*) and GPR43 (*Ffar2*) are expressed by $CD8^+$ T cells, we used RT-qPCR to detect gene expression. We focused on *Ffar2* and *Ffar3* mRNA levels at various differentiation stages of $CD8^+$ T cells, including T cells in activated and developing (thymocyte) stages. During thymic development, $CD4^-CD8^-$ precursors expressing pre-TCRs progress to the $CD4^+CD8^+TCR^+$ stage, followed by maturation into either $CD4^+CD8^-TCR^+$ or $CD4^-CD8^+TCR^+$ cells that enter the circulation. To assess whether T cells expressed GPR41/43 during thymic development, we sorted $CD4^+CD8^-$, $CD4^-CD8^+$, $CD4^-CD8^-$, and $CD4^+CD8^+$ cells from thymi of WT and GPR41/GPR43-deficient mice, and measured *Ffar2* and *Ffar3* gene expression. $CD11b^+$ DCs were used as a positive control for *Ffar*2 and *Ffar3* detection as DCs have been shown to express these genes [184, 185, 291]. GPR41/GPR43-deficient thymocytes served as a background control. *Ffar2* expression levels in WT $CD4^+CD8^-$, $CD4^-CD8^+$ and $CD4^-CD8^-$ thymocytes were more than 100 times lower than in $CD11b^+$ DCs (Figure 3.1A), confirming previous published data. While $CD4^+CD8^-$ and $CD4^-CD8^-$ thymocytes expressed comparable levels of *Ffar2*, expression in $CD4^-CD8^+$ cells was lower. *Ffar2* expression was not observed in WT $CD4^+CD8^+$ cells. In contrast to *Ffar2* expression, *Ffar3* expression was undetectable at all stages of T cell thymic development (Figure 3.1A). In summary, while thymocytes did not appear to express *Ffar2* at an intermediate stage of thymic development ($CD4^+CD8^+$), *Ffar2* was detectable at the earlier ($CD4^-CD8^-$) and later ($CD4^+CD8^-$ and $CD4^-CD8^+$) stages.

The analysis of *Ffar2* and *Ffar3* expression on activated $CD8^+$ T cells was performed using MHC-I-restricted transgenic $CD8^+$ T cells that are specific to the HSV-1 glycoprotein B, $gB_{498\text{-}505}$ (gBT-I cells), that were isolated from spleens and lymph nodes, followed by *in vitro* activation with splenocytes that had been pulsed with the $gB_{498\text{-}505}$ antigen. We pre-treated the cells with butyrate for 2 days to investigate if SCFAs exposure alters the receptor expression through feedback loops. *In vitro* activated WT $CD8^+$ T cells expressed *Ffar2* at low but detectable levels, with butyrate pre-treatment doubling the expression (Figure 3.1B). This suggested *Ffar2* was upregulated by butyrate. *Ffar3* was detected in activated WT $CD8^+$ T cells, but its

expression was reduced in butyrate-pre-treated cells (Figure 3.1B). Altogether, these data demonstrated that *Ffar2* and *Ffar3* are expressed by activated $CD8^+$ T cells derived from the secondary lymphoid organs, and their expression may be regulated by butyrate.

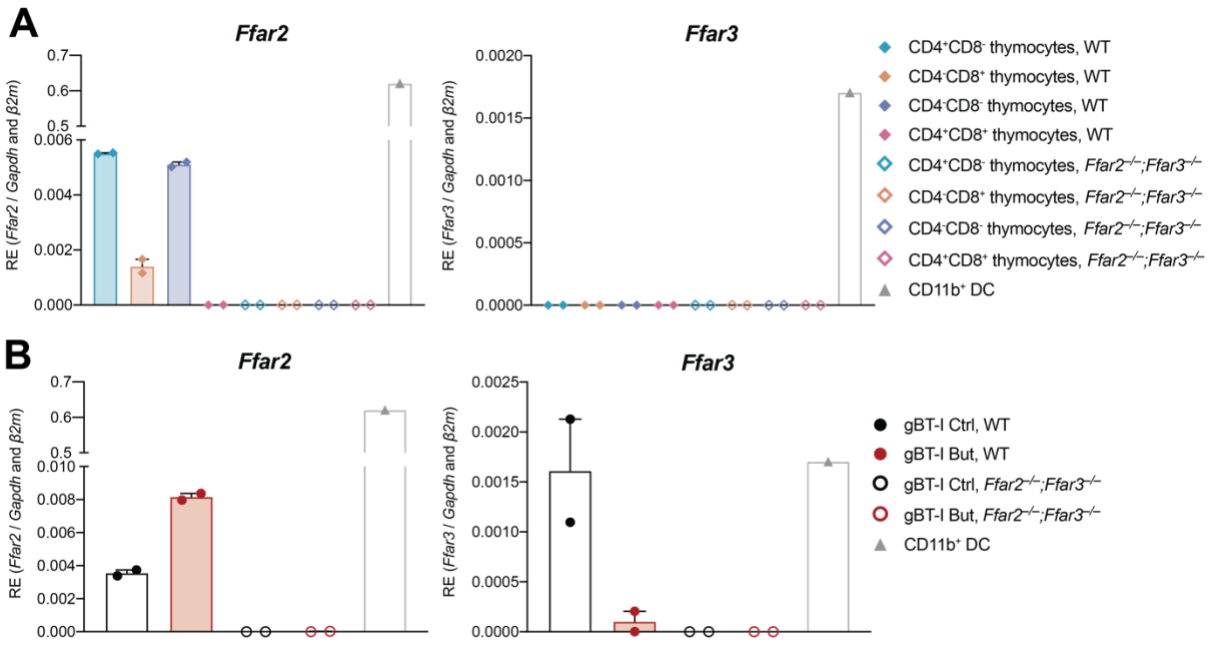

Figure 3.1 *Ffar2* and *Ffar3* are co-expressed on activated CD8⁺ T cells.

Ffar2 and *Ffar3* expression in T cells and primary CD11b⁺ dendritic cells (DC) were analysed using real-time quantitative polymerase chain reaction (RT-qPCR). The relative expression (RE) of *Ffar2* and *Ffar3* to *Gapdh* and *β2m* is shown. **(A)** $CD4^{-}CD8^{-}$, $CD4^{+}CD8^{-}$, $CD4^{-}CD8^{+}$, $CD4^{+}CD8^{+}$ thymocytes were sorted from wildtype (WT) and $Ffar2^{-/-};Ffar3^{-/-}$ mice. **(B)** Transgenic $CD8^{+}$ T cells (gBT-I) that recognise the HSV-1 peptide glycoprotein B ($gB_{498\text{-}505}$) from WT and $Ffar2^{-/-};Ffar3^{-/-}$ mice were activated *in vitro* by $gB_{498\text{-}505}$-pulsed splenocytes. Cells either remained untreated or were treated with 0.5 mM butyrate on days 2 and 3 post-activation. The expression levels of *Ffar2* and *Ffar3* relative to *Gapdh* and *β2m* are shown. Data are presented as mean + SEM from technical duplicates. No statistical testing was performed due to the sample size.

3.2.2 Optimal memory precursor differentiation of CD8$^+$ T cells is partially dependent on GPR41 and GPR43

To test whether GPR41 and GPR43 signalling influenced CD8$^+$ T cell priming, we infected WT and GPR41/GPR43-deficient mice with HSV-1 on the flank skin. Taking into consideration the possiblility of redundant effects of GPR41 and GPR43, mice that lacked both receptors was used. 9 days after infection, we examined the immunodominant CD8$^+$ T cell response to HSV-1 infection using flow cytometric analysis of the spleen (Figure 3.2A). H2-K^b-gB$_{498\text{-}505}$ tetramer staining revealed that approximately 6.3×10^6 gB-specific CD8$^+$ T cells were present in spleens of WT mice, accounting for 8.8 ± 1.3% of total splenic CD8$^+$ T cells (Figure 3.2B). GPR41/GPR43-deficient mice possessed comparable numbers and frequencies of gB-specific CD8$^+$ T cells, implying that there was no defect in the primary expansion of activated CD8$^+$ T cells in the absence of GPR41 and GPR43 expression (Figure 3.2B). In line with this, comparable numbers and proportions of gB-specific CD8$^+$ T cells were detected at the site of infection in the skin of both the WT and GPR41/GPR43-deficient mice following HSV-1 infection (Figure 3.2C), indicating that the ability of antigen-specific CD8$^+$ T cells to expand and enter the skin was intact in mice lacking GPR41 and GPR43 expression.

Although GPR41 and GPR43 did not affect the magnitude of the CD8$^+$ T cell response in the spleen and skin, it was important to assess the quality of the response. Activated CD8$^+$ T cells differentiate from KLRG1$^-$CD127$^-$ EECs with greater plasticity into more differentiated KLRG1$^-$CD127$^+$ MPECs and KLRG1$^+$CD127$^-$ SLECs [30]. These subsets are known to infiltrate the skin in e.c. HSV-1 infection [292]. The MPEC/SLEC balance is determined by a diverse set of input signals from surrounding cells and the microenvironment, including metabolite availability which can skew EEC differentiation [29, 214, 293, 294]. We therefore analysed splenic gB-specific CD8$^+$ T cells for their expression of KLRG1 and CD127. Interestingly, clear differences in subset proportions between the WT and GPR41/GPR43-deficient groups were detected. GPR41/GPR43-deficient mice possessed a significantly lower frequency of EECs than WT mice (Figure 3.2D), suggesting that GPR41 and GPR43 restrained differentiation of EECs. Further discrepancies were observed amongst the cells that did progress into MPECs or SLECs. The frequency of GPR41/GPR43-deficient

MPECs was significantly lower than that of the WT group (11 ± 0.84% and 17 ± 1.6% respectively) (Figure 3.2D). In contrast, SLEC frequencies were greater in GPR41/GPR43-deficient mice than their WT counterparts (55 ± 8.6% and 48 ± 7.9% respectively) (Figure 3.2D). GPR41 and GPR43 hence support the ability of $CD8^+$ T cells in the spleen to form MPECs.

A similar defect was observed in the skin, with a greater proportion of $KLRG1^-$ $CD127^-$ cells in the skin of WT mice than GPR41/GPR43-deficient mice (Figure 3.2E). $KLRG1^-CD127^+$ cell frequencies were reduced from 18 ± 1.5% in WT mice to 13 ± 0.56% in GPR41/GPR43-deficient mice, and $KLRG1^+CD127^-$ cell frequencies were increased from 36 ± 2.2% to 47 ± 0.85% in WT and GPR41/GPR43-deficient mice respectively (Figure 3.2E). This suggest that $CD8^+$ T cells GPR41 and GPR43 can influence fate decisions in both the spleen and site of infection.

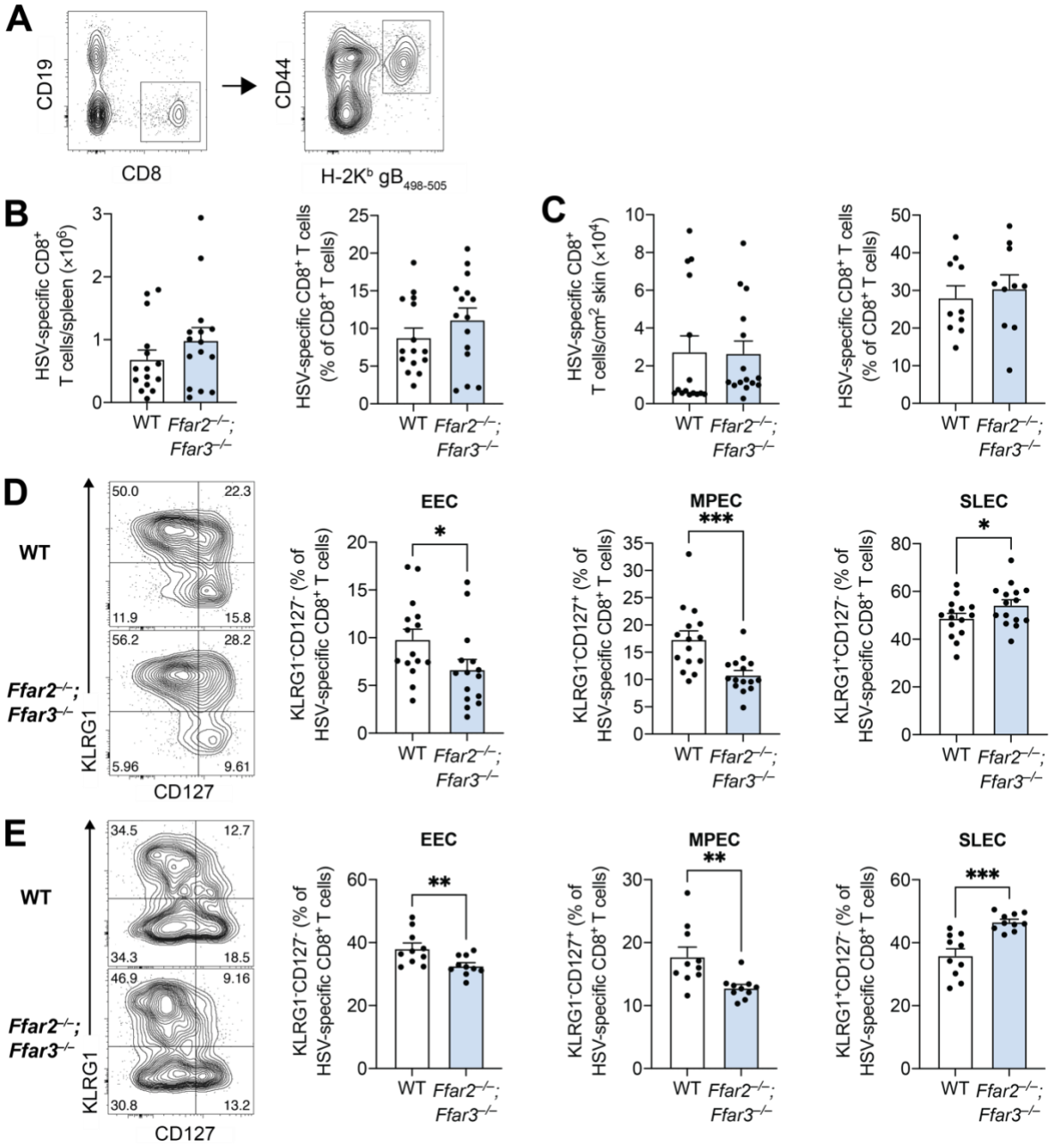

Figure 3.2 GPR41 and GPR43 promote CD8⁺ T cell differentiation into MPECs following HSV-1 infection.

Ffar2$^{-/-}$*;Ffar3*$^{-/-}$ and wildtype (WT) mice were infected with 1 x 10^6 plaque forming units (PFUs) HSV-1 epicutaneously. 9 days after infection, endogenous $gB_{498\text{-}505}$-specific CD8⁺ T cells from spleen and skin tissues were analysed using H-2K^b-$gB_{498\text{-}505}$-restricted tetramers. **(A)** Representative plots of the gating strategy to identify $gB_{498\text{-}505}$-specific CD8⁺ T cells are shown. **(B, C)** The absolute numbers and frequencies of $gB_{498\text{-}505}$-specific CD8⁺ T cells in the spleen (B) and skin (C), as analysed by tetramer staining. **(D, E)** The proportions of EEC, MPEC, and SLEC populations within HSV-specific CD8⁺ T cells in the spleen (D) and skin (E). Representative contour plots of KLRG1 and CD127 expression on $gB_{498\text{-}505}$-specific

$CD8^+$ T cells of WT and *Ffar2*$^{-/-}$;*Ffar3*$^{-/-}$ mice are depicted. Data are presented as mean + SEM of n = 10 – 15 WT or *Ffar2*$^{-/-}$;*Ffar3*$^{-/-}$ mice from 2 to 3 independent experiments. Asterisks indicate statistically significant differences as analysed by unpaired Student's *t*-tests (* $p < 0.05$, ** $p < 0.01$, *** $p < 0.001$).

3.2.3 TNF-α production by CD8$^+$ T cells and viral control are GPR41- and GPR43-dependent

Apart from the MPEC/SLEC differentiation, the quality of the effector response is also determined by effector molecule expression. It has been reported that GPR41 can promote the degranulation and release of IFN-γ by CD8$^+$ T cells [181]. Furthermore, our group has previously shown that the IFN-γ response of GPR41/GPR43-deficient secondary effector CD8$^+$ T cells was reduced compared to their WT counterparts in mixed BM chimera mice after antigen re-exposure [31]. We therefore tested whether CD8$^+$ T cell effector molecule expression was affected by GPR41 and GPR43 in the initial response following HSV-1 infection. WT and GPR41/GPR43-deficient mice infected on the skin with HSV-1 were analysed 9 days later. Re-stimulation of splenocytes with the $gB_{498-505}$ peptide allowed us to probe for intracellular cytokine expression. The CD8$^+$ T cell population was analysed for IFN-γ, and the antigen-responsive cells denoted by IFN-γ and CD44 co-expression were further divided into MPEC/SLEC subsets (Figure 3.3A). IFN-γ$^+$CD44$^+$ cells accounted for about 5% of the total CD8$^+$ T cells in both WT and GPR41/GPR43-deficient mice in line with most gB-specific CD8$^+$ T cells (Figure 3.2B) responding to *ex vivo* re-stimulation (Figure 3.3B). Interestingly, dividing this population into MPECs and SLECs uncovered significant differences in the expression of the pro-inflammatory cytokine TNF-α. While TNF-α production by SLECs was not affected by GPR41 and GPR43 deficiency, this cytokine was downregulated in the MPEC compartment from 59 ± 2.0% in WT cells to 44 ± 4.1% in GPR41/GPR43-deficient cells (Figure 3.3C). These results demonstrated that MPECs relied on SCFA receptor signalling for optimal TNF-α expression.

TNF-α is an important molecule in the control and clearance of viruses, as shown by the heightened risk of cutaneous HSV infection in patients receiving TNF- α inhibitors [295, 296]. As such, we next assessed the influence of GPR41 and GPR43 on HSV-1 control. Viral burden in the skin was measured 2 and 5 days post-infection as the virus migrates from the primary site of infection to the innervating dorsal root ganglion by day 2, and re-emerges at the secondary infection site at around day 5 [288]. 2 days after infection, there was a small but significantly greater viral PFUs in skins of GPR41/GPR43-deficient mice compared to WT mice (Figure 3.3D). While the anti-viral response is mainly mediated by the innate immune system at 2 days post-

infection, it has been reported that viral control by $CD8^+$ T cells occurs at approximately 5 days after infection [288]. On day 5 post-infection, we detected that the difference in viral burden between WT and GPR41/GPR43-deficient mice further increased (Figure 3.3D). These results suggest that the expression of GPR41 and GPR43 within both the innate and adaptive immune compartments contribute to viral control.

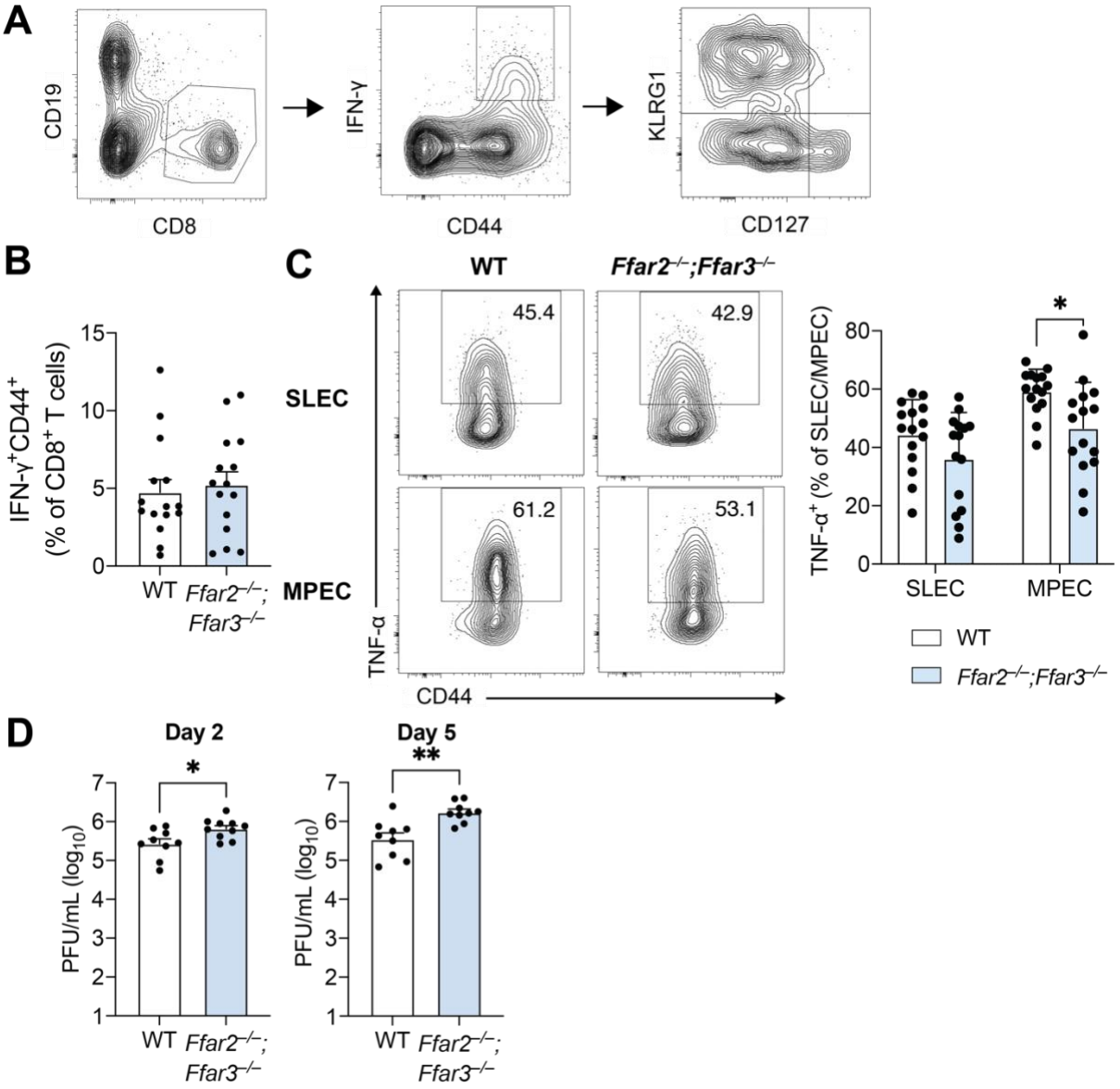

Figure 3.3 GPR41 and GPR43 expression contributes towards effector function of CD8⁺ T cells and immune control of HSV-1.

Ffar2$^{-/-}$*;Ffar3*$^{-/-}$ and wildtype (WT) mice were infected with 1 x 10^6 plaque forming units (PFUs) HSV-1 epicutaneously. **(A – C)** *Ex vivo* $gB_{498-505}$ peptide re-stimulation was performed for 5 hours on splenocytes 9 days post-infection in the presence of brefeldin A. Intracellular cytokine stains were analysed using flow cytometry by gating on $CD19^-CD8^+$ T cells, followed by antigen-responsive $CD8^+$ T cells denoted by IFN-γ and CD44 co-expression, then $KLRG1^-CD127^+$ MPECs and $KLRG1^+CD127^-$ SLECs (A). The frequency of $IFN\text{-}\gamma^+CD44^+$ T cells of total $CD8^+$ T cells of WT and *Ffar2*$^{-/-}$*;Ffar3*$^{-/-}$ mice was measured (B). The frequency of TNF-α expression in $IFN\text{-}\gamma^+CD44^+CD8^+$ MPEC and SLEC populations, and representative contour plots of TNF-α against CD44 in SLECs and MPECs are shown (C). **(D)** Skin from the flanks of WT and *Ffar2*$^{-/-}$*;Ffar3*$^{-/-}$ mice were harvested on day 2 and 5 post-infection for

analysis of viral titres using PFU assays. Cytokine expression in (A – C) was measured in 3 independent experiments, with n = 15 per group. Viral PFUs were measured in 2 independent experiments, with n = 10 per group. Data are represented as mean + SEM. Asterisks indicate statistically significant differences as analysed by unpaired Student's *t*-tests or a two-way ANOVA test (* $p < 0.05$, ** $p < 0.01$).

3.2.4 GPR41 and GPR43 expression modulate CD8$^+$ T cell differentiation following systemic antigen challenge

The higher viral titres observed in GPR41/GPR43-deficient mice indicate greater antigen abundance, which may have been a confounder in TCR stimulation and resulting effector differentiation. To validate that our results in the previous section were attributed SCFA receptors and not antigen load, we infected naïve mice with HSV-1 via i.v. injection. This route of infection was used as the virus cannot replicate in the spleen, thus ensuring T cell responses were not influenced by differences in antigen load.

To study effector differentiation, the endogenous CD8$^+$ T cell response of WT and GPR41/GPR43-deficient mice was analysed at day 8 post-infection. H-2K$_b$-gB$_{498\text{-}505}$ tetramer staining indicated that peripheral blood of WT and GPR41/GPR43-deficient mice possessed similar numbers and frequencies of gB-specific CD8$^+$ T cells (Figure 3.4A). However, clear qualitative differences within the HSV-specific response existed between the WT and GPR41/GPR43-deficient groups, consistent with our observations in the epicutaneous HSV-1 model. EECs comprised of a smaller proportion of gB-specific CD8$^+$ T cells in GPR41/GPR43-deficient mice compared to their WT counterparts (Figure 3.4B). Mice deficient for GPR41 and GPR43 also possessed a reduced frequency of MPECs (WT, 30 ± 2.4%; *Ffar2*$^{-/-}$*;Ffar3*$^{-/-}$, 22 ± 1.4%), and preferential differentiation into SLECs (WT, 32 ± 2.6%; *Ffar2*$^{-/-}$*;Ffar3*$^{-/-}$, 42 ± 2.2%) (Figure 3.4B). These findings indicate that the defect in effector differentiation of gB-specific CD8$^+$ T cells lacking GPR41 and GPR43 was not a consequence of antigen availability, and instead was a result of SCFA receptor expression.

MPECs have a greater ability to survive the contraction phase of the immune response and transition into long-lived Memory T cells cells over time [29]. We evaluated whether alterations in the differentiation observed during the effector phase would also be observed during the memory phase. As expected, 4 weeks post-infection, the numbers and frequencies of gB-specific CD8$^+$ T cells in the spleen were similar between groups (Figure 3.4C). Consistent with our earlier results from an effector timepoint, GPR41 and GPR43 did not alter the magnitude of the CD8$^+$ T cell response during the memory phase.

4 weeks after infection, the proportion of KLRG1$^-$CD127$^-$ gB-specific CD8$^+$ T cells was comparable between WT and GPR41/GPR43-deficient mice (Figure 3.4D). However, GPR41/GPR43-deficient mice had a reduced frequency of KLRG1$^-$CD127$^+$ gB-specific CD8$^+$ T cells and an augmentation in KLRG1$^+$CD127$^-$ gB-specific CD8$^+$ T cells compared to WT mice (Figure 3.4D). These differenitation trends were in line with that at an effector timepoint (Figure 3.2D). Furthermore, there was a relatively lower number of KLRG1$^-$CD127$^-$ and KLRG1$^-$CD127$^+$ gB-specific CD8$^+$ T cells in GPR41/GPR43-deficient mice compared to their WT counterparts, although significance was only reached in the KLRG1$^-$CD127$^+$ population (Figure 3.4E). The KLRG1$^+$CD127$^-$ gB-specific CD8$^+$ T cell population was a similar size in both groups (Figure 3.4E). GPR41 and GPR43 therefore contribute significantly to CD8$^+$ T cell priming and differentiation, with their effects remaining discernible after the resolution of the infection, at a memory timepoint.

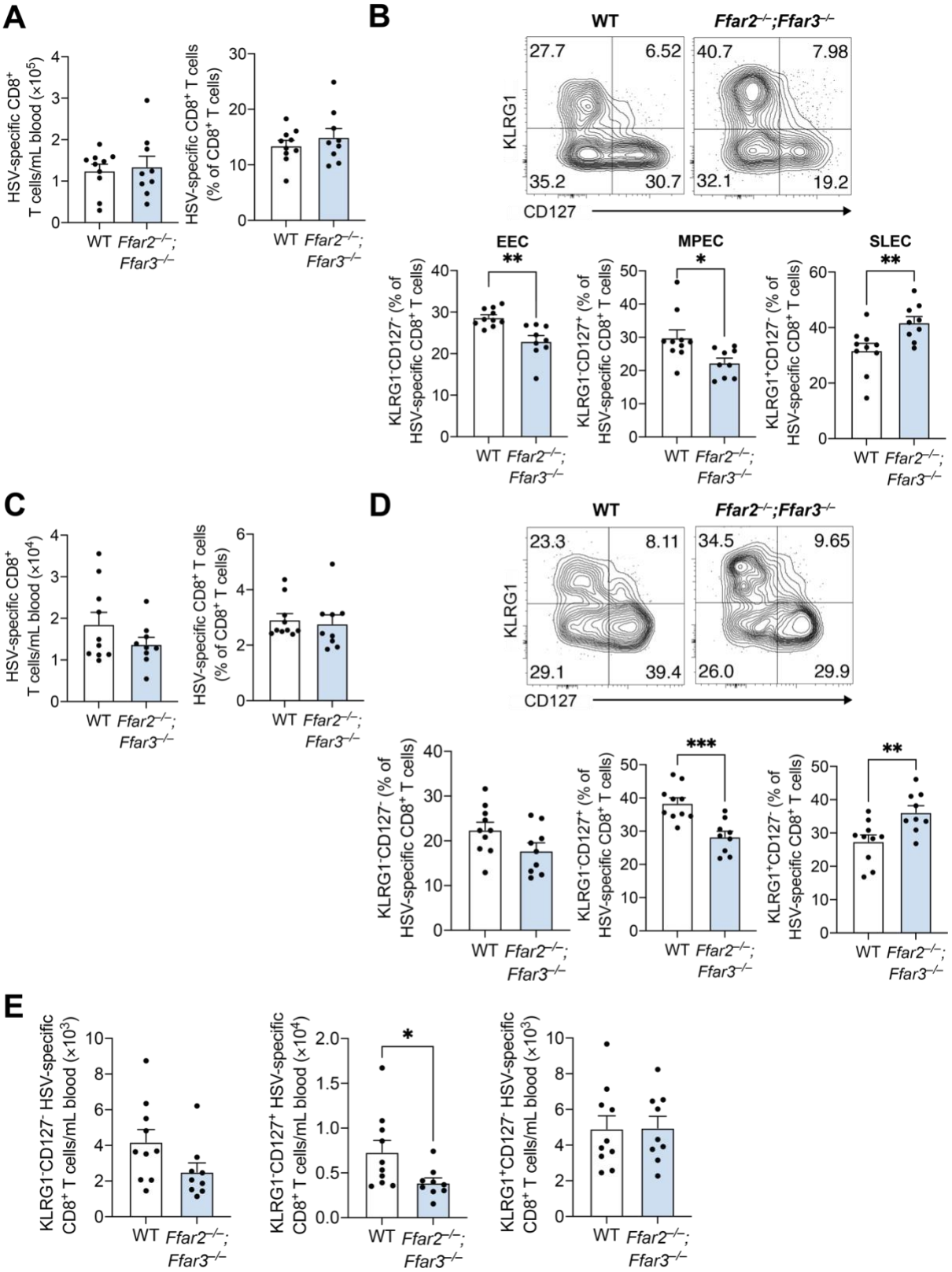
A
HSV-specific CD8+ T cells/mL blood (×10^5)
HSV-specific CD8+ T cells (% of CD8+ T cells)
WT
Ffar2−/−; Ffar3−/−
B
WT
Ffar2−/−;Ffar3−/−
27.7
6.52
35.2
30.7
40.7
7.98
32.1
19.2
KLRG1
CD127
EEC
MPEC
SLEC
KLRG1-CD127- (% of HSV-specific CD8+ T cells)
KLRG1-CD127+ (% of HSV-specific CD8+ T cells)
KLRG1+CD127- (% of HSV-specific CD8+ T cells)
C
HSV-specific CD8+ T cells/mL blood (×10^4)
HSV-specific CD8+ T cells (% of CD8+ T cells)
D
23.3
8.11
29.1
39.4
34.5
9.65
26.0
29.9
E
KLRG1-CD127- HSV-specific CD8+ T cells/mL blood (×10^3)
KLRG1-CD127+ HSV-specific CD8+ T cells/mL blood (×10^4)
KLRG1+CD127- HSV-specific CD8+ T cells/mL blood (×10^3)

Figure 3.4 GPR41- and GPR43-mediated CD127 upregulation is maintained at a memory timepoint.

Wildtype (WT) and *Ffar2*$^{-/-}$*;Ffar3*$^{-/-}$ mice were intravenously infected with 2 × 10^5 plaque-forming units (PFU) HSV-1. **(A, B)** Analysis of endogenous $gB_{498\text{-}505}$-specific $CD8^+$ T cells using H-$2K^b$-$gB_{498\text{-}505}$-restricted tetramers was performed on submandibular bleeds 8 days post-infection. Absolute numbers and frequencies of $gB_{498\text{-}505}$-specific $CD8^+$ T cells are shown (A). Frequencies of EECs, MPECs, and SLECs in $gB_{498\text{-}505}$-specific $CD8^+$ T cells were measured (B). **(C – E)** Analysis of endogenous $gB_{498\text{-}505}$-specific $CD8^+$ T cells using H-$2K^b$-$gB_{498\text{-}505}$-restricted tetramers was performed on spleens 4 weeks post-infection. Absolute numbers and frequencies of $gB_{498\text{-}505}$-specific $CD8^+$ T cells in the blood 4 weeks after infection are shown (C). Frequencies (D) and absolute numbers (E) of $KLRG1^-CD127^-$, $KLRG1^-CD127^+$, and $KLRG1^+CD127^-$ $gB_{498\text{-}505}$-specific $CD8^+$ T cell population were measured. Representative contour plots of KLRG1 and CD127 expression on $gB_{498\text{-}505}$-specific $CD8^+$ T cells of WT and *Ffar2*$^{-/-}$*;Ffar3*$^{-/-}$ mice are depicted in (B and D). Data are presented as mean + SEM of n = 10 WT or *Ffar2*$^{-/-}$*;Ffar3*$^{-/-}$ mice from 2 independent experiments. Asterisks indicate statistically significant differences as analysed by unpaired Student's *t*-tests (* $p < 0.05$, ** $p < 0.01$, *** $p < 0.001$).

3.2.5 GPR41 and GPR43 expression supports MPEC differentiation through CD8$^+$ T cell-extrinsic mechanisms

Having identified a reduction in CD8$^+$ T cell MPEC differentiation and function with global deficiencies in GPR41 and GPR43, we next sought to delineate whether this receptor signalling requirement was CD8$^+$ T cell-intrinsic or extrinsic. We adoptively transferred naïve WT gBT-I cells into recipients deficient or sufficient for GPR41 and GPR43 a day prior to epicutaneous HSV-1 infection. As gBT-I cells were competent for GPR41 and GPR43, they could sense SCFAs via these receptors while all endogenous cells could not. 9 days after infection, we analysed the gBT-I population in the spleen and skin (Figure 3.5A). The absolute numbers and frequencies of gBT-I cells in the spleen and skin were similar between both recipient groups (Figure 3.5B and C). The expression of GPR41 and GPR43 by the gBT-I cells did not affect the magnitude of the response in the spleen and skin. This recapitulated our observations for the endogenous CD8$^+$ T cell response (Figure 3.2B and C).

Nevertheless, further analysis of gBT-I cell differentiation in the spleen uncovered differences in KLRG1 and CD127 expression. A similar proportion of EECs was detected in both recipient groups (Figure 3.5D). However, the gBT-I population in GPR41/GPR43-deficient recipients contained a lower proportion of MPECs than WT recipients (12 ± 0.60% and 19 ± 1.6% respectively); while the relative prevalence of SLECs was greater in GPR41/GPR43-deficient mice (*Ffar2*$^{-/-}$*;Ffar3*$^{-/-}$, 51 ± 1.3%; WT, 42 ± 1.4%) (Figure 3.5D). In the skin, only KLRG1 was used to discriminate between effector subsets as CD127 was cleaved during enzymatic digestion with dispase. This is opposed to the use of liberase in Figure 3.2E which preserved CD127 and CD8 expression, enabling us to identify endogenous CD8$^+$ T cells. GPR41/GPR43-deficient hosts possessed a lower frequency of KLRG1$^-$ cells which represented less differentiated effector subsets, EECs and MPECs (Figure 3.5E). In contrast, the proportion of the KLRG1$^+$ cells (consisting mainly of SLECs) in receptor-deficient mice was relatively larger compared to WT mice (Figure 3.5E). This indicated that CD8$^+$ T cell differentiation was skewed by GPR41 and GPR43 expression in the recipient, not the transferred CD8$^+$ T cells. The influence of GPR41 and GPR43 expression on MPEC/SLEC formation during priming can thus be attributed to CD8$^+$ T cell-extrinsic mechanisms.

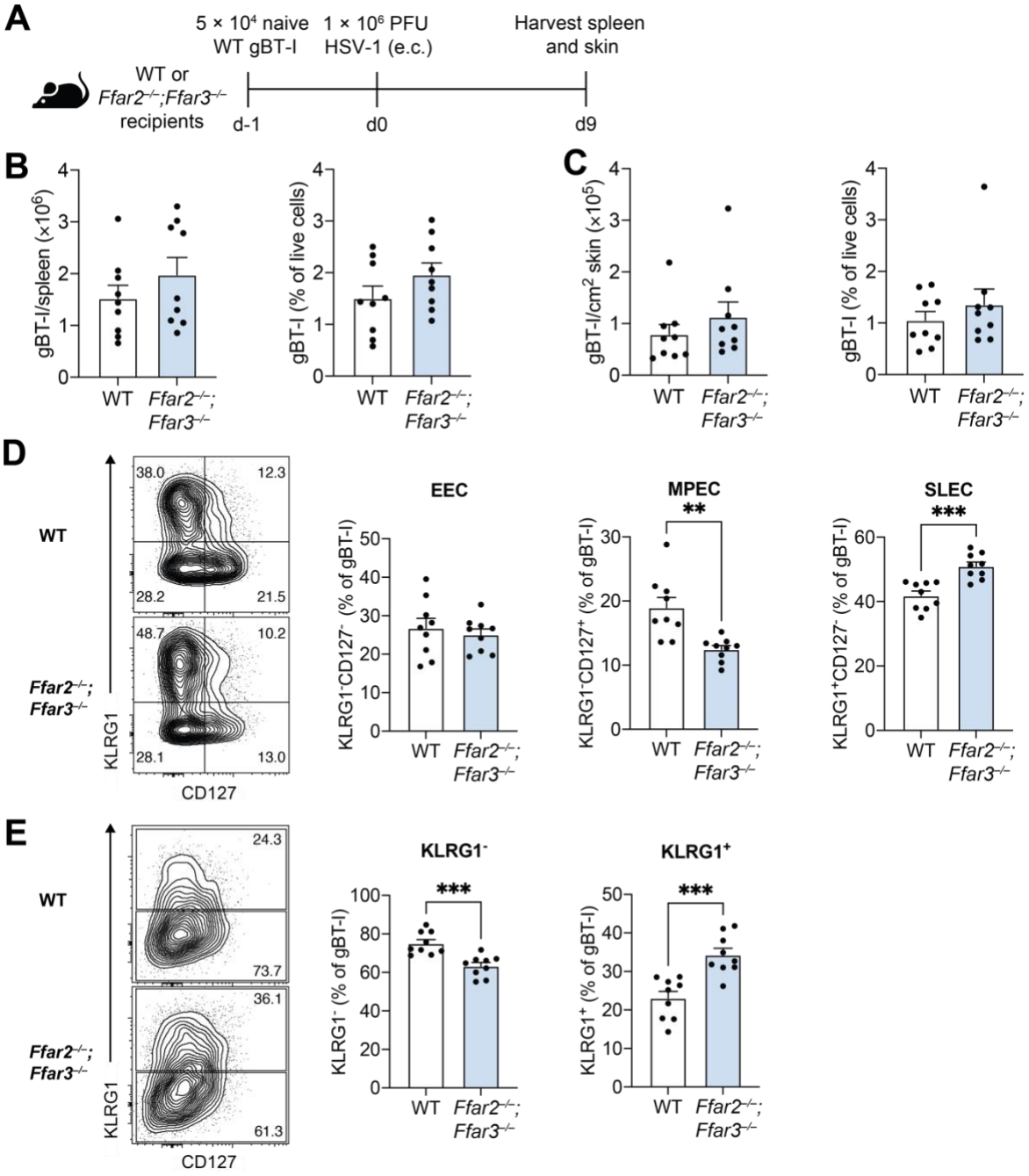

Figure 3.5 Differentiation into MPECs is hindered in a priming environment deficient in GPR41 and GPR43.

5 × 10^4 naïve wildtype (WT) gBT-I cells were transferred into *Ffar2*$^{-/-}$*;Ffar3*$^{-/-}$ and WT recipients which were subsequently epicutaneously (e.c.) infected with 1 × 10^6 plaque-forming units (PFU) HSV-1. gBT-I cells from spleens and skin tissues were analysed 9 days after infection. **(A)** The experimental schematic is shown. **(B, C)** The number and frequencies of gBT-I cells in the spleen (B) and skin (C) are shown. **(D, E)** KLRG1$^-$CD127$^-$ EEC, KLRG1$^+$CD127$^-$ SLEC, and KLRG1$^-$CD127$^+$ MPEC frequencies in gBT-I cells from the spleen (D) in *Ffar2*$^{-/-}$*;Ffar3*$^{-/-}$ and WT recipients were compared, as well

as KLRG1^{+} and KLRG1^{-} cells as a frequency of gBT-I cells from the skin (E). Representative contour plots of KLRG1 and CD127 expression in WT and *Ffar2*$^{-/-}$*; Ffar3*$^{-/-}$ mice are depicted. Data are presented as mean + SEM of n = 10 mice per group from 2 pooled independent experiments. Asterisks indicate statistically significant differences as analysed by unpaired Student's *t*-tests (** $p < 0.01$, and *** $p < 0.001$).

3.2.6 GPR41- and GPR43-expressing CD8$^+$ T cells compensate for the sub-optimal viral control in receptor-deficient mice

We observed that endogenous gB-specific CD8$^+$ T cells from GPR41/GPR43-deficient mice possessed a dampened TNF-α response, likely contributing to poorer viral control (Figure 3.3C and D). To examine if this was the result of a deficiency in GPR41 or GPR43 presence on CD8$^+$ T cells or other cell types, we measured effector molecule expression of WT gBT-I cells that had been adoptively transferred into WT or GPR41/GPR43-deficient mice. On day 9 post-infection, gBT-I cells from the spleen were re-stimulated with the $gB_{498-505}$ peptide, then sub-typed into MPECs and SLECs to analyse each subset's expression of IFN-γ, TNF-α and granzyme B (Figure 3.6A).

We observed similar IFN-γ, TNF-α and granzyme B expression between gBT-I SLECs from WT and GPR41/GPR43-deficient hosts (Figure 3.6B). Similarly, effector molecule production was comparable between MPECs from both groups, indicating that gBT-I function was in part dependent on GPR41 and GPR43 expression on CD8$^+$ T cells themselves (Figure 3.6B). Furthermore, viral tires in the skin of WT and GPR41/GPR43-deficient hosts were similar 5 days after infection (Figure 3.6C). The transfer of WT gBT-I cells into GPR41/GPR43-deficient recipients therefore compensated for deficiencies in the endogenous effector response, enabling competent viral control. Thus, optimal TNF-α production appear to be dependent on CD8$^+$ T cell-intrinsic GPR41 and GPR43 signalling, resulting in the WT gBT-I cells being capable of producing similar levels of TNF-α regardless of host phenotype. Cytokine production seems to be differentially regulated from MPEC development which required CD8$^+$ T cell-extrinsic expression of GPR41 and GPR43.

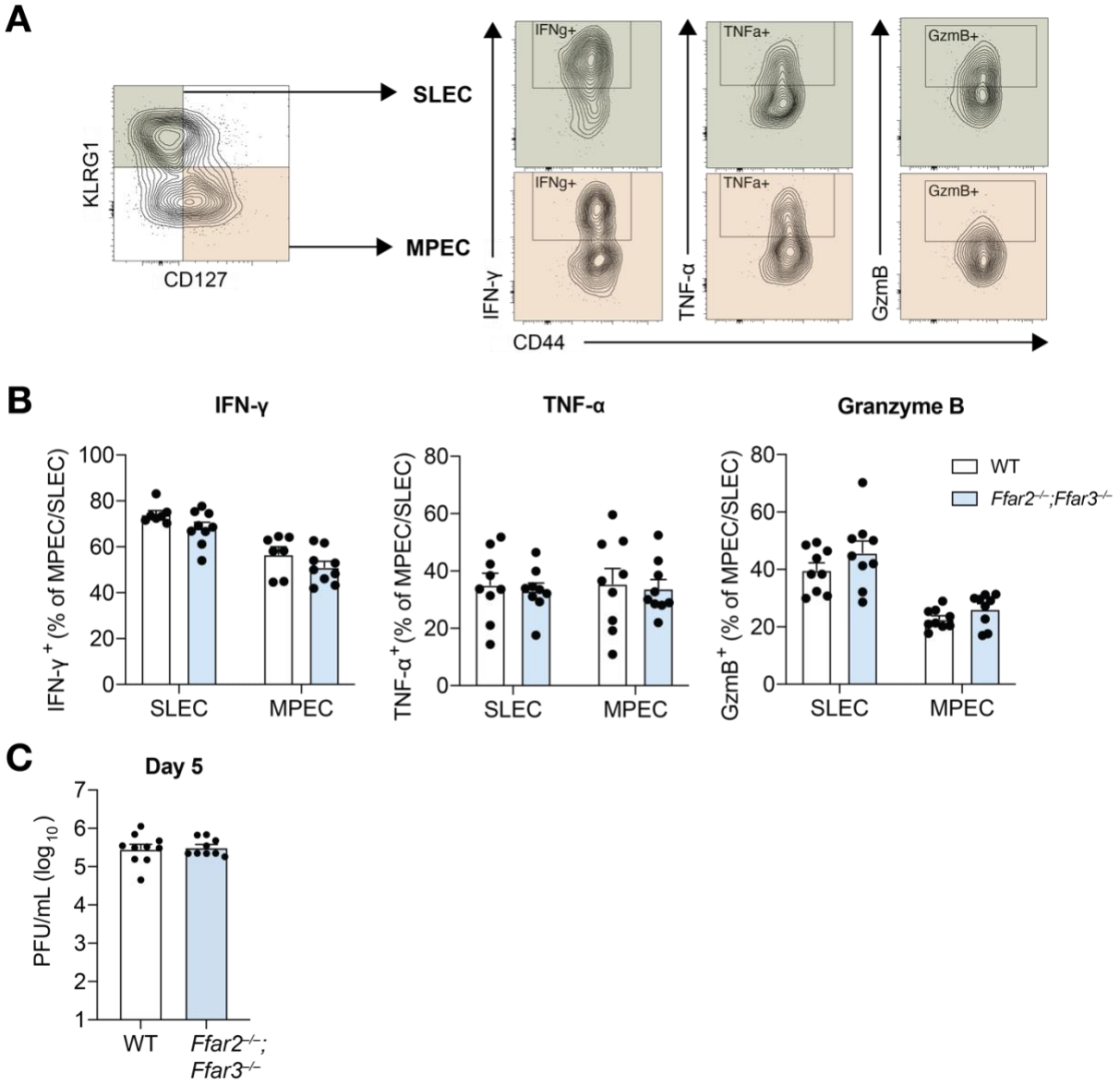

Figure 3.6 The effector function of CD8⁺ T cells in an environment deficient for GPR41 and GPR43 is not altered.

5×10^4 naïve wildtype (WT) gBT-I cells were transferred into WT and *Ffar2*$^{-/-}$*;Ffar3*$^{-/-}$ recipients, which were epicutaneously infected with 1×10^6 plaque forming units (PFU) HSV-1 the following day. **(A, B)** On day 9 post infection, splenocytes were harvested and restimulated with $gB_{498\text{-}505}$ peptide for 5 hours in the presence of brefeldin A. Vα2$^+$CD45.1$^+$ gBT-I cells were analysed for KLRG1 and CD127 expression, followed by effector molecule expression in MPECs and SLECs, according to the representative gating shown in (A). Frequencies of SLECs and MPECs expressing IFN-γ, TNF-α and granzyme B were measured (B). **(C)** Skin from WT and *Ffar2*$^{-/-}$*;Ffar3*$^{-/-}$ mice were harvested 5 days after HSV-1 infection (e.c.) to measure viral titres using PFU assays. Cytokine expression was measured in 2 independent experiments, with n = 7 – 9 per group in (A, B). Viral PFUs were measured in 2 independent

experiments with n = 9 – 10 per group in (C). Data are represented as mean + SEM. Statistical significance was evaluated using two-way ANOVA tests or an unpaired Student's *t*-test.

3.3 Discussion

There is a growing appreciation for the influence of SCFAs on $CD8^+$ T cell immunity, with implications shown in various infections and disorders where SCFAs can improve cytokine responses [31, 123, 160, 168]. SCFAs can elicit effects in T cells through various mechanisms, including receptor-mediated effects through GPR41 and GPR43. These receptors have been studied in the context of viral infections, colitis and asthma [31, 181, 284, 285]. Our group previously reported the positive role of GPR41 and GPR43 in the expansion of secondary effector $CD8^+$ T cells and their IFN-γ production [31]. However, the potential involvement of the GPR41 and GPR43 receptors in $CD8^+$ T cell priming and differentiation *in vivo* has not been explored in great detail. A reason why the role of GPR41 and GPR43 in $CD8^+$ T cell responses is not well understood is due to the lack of clarity about their expression [160, 174, 184, 185]. In our investigation, *Ffar2* and *Ffar3* were detectable at an RNA level in $CD8^+$ T cells. The key findings in our study included the contribution of GPR41 and GPR43 in MPEC differentiaton, TNF-α production, and viral control. While MPEC differentiation was promoted by SCFA receptors in a $CD8^+$ T cell extrinsic manner, TNF-α expression was influenced by $CD8^+$ T cell intrinsic mechanisms.

Currently, clonal antibodies against murine GPR41 and GPR43 are not commercially available which has hindered the analysis of GPR41 and GPR43 protein expression levels. Hence, we used RT-qPCR to measure mRNA levels expressed in T cells. In our study, we validated that despite being detected at low levels, *Ffar2* and *Ffar3* expression was indeed found in *in vitro*-activated $CD8^+$ T cells derived from the spleen. Developing thymocytes, in contrast, expressed only *Ffar2* at detectable levels. This implied that even at an immature developmental phase, T cells may have the potential to detect SCFAs in their microenvironment through GPR43. Our findings that mature $CD8^+$ T cells express both receptors suggest that they may become more sensitive to SCFAs at an activated stage. Furthermore, butyrate appeared to regulate GPR41 and GPR43 receptor expression. This is in line with a separate study where $CD4^+$ T cells treated with acetate and propionate upregulated SCFA receptor expression [124]. These results demonstrate that activated $CD8^+$ T cells are likely able respond to SCFAs in their surroundings by regulating receptor expression which may increase their sensitivity to lower levels of SCFAs.

We found that $CD8^+$ T cell priming was impacted by GPR41 and GPR43. These receptors significantly promoted the differentiation of endogenous $CD8^+$ T cells into EECs and MPECs, in preference to SLECs. The EEC subset is the least differentiated of the three, followed by MPECs, and then SLECs [16]. SCFA sensing through GPR41 and GPR43 therefore seems to play a role in slowing down or restraining differentiation following priming. MPECs are known to differentiate into long-lived and protective memory cells [29], suggesting that GPR41 and GPR43 may contribute to the optimal development of $CD8^+$ T cell memory. MPEC/SLEC fate decisions are contingent on the level of inflammation [29], which is influenced by antigen levels. While GPR41/43-deficient mice were less capable of viral control and hence possessed higher antigen levels than WT mice in our model of epicutaneous infection, this was not a confounder in the observed differentiation outcomes. GPR41/43-induced effects on MPEC formation could be reproduced in an i.v. infection model where antigen abundance was equal between groups. These results suggested that receptor signalling, not the antigen abundance, was the reason for differences in MPEC/SLEC differentiation between WT and GPR41/43-deficient mice.

We only observed lower MPEC differentiation when $CD8^+$ T cells were in an environment lacking GPR41 and GPR43, while receptor expression on the $CD8^+$ T cells themselves did not affect differentiation outcomes. This pointed to GPR41/GPR43-associated MPEC differentiation being attributed to receptor activity in other cell types. A potential experiment to further investigate the $CD8^+$ T cell intrinsic and extrinsic roles of these receptors would be the transfer of GPR41/GPR43-deficient gBT-I cells into WT recipients. Moving forward, further work is necessary to elucidate which cell types account for the MPEC/SLEC differentiation defects when GPR41/43 signalling is lacking. DCs are an obvious cell type involved in priming. They are known to express GPR43 and upon binding to SCFAs, exhibit phenotypic as well as functional effects which include the skewing of B cell reponses [297, 298]. DCs may hence be potential candidates that mediate GPR41/43-dependent effects. $CD4^+$ T cells promote effective $CD8^+$ T cell priming through the provision of help signals [227] and guide them to form memory cells [299]. SCFA receptors may also influence such signals generated by $CD4^+$ T cells during $CD8^+$ T cell priming, although this has yet to be investigated.

Apart from a role for SCFA receptor signalling in the MPEC/SLEC axis, we demonstrated that the functional response of the $CD8^+$ T cells was also affected upon priming. Mice lacking GPR41 and GPR43 exhibited reduced TNF-α expression. Furthermore, we showed that GPR41 and GPR43 supported anti-viral immunity. Greater TNF-α expression by MPECs was associated with improved HSV-1 control in mice that were able to signal through GPR41 and GPR43. This was in line with reports that TNF-α was required for the immune control of HSV-1 [300, 301]. Although T cell-extrinsic GPR41 and GPR43 activity influenced differentiation, optimal cytokine production depended on $CD8^+$ T cell-intrinsic receptor signalling. When analysing the primary endogenous $CD8^+$ T cell response, we observed an inferior TNF-α response in endogenous MPECs of GPR41/GPR43-deficient mice. Yet, TNF-α levels were similar in adoptively transferred WT gBT-I cells regardless of receptor expression in recipient mice, indicating that optimal TNF-α production was not disrupted so long as the T cells themselves expressed GPR41 and GPR43.

In influenza-specific $CD8^+$ T cells, GPR41 and GPR43 have been shown to promote TNF-α at an effector timepoint [181]. We furthered these findings in the context of HSV-1 infection by identifying the effector subset that this difference in expression arose from. Interestingly, we observed that the GPR41- and GPR43-mediated induction of TNF-α was isolated to the MPEC compartment. Cytokine production of MPECs therefore could have been more dependent on SCFA sensing through GPR41 and GPR43 than SLECs were. This implies that SCFA receptors influence MPEC differentiation and function, conveying microbiome- and stress-related changes in SCFA levels during viral infection. Of note, acetate levels rise following bacterial infection and other inflammatory conditions [160, 188] and could act as DAMPs on MPECs, regulating their effector function and differentiation into memory.

In summary, our data highlight a role for GPR41 and GPR43 in $CD8^+$ T cell priming. SCFA sensing through GPR41 and GPR43 promoted differentiation into MPECs and increased TNF-α expression of MPECs, which correlated with better viral control. In particular, we identified alterations in priming attributed to receptor signalling in a $CD8^+$ T cell-intrinsic and extrinsic manner. GPR41 and GPR43

signalling are mechanisms by which SCFAs exert effects on cells. The immunomodulatory potential of SCFAs has led to the idea that these gut microbiota-derived metabolites may hold promise as a therapeutic [302, 303]. Indeed, synthetic compounds with GPR43 agonistic properties reportedly attenuated dextran sulfate sodium-induced colitis in mice, suggesting potential clinical benefit [284]. Improving our knowledge of how GPR41 and GPR43 receptors influence $CD8^+$ T cell priming will hence enable us to better understand mechanisms by which SCFAs interact with the immune system, and how SCFAs or GPR41/GPR43 agonists can be harnessed to promote T cell responses in diseases such as cancer.

Chapter 4:
Establishing the role of butyrate in $CD4^+$ T cell differentiation

Chapter 4 Establishing the role of butyrate in $CD4^+$ T cell differentiation

4.1 Introduction

$CD4^+$ T cells are important for co-ordinating and executing adaptive immune responses against pathogens and disorders including cancer. Their ability to differentiate into distinct subsets, such as Th1, Th2, Th17, Tregs and Tfh cells, allows them to respond in a context-specific manner induced by the modulation of master transcriptional regulators. For example, intracellular infections and cancer predominantly trigger polarisation into Th1 cells. Classical Th1 cells are characterised by the expression of the transcription factor T-bet and the pro-inflammatory cytokines IFN-γ and TNF-α, as well as low FoxO1 expression [304]. However, heterogeneity exists even within the Th1 population. For example, $Ly6C^+$ Th1 cells have a stronger effector phenotype resulting in higher expression levels of IFN-γ [305]. The differentiation of $CD4^+$ T cells hinges on a multitude of factors including antigen stimulation, exposure to cytokines and environmental influences, such as metabolite availability, although the latter remains unclear. Differentiation involves profound changes to the metabolic and epigenetic landscape of the cell, which specific metabolites are capable of inducing [13, 207, 306].

The association between diet and disease outcome has been illustrated in the context of cancer immunotherapy. Dietary fibre, a substrate of microbiota fermentation resulting in the SCFA production, was found to be positively associated with patient responsiveness to ICB therapy in the form of anti-PD-1 and anti-PD-L1 [153, 256, 307, 308]. Furthermore, faecal and plasma butyrate concentrations correlated with progression-free survival in patients with solid tumours [153, 309]. Gopalakrishnan *et al.* found an enrichment of Clostridiales, Ruminococcaceae, and *Faecalibacterium* in melanoma patients who had higher frequencies of effector $Foxp3^-CD4^+$ T cells and better anti-tumour cytokine responses, in particular the Th1 cytokine TNF-α [248]. Interestingly, other studies revealed that the bacteria identified by Gopalakrishnan *et al.* were known to be SCFA-producing gut commensals [310-313]. This perhaps hints at the ability of SCFAs to alter $CD4^+$ T cell differentiation towards anti-tumour subsets.

Park *et al.* have proposed that acetate and propionate promoted the expression of T-bet and IFN-γ under Th1 polarising conditions, enhancing Th1 formation [124]. However, a direct link between butyrate and $CD4^+$ T cell differentiation into Th1 cells has yet to be uncovered.

The role of the butyrate in Th1 cell differentiation is not well-explored as the original studies focused on the role of SCFA on inducible Tregs, followed up by work demonstrating the suppression of Th17 cell differentiation [313, 314]. Interestingly, using an *in vitro* setup, Kespohl and colleagues demonstrated that while low concentrations of butyrate promoted Treg formation, $CD4^+$ T cells exposed to high levels of butyrate expressed increased the expression of T-bet and the Th1-associated cytokine IFN-γ [152]. This raised the question of whether butyrate is capable of inducing more than a regulatory phenotype in $CD4^+$ T cells. Indeed, butyrate triggered Th0 cells to produce IFN-γ [152], but how closely the resulting cells resembled classical Th1 cells remains in question. Due to the potential link between diet, SCFAs and improved ICB therapy success in cancer patients, understanding the effects of the SCFA butyrate on Th1 cells in a systematic manner possesses clinical relevance.

A subfraction of $CD4^+$ T cells can exert cell-mediated cytotoxicity through granzyme, perforin and FasL, which are traditionally thought to be effector molecules of $CD8^+$ T cells [46, 315]. Although the functional importance of cytotoxic $CD4^+$ T cells has been demonstrated in cancer and viral infections [316, 317], their development remains relatively elusive. It has not yet been established whether they represent an independent lineage or originate from classical $CD4^+$ T cell subsets such as Th1 cells, which can indeed possess overlapping features with cytotoxic $CD4^+$ T cells [318-320]. Due to recent correlative studies, there is a growing interest in targeting selective $CD4^+$ T cell subsets to enhance the effectiveness of cancer immunotherapies [321-323]. As such, further knowledge encompassing the consequences of butyrate on cytotoxic Th1 cell differentiation is required. In this chapter, we aimed to study whether butyrate could promote differentiation into and functionality of this subset, as well as the mechanisms through which butyrate induces these changes.

4.2 Results

4.2.1 The SCFA butyrate is more effective than acetate and propionate in inducing a Th1-like phenotype in CD4$^+$ T cells

As a detailed analysis of the role of butyrate in CD4$^+$ T cell differentiation is lacking, we used gDT-II cells, which are transgenic I-Ab-restricted CD4$^+$ T cells specific for the HSV-1 glycoprotein D-derived epitope $gD_{315-327}$. Using splenocytes pulsed with their cognate antigen, we *in vitro*-activated gDT-II cells without the addition of polarising cytokines or blocking antibodies but with the addition of LPS and IL-2. In addition to earlier reports identifying a default Th1 polarisation in mice of B6 background [324, 325], IL-2 supplementation is known to induce the expression of Th1-associated factors such as T-bet and IFN-γ [293, 326]. As majority of DCs undergo apoptosis within the initial 2 days of culture, SCFAs treatment was provided on days 3 to 5 to reflect direct SCFA exposure upon activation. gDT-II cells were identified by gating on live CD45.1$^+$CD4$^+$Vα3.2$^+$ cells (Figure 4.1A). As expected, we observed a preference for gDT-II cells activated using this protocol to express the Th1 master transcription factor T-bet (Figure 4.1B). These cells expressed very low levels of the Treg and Tfh master transcription factors Foxp3 and Bcl-6 respectively, and all 3 types of SCFAs did not induce significant changes to the expression of these transcription factors (data not shown). Interestingly, butyrate further promoted T-bet expression more effectively than acetate or propionate (Figure 4.1B).

To validate that the butyrate-mediated T-bet upregulation was not simply a feature of transgenic CD4$^+$ T cells, we similarly treated polyclonal CD4$^+$ T cells that had been activated with anti-CD3 and anti-CD28 in the absence of LPS. Comparable results were observed in T-bet expression in antigen- and polyclonally-activated CD4$^+$ T cells, indicating that the effects of butyrate on T-bet expression were not specific to gDT-II cells and furthermore were not confounded by activation protocols (Figure 4.1C). The ability of butyrate to enhance T-bet expression more than acetate and propionate prompted us to further investigate the effects of butyrate on CD4$^+$ T cell differentiation and function in this chapter.

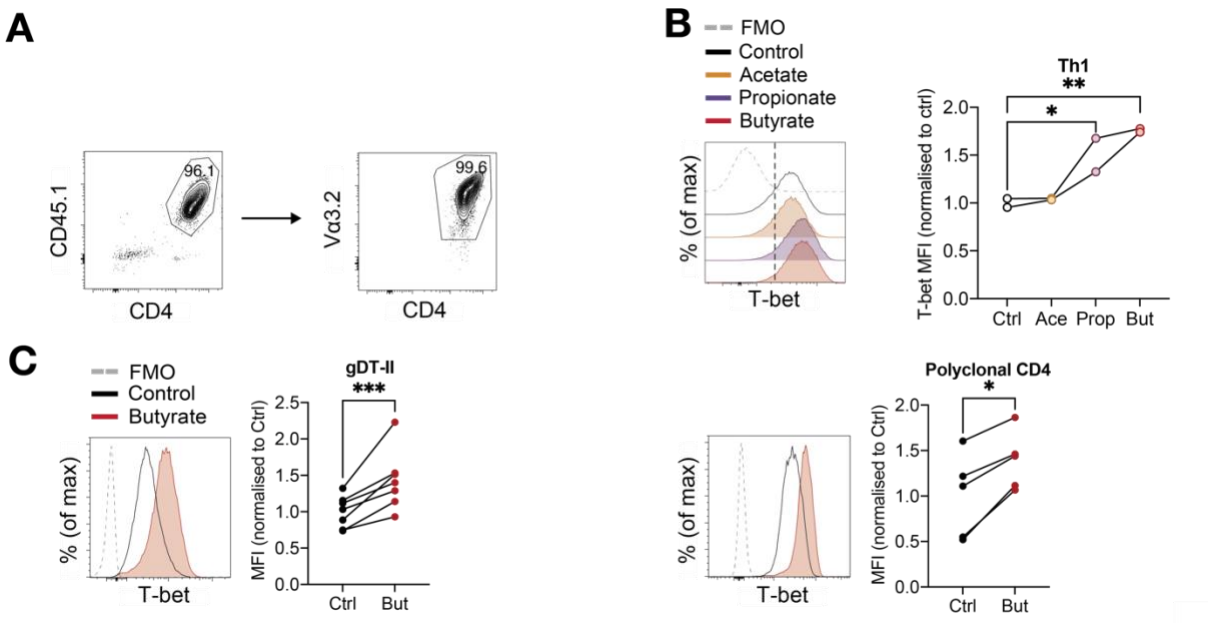

Figure 4.1 Butyrate is more effective at promoting a Th1-like phenotype than acetate and propionate.

(A and B) gDT-II cells were activated *in vitro* with splenocytes pulsed with the $gD_{315-327}$ peptide, and cultured in the presence of LPS and IL-2. Cells were treated with 0.5 mM acetate (Ace), propionate (Prop) or butyrate (But) from days 3 to 5. No short chain fatty acid treatment was provided to the control (Ctrl) group. Analysis of gDT-II cells was performed on day 6 post-activation by gating on live cells that expressed CD45.1, CD4 and Vα3.2. The representative gating strategy is shown in (A). T-bet expression of gDT-II cells is shown as the mean fluorescence intensity (MFI), normalised to that of the untreated group (B). **(C)** Polarisation of in *vitro-activated* gDT-II cells and polyclonal $CD4^+$ T cells activated with anti-CD3 and anti-CD28 into Th1 cells are expressed as the normalised mean fluorescence intensities (MFI) of T-bet. Data in (B and C) are presented as the MFI of n = 2 – 7 independent experiments. Asterisks indicate statistically significant differences as analysed by a one-way ANOVA test or Student's *t*-tests (* $p < 0.05$, ** $p < 0.01$, *** $p < 0.001$).

4.2.2 Butyrate promotes CD4$^+$ T cell differentiation into cytotoxic Th1 cells

To obtain a broad overview on how butyrate affects CD4$^+$ T cell activation, we studied the lymph node-homing molecule CD62L as well as the activation markers CD25 and PD-1, which undergo changes in expression upon T cell stimulation. 61 $\pm$ 5.9% and 93 $\pm$ 1.7% of control CD4$^+$ T cells expressed CD62L and CD25 respectively, while PD-1 was expressed at very low levels (0.90 $\pm$ 0.22%) (Figure 4.2A). The expression of all three markers were minimally changed by butyrate, indicating that butyrate did not alter CD4$^+$ T cell activation. We proceeded to analyse the expression of markers that are functionally relevant to T-bet-expressing CD4$^+$ T cells, such as Ly6C [327] and CXCR3 [328]. Ly6C which is upregulated by effector Th1 cells [305] was augmented from 51 $\pm$ 2.7% to 77 $\pm$ 2.9% upon butyrate treatment (Figure 4.2B). In contrast, butyrate did not alter the expression of CXCR3 (Figure 4.2C), a chemokine receptor inducing migration to inflammatory sites [329]. These results indicated that butyrate induced an Th1-like effector phenotype in CD4$^+$ T cells, but did not influence the expression of the chemokine receptor CXCR3.

Apart from Ly6C and CXCR3 expression, another characteristic of Th1 cells is the downmodulation of the transcription factor FoxO1 that opposes T-bet expression [57, 304, 330] and can induce memory formation [52]. Despite the upregulation of T-bet, butyrate mediated an increase in FoxO1 expression (Figure 4.2D). This suggested that butyrate did not induce classical Th1 cells. A subset of cytotoxic CD4$^+$ T cells shares features with Th1 cells, such as T-bet expression [46]. Eomes has been suggested to be amongst one of the main transcription factors driving this cytotoxic phenotype [293]. We observed that Eomes expression was similar between control and butyrate-treated CD4$^+$ T cells, suggesting that Eomes-driven effector function may not be altered by butyrate (Figure 4.2E).

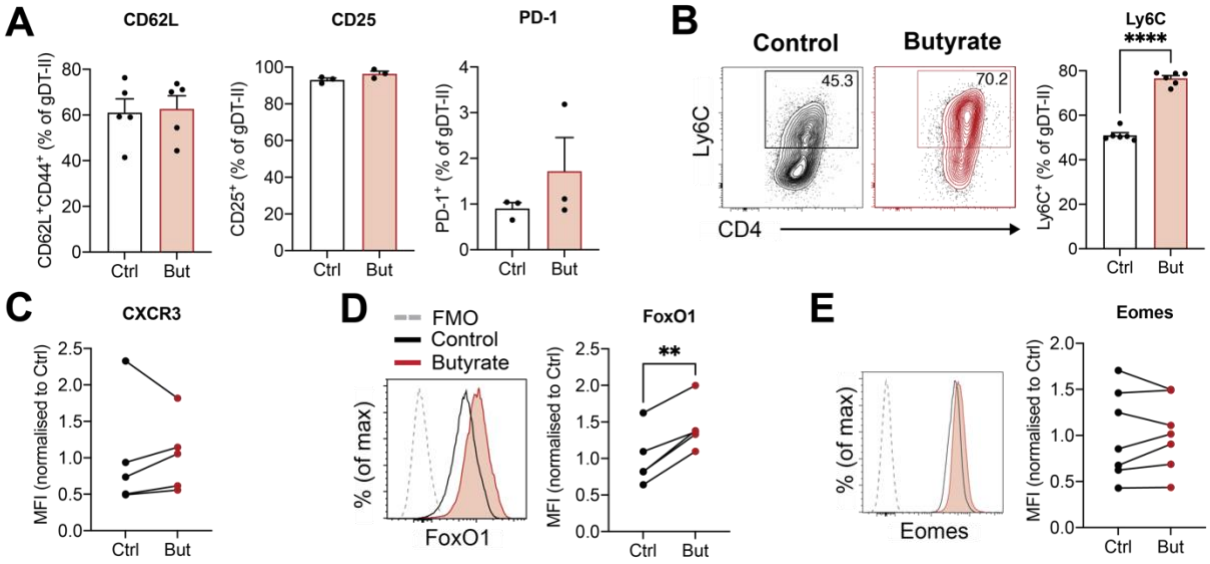

Figure 4.2 Butyrate upregulates classical and non-classical Th1 cell features in CD4⁺ T cells.

gDT-II cells were *in vitro* activated by co-culture with splenocytes pulsed with the $gD_{315-327}$ peptide, LPS and IL-2 supplementation. Cells were treated with 0.5 mM butyrate (But) on days 3 to 5 after activation, or remained untreated (control; Ctrl). Analysis was performed 6 days after activation. **(A)** The proportions of gDT-II cells expressing the activation markers CD62L, CD25 and PD-1 were measured. **(B)** The proportion of gDT-II cells expressing Ly6C is shown. Representative contour plots display Ly6C expression against CD4 within the total gDT-II cell population. **(C)** The normalised mean fluorescence intensity (MFI) of chemokine receptor CXCR3 was measured. **(D)** FoxO1 expression in control and butyrate-treated gDT-II cells is expressed as MFIs normalised to the average expression in the untreated group. **(E)** Eomes expression in gDT-II cells is expressed as MFIs normalised to the average expression in the untreated group. Representative histograms showing transcription factor expression in gDT-II cells are depicted in (D, E). Data are presented as MFI values or mean + SEM of n = 3 – 7 from independent experiments. Asterisks indicate statistically significant differences as analysed by paired Student's *t*-tests (* $p < 0.01$, **** $p < 0.0001$).

Both T-bet and Eomes are known to be regulators of cytotoxic Th1-associated cytokines and cytotoxic mediators [58, 293, 331-333]. We therefore restimulated the $CD4^+$ T cells and investigated the effects of butyrate on the expression of pro-inflammatory cytokines, as well as the cytotoxic mediators granzyme B, perforin and FasL. Control $CD4^+$ T cells produced low levels of IFN-γ (25 ± 2.5%), but butyrate promoted its expression by approximately 2.5-fold to 63 ± 5.5% (Figure 4.3A). TNF-α expression was similarly high in both groups at an estimated level of 93% (Figure 4.3A). Butyrate was also effective at increasing the expression of granzyme B (Ctrl, 61 ± 2.5%; But, 74 ± 1.8%) and FasL (Ctrl, 64 ± 3.2%; But, 84 ± 3.0%) (Figure 4.3A). Perforin too was upregulated by butyrate by more than 2-fold, but its expression remained low (Ctrl, 3.0 ± 0.58%; But, 7.3 ± 1.0%) (Figure 4.3A). This highlighted that despite not regulating Eomes expression, butyrate triggered greater cytotoxic Th1-associated effector molecule production.

It has been demonstrated that Ly6C can be used as a marker for Th1 cells that are better equipped to produce IFN-γ and granzyme B in LCMV infection [305]. As we observed that the effector Th1 marker Ly6C was augmented upon butyrate treatment (Figure 4.2B), we tested whether $Ly6C^+$ and $Ly6C^-$ cells differed in their responses to butyrate. We analysed the expression of IFN-γ, TNF-α and granzyme B within the $Ly6C^+$ and $Ly6C^-$ $CD4^+$ T cell populations. IFN-γ and granzyme B expression were approximately doubled in $Ly6C^+$ effectors compared to their $Ly6C^-$ counterparts in the untreated controls (Figure 4.3B). With the addition of butyrate, IFN-γ was significantly upregulated by more than 2-fold in the $Ly6C^-$ (Ctrl, 16 ± 1.3%; But, 35 ± 3.2%) and $Ly6C^+$ cells (Ctrl, 26 ± 1.9%; But, 51 ± 3.1%). Butyrate also promoted granzyme B both in the $Ly6C^-$ (Ctrl, 27 ± 3.4%; But, 48 ± 5.1%) and $Ly6C^+$ (Ctrl, 52 ± 0.66%; But, 66 ± 1.9%) populations (Figure 4.3B). In contrast, TNF-α production appeared independent of Ly6C expression and butyrate treatment (Figure 4.3B). Butyrate therefore promoted cytokine and cytotoxic molecule expression in $CD4^+$ T cells independently of Ly6C-demarkated populations. Of note, butyrate enabled $Ly6C^-$ $CD4^+$ T cells, which are known to be poorer effectors, to resemble control $Ly6C^+$ cells.

Altogether, butyrate promoted the upregulation of classical Th1 markers T-bet, Ly6C and effector molecules. Although cytotoxic mediator expression was augmented

by butyrate, this was Eomes-independent and appeared unique compared to typical cytotoxic $CD4^+$ T cells that have been previously described. Furthermore, the stemness-associated marker FoxO1 that butyrate upregulated typically represses classical Th1 differentiation. This suggests that while butyrate induces a pro-inflammatory phenotype in $CD4^+$ T cells that shares some features with cytotoxic Th1 cells, butyrate-treated cells show non-classical transcriptional control.

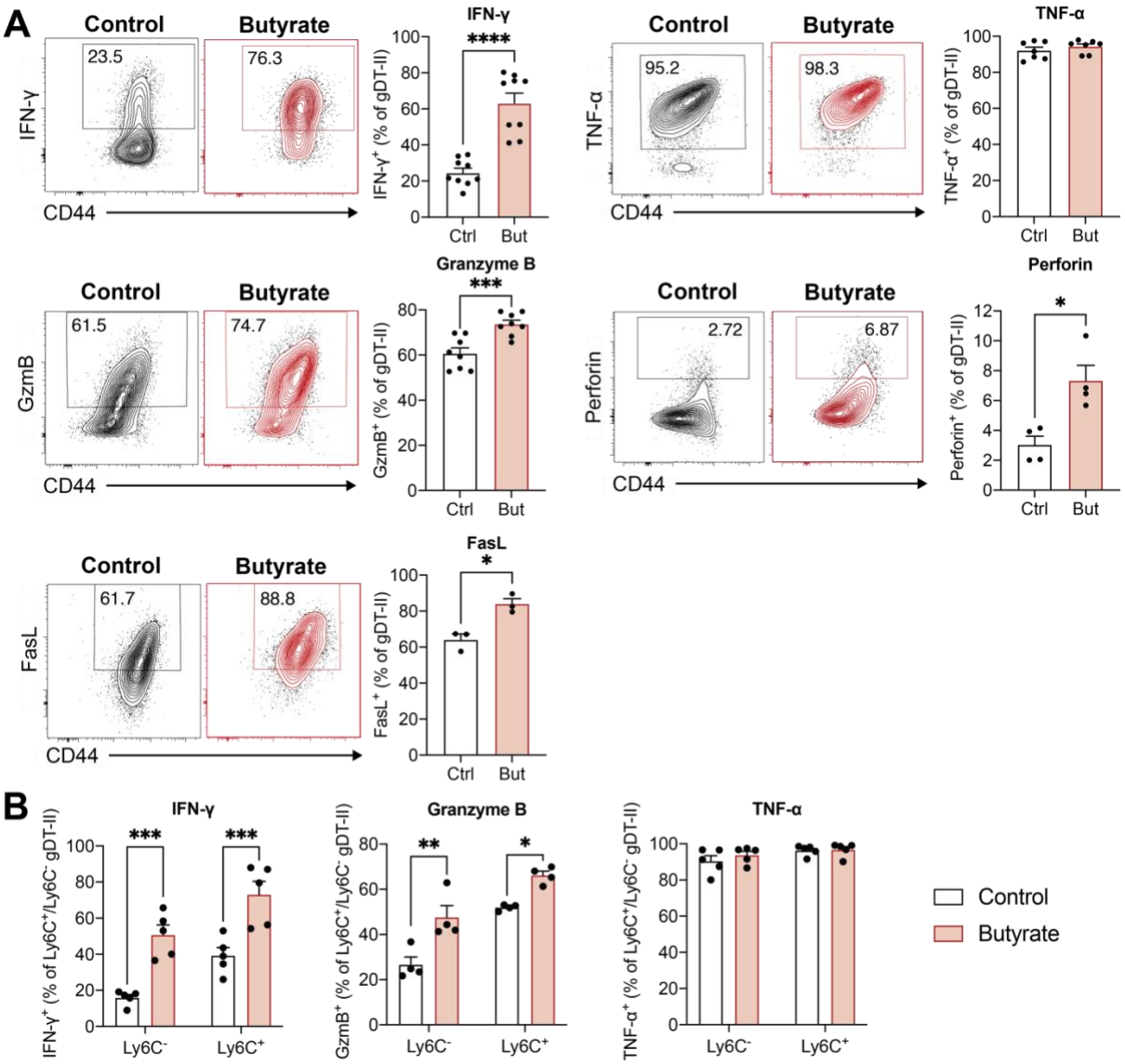

Figure 4.3 Butyrate promotes pro-inflammatory effector molecule expression.

gDT-II cells were activated *in vitro* using splenocytes pulsed with the $gD_{315-327}$ peptide and treated with 0.5 mM butyrate (But) on days 3 to 5 post-activation. Untreated gDT-II cells were used as controls (Ctrl). On day 6, cells were re-stimulated with PMA and ionomycin. Intracellular staining for cytokines and cytotoxic mediators was performed. **(A)** The frequencies of gDT-II cells expressing IFN-γ, TNF-α, granzyme B (GzmB), perforin and Fas ligand (FasL) are shown. Representative contour plots showing effector molecules expression of gDT-II cells against CD44 are depicted. **(B)** gDT-II cells were subdivided into $Ly6C^-$ and $Ly6C^+$ populations. The expression in IFN-γ, TNF-α, and granzyme B by $Ly6C^-$ and $Ly6C^+$ subsets are indicated. Data are presented as normalised MFI values or mean + SEM of n = 3 – 9 independent experiments. Asterisks indicate statistically significant differences as analysed by paired Student's *t*-tests or two-way ANOVA tests (* $p < 0.05$, ** $p < 0.01$, *** $p < 0.001$, **** $p < 0.0001$).

4.2.3 Butyrate-treated CD4$^+$ T cells express more FoxO1 than classical Th1 cells

Having demonstrated the ability of butyrate to promote a pro-inflammatory phenotype in CD4$^+$ T cells, we sought to assess how closely butyrate-treated CD4$^+$ T cells resembled classical Th1 cells. We generated classical Th1 cells by activating gDT-II cells in the presence of IL-12 and anti-IL-4, and compared them to butyrate-treated gDT-II cells cultured without these polarising factors. Butyrate-treated and classical Th1 cells both upregulated T-bet to similar extents, relative to untreated controls (Figure 4.4A). This indicated that butyrate was able to induce T-bet expression to the same extent as IL-12 and anti-IL-4. Interestingly, we detected a difference in FoxO1 expression between butyrate-treated cells and classical Th1 cells, where butyrate induced FoxO1 expression more than the latter (Figure 4.4B). This signified that despite the upregulation of T-bet, this aspect of butyrate-induced transcriptional regulation was distinct from classical Th1 cells.

As we had detected increased cytokine expression following butyrate treatment, we next compared these levels to the cytokine profile of classical Th1 cells. CD4$^+$ T cells from the butyrate and classical Th1 groups expressed similar levels of IFN-γ, TNF-α and granzyme B (Figure 4.4C). Interestingly, the frequency of Th1 cells expressing perforin was comparable to the untreated controls but consistently lower than butyrate-treated cells (Figure 4.4C). FasL expression was marginally elevated in the butyrate-treated group compared to classical Th1 cells but this difference did not reach significance (Figure 4.4C). Butyrate-treated CD4$^+$ T cells hence have a similar effector molecule profile as classical Th1 cells.

Together, we showed that classical Th1 polarising factors did not completely replicate the effects of butyrate, suggesting that butyrate's mechanism may be distinct to that of IL-12 and anti-IL-4. Importantly, the upregulation of stemness-associated factor FoxO1 by butyrate and not IL-12/anti-IL-4-mediated polarisation was unique to butyrate-treated CD4$^+$ T cells.

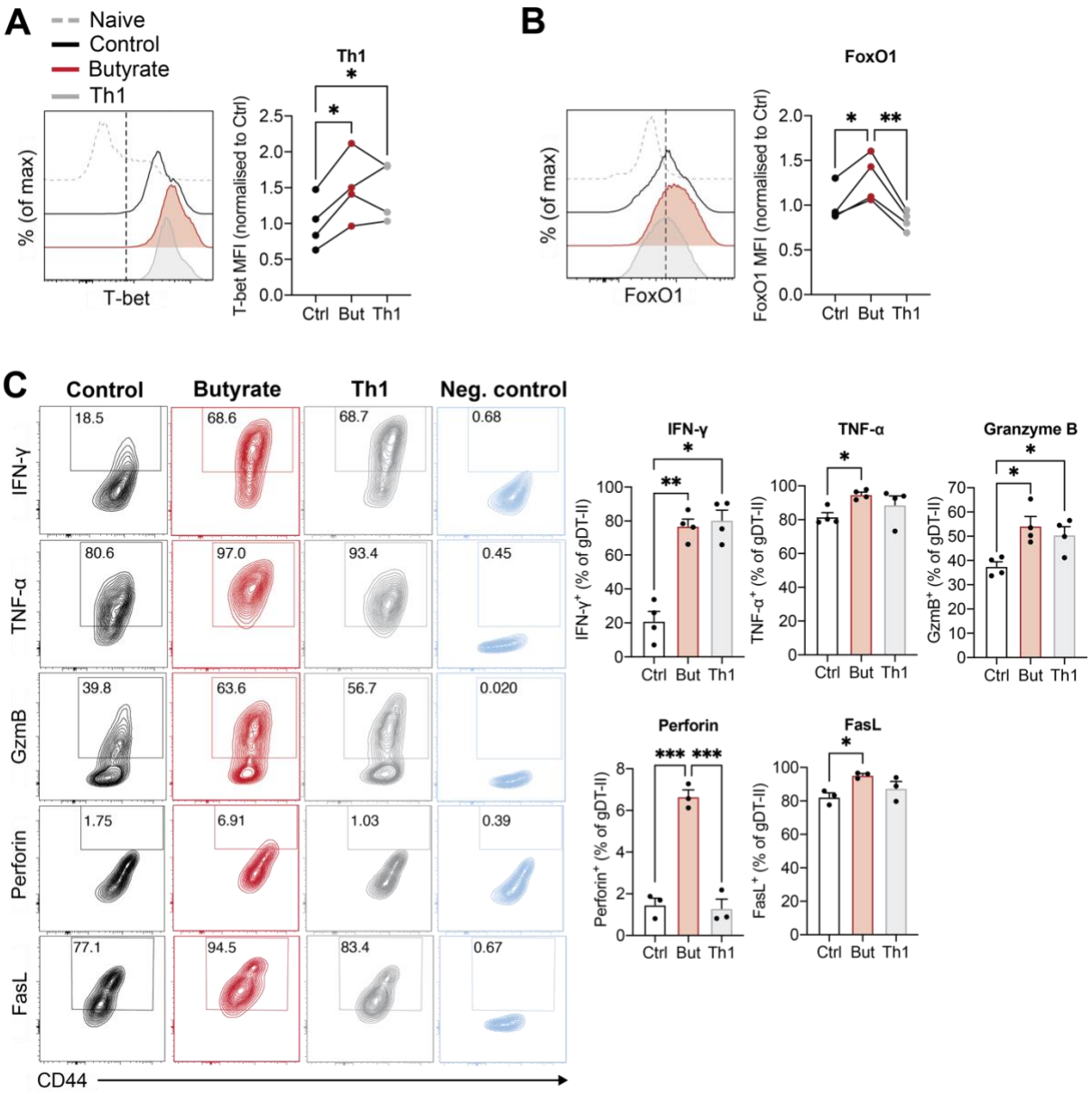

Figure 4.4 Butyrate simultaneously promotes classical Th1-associated marker expression and FoxO1.

gDT-II cells were activated *in vitro* with splenocytes pulsed with the $gD_{315-327}$ peptide in the absence or presence of the classical Th1 polarising conditions IL-12 and anti-IL-4. Cells that were not exposed to Th1 polarising factors were either cultured with 0.5 mM butyrate (But) on days 3 to 5 post-activation, or remained untreated (control; Ctrl). Classical Th1 cells were not treated with butyrate. Analysis was performed on day 6 after activation. **(A)** Th1 polarisation is shown as the mean fluorescence intensity (MFI) of T-bet normalised to the untreated gDT-II cells. Representative histograms are indicative of T-bet expression in naïve gDT-II cells, untreated gDT-II controls, But-treated gDT-II cells and gDT-II Th1 cells. **(B)** The MFI of FoxO1 was normalised to the untreated group. Representative histograms are indicative of FoxO1 expression in naïve gDT-II cells, untreated gDT-II controls, But-treated gDT-II cells and gDT-II Th1

cells. **(C)** Intracellular staining for cytokines and cytotoxic mediators was performed using PMA and ionomycin for re-stimulation for 5 hours. The frequencies of gDT-II cells expressing IFN-γ, TNF-α, granzyme B (GzmB), perforin and Fas ligand (FasL) are shown. IFN-γ and TNF-α expression of unstimulated cells and GzmB, perforin and FasL of fluorescence minus one samples were used as negative controls (blue). Representative contour plots show effector molecule expression against CD44 within the gDT-II population. Data are presented as normalised MFI values or mean + SEM of n = 3 – 4 independent experiments. Asterisks indicate statistically significant differences as analysed by one-way ANOVA tests (* $p < 0.05$, ** $p < 0.01$, *** $p < 0.001$).

4.2.4 The Th1-like phenotype induced by butyrate is maintained *in vivo* upon HSV-1 infection

To investigate the effects of butyrate-induced upregulation of T-bet and Ly6C in an infection model, we tested their expression following adoptive transfer and HSV-1 infection (e.c.). gDT-II cells were activated with $gD_{315-327}$-loaded splenocytes as described above and treated with butyrate daily from day 2 to 5 (Figure 4.5A). On day 6, $CD45.1^+$ gDT-II cells were adoptively transferred into naïve $CD45.2^+$ B6 recipients. To allow cells to rest, mice were infected with HSV-1 by flank scarification 14 days post-transfer. $V\alpha3.2^+CD45.1^+CD4^+$ gDT-II cells in the spleens, skin, and draining brachial lymph nodes (bLNs) of mice were analysed on day 7 post-infection.

As expected, a high proportion of splenic gDT-II cells expressed T-bet following HSV-1 infection, validating their differentiation into Th1-like cells (Figure 4.5B). Butyrate pre-treatment importantly enhanced T-bet expression further (Ctrl, 74 ± 4.9%; But, 86 ± 2.4%) (Figure 4.5B), in line with their phenotype prior to adoptive transfer. Similarly, higher T-bet expression was observed in the bLN of the butyrate group (73 ± 2.8%) than controls (57 ± 2.7%) (Figure 4.5B). These results suggested that T-bet upregulation by butyrate was stable and detectable even after secondary antigen exposure. Ly6C expression marked cells that produced IFN-γ and granzyme B at high levels *in vitro* (Figure 4.3B). Following infection, Ly6C expression in the spleen, skin and bLN of the butyrate treatment group was at least greater than the controls by 1.4-fold, 1.7-fold and 1.5-fold respectively (Figure 4.5C). Hence, gDT-II cells that were pre-treated with butyrate promoted this Th1 effector marker in both the secondary lymphoid organs and at the site of infection. Short-term *in vitro* butyrate exposure therefore induces long-lasting effects, which persists even after pathogenic infection.

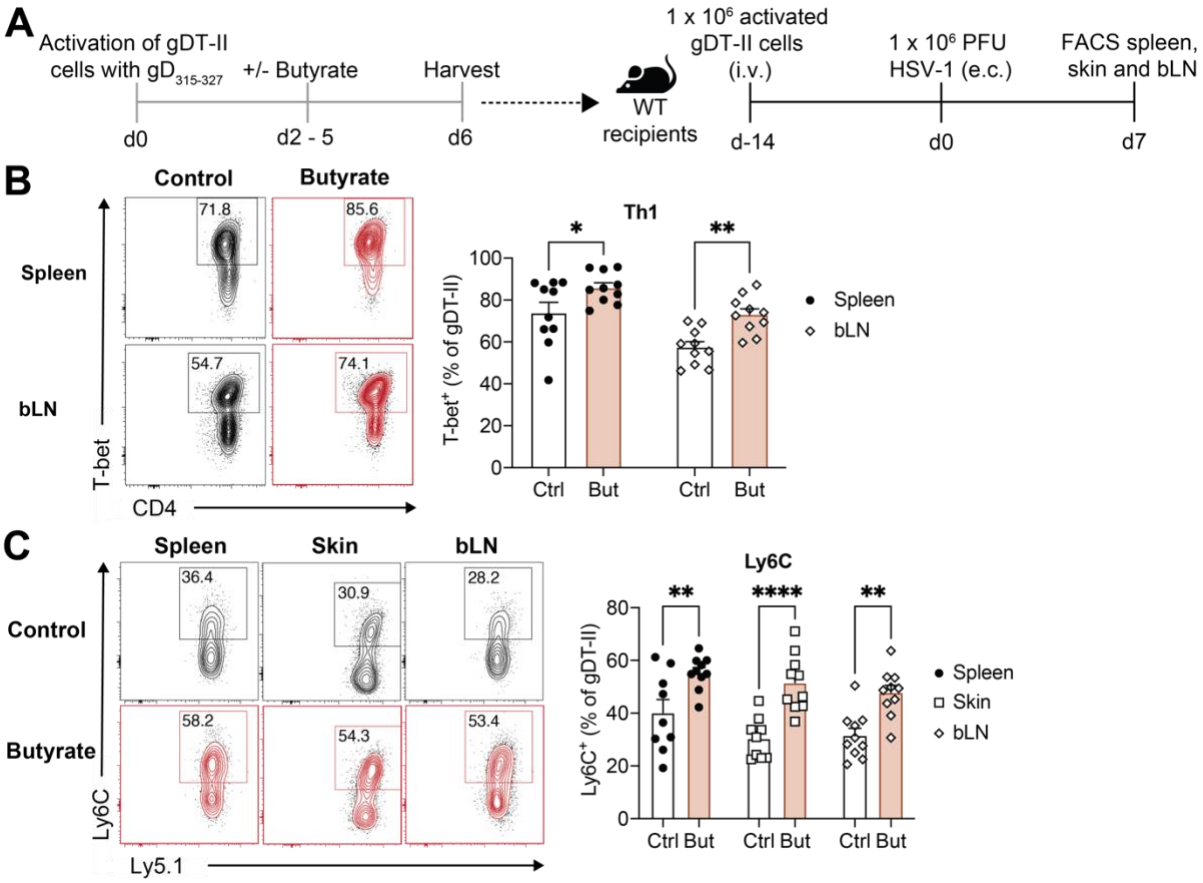

Figure 4.5 The stronger Th1-like differentiation induced by butyrate *in vitro* is maintained following HSV-1 infection *in vivo.*

Ly5.1$^+$ gDT-II cells were activated *in vitro* with $gD_{315-327}$-pulsed splenocytes, and were either untreated (control; Ctrl) or treated with 0.5 mM butyrate (But) on days 2 to 5. On day 6, 1 x 10^6 cells were intravenously (i.v.) transferred into Ly5.2$^+$ wildtype (WT) recipients. 14 days later, mice were epicutaneously (e.c.) infected with 1 x 10^6 plaque forming units (PFU) HSV-1. The spleen, skin and the draining brachial lymph nodes (bLNs) were collected on day 7 post-infection. **(A)** Schematic of experimental setup. **(B)** The frequency of gDT-II cells from the spleen and bLNs that expressed T-bet. The representative contour plots show T-bet expression of gDT-II cells against CD4. **(C)** Ly6C$^+$ cells in spleens, skins and bLNs were expressed as a frequency of total gDT-II cells. Representative contour plots show Ly6C expression against Ly5.1 within the gDT-II population. Data are presented as mean + SEM of n = 7 – 10 mice from at least 2 pooled independent experiments. Asterisks indicate statistically significant differences as analysed by two-way ANOVA tests (* $p < 0.05$, ** $p < 0.01$, **** $p < 0.0001$).

4.2.5 The mechanisms of butyrate: receptors, metabolism and epigenetic modifications

The complex regulatory effects of SCFAs in different cell types have mainly been attributed to the following mechanisms of action: SCFA receptor signalling, epigenetic modifications, and metabolic rewiring [186, 334, 335]. In this sub-chapter, we aimed to identify which of these mechanisms resulted in the observed non-classical cytotoxic Th1-like phenotype. Of note, butyrate-engaged mechanisms overlap with mechanisms required for Th1 lineage commitment. This includes specific molecules that participate in the GPR41 and GPR43 signalling cascades, metabolic changes and hyperacetylation of *Ifng* and *Tbet* promoters [89, 173, 336-341]. As such, we investigated the importance of these mechanisms in butyrate-driven differentiation and functionality.

4.2.5.1 The expression of GPR41 and GPR43 is dispensable for Th1 induction by butyrate *in vitro*

In Chapter 3, we highlighted a role for GPR41 and GPR43 in supporting optimal memory potential and effector function of $CD8^+$ T cells. We hence sought to evaluate whether butyrate may be inducing changes in $CD4^+$ T cell differentiation and function through its G protein-coupled receptors. Using RT-qPCR, we measured the expression of *Ffar2*, *Ffar3* and *Hcar2* (which encode GPR43, GPR41 and GPR109a respectively) in activated $CD4^+$ T cells that were cultured in the presence and absence of butyrate to determine if $CD4^+$ T cells expressed these receptors and if butyrate was capable of regulating their expression. mRNA transcripts of *Ffar2* and *Hcar2*, but not *Ffar3*, were detected in untreated control $CD4^+$ T cells (Figure 4.6A). Importantly, all SCFA receptor transcripts were upregulated after butyrate treatment by up to 8-fold (Figure 4.6A). As such, this suggests that $CD4^+$ T cells can detect SCFAs via receptors, and butyrate positively regulated SCFA receptor gene expression.

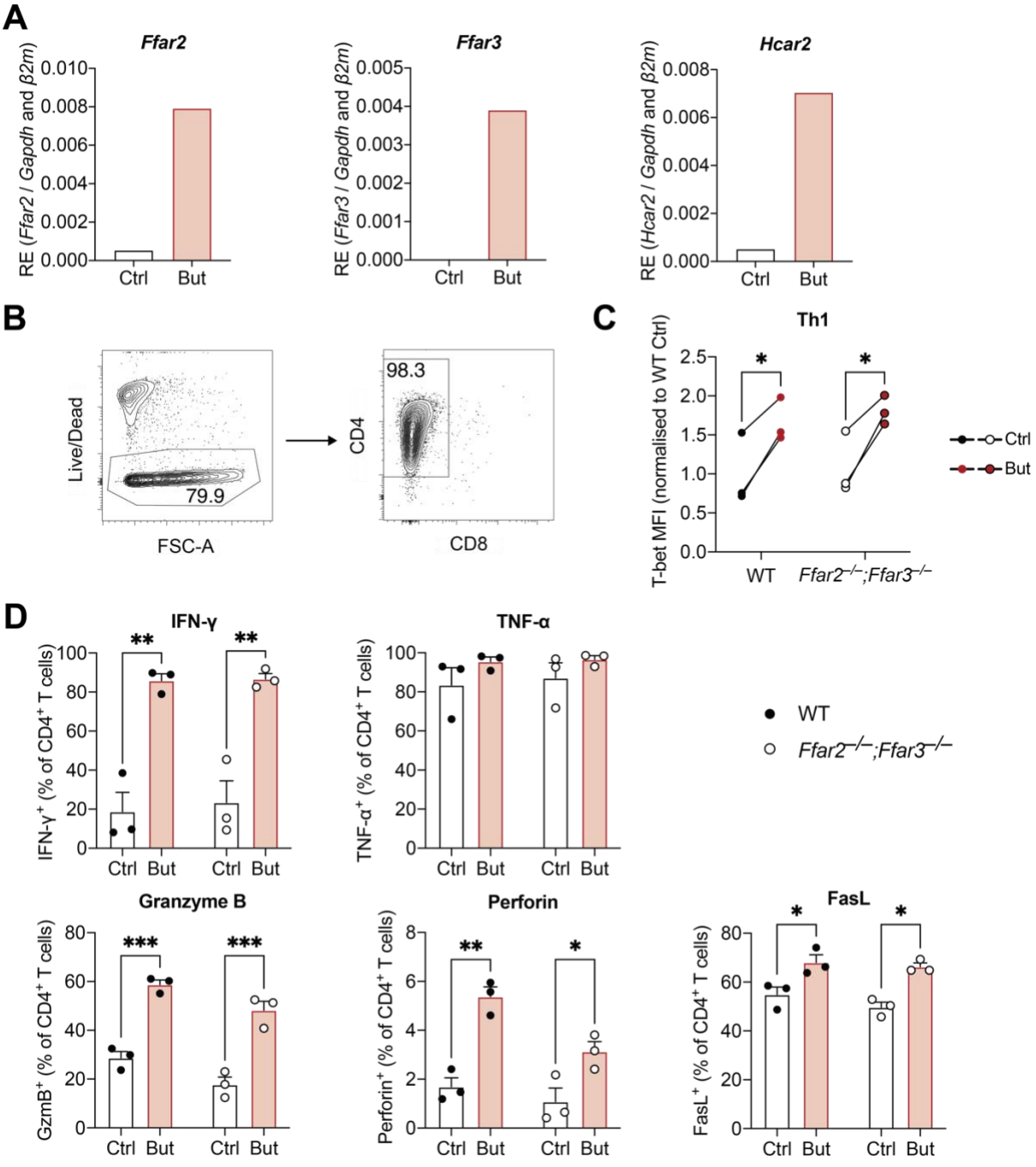

Figure 4.6 Butyrate does not alter CD4⁺ T cell polarisation through GPR41 and GPR43.

(A) Wildtype (WT) gDT-II cells were activated *in vitro* with splenocytes pulsed with the $gD_{315-327}$ peptide and LPS, and supplemented with IL-2. Cells were cultured in the absence (Control; Ctrl) or presence of 0.5 mM butyrate (But) from days 3 to 5, and analysed on day 6. *Ffar2*, *Ffar3* and *Hcar2* expression in activated WT CD4⁺ T cells were analysed using real-time quantitative polymerase chain reaction. **(B – D)** WT and *Ffar2*$^{-/-}$;*Ffar3*$^{-/-}$ polyclonal CD4⁺ T cells were activated *in vitro* using anti-CD3ε and anti-CD28. Cells were cultured in the absence or presence of 0.5 mM butyrate from

days 3 to 5, and analysed on day 6 using flow cytometry by gating on live $CD4^+CD8^-$ cells. The representative gating strategy is shown in (B). The mean fluorescence intensity (MFI) of T-bet expression in untreated control and butyrate-treated cells from WT and *Ffar2*$^{-/-}$*;Ffar3*$^{-/-}$ mice (C). Cells were re-stimulated with PMA and ionomycin. IFN-γ, TNF-α, granzyme B (GzmB), perforin and Fas ligand (FasL) expression is shown as the frequency of $CD4^+$ T cells (D). Data are presented as mean of n = 2 replicates in a single experiment in (A), and normalised MFI values or mean + SEM of n = 3 independent experiments in (C and D). Asterisks indicate statistically significant differences as analysed by two-way ANOVA tests (* $p < 0.05$, ** $p < 0.01$, *** $p < 0.001$). No statistical testing was performed in (A) due to the sample size.

Next, we tested the role of GPR41 and GPR43 expression in butyrate-mediated T-bet upregulation using polyclonal $CD4^+$ T cells that were isolated from WT and *Ffar2*$^{-/-}$;*Ffar3*$^{-/-}$ mice and activated with anti-CD3ε and anti-CD28 *in vitro*. Live $CD4^+CD8^-$ cells were gating on using flow cytometric analysis (Figure 4.6B). Regardless of GPR41 and GPR43 expression, T-bet expression was comparable in $CD4^+$ T cells cultured in the absence of butyrate (Figure 4.6C). Moreover, butyrate promoted T-bet expression to similar extents in both the WT and *Ffar2*$^{-/-}$;*Ffar3*$^{-/-}$ groups. As GPR41/43 were required by $CD8^+$ T cells to induce optimal TNF-α production (Chapter 3), Th1 effector molecule expression was compared in these experiments. Butyrate-treated GPR41- and GPR43-deficient $CD4^+$ T cells expressed greater levels of IFN-γ, granzyme B, perforin and FasL compared to their untreated counterparts (Figure 4.6D). This trend was similar to the WT groups (Figure 4.6D). TNF-α remained comparable in both groups (Figure 4.6D). This indicated that *in vitro* induction of T-bet expression and Th1 effector molecules were independent of butyrate sensing by GPR41 and GPR43.

4.2.5.2 Butyrate- and histone acetylation-induced effector molecule expression are similar

Butyrate is a well-known inhibitor of HDACs, and its metabolic intermediate acetyl-CoA can act as a substrate for histone acetyltransferases [166, 339, 342]. Increased histone acetylation provides a more permissive chromatin state, allowing for gene transcription. Acetate's induction of the Th1 lineage has been suggested to be a result of histone acetylation [124]. We therefore measured histone acetylation in butyrate-treated cells directly and compared this to cells treated with TSA, a pan-HDAC inhibitor. Our Western blot analyses detected that butyrate induced more total histone H3 acetylation (H3ac) compared to untreated cells, and was similar to the positive control TSA (Figure 4.7A).

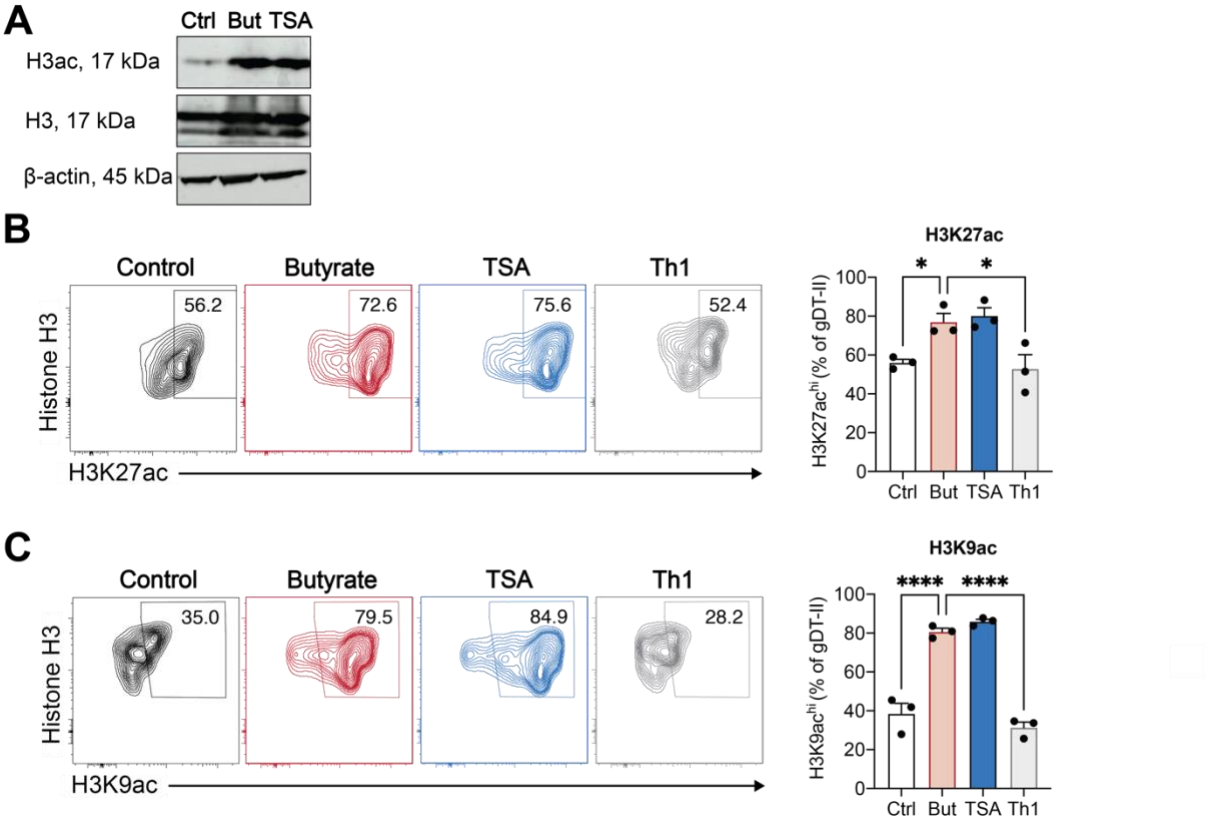

Figure 4.7 Butyrate induces histone H3 acetylation.

gDT-II cells were were activated *in vitro* with splenocytes pulsed with the $gD_{315-327}$ peptide and LPS, and supplemented with IL-2. Cells were cultured in the absence or presence of 0.5 mM butyrate (But) or 15 nM Trichostatin A (TSA) from days 3 to 5. Th1 cells were generated from IL-12 and anti-IL-4 treatment. Analysis was performed on day 6. **(A)** Representative Western blots of histone H3 acetylation (H3ac) are shown. Histone H3 and β-actin were used as loading controls. **(B)** The frequency of gDT-II cells possessing histone H3 lysine 27 acetylation (H3K27ac) was measured. **(C)** The frequency of gDT-II cells possessing histone H3 lysine 9 acetylation (H3K9ac) was measured. Representative contour plots showing histone H3K27ac and H3K9ac against histone H3 of gDT-II cells are depicted in (B and C). Data are representative of n = 3 experiments. Asterisks indicate statistically significant differences as analysed by one-way ANOVA tests (* $p < 0.05$, **** $p < 0.0001$).

To extend these findings on histone H3 acetylation, we investigated quantitative changes in acetylation of specific lysine residues of histone 3 using a flow cytometric approach. Acetylation of histone H3 lysine 27 (H3K27ac) and histone H3 lysine 9 (H3K9ac) have been identified at promoters of genes encoding pro-inflammatory cytokine and cytotoxic mediators in classical Th1 cells [341, 343]. We discovered that 56 ± 1.8% of untreated *in vitro*-activated $CD4^+$ T cells possessed high levels of H3K27ac, whereas these levels were greater in butyrate- and TSA-treated cells (But, 77 ± 4.4%; TSA, 80 ± 4.2%) (Figure 4.7B). This indicated that butyrate had a high capacity to induce acetylation of H3K27. In contrast, 53 ± 7.4% of classical Th1 cells possessed H3K27 hyperacetylation, suggesting that butyrate induced more acetylation of H3K27 than Th1 polarising factors. H3K9 acetylation was also detected in 81 ± 1.8% of butyrate-treated cells and 86 ± 1.2% of TSA-treated cells, which were considerably greater than untreated controls (38 ± 5.3%) and Th1 cells (31 ± 2.8%) (Figure 4.7C). Butyrate therefore led to hyperacetylation of histone H3 residues which are known to carry functional importance in Th1 lineage commitment and function.

To determine if butyrate induced this phenotype specifically by histone acetylation, we next aimed to identify if TSA-mediated histone acetylation induced a similar non-classical cytotoxic Th1 phenotype. Activated gDT-II cells that received either butyrate or TSA treatment for 3 days were analysed for their subset differentiation and memory-associated phenotype. The range of 5 – 15 nM TSA that we selected had been found to be effective in prior T cell studies [162, 344]. While a small but insignificant dose-dependent effect on T-bet was recorded, FoxO1 expression was comparable to untreated $CD4^+$ T cells after TSA treatment (Figure 4.8A and B). As butyrate-induced T-bet and FoxO1 levels were significantly greater than that of TSA-treated cells at all concentrations tested, histone acetylation alone could not reproduce butyrate's induction of T-bet and FoxO1.

$CD4^+$ T cells were re-stimulated to evaluate how histone acetylation modulates effector molecule expression. Interestingly, TSA had a dose-dependent effect on most effector molecules, indicating some level of regulation by histone acetylation. IFN-γ was expressed by 75 ± 1.0% of butyrate-treated cells, compared to 68 ± 4.7% of 15 nM TSA-treated cells (Figure 4.8C). This highest concentration of TSA was also able to

promote TNF-α and FasL to a similar level as butyrate (Figure 4.8C). Both butyrate and TSA (at a concentration as low as 5 nM) increased granzyme B expression to a comparable level (Figure 4.8C). In contrast, butyrate upregulated perforin considerably more than TSA (But, 14 ± 1.3 %; 15 nM TSA, 3.5 ± 0.79%) (Figure 4.8C). This provides evidence that histone acetylation facilitates cytokine and cytotoxic mediator upregulation. The relatively greater dependency of IFN-γ, TNF-α, granzyme B, and FasL expression on histone acetylation was evident, while histone acetylation only had a minor contribution to perforin expression. As butyrate and TSA induced similar levels of histone H3 acetylation, it is tempting to speculate that butyrate-induced histone acetylation may play a major role in the augmentation of effector molecule expression, with the exception of perforin.

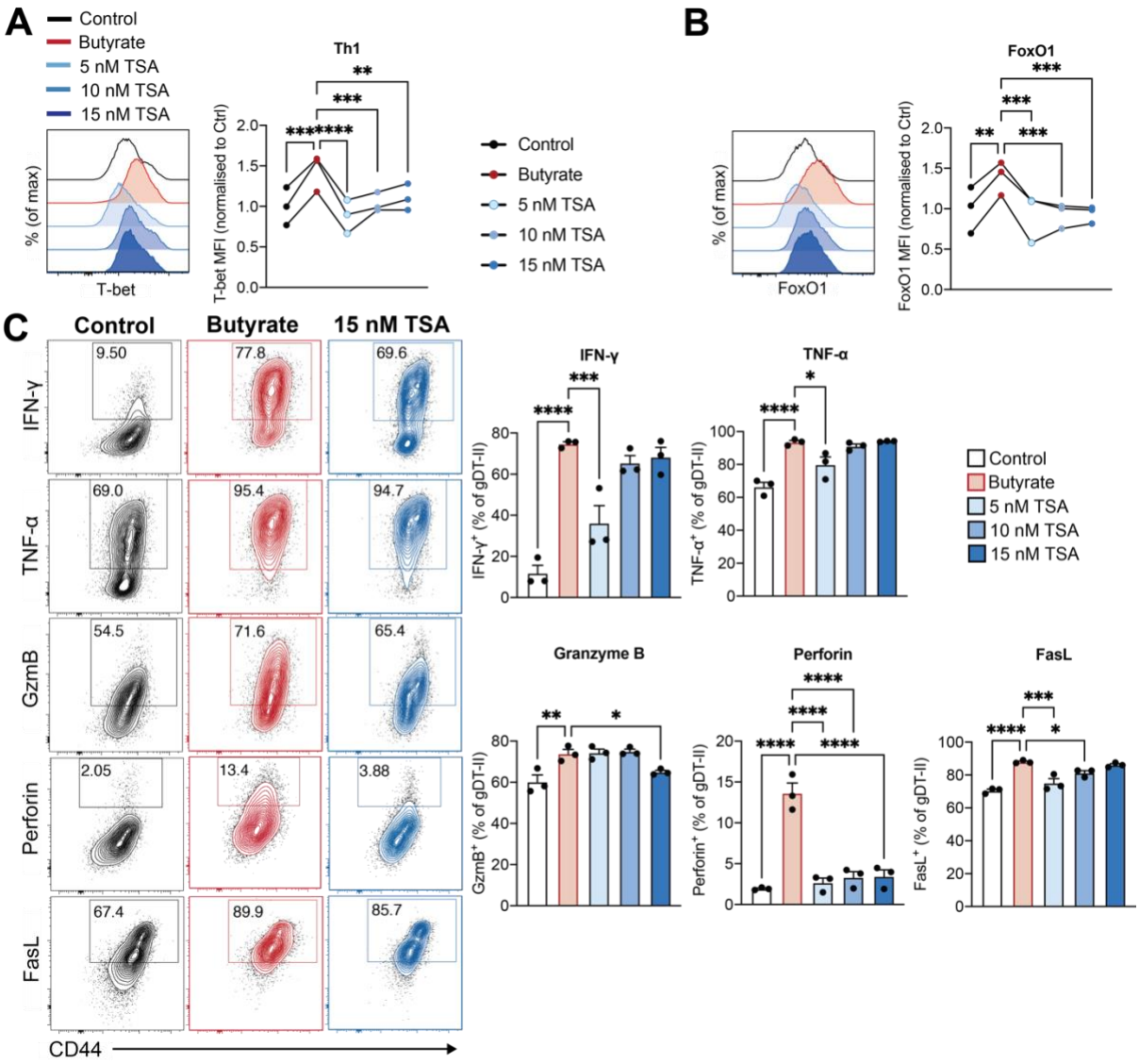

Figure 4.8 Histone acetylation promotes effector molecule expression.

gDT-II cells were activated *in vitro* with splenocytes pulsed with the $gD_{315-327}$ peptide and LPS, and supplemented with IL-2. Cells were cultured with 0.5 mM butyrate (But), 5 – 15 nM Trichostatin A (TSA) or were left untreated (Control; Ctrl) from days 3 to 5, and analysed on day 6. **(A)** The mean fluorescence intensity (MFI) of T-bet in gDT-II cells was normalised to the average T-bet MFI of the untreated group. Representative histograms depicting T-bet expression within gDT-II cells is shown. **(B)** The MFI of FoxO1 in gDT-II cells was normalised to the average FoxO1 MFI of the untreated group. Representative histograms depicting FoxO1 expression within gDT-II cells is shown. **(C)** Cells were restimulated with PMA and ionomycin for 5 hours. IFN-γ, TNF-α, granzyme B (GzmB), perforin and Fas ligand (FasL) expression are expressed as the frequencies of gDT-II cells. Representative contour plots depict effector molecule expression of gDT-II cells against CD44. Data are presented as mean + SEM, n = 3 independent experiments. Asterisks indicate statistically significant differences as

analysed by one-way ANOVA tests (* $p < 0.05$, ** $p < 0.01$, *** $p < 0.001$, **** $p < 0.0001$).

4.2.5.3 The glycolytic reserve and spare respiratory capacity of CD4$^+$ T cells are enhanced by butyrate

Th1 polarisation is accompanied by a shift towards anabolic metabolism characterised by cell growth and the synthesis of cellular products [345]. Upregulated glucose uptake and glycolysis in Th1 cells are particularly crucial in the effector phase to facilitate greater cytokine production [346, 347]. To assess the impact of butyrate on glycolysis, we performed a Seahorse Glycolysis Stress Test. Changes in the extracellular acidification rate (ECAR), a result of proton extrusion during glycolysis, were measured at various timepoints upon sequential addition of glucose as substrate for glycolysis, followed by oligomycin to inhibit mitochondrial ATP production and shift metabolic reliance to glycolysis, and finally 2-deoxy-D-glucose (2-DG) that inhibited glycolysis (Figure 4.9A). We compared untreated and butyrate-treated CD4$^+$ T cells to classical Th1 cells due to their known high glycolytic rate, which is understood to be intimately linked to their IFN-γ production [348]. As expected, classical Th1 cells exhibited a higher glycolytic level than untreated controls (Ctrl, 25 ± 2.3 mpH/min; Th1, 34 ± 1.5 mpH/min) (Figure 4.9B). We identified a low rate of glycolysis in butyrate-treated CD4$^+$ T cells (10 ± 0.39 mpH/min), which was less than half of that of their untreated counterparts and a third of Th1 cells (Figure 4.9B). Compared to Th1 cells, butyrate-treated cells also exhibited significantly lower levels of glycolytic capacity, which refers to the maximum ECAR rate (Figure 4.9B). Interestingly, butyrate increased the glycolytic reserve of CD4$^+$ T cells relative to untreated controls and Th1 cells (Figure 4.9B). This implied that butyrate-treated cells possessed a greater potential to increase ATP production through glycolysis under stress. Together, these findings suggested that butyrate-treated cells and classical Th1 cells were metabolically distinct.

Epigenetic modifications and cellular metabolism are able to influence each other bi-directionally [349, 350]. In particular, HATs and HDACs can regulate the expression and activity of metabolic enzymes [351]. To understand how histone acetylation influences glycolysis in CD4$^+$ T cells and if this mechanism contributed to butyrate-mediated glycolytic changes, we compared the effect of TSA to butyrate. We made the interesting observation that TSA-induced changes in CD4$^+$ T cell metabolism trended similarly to butyrate, although the differences in glycolysis, glycolytic capacity and glycolytic reserve compared to untreated controls were not

statistically significant (Figure 4.9B). This suggests that histone acetylation likely influenced glycolysis, and is potentially a mechanism by which butyrate reduced glycolytic metabolism.

Both glycolysis and FAO provide substrates for the TCA cycle and oxidative phosphorylation which occur in the mitochondria. Mitochondrial respiratory Complex I is reportedly important for $CD4^+$ T helper cell epigenetic remodelling at early timepoints, while Complex II supports Th1 terminal effector cell function [352]. To analyse the effects of butyrate on $CD4^+$ T cell mitochondrial respiration, we measured the oxygen consumption rate (OCR), which is proportional to mitochondrial respiration, using a Seahorse Cell Mito Stress Test (Figure 4.9C). These measurements were performed upon sequential addition of oligomycin, carbonyl cyanide-4 (trifluoromethoxy) phenylhydrazone (FCCP) which disrupts the mitochondrial membrane potential, and Complex I and III inhibitors rotenone and antimycin A that inhibit mitochondrial respiration and enable measurements of acidification (Figure 4.9C). Butyrate had negligible effects on the basal respiration, maximal respiration and mitochondrial ATP production of $CD4^+$ T cells relative to untreated controls (Figure 4.9D). Furthermore, the basal respiration and mitochondrial ATP production rate of butyrate-treated $CD4^+$ T cells were lower than that of Th1 cells, although these differences were not statistically significant (Figure 4.9D). We however, detected that the spare respiratory capacity, indicative of the ability of the cell to respond to an energetic demand through mitochondrial respiration, was greater in butyrate-treated $CD4^+$ T cells than untreated controls and Th1 cells (Figure 4.9D). Our findings indicated that butyrate may enable $CD4^+$ T cells to adapt better to metabolically stressful conditions through mitochondrial respiration.

When assessing the effects of histone acetylation in mitochondrial metabolism, we found that TSA-treated $CD4^+$ T cells did not significantly differ from all other groups in terms of their basal respiration, maximal respiration and mitochondrial ATP production (Figure 4.9D). The spare respiratory capacity of the TSA and butyrate groups showed a similar trend relative to untreated controls and Th1 cells (Figure 4.9D). Altogether, butyrate may increase the propensity of the cell to meet sudden rises in energy demands through glycolysis and mitochondrial respiration. Butyrate alters the metabolic profile of $CD4^+$ T cells in a manner that is distinct from classical

Th1 cells, and instead bears a closer resemblance to cells possessing histone hyperacetylation.

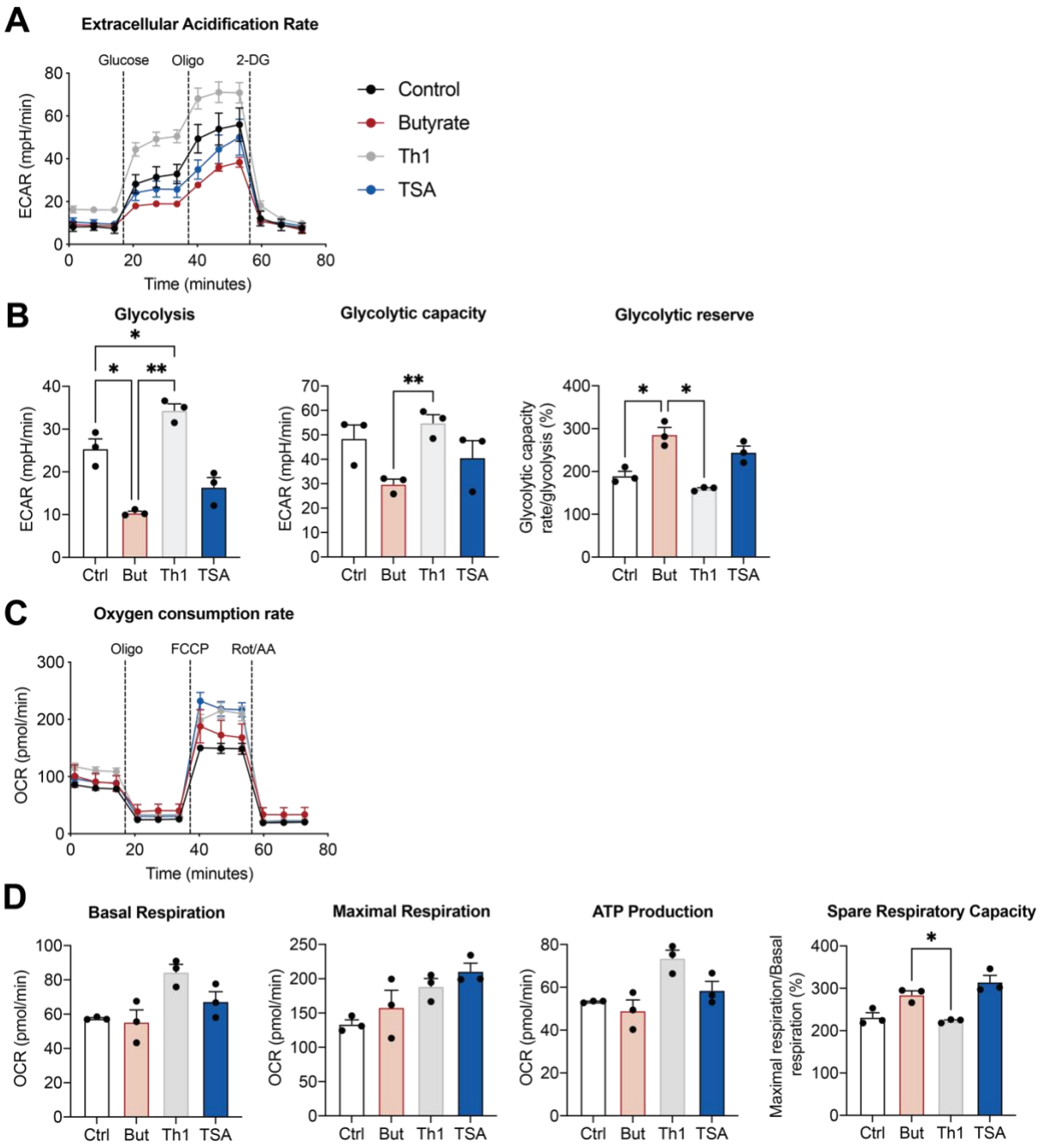

Figure 4.9 Butyrate increases CD4⁺ T cell glycolytic reserve and spare respiratory capacity.

gDT-II cells were activated *in vitro* with splenocytes pulsed with the $gD_{315-327}$ peptide and LPS, in the absence or presence of classical Th1 polarising conditions (IL-12 and anti-IL-4). Cells that were not exposed to Th1 polarising factors were either cultured with 0.5 mM butyrate (But) or 15 nM Trichostatin A (TSA) on days 3 to 5 post-activation, or remained untreated (Control; Ctrl). Seahorse metabolic assays were performed on day 6 after activation. **(A, B)** Glycolysis Stress Tests were performed. The extracellular acidification rates (ECAR) of CD4⁺ T cells were measured under

basal conditions, and in response to glucose, oligomycin (Oligo) and 2-deoxy-D-glucose (2-DG) (A). Glycolysis, glycolytic capacity and glycolytic reserve are shown in (B). **(C, D)** Mito Stress Tests were performed. The oxygen consumption rate (OCR) of $CD4^+$ T cells was measured under basal conditions, and in response to Oligo, carbonyl cyanide-4 (trifluoromethoxy) phenylhydrazone (FCCP), and rotenone and antimycin A (Rot/AA) (C). The basal respiration, maximal respiration, ATP production and spare respiratory capacity of groups are shown in (D). Data are presented as mean ± SEM (A, C) or mean + SEM (B, D) of n = 3 experiments. Asterisks indicate statistically significant differences as analysed by one-way ANOVA tests (* $p < 0.05$, ** $p < 0.01$).

4.2.6 Butyrate regulates Th1-like differentiation through FoxO1

FoxO1 is a transcription factor that regulates T cell survival, homeostasis and differentiation [52, 353, 354]. As FoxO1 is reportedly downregulated upon Th1 polarisation [354], we found it interesting that butyrate induced both a Th1 phenotype and FoxO1 expression simultaneously. To better understand the role of FoxO1 induction, we studied this relationship further by treating activated gDT-II cells with the FoxO1 inhibitor (FoxO1i) AS1842856 at a range of concentrations, 30 minutes prior to daily butyrate treatment. FoxO1i treatment did not appreciably alter FoxO1 expression in control $CD4^+$ T cells, but completely negated butyrate-mediated FoxO1 upregulation at all FoxO1i concentrations (Figure 4.10A). This suggests that FoxO1 likely upregulated its own expression in butyrate-treated $CD4^+$ T cells. To better understand the interplay between FoxO1, butyrate and $CD4^+$ T cell differentiation, we analysed if the FoxO1i influenced the expression of T-bet. Although FoxO1 inhibition did not influence T-bet expression in untreated controls, $CD4^+$ T cells that had been exposed to a combination of butyrate and FoxO1i showed a partial reduction in Th1 polarisation in a FoxO1i dose-dependent manner (Figure 4.10B). Even at the highest FoxO1i concentration of 1 mM, Th1 polarisation of the butyrate-treated cells was still greater than the untreated controls. This suggested that butyrate-induced Th1 polarisation was in part dependent on FoxO1 regulation.

We sought to gain insights into the butyrate-mediated regulation of the Th1 effector markers through FoxO1. Similar to T-bet, Ly6C expression was not altered by FoxO1i in $CD4^+$ T cells that were cultured in the absence of butyrate (Figure 4.10C). However, butyrate-induced upregulation of Ly6C was completely abrogated by treatment with 1 mM FoxO1i (Figure 4.10C). As we previously showed that Ly6C correlated with IFN-γ and granzyme B expression, we proceeded to investigate the relationship between butyrate, FoxO1 and effector molecule expression. FoxO1 inhibition partially reduced IFN-γ expression from 41 ± 9.4% (0 mM FoxO1i) to 21 ± 1.8% (1 mM FoxO1i) in cells that were cultured with butyrate (Figure 4.10D). Less than 4% of cells lacking butyrate treatment produced IFN-γ regardless of FoxO1 inhibition. The lower IFN-γ expression in this experiment was due to the weaker batch of PMA used in comparison to other experiments in this chapter. Regardless, there remained a prominent difference between the control and butyrate groups. The inhibition of

FoxO1 reduced granzyme B expression by control $CD4^+$ T cells from 45 ± 1.9% to 1.6 ± 0.31% (Figure 4.10D). Interestingly, granzyme B expression of butyrate-treated cells peaked at 0.25 mM FoxO1i but remained relatively unchanged at the highest FoxO1i dose (Figure 4.10D). This indicated that butyrate does not positively regulate granzyme B through FoxO1 in $CD4^+$ T cells. TNF-α expression was not influenced by FoxO1 inhibition in both control and butyrate groups (Figure 4.10D). This signified a major role for FoxO1 as a positive regulator in the butyrate-driven induction of the Th1 effector markers Ly6C and IFN-γ. FoxO1 was hence important in the modulation of $CD4^+$ T cell differentiation and function by butyrate.

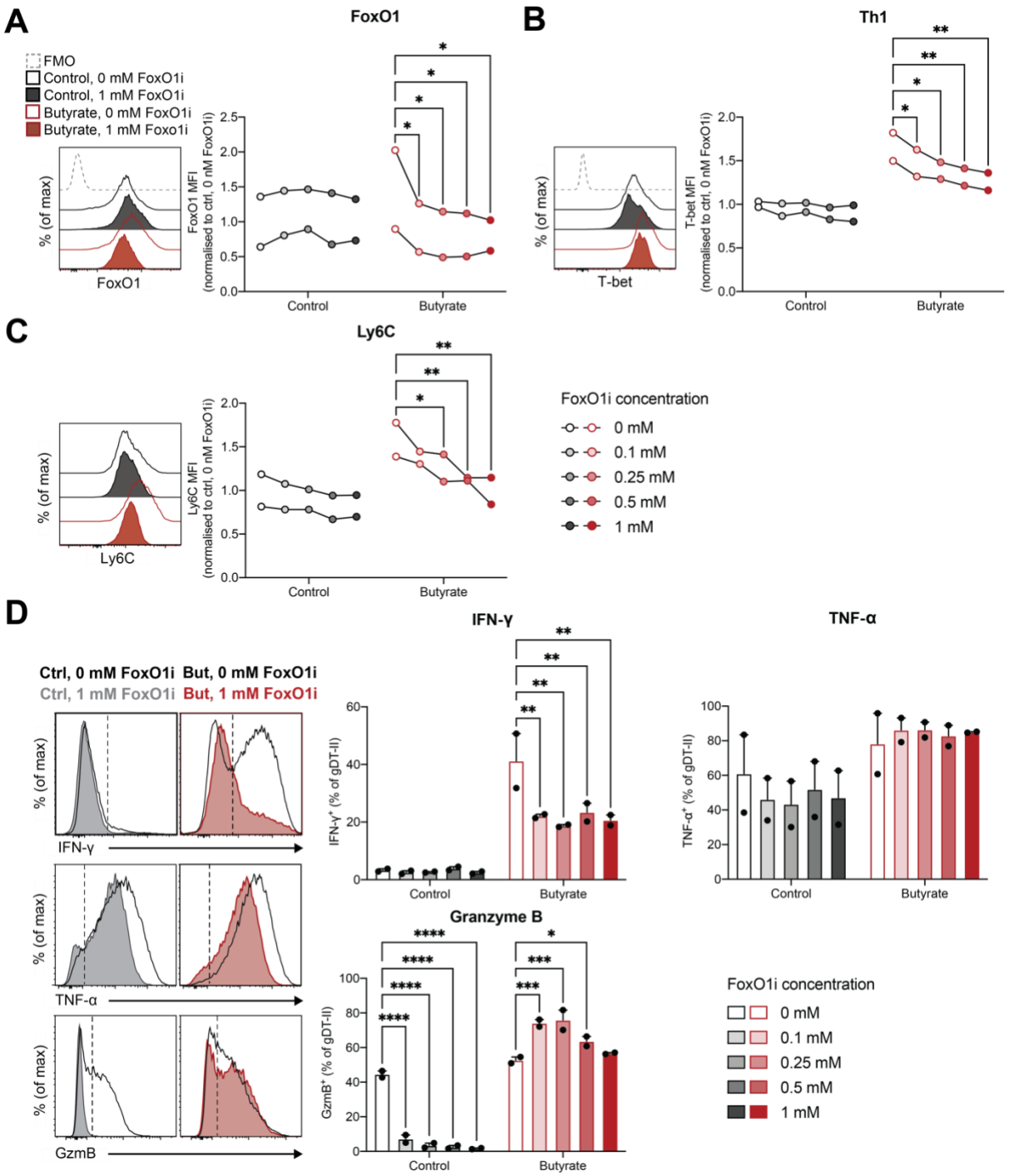

Figure 4.10 FoxO1 is a regulator of butyrate-induced Th1-like polarisation in CD4⁺ T cells.

In vitro-activated gDT-II cells were either untreated (control) or treated with 0.5 mM butyrate on days 3 to 5. FoxO1 activity was inhibited through daily pre-incubation with 0 mM. 0.1 mM, 0.25 mM, 0.5 mM or 1 mM FoxO1 inhibitor (FoxO1i) AS1842856 before butyrate treatment. Cells were analysed on day 6. **(A – C)** The mean fluorescence intensities (MFIs) of FoxO1 (A), T-bet (B) and Ly6C (C) were normalised to untreated controls that were not exposed to FoxO1i. Representative histograms of FoxO1, T-bet

and Ly6C MFIs of gDT-II cells are depicted. **(D)** Cells were re-stimulated with PMA and ionomycin for 5 hours. The intracellular expression of IFN-γ, TNF-α and granzyme B (GzmB) are shown. Representative histograms gated on total gDT-II cells show an overlay of untreated cells incubated with 0 nM (black) and 1 mM (grey) FoxO1i in the left column, and butyrate-treated cells incubated with 0 nM (black) and 1 mM (red) FoxO1i in the right column. Data are presented as mean + SEM from n = 2 independent experiments. Asterisks indicate statistically significant differences as analysed by two-way ANOVA tests (* $p < 0.05$, ** $p < 0.01$, *** $p < 0.001$, **** $p < 0.0001$).

4.2.7 Butyrate enhances CD4$^+$ T cell cytotoxicity against tumour cells through Fas ligand and histone acetylation

Given that butyrate promoted a cytotoxic phenotype, we evaluated whether this translated into an improved killing capacity. An underappreciated but crucial feature of *in vitro* activated CD4$^+$ T cells is their ability to exhibit direct cytotoxicity against targets (Emma Bawden, unpublished results). We performed *in vitro* real-time killing assays using B16.gD melanoma cells as target cells. IFN-γ pre-treatment of B16.gD cells induced upregulation of MHC-II expression, whereas untreated target cells lacking MHC-II expression were used as a negative control (Figure 4.11A). This allowed us to measure MHC-specific killing. B16.gD cells were co-cultured with control or butyrate-treated gDT-II cells for 16 hours. B16.gD cell death was tracked using PI which permeates dead cells. CD4$^+$ T cells were not able to kill target cells if the latter were not pre-treated with IFN-γ, indicating that MHC-II upregulation and hence antigen recognition was required (Figure 4.11A). As expected, untreated CD4$^+$ T cells did, Butyrate drastically increased CD4$^+$ T cell-mediated killing of melanoma cells through faster killing and augmenting the total maximum killing (Figure 4.11B). These results were in line with the augmented cytokine and cytotoxic mediator expression after butyrate treatment. This showed for the first time that butyrate enhances the capacity of CD4$^+$ T cells to directly kill target cells.

We next investigated which effector molecules were required for improved killing mediated by butyrate. In this chapter, we consistently showed that IFN-γ, granzyme B, perforin and FasL were upregulated by butyrate. IFN-γ facilitates the expression of pro-apoptotic genes and sensitises tumour cells to FasL-induced killing [355, 356], while granzyme B, perforin and FasL mediate programmed cell death through caspase cascades [357, 358]. We firstly analysed the role of perforin by comparing the killing abilities of perforin-deficient and WT gDT-II cells. Without butyrate pre-treatment, perforin-deficient and WT cells showed virtually identical killing kinetics and degrees of cytotoxicity (Figure 4.11C). The same trend was observed between butyrate-treated groups regardless of perforin production, indicating that butyrate did not promote the cytotoxic function of CD4$^+$ T cells through perforin. To evaluate whether butyrate promoted cytotoxicity via IFN-γ, we co-cultured gDT-II cells and B16.gD cells in media containing anti-IFN-γ antibodies. IFN-γ blockade did not have an effect on neither the untreated groups nor butyrate-treated groups (Figure

4.11D), suggesting that IFN-γ had a negligible role in $CD4^+$ T cell-mediated cytotoxicity *in vitro*. In contrast to the other molecules tested, neutralising FasL activity using a FasL blocking antibody decreased the killing ability of untreated gDT-II cells by approximately 75% (Figure 4.11E). While the killing capacity of butyrate-treated cells was appreciably greater than untreated controls, FasL blockade completely abrogated the cytotoxicity induced by butyrate (Figure 4.11E). Hence, FasL, not perforin or IFN-γ, was the main mediator of $CD4^+$ T cell and butyrate-induced cytotoxicity *in vitro*.

To study whether histone acetylation influenced the $CD4^+$ T cell killing capacity, we compared the effects of butyrate to TSA. Interestingly, butyrate and TSA induced a comparable level of killing with similar kinetics (Figure 4.11F). This indicated that histone acetylation was an important mechanism for inducing $CD4^+$ T cell cytotoxicity. As butyrate and TSA mediated histone acetylation (Figure 4.7), it is tempting to speculate that histone acetylation induced by butyrate may mediate more effective killing.

Finally, given that cytotoxic $CD4^+$ T cells can arise from the Th1 lineage [46], we hypothesised that butyrate-treated gDT-II cells may be more potent killers than classical Th1 cells. Indeed, classical Th1 cells displayed a comparable level of killing to control gDT-II cells, with butyrate inducing greater B16.gD cell death (Figure 4.11G). Butyrate-treated cells were thus more effective than Th1 cells in direct targeting tumour cells. In this series of killing assays, we showed that butyrate-induced killing was mainly FasL-dependent, with a probable role for histone acetylation in mediating these functional outcomes. These results are striking as it shows that the microbiota-derived metabolite, butyrate, induces $CD4^+$ T cells to possess an even greater cytotoxic capacity than classical Th1 cells.

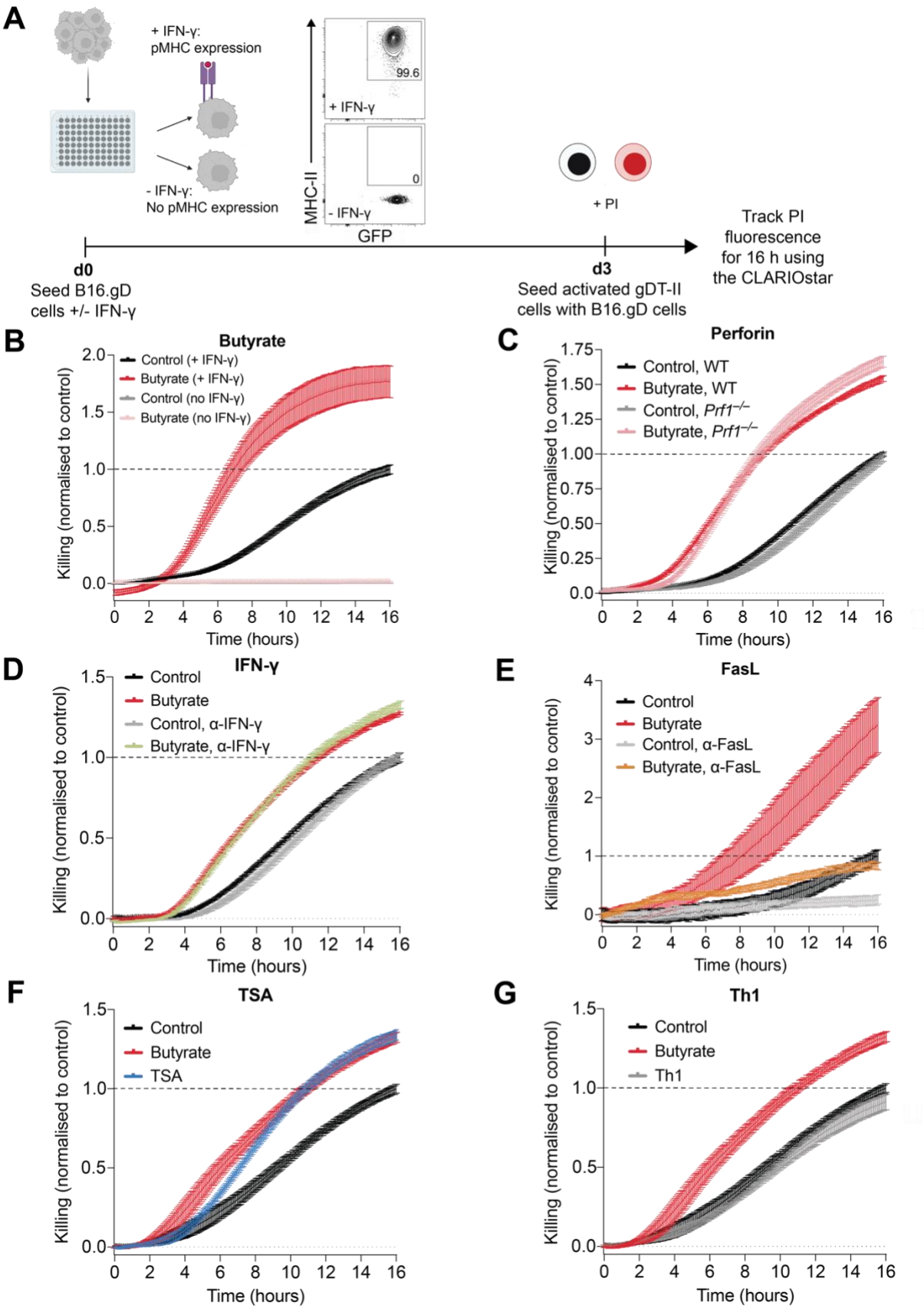
A
+ IFN-γ:
pMHC expression
- IFN-γ:
No pMHC expression
MHC-II
99.6
+ IFN-γ
0
- IFN-γ
GFP
+ PI
d0
Seed B16.gD
cells +/- IFN-γ
d3
Seed activated gDT-II
cells with B16.gD cells
Track PI
fluorescence
for 16 h using
the CLARIOstar
B
Butyrate
Control (+ IFN-γ)
Butyrate (+ IFN-γ)
Control (no IFN-γ)
Butyrate (no IFN-γ)
Killing (normalised to control)
Time (hours)
C
Perforin
Control, WT
Butyrate, WT
Control, Prf1−/−
Butyrate, Prf1−/−
D
IFN-γ
Control
Butyrate
Control, α-IFN-γ
Butyrate, α-IFN-γ
E
FasL
Control
Butyrate
Control, α-FasL
Butyrate, α-FasL
F
TSA
Control
Butyrate
TSA
G
Th1
Control
Butyrate
Th1

Figure 4.11 Butyrate improves FasL-mediated antigen-specific killing of melanoma cells by CD4$^+$ T cells.

B16 melanoma cells transduced to express HSV-1 glycoprotein D (B16.gD) were seeded in the absence or presence of IFN-γ, where IFN-γ induced MHC-II upregulation. After 3 days, *in vitro*-activated control or butyrate-treated gDT-II cells were co-cultured with the plated B16.gD cells which had been washed to remove IFN-γ. Propidium iodide (PI) uptake was recorded for 16 hours using the CLARIOstar Plus. Killing of B16.gD cells was calculated by subtracting cell death in samples cultured in the absence of IFN-γ from samples with IFN-γ pre-treatment. **(A)** The experimental schematic is depicted. **(B)** Killing of IFN-γ-treated and non-IFN-γ treated B16.gD tumour cells by gDT-II cells was normalised to group that lacked butyrate treatment. **(C – E)** Effector molecules mediating cytotoxicity was investigated by comparing control and butyrate-treated gDT-II cells from perforin-deficient (*Prf1*$^{-/-}$) and wildtype (WT) mice (C). Control and butyrate-treated gDT-II cells were incubated with IFN-γ blocking antibody (α-IFN-γ) (D), FasL blocking antibody (α-FasL) (E) or in the absence of blocking antibodies. **(F)** Tumour cell killing was compared between untreated gDT-II cells, butyrate-pre-treated cells, and gDT-II cells treated with Trichostatin A (TSA). **(G)** The killing capacity of untreated and butyrate-pre-treated cells was compared to classical Th1 cells. Data in (B – G) are presented as mean ± SEM of n = 5 – 12 from at least 2 pooled independent experiments.

4.3 Discussion

Research focusing on the importance of the gut microbiome in anti-viral and anti-cancer responses has gained traction over the past decade. A number of reports have pinpointed the enrichment of butyrate-producing gut microbiota as a factor that differentiates healthy individuals from patients [359-362]. Butyrate can directly regulate immune responses in various immune cell types [31, 164, 210], but has mainly been investigated in the context of Tregs in autoimmunity [183, 313, 363]. Th1 cells are an important prognostic marker in cancer and infection [241, 364]. Nevertheless, knowledge linking butyrate to Th1-type responses is limited. In this study, we therefore investigated the ability of the microbiota-derived metabolite butyrate to promote pro-inflammatory $CD4^+$ T cell differentiation and function. We report that butyrate promoted $CD4^+$ T cell differentiation into a unique subset of Th1-like cells that expressed elevated levels of the memory marker FoxO1 and a greater killing capacity against tumour cells. Majority of the phenotypic, metabolic and functional effects that butyrate induced strongly resembled that of TSA-mediated histone acetylation.

We treated $CD4^+$ T cells with butyrate from day 3 of activation when majority of APCs and non-TCR transgenic T cells that were initially present in the co-culture had undergone cell death. This enabled us to study the direct effects of butyrate on $CD4^+$ T cells. Our first key finding highlighted that *in vitro* butyrate treatment was able to induce the differentiation of $CD4^+$ T cells into non-classical cytotoxic Th1-like cells, with butyrate-mediated T-bet upregulation sustained upon *in vivo* viral infection. One of the most striking features of this butyrate-mediated phenotype was the increase in many Th1-associated effector molecules, with IFN-γ upregulation being the most profound. The panel of upregulated effector molecules included the cytotoxic mediators granzyme B, perforin and FasL. In general, heterogeneity within the Th1 subset is common, with only a proportion of the cells being capable of cytotoxic function [46]. Butyrate appeared to increase the frequency of this cytotoxic subset, which could be beneficial in settings that require the clearance of infected or metastatic cells [365]. While butyrate-treated $CD4^+$ T cells resembled classical Th1 cells in T-bet and cytokine expression, distinct differences also existed between the groups. A key distinguishing feature was the enhanced FoxO1 expression which was unique to the

butyrate group. FoxO1 is a master regulator of memory T cells, and is known to repress T-bet expression [52]. The upregulation of both FoxO1 and T-bet may suggest that butyrate disrupted the ability of FoxO1 to inhibit T-bet expression. Eomes, a downstream molecule of FoxO1, has been suggested to direct target T-bet [57]. The similar Eomes expression upon butyrate treatment presented further evidence that the transcriptional regulation of T-bet was likely altered by butyrate. Together, these data highlighted that butyrate-treated $CD4^+$ T cells and classical Th1 cells were distinct.

We further elucidated the role of FoxO1 in butyrate-mediated effects. As a key transcriptional regulator of stemness, FoxO1 counteracts senescence in T cells by integrating mitogenic and metabolic signals, thus maintaining the cell's fitness [35, 52, 366]. Butyrate-treated $CD4^+$ T cells possessed high FoxO1 expression and elevated spare respiratory capacity, which are both features of memory T cells [61, 367]. This raises the possibility that butyrate may direct $CD4^+$ T cells to differentiate into functionally competent memory cells, but further work focusing on memory timepoint analyses must be carried out to provide stronger evidence for this. Another noteworthy finding in our experiment was that FoxO1 was partially responsible for the butyrate-mediated increase in T-bet, Ly6C and IFN-γ expression. The ability of butyrate to increase the expression of such Th1-associated markers through FoxO1 highlights FoxO1 as an important transcriptional modulator that butyrate acts through.

We furthermore investigated the mechanisms of butyrate. In our study, despite the fact that $CD4^+$ T cells expressed detectable levels of GPR41 and GPR43 upon butyrate exposure, butyrate did not induce changes in differentiation or function through these receptors *in vitro*. This corresponds to a report that showed the induction of IFN-γ in *in vitro* generated Tregs was not dependent on GPR41/GPR434, but on HDAC inhibition [152]. Importantly, our results highlighted that butyrate induced high levels of histone H3 acetylation, which is known to occur in actively transcribed genes [368]. We additionally showed that acetylation of histone H3K9 and H3K27 positively correlated with increased effector molecule expression. A further causative relationship is likely to exist as H3K9ac and H3K27ac promotes *Ifng*, *Tnf*, and *Gzmb* expression in T cells [80, 81, 341, 343]. SCFAs can induce histone acetylation through HDAC and HAT regulation [166, 339]. HDAC inhibition by butyrate has been clearly demonstrated in a range of cell types [339, 369, 370]. As HDAC1 and HDAC2 inhibit

$CD4^+$ T cell expression of IFN-γ and granzyme B [222], HDAC inhibition may be a way by which butyrate upregulated these molecules in our study. Indeed, butyrate has been suggested to increase IFN-γ expression by macrophages and $CD4^+$ T cells at least in part through its HDAC inhibitor properties [152, 371]. The second mechanism of histone acetylation may be through butyrate metabolism which generates acetyl-CoA, a substrate for HATs [342]. Butyrate can enhance the activity of the HAT p300 [166], which is an activator of *Ifng* and *Fasl* in Jurkat T cells and cancer stem-like cells respectively [372, 373]. Butyrate-mediated histone acetylation may alter gene transcription through butyrate response elements (BREs). These are binding sites of the transcription factor Sp1 on promoters of certain butyrate-regulated genes, and are known to recruit regulatory complexes containing HDAC1, HDAC2 and the HAT p300/CBP [339]. BREs have not been characterised in $CD4^+$ T cells, though this may be how butyrate can upregulate molecules such as IFN-γ through HDACs and HATs.

Butyrate has been shown to influence glycolysis and mitochondrial respiration in Tregs and $CD8^+$ T cells through direct and indirect modes of action [31, 160, 210]. In our study, butyrate reduced glycolysis and showed minimal effects on the mitochondrial respiration of $CD4^+$ T cells. Intriguingly, butyrate induced a greater glycolytic reserve and mitochondrial spare respiratory capacity in $CD4^+$ T cells. These characteristics are known to reflect the potential of a cell to cope with increases in energetic demands, such as under physiologically stressed conditions and re-activation [374, 375]. High levels of these parameters indicate greater plasticity in metabolic capacity, which confers better resistance to senescence and apoptosis [376, 377]. Indeed, the ability to withstand metabolic stress is a feature of memory T cells [53, 61]. Together with FoxO1 upregulation, the increased glycolytic reserve and mitochondrial spare respiratory capacity are memory-associated characteristics that butyrate induced. Moreover, butyrate-treated $CD4^+$ T cells relied less on glycolysis than classical Th1 cells that are particularly dependent on this metabolic process for effector molecule production [378, 379]. This distinguished butyrate-treated $CD4^+$ T cells from their more metabolically active Th1 counterparts. Our group has demonstrated that butyrate upregulates $CD8^+$ T cell glycolysis and mitochondrial respiration, and was even used as a substrate in the TCA cycle [31]. This discrepancy between $CD4^+$ and $CD8^+$ T cells despite similar treatments with butyrate calls into question whether the role of butyrate as a metabolic substrate differed between $CD4^+$

and $CD8^+$ T cells. Perhaps most strikingly, the metabolic effects of butyrate resembled that of TSA-induced histone acetylation. Histone acetylation may therefore not only promote effector molecule expression as mentioned above, but could also contribute to metabolic regulation. As acetylation can determine metabolic protein expression and activity [380, 381], butyrate-mediated post-translational modifications of metabolic proteins may be a key mechanism in inducing metabolic effects. As butyrate appeared to act primarily through histone acetylation in $CD4^+$ T cells, it may have been preferentially directed into the nucleus rather than the mitochondria. This would have enabled butyrate to act as an epigenetic regulator while decreasing its availability as a metabolic fuel source.

In the last few years, single cell RNA sequencing (RNAseq) of peripheral blood and tumour biopsies from cancer patients has revealed the importance of cytotoxic $CD4^+$ T cells in the elimination of various solid cancers including melanoma [382-384]. We proceeded to prove that butyrate-mediated upregulation of cytotoxic mediators translated into an enhanced the ability of $CD4^+$ T cells to directly kill melanoma cells. The cytotoxic functionality of butyrate-treated $CD4^+$ T cells *in vitro* was predominantly reliant on FasL. This was particularly interesting as other groups have demonstrated FasL functional activity by $CD4^+$ T cells against $CD8^+$ target cells *in vitro* [385] and showed that the main mediator of killing by LCMV-specific $CD4^+$ T cells *in vivo* was FasL rather than the perforin pathway [386, 387]. We noted that histone acetylation appeared to be crucial for $CD4^+$ T cell cytotoxicity. This may occur through the regulation FasL by H3K9ac, which has been shown to occur in human $CD4^+$ T cells [388]. Notably, the killing capacities of untreated controls and classical Th1 cells, both of which possessed less histone acetylation, were lower than butyrate-treated cells. This demonstrated a link between histone acetylation and robust cytotoxicity, which the ability of butyrate-treated $CD4^+$ T cells to kill tumour cells may depend on. From a metabolic perspective, energetic demands are increased in T cells during re-stimulation [389], for example upon encountering tumour cells expressing the T cell cognate antigen. T cells which are capable of rapidly adapting their metabolic programs therefore produce a more robust response [375, 389]. The ability of butyrate to enhance the killing potential of $CD4^+$ T cells similar to TSA but greater than Th1 cells was therefore in line with our metabolic data. We thus propose the novel concept that butyrate is able to induce greater cytotoxic ability of $CD4^+$ T cells which is

dependent on histone acetylation. Butyrate availability can vary widely between individuals [390], and may hence be one of the factors contributing towards the effective clearance of infected or cancerous cells.

In conclusion, our study reports that butyrate mediates non-classical cytotoxic Th1 polarisation and function. We discovered that epigenetic alterations likely played a significant role in transcriptional, metabolic and functional changes. Enhanced responses upon butyrate exposure were strongly associated with its induction of histone acetylation. The ability of butyrate to alter the expression of various molecules and $CD4^+$ T cell killing potential may further stem from its alteration of transcriptional complexes containing regulators such as HATs, HDACs, FoxO1 and T-bet. From our results, it was evident that the role of butyrate on $CD4^+$ T cell immunity that is described in the existing literature may be over-simplified. Butyrate likely possesses a multifaceted role which is highly context-dependent. While butyrate indeed has immunoregulatory potential that is beneficial in autoimmune conditions such as ulcerative colitis and type 1 diabetes [221, 363], it can also elicit pro-inflammatory responses that are desirable in immunity against cancer. Our findings thus challenge the dogma which largely paints butyrate to induce anti-inflammatory $CD4^+$ T cell responses. The results of our study highlight that metabolite-targeting of the $CD4^+$ T cell arm can improve their cytotoxic capacity which to date, has not yet been thoroughly explored in the context of immunotherapy. Butyrate supplementation to the diet or probiotic supplementation with butyrate-producing bacteria may be feasible methods of increasing T cell exposure to this SCFA. We believe that a deeper understanding of butyrate's ability to skew $CD4^+$ T cell differentiation towards non-classical cytotoxic Th1 cells could provide novel targets for immunotherapies such as CAR T cell therapy.

Chapter 5:
Exploring the therapeutic application of butyrate in CAR T cell therapy

Chapter 5 Exploring the therapeutic application of butyrate in CAR T cell therapy

5.1 Introduction

CAR T cell therapy is a form of cancer treatment where T cells are engineered to express receptors that recognise specific tumour antigens. To date, 6 CAR T cell therapies have been approved by the FDA for patients with aggressive haematological malignancies [391]. Its success against blood cancers has led to clinical trials that seek to optimise CAR T cells against solid tumours [392-394]. Such tumours often evade the endogenous immune response, which in many cases involves the downregulation of MHC expression by the tumour [395, 396]. The promise of CAR T cells lies in the fact MHC downregulation will not influence their effectiveness as long as the relevant tumour antigen remains expressed [397]. This non-classical immune synapse established between the CAR and the tumour results in the release of cytotoxic mediators granzyme and perforin, and exposes the tumour cell to FasL, as well as proinflammatory cytokines IFN-γ and TNF-α that can induce tumour cell death through direct and indirect mechanisms, such as myeloid cell activation [398-401].

The majority of studies manufacture CAR T cell products from unselected T cells consisting of a mix of $CD4^+$ and $CD8^+$ CAR T cells in patient-dependent ratios [402]. The initial anti-tumour response has been reported to be dominated by $CD8^+$ CAR T cells, while long-term remission relied on $CD4^+$ CAR T cells [403]. A key determinant for the effectiveness of therapy is the differentiation status of CAR T cells. Animal and clinical studies have demonstrated that Th1 cells are positively associated with responsiveness to cancer immunotherapy and overall anti-tumour responses [404-406]. In a lymphoma model, Th1-polarised $CD4^+$ CAR T cells showed proinflammatory cytokine secretion and cytotoxicity, improving survival rates of tumour-bearing mice [407]. Single cell RNAseq of tumour and peripheral blood samples from cancer patients has additionally revealed the importance of cytotoxic $CD4^+$ T cells in the elimination of various solid cancers including melanoma [382-384]. Expanded $CD4^+$ and $CD8^+$ T cell memory subsets have also been shown to be good prognostic markers for long-term clinical responsiveness, owing to the persistence and

preserved function of the CAR T cells over extended periods of time [408, 409]. Indeed, human $CD8^+$ CAR T cells with a central memory phenotype conferred better survival than naïve and effector memory subsets in Raji-bearing mice [410]. In a longitudinal study where leukemia patients received a mix of $CD4^+$ and $CD8^+$ CAR T cells, 97% of remaining CAR T cells after more than 7 years post-infusion were cytotoxic $CD4^+$ CAR T cells [403]. This indicates the importance of reinforcing $CD4^+$ CAR T cell functionality and developing $CD8^+$ CAR T cell products with superior memory T cell characteristics, such as prolonged survival, to better contribute to long-term tumour control.

While CAR T cell therapy has the potential to augment both immediate and long-term anti-tumour responses, its success in solid tumours is hampered by a multitude of factors including an immunosuppressive tumour microenvironment (TME). In particular, a glucose-poor and adenosine-rich TME causes metabolic instability and apoptosis of glycolytically-reliant CAR T cells that are unable to produce sufficient ATP [411, 412]. Further metabolic barriers induced by the TME include mitochondrial dysfunction of T cells [413, 414], in part through the inhibition of Foxo transcription factor activity [415]. This correlates with inhibitory molecule expression and T cell exhaustion, thereby weakening T cell persistence and effector capacity [415, 416].

The ability of a cell to proliferate, self-renew and retain functionality is known as stemness. In a chronic disease setting such as cancer, continuous stimulation of T cells leads them to be susceptible to dysfunction. CAR T cells with stem-like qualities are therefore beneficial as they possess greater plasticity and therefore have a higher potential to survive and contribute to the functional response. As such, a strong focus has been placed on methods to enhance stemness and functionality of CAR T cell products. Firstly, manufacturing methods can be altered to optimise CAR T cell stemness. Suggested strategies include promoting mitochondrial metabolism through careful selection of CAR domains and cell culture conditions such as supplementation with the memory-promoting cytokines IL-7 and IL-15 [415, 417-419]. Another avenue that is being explored is the selection of CAR T cell subsets for infusion. This may be in the form of preferential infusion of memory CAR T cells rather than effector cells [420], or infusion of both $CD4^+$ and $CD8^+$ CAR T cells in precise ratios [392, 410].

Synergy between $CD4^+$ and $CD8^+$ CAR T cells was shown to improve anti-tumour responses, with the $CD4^+$ subset supporting the proliferation of their $CD8^+$ counterparts [410]. In patients with B cell acute lymphoblastic leukemia, a defined composition of 1:1 $CD4^+/CD8^+$ CAR T cells correlated with improved disease-free survival through expansion and the persistence of CAR T cells [392]. Additionally, to overcome T cell exhaustion, combination therapy with ICB can be used to rescue the function of CAR T cells and endogenous T cells [421]. For example, increased proliferative and effector capacity of CAR T cells were demonstrated in a breast cancer model using anti-HER2 CAR T cells and anti-PD-1 [422], possibly through ICB-mediated reversal of metabolic dysfunction [423, 424]. This led to tumour growth inhibition and better survival of mice [422].

While the maintenance of stemness has proven crucial for long-term effectiveness of therapy, amplified cytotoxicity is another desired feature that is routinely assayed as a part of the manufacturing process and is necessary for anti-tumour effects [425]. It was recently shown that memory $CD8^+$ CAR T cells with elevated cytotoxicity enhanced treatment efficacy against mouse melanoma [111]. This indicates the need to harness both stemness and functionality to create superior CAR T cell products. In Chapters 3 and 4, as well as Bachem *et al.* [31], we showed that SCFAs such as butyrate increased the expression of stemness markers and altered cellular metabolism. Butyrate promoted $CD8^+$ T cell differentiation into MPECs in acute viral infection and promoted FoxO1 expression in $CD4^+$ T cells. We also found that butyrate regulated $CD4^+$ and $CD8^+$ T cell effector responses. Importantly, butyrate encouraged the differentiation of $CD4^+$ T cells into cytotoxic Th1-like cells with an increased ability to directly kill tumour cells. Together, these findings have led us to hypothesise that butyrate may improve CAR T cell responses by inducing effector and memory phenotypes simultaneously. We aimed to use *in vitro* and *in vivo* models to assess whether butyrate could be employed to promote CAR T cell efficacy.

5.2 Results

5.2.1 Butyrate promotes the memory program, metabolism and effector function of murine CAR T cells *in vitro*

To assess whether butyrate could improve stemness and functional phenotypes of CAR T cells, we activated murine T cells with anti-CD3ε and anti-CD28, and retrovirally transduced them to express anti-HER2 CAR constructs that recognised E0771-HER2 breast cancer cells leading to about 60% transduction rate (Figure 5.1A). These second generation CAR T cells were treated with either butyrate or PBS for 2 days after transduction. On day 5 post-activation, successfully transduced $CD4^+$ and $CD8^+$ CAR T cells that expressed mCherry-tagged CARs were analysed (Figure 5.1B). The control and butyrate groups both consisted of $CD8^+$ and $CD4^+$ T cells in an approximate 3:1 ratio (Figure 5.1C). We firstly assessed the effects of butyrate on the activation status of CAR T cells. We detected increased CD44 and decreased CD62L expression in both the $CD4^+$ and $CD8^+$ sub-populations upon butyrate treatment (Figure 5.1D and E), signifying stronger activation of CAR T cells. Butyrate induced statistically significant increases in FoxO1 expression in both $CD4^+$ and $CD8^+$ CAR T cells (Figure 5.1F). As mitochondrial function contributes to metabolic fitness and has been shown to support CAR T cell plasticity [426], we also measured the effect of butyrate on mitochondrial activity and mass, and found that butyrate indeed enhanced mitochondrial membrane potential (TMRM) and mitochondrial mass (Mitotracker) of CAR T cells (Figure 5.1G and H). The increases in FoxO1 expression and mitochondrial function are consistent with the notion that butyrate promoted stemness-associated factors and mitochondrial metabolism.

As we demonstrated in previous chapters that butyrate enhanced effector-associated marker expression, we proceeded to study whether this effect was also present in CAR T cells. In line with our earlier observations, butyrate enhanced T-bet expression (Figure 5.2A), suggesting that the butyrate-treated group comprised of more Th1-like $CD4^+$ CAR T cells and $CD8^+$ CAR T cells with a stronger effector program. We next confirmed whether the butyrate-induced changes in transcription factor expression correlated with effector molecule expression. Relative to untreated $CD4^+$ CAR T cells, butyrate-treated CAR T cells expressed significantly greater levels of IFN-γ (Ctrl, $14 \pm 5.3\%$; But, $56 \pm 8.9\%$) and granzyme B (Ctrl, $27 \pm 4.4\%$; But, $55 \pm$

0.91%) (Figure 5.2B). Small but consistent increases in TNF-α (Ctrl, 73 ± 2.9 %; But, 87 ± 3.4%) and perforin (Ctrl, 1 ± 0.56%; But, 7 ± 0.53%) expressions were also observed in butyrate-treated $CD4^+$ CAR T cells (Figure 5.2B). Likewise, butyrate promoted the production of most effector molecules in $CD8^+$ CAR T cells, with the most notable increases observed in TNF-α (Ctrl, 57 ± 7.2%; But, 83 ± 2.1%) and perforin (Ctrl, 58 ± 1.0%; But, 94 ± 1.8%) (Figure 5.2C). Small upregulations in granzyme B (Ctrl, 85 ± 2.5%; But, 96 ± 0.0059%) were recorded but alterations in IFN-γ expression were inconsistent (Figure 5.2C). Taken together, this demonstrated that butyrate increased pro-inflammatory cytokine and cytotoxic mediator production by both $CD4^+$ and $CD8^+$ CAR T cell subsets.

To understand whether the butyrate-mediated increases in effector molecule expression altered the ability of CAR T cells to exert cytotoxicity, we performed killing assays. We co-cultured a mixture of $CD4^+$ and $CD8^+$ CAR T cells with E0771-HER2 breast cancer cells to closely mimic clinical protocols where the $CD4^+$ and $CD8^+$ CAR T cells are co-transfused into patients. We compared tumour cell lysis at various E:T ratios using chromium-51 release assays. The degree of tumour cell lysis by untreated CAR T cells increased from approximately 1.6% to 28% at E:T ratios of 0.156 and 40 respectively (Figure 5.2E). Butyrate enhanced the killing capacity of CAR T cells at all E:T ratios, from approximately 8.1% to 32% (Figure 5.2E). Importantly, 8 butyrate-treated CAR T cells were as effective as 2 control CAR T cells at a lysis level of 20.5% (Figure 5.2E). Our findings hence demonstrated that butyrate improved cytotoxicity of CAR T cells against tumour cells *in vitro*.

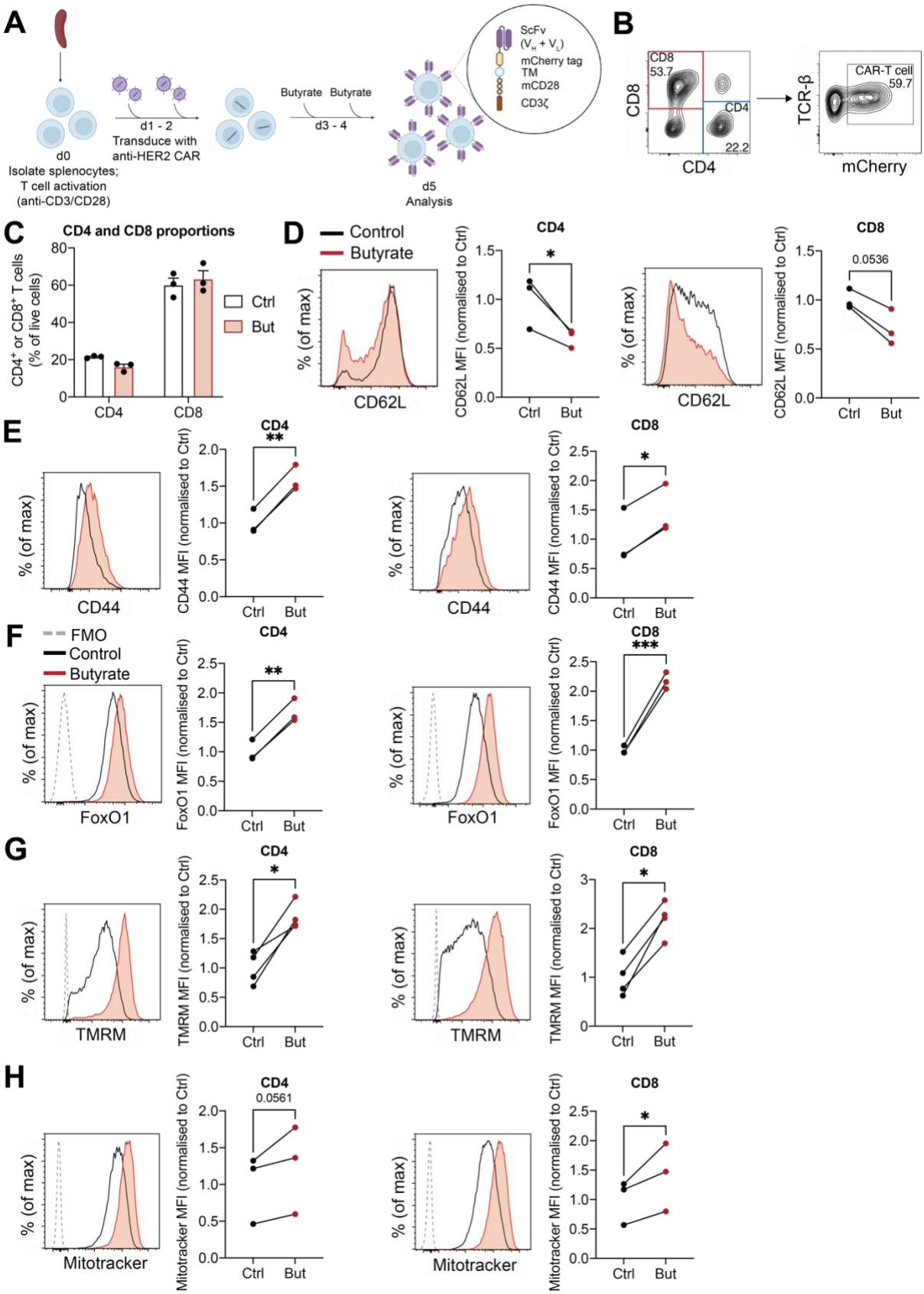
A
d0
Isolate splenocytes;
T cell activation
(anti-CD3/CD28)
d1 - 2
Transduce with
anti-HER2 CAR
Butyrate Butyrate
d3 - 4
d5
Analysis
ScFv
(VH + VL)
mCherry tag
TM
mCD28
CD3ζ
B
CD8
53.7
CD4
22.2
CD4
CD8
TCR-β
CAR-T cell
59.7
mCherry
C
CD4 and CD8 proportions
CD4+ or CD8+ T cells
(% of live cells)
Ctrl
But
CD4
CD8
D
Control
Butyrate
% (of max)
CD62L
CD62L MFI (normalised to Ctrl)
CD4
CD8
0.0536
E
CD44
CD44 MFI (normalised to Ctrl)
F
FMO
Control
Butyrate
FoxO1
FoxO1 MFI (normalised to Ctrl)
G
TMRM
TMRM MFI (normalised to Ctrl)
H
Mitotracker
Mitotracker MFI (normalised to Ctrl)
0.0561

Figure 5.1 Butyrate promotes a memory program and mitochondrial membrane potential in murine CAR T cells.

T cells from C57BL/6 splenocytes were activated with anti-CD3 and anti-CD28, and transduced to express 2-tail (CD3ζ/CD28) chimeric antigen receptor (CAR) constructs specific to human HER2. Anti-HER2 CAR T cells were treated with PBS (Control; Ctrl) or 0.5 mM butyrate (But) *in vitro* on days 3 and 4. Analysis was performed on day 5 post-activation. **(A)** The experimental schematic is depicted. **(B)** Successfully transduced $CD4^+$ and $CD8^+$ CAR T cells were identified using mCherry and TCR-β, as shown in the representative gating strategy. **(C)** Proportions of $CD4^+$ and $CD8^+$ CAR T cells on day 5 post-activation, as a frequency of live cells. **(D, E)** The mean fluorescence intensities (MFIs) of the activation markers CD44 (D) and CD62L (E) of $CD4^+$ and $CD8^+$ CAR T cells. MFIs were normalised to the average PBS group MFI. **(F)** The FoxO1 MFIs of control and butyrate-treated $CD4^+$ and $CD8^+$ CAR T cells expression are shown. MFIs were normalised to the average PBS group MFI. Representative histograms depict the MFIs of FoxO1 in fluorescence minus one (FMO) controls, untreated and butyrate-treated CAR T cells. **(G, H)** $CD4^+$ and $CD8^+$ CAR T cell mitochondrial membrane potential (G) and mitochondrial size (H) were compared using the metabolic probes tetramethylrhodamine methyl ester (TMRM) and Mitotracker respectively. Their mean fluorescence intensities (MFI) were normalised to the average PBS group MFI. Representative histograms depict the MFIs of TMRM or Mitotracker fluorescence in fluorescence minus one (FMO) controls, untreated and butyrate-treated CAR T cells. Data are presented as mean + SEM or normalised MFIs with n = 2 – 3 independent experiments. Asterisks indicate statistically significant differences as analysed by a two-way ANOVA test or paired Student's *t*-tests (* $p < 0.05$, ** $p < 0.01$, *** $p < 0.001$).

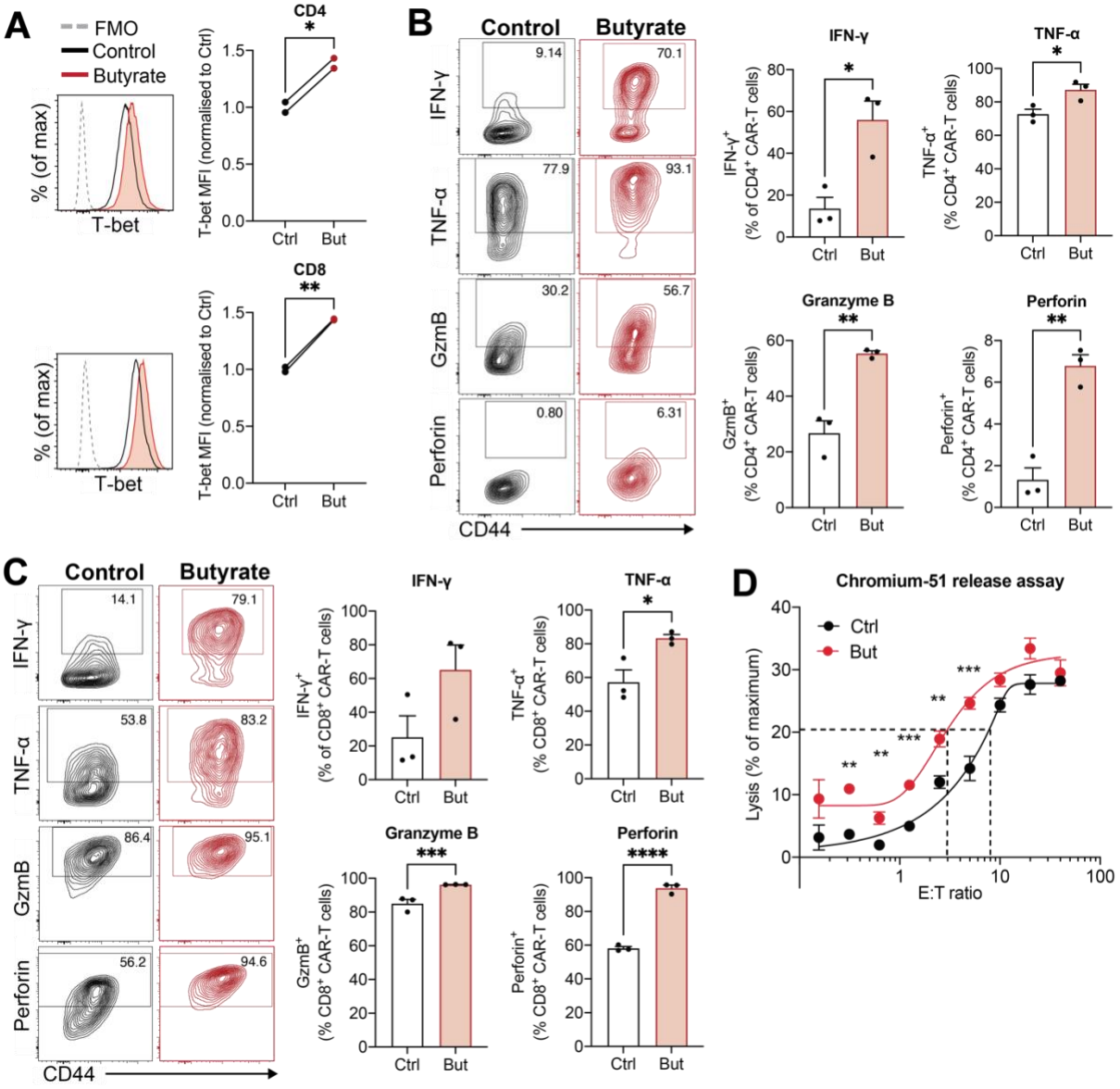

Figure 5.2 The effector molecule expression and *in vitro* killing capacity of murine CAR T cells are enhanced by butyrate.

Anti-HER2 murine CAR T cells were treated with PBS or 0.5 mM butyrate (But) *in vitro* 3 and 4 days after activation. CAR T cells were analysed on day 5 post-activation. **(A)** The T-bet mean fluorescence intensities (MFI) of control and butyrate-treated CD4$^+$ CAR T cells were compared. MFIs were normalised to the average PBS group MFI. Representative histograms depict the MFIs of T-bet expression in fluorescence minus one (FMO) controls, untreated and butyrate-treated CAR T cells. **(B, C)** Re-stimulation of CAR T cells with PMA and ionomycin for 5 hours was performed, followed intracellular cytokine staining. The expression of IFN-γ, TNF-α, granzyme B and perforin by CD4$^+$ (B) and CD8$^+$ (C) CAR T cells was measured. Representative contour plots show effector molecule expression against CD44 in CD8$^+$ CAR T cells. **(D)** Chromium-51 release assays were performed by co-culturing a mix of CD4$^+$ and

$CD8^+$ CAR T cells with E0771-HER2 cells at effector to target cell (E:T) ratios of 0.156:1 to 40:1 for 4 hours. Data are presented as the normalised MFI (A), mean + SEM (B, C) or mean ± SEM (D) of at least n = 2 independent experiments. Asterisks indicate statistically significant differences as analysed by paired Student's *t*-tests (* $p < 0.05$, ** $p < 0.01$, *** $p < 0.001$, **** $p < 0.0001$).

5.2.2 Butyrate-treated CAR T cells confer better control of breast cancer growth *in vivo*

CAR T cells are known to show limited success against solid tumours, which is thought to be related to metabolically hostile TMEs. However, improved CAR T cell stemness and a greater reliance on mitochondrial respiration can enhance the effectiveness of therapy in these settings [427]. Our observations that butyrate promoted mitochondrial activity, enhanced the expression of the stemness marker FoxO1 and improved killing of tumour cells *in vitro* led us to hypothesise that butyrate may enhance CAR T cell efficacy against solid cancers. To test this *in vivo*, we used an aggressive orthotopic model of E0771-HER2 breast cancer, where tumour-bearing mice were treated with CAR T cells (Figure 5.3A). Selected groups were co-treated with the ICB agent anti-PD-1 or the isotype control 2A3, and tumour growth was monitored (Figure 5.3A). The average tumour area of mice surpassed 100 mm^2 by 14 days post-inoculation in the absence of treatment (Figure 5.3B). Compared to untreated mice, control CAR T cell monotherapy reduced the rate of tumour growth to a small extent and was minimally effective (Figure 5.3B). In contrast, butyrate-treated CAR T cell monotherapy significantly reduced tumour growth, with the average tumour area exceeding 100 mm^2 only after 23 days post-inoculation (Figure 5.3B). While anti-PD-1 therapy alone did not induce significant effects on tumour growth, combination therapy with ICB and control or butyrate-treated CAR T cells delayed the average tumour outgrowth by 1.5-fold relative to the untreated group (Figure 5.3B). Strikingly, butyrate-treated CAR T cell monotherapy as effective as CAR T cell/ICB combination therapy in reducing tumour growth (Figure 5.3B). Like combination therapy, butyrate-treated CAR T cell monotherapy successfully enabled tumour control in a low proportion of mice; whereas tumour progression was noted in all mice that received control CAR T cell monotherapy (Figure 5.3B). These results suggested that butyrate was able to induce similar effects as ICB.

We additionally assessed how butyrate treatment of CAR T cells affected the survival of tumour-bearing mice. Survival was defined by a tumour area of less than 150 mm^2. Although all treatments prolonged survival, control CAR T cell monotherapy was the only treatment where all mice succumbed to disease and did not improve survival rates (Figure 5.3C). Butyrate-treated CAR T cell monotherapy was more effective than their control CAR T cell counterparts with a survival rate of 8.4% and

0% respectively. However, butyrate-treated CAR T cell monotherapy showed a comparable efficacy to CAR T cell/ICB combination therapy (Control CAR T cell/ICB, 25%; Butyrate CAR T cell/ICB, 8.4%) (Figure 5.3C). Together, these results demonstrated that treating CAR T cells with butyrate during manufacturing enhances their anti-tumour response even towards an aggressive form of solid cancer. Most importantly, butyrate reduced the need for treatment supplementation with ICB.

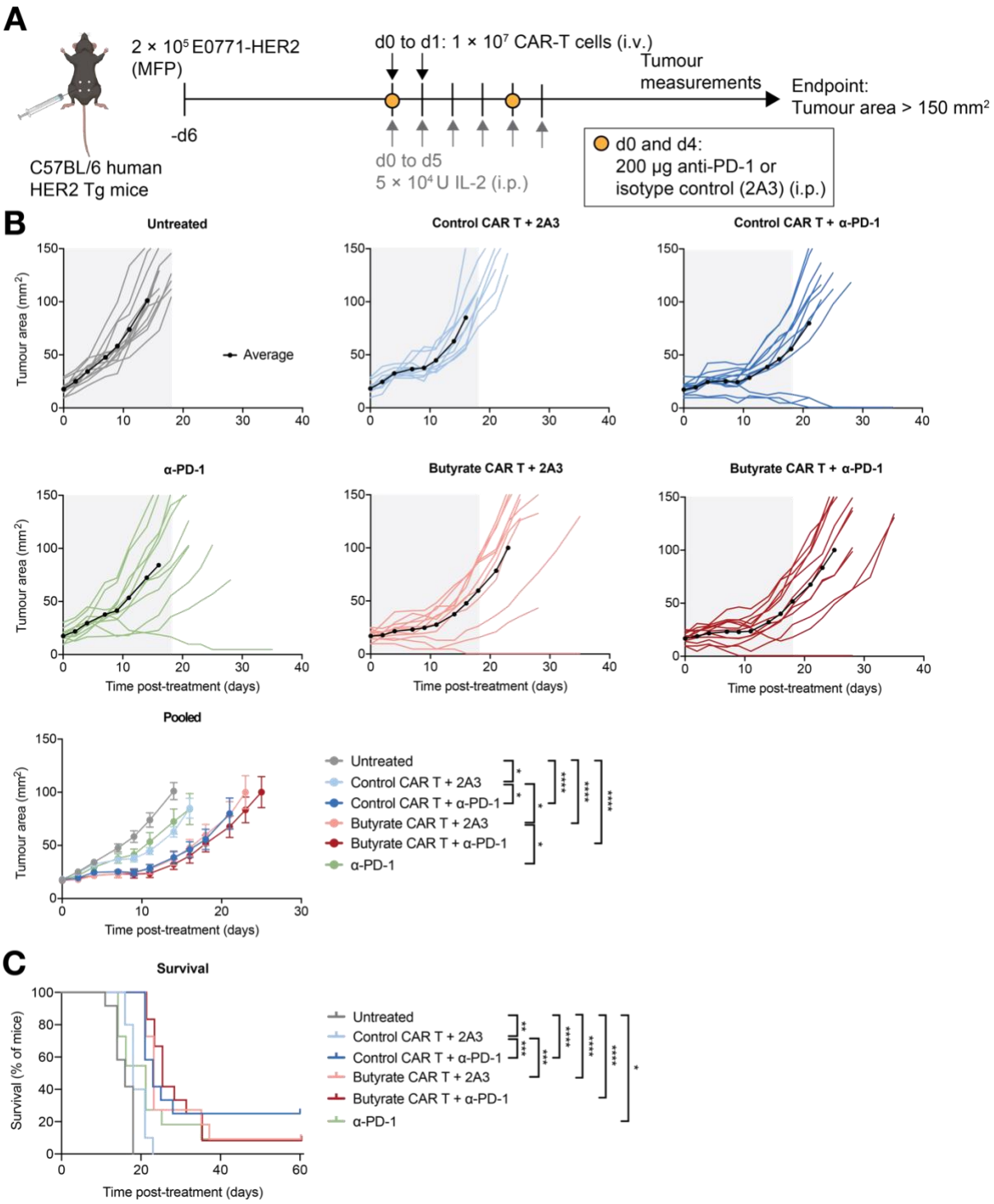

Figure 5.3 CAR T cells treated with butyrate confer superior control of E0771 breast cancer in mice.

Mammary fat pads (MFP) of female mice were inoculated with 2×10^5 E0771-HER2 tumour cells. 1×10^7 anti-HER2 CAR T cells that had been treated with PBS or 0.5 mM butyrate were adoptively transferred into tumour bearing mice that had been pre-conditioned by irradiation (4 Gy). Mice were treated with 5×10^4 units (U) IL-2

(intraperitoneally; i.p.) into the mice daily from days 0 to 5. Certain groups were treated with either anti-PD-1 (α-PD-1) or an isotype control (2A3) (200 μg) on days 0, 4, and 8. Tumours were measured until the experimental endpoint (when the tumour area was greater than 150 mm^2, or day 60). **(A)** The experimental schematic is shown. **(B)** Tumour areas calculated as (length × width) were measured in untreated, control CAR T cell + 2A3, control CAR T cell + α-PD-1, butyrate-treated CAR T cell + 2A3, butyrate-treated CAR T cell + α-PD-1, α-PD-1 only groups. The average tumour area of each group is denoted by a black line in graphs of individual groups. The pooled average tumour growth of each group is compared in a single graph which depicts the mean tumour sizes in the aforementioned graphs. **(C)** Survival curves of mice from all groups. Data are presented the mean + SEM of n = 10 – 11 mice per group from 2 independent experiments. Asterisks indicate statistically significant differences as analysed by log-rank (Mantel-Cox) tests (* $p < 0.05$, ** $p < 0.01$, *** $p < 0.001$, **** $p < 0.0001$).

5.2.3 Human CAR T cells upregulate memory and effector molecules upon butyrate treatment

We aimed to validate that the effects of butyrate on murine CAR T cells were translatable and could improve the quality of human CAR T cell products. The majority of human epithelial cancers express the LeY antigen [428, 429]. We therefore synthesised CAR T cells directed against this antigen. This was performed by activating PBMCs from a healthy human donor with anti-CD3 and transducing them to express anti-LeY CAR constructs. Human CAR T cells were supplemented with IL-2 and treated with butyrate for 3 days following transduction, and were analysed on day 7 post-activation. The proportion of $CD4^+$ and $CD8^+$ CAR T cells was 24% and 72% in untreated controls, and 28% and 63% in the butyrate-treated group respectively (Figure 5.4A). Butyrate may possess a minor effect on the proliferation or survival of $CD4^+$ and $CD8^+$ CAR T cells. We assessed the impact of butyrate on the activation status of human CAR T cells. Increased CD44 and PD-1 expression were observed after butyrate treatment (Figure 5.4B). In particular, PD-1 was strikingly upregulated beyond 3- and 4-fold in $CD4^+$ and $CD8^+$ CAR T cells respectively (Figure 5.4B). We additionally measured the expression of CD62L and CD45R. CD62L is typically downregulated during early activation and is linked to the acquisition of lytic function [430]. As expected, untreated $CD4^+$ and $CD8^+$ CAR T cells expressed low CD62L expression, reflecting activation (Figure 5.4C). CD45RA is progressively downregulated by $CCR7^+$ naïve human T cells over a 2-week period post-activation but can also be expressed by $CCR7^-$ terminal effector memory T cells [62, 431, 432]. Majority of untreated CAR T cells expressed CD45RA at this timepoint, although CCR7 co-staining was not performed to distinguish naïve from terminal effector cells (Figure 5.4C). CD62L and CD45RA were both further downregulated by butyrate-treated CAR T cells (Figure 5.4C). In line with our observations in murine CAR T cells, this suggested that butyrate promoted stronger activation of human CAR T cells.

Various discrepancies exist between the murine and human immune system, but the roles of transcription factors such as *Tbet* and *Foxo* are largely conserved between both species [433-435]. As we recorded an increase in the memory- and effector-associated markers in murine CAR T cells after butyrate treatment (Figure 5.1F), we investigated whether similar trends would occur in human CAR T cells.

Indeed, butyrate induced FoxO1 upregulation in human $CD4^+$ and $CD8^+$ CAR T cells (Figure 5.4D), signifying regulation of this memory-associated marker.

In terms of effector-associated markers, T-bet was upregulated by butyrate (Figure 5.5A) to a degree comparable to murine CAR T cells (Figure 5.2A). To test if butyrate influenced effector molecule expression in human CAR T cells, we performed an intracellular cytokine stain after T cell re-stimulation. In $CD4^+$ CAR T cells, IFN-γ, TNF-α, granzyme B and perforin production were increased by butyrate (Figure 5.5B). Interestingly, butyrate showed stronger effects in the upregulation of TNF-α (Ctrl, 36%; But, 59%) and perforin (Ctrl, 6%; But, 28%) in human $CD4^+$ CAR T cells (Figure 5.5B) compared to their murine counterparts (Figure 5.2B). IFN-γ, TNF-α, and perforin production by human $CD8^+$ CAR T cells were improved by butyrate treatment, reflecting similar trends as murine $CD8^+$ CAR T cells (Figure 5.5C). In contrast, granzyme B expression was comparable between the control and butyrate-treated $CD8^+$ CAR T cells (Figure 5.5C). Our findings suggest that butyrate has similar effects on the regulation of activation, memory- and effector-associated markers in human and murine CAR T cells. This is a first step in demonstrating the therapeutic potential of the microbiota-derived SCFA butyrate in CAR T cell therapy, and strongly justifies the need for further inquisition into whether butyrate can promote anti-LeY CAR T cell efficacy in pre-clinical models.

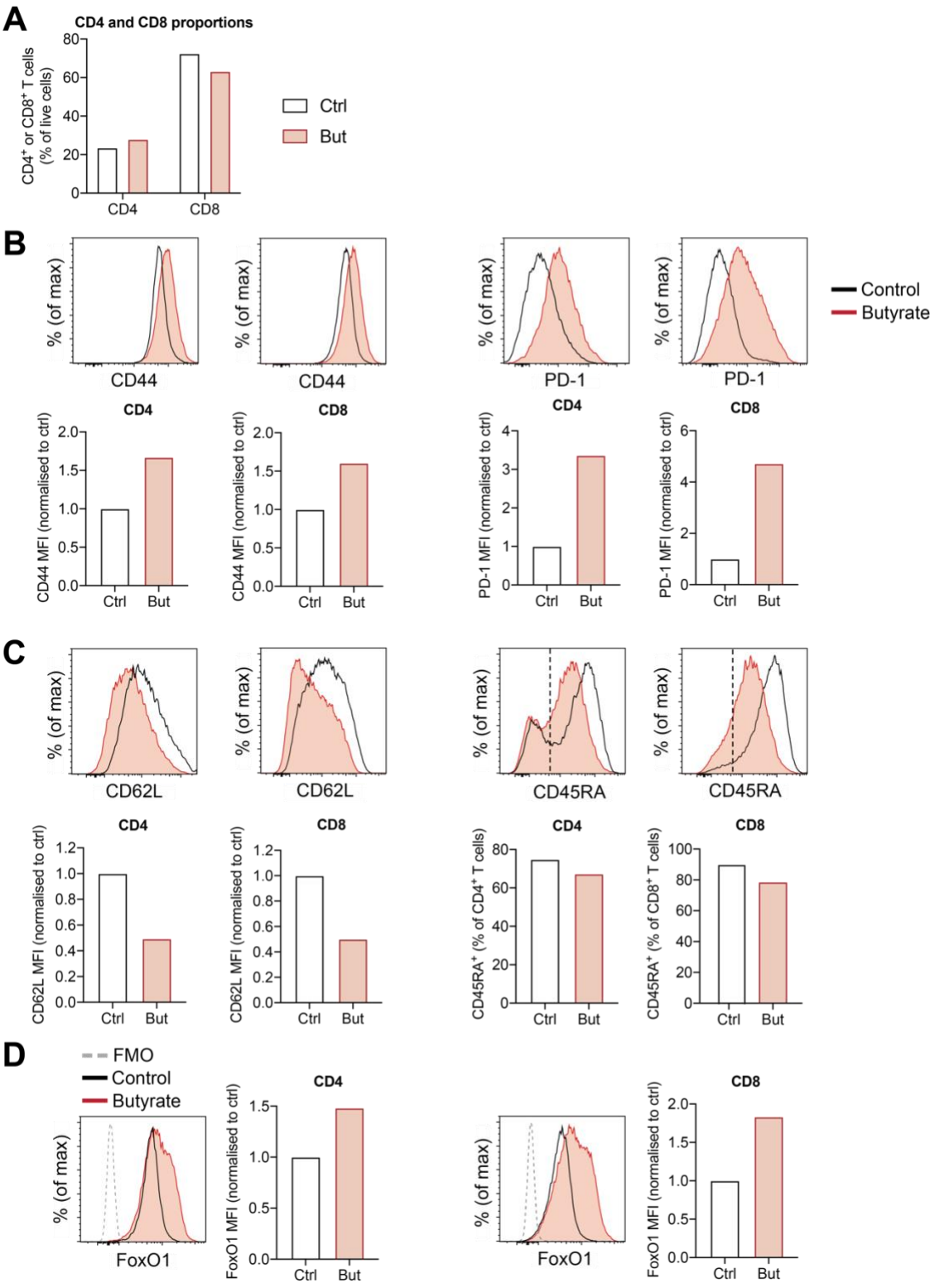

Figure 5.4 Butyrate upregulates activation and memory-type markers of human CAR T cells.

PBMCs of a healthy human donor were activated with anti-CD3, and transduced to express chimeric antigen receptor (CAR) constructs specific to human Lewis Y antigen (LeY). Anti-LeY CAR T cells were treated with 0.5 mM butyrate (But) *in vitro* on days 4 to 6. Untreated CAR T cell were used as controls (Ctrl). Analysis was performed on

day 7 post-activation. **(A)** The proportion of $CD4^+$ and $CD8^+$ CAR T cells within live cells is shown. **(B)** The mean fluorescence intensities (MFIs) of CD44 and PD-1 were compared within the $CD4^+$ and $CD8^+$ CAR T cell subsets. MFIs were normalised to the control group. MFIs were normalised to the untreated group. **(C)** The MFIs of CD62L and CD45RA in $CD4^+$ and $CD8^+$ CAR T cells are shown. MFIs were normalised to the untreated group. **(D)** The MFIs of the memory-associated marker FoxO1 of $CD4^+$ and $CD8^+$ CAR T cells. MFIs were normalised to the untreated group. Representative histograms depict the MFIs of the respective markers expressed by $CD4^+$ or $CD8^+$ CAR T cells in the fluorescence minus one (FMO) controls, untreated and butyrate-treated groups. Data are presented as the mean of n = 2 – 3 replicates from a single experiment. No statistical testing was performed due to the sample size.

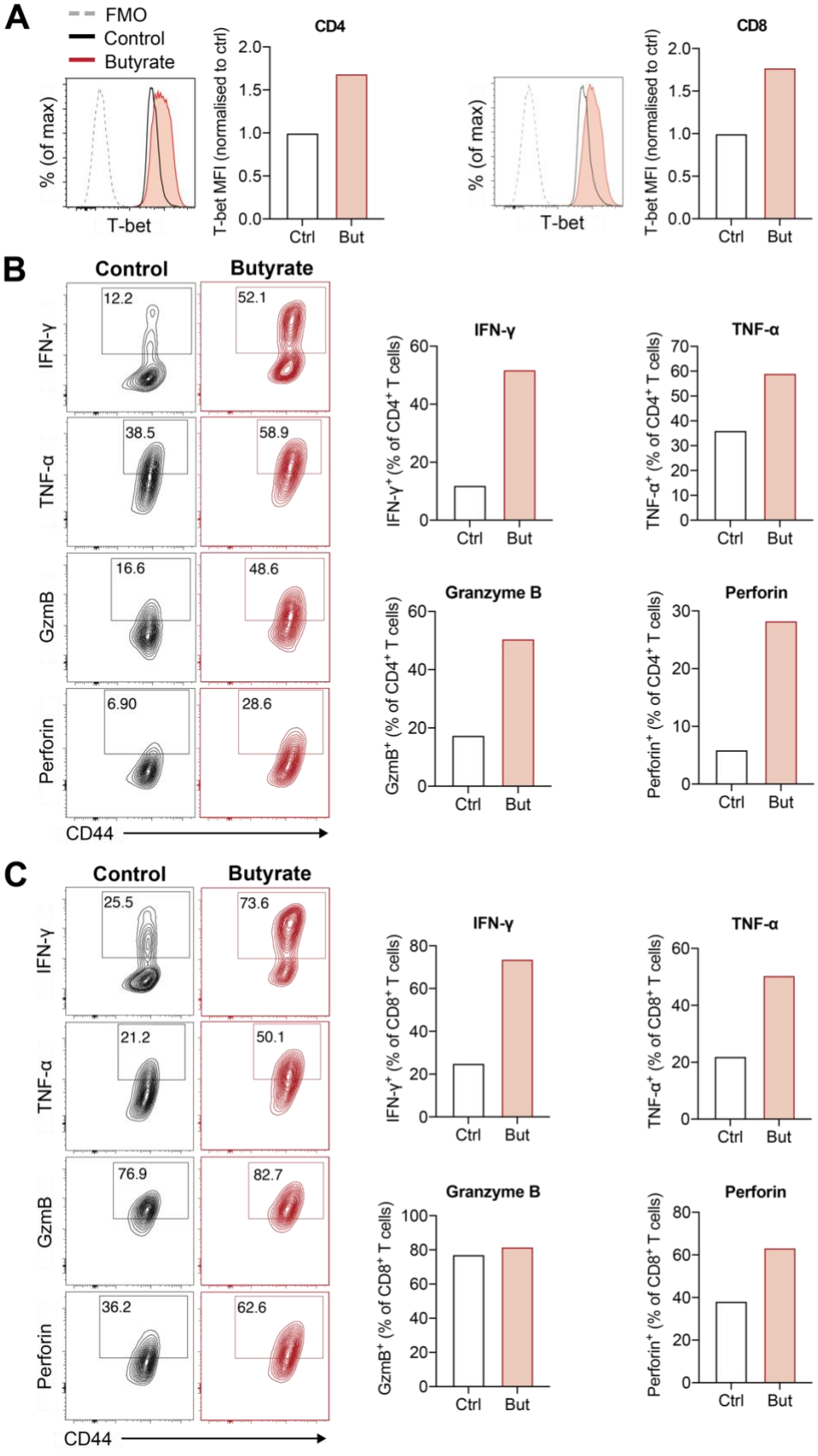
A
FMO
Control
Butyrate
% (of max)
T-bet
CD4
T-bet MFI (normalised to ctrl)
Ctrl
But
CD8
B
Control
Butyrate
IFN-γ
TNF-α
GzmB
Perforin
12.2
52.1
38.5
58.9
16.6
48.6
6.90
28.6
CD44
IFN-γ+ (% of CD4+ T cells)
TNF-α+ (% of CD4+ T cells)
Granzyme B
GzmB+ (% of CD4+ T cells)
Perforin
Perforin+ (% of CD4+ T cells)
C
25.5
73.6
21.2
50.1
76.9
82.7
36.2
62.6
IFN-γ+ (% of CD8+ T cells)
TNF-α+ (% of CD8+ T cells)
GzmB+ (% of CD8+ T cells)
Perforin+ (% of CD8+ T cells)

Figure 5.5 Butyrate promotes an anti-tumour effector phenotype in human CAR T cells.

PBMCs of a healthy human donor were activated with anti-CD3, and transduced to express chimeric antigen receptor (CAR) constructs specific to human Lewis Y antigen (LeY). Anti-LeY CAR T cells were treated with 0.5 mM butyrate (But) *in vitro* on days 4 to 6. Untreated CAR T cell were used as controls (Ctrl). Analysis was performed on day 7 post-activation. **(A)** The mean fluorescence intensities (MFI) of T-bet was compared in control and butyrate-treated $CD4^+$ and $CD8^+$ CAR T cells. MFIs were normalised to the untreated group. Representative histograms depict the T-bet MFIs of CAR T cells in the fluorescence minus one (FMO) controls, untreated control and butyrate-treated groups. **(B, C)** Cells were re-stimulated with PMA and ionomycin. Intracellular expression of IFN-γ, TNF-α, granzyme B and perforin are expressed as a frequency of $CD4^+$ (B) and $CD8^+$ CAR T cells (C). Representative contour plots show CAR T cell effector molecule expression against CD44. Data are presented as the mean of n = 2 – 3 replicates from a single experiment. No statistical testing was performed due to the sample size.

5.3 Discussion

While CAR T cell therapy has shown success in limiting clinical progression of haematological malignancies [391], its use against solid tumours requires further optimisation [436, 437]. This is believed to be at least partially due to an immunosuppressive TME that is deficient for metabolites, inducing terminal differentiation and T cell dysfunction. In this chapter, we sought to evaluate whether butyrate could improve CAR T cell efficacy. We detected a role for butyrate in mediating both memory- and effector-associated molecule upregulation, mitochondrial alterations, and increases in cytotoxic capacity of CAR T cells. Most importantly, butyrate-treated CAR T cell monotherapy improved *in vivo* tumour control to a greater extent than CAR T cell/ICB combination therapy.

A major factor that determines CAR T cell functionality *in vivo* is their metabolic profile, where metabolic fitness is impaired in dysfunctional cells but intact in cells that are able to proliferate and maintain effector molecule expression [438]. Our data indicated that butyrate promoted the mitochondrial activity and mass of both $CD4^+$ and $CD8^+$ CAR T cells. These readouts may reflect butyrate metabolism, similar to our group's previous findings that $CD8^+$ T cells utilised butyrate as a metabolic substrate [31]. T cells with an enhanced mitochondrial membrane potential have been shown to possess greater stemness and produced robust responses in ACT therapy [439]. A larger mitochondrial mass reflects a greater ability to perform electron transport chain activity and hence confer a higher spare respiratory capacity [61]. It would be interesting to measure glycolytic reserve and mitochondrial spare respiratory capacity to further predict the butyrate-induced changes in response to metabolic stress, similar to Section 4.2.5.3. In line with our metabolic results in Chapter 4, we speculate that the ability of butyrate to induce histone acetylation may at least in part be responsible for the observed metabolic effects in CAR T cells. Another prominent finding was the correlation between mitochondrial membrane potential and stemness markers. Butyrate treatment of $CD4^+$ and $CD8^+$ CAR T cells resulted in elevated FoxO1 expression, in line with our findings in previous chapters. Not only does FoxO1 limit senescence by inducing the expression of the anti-apoptotic molecule Bcl-2 in MPECs and central memory T cells [52, 367, 440], it also supports mitochondrial biogenesis and respiration through PGC-1α [415, 441]. Furthermore, we detected butyrate-

mediated CD44 upregulation in both murine and human CAR T cells. High CD44 expression denotes Th1 cells with increased resistance to Fas-mediated apoptosis [442], and correlates to $CD4^+$ and $CD8^+$ T cell expansion via interleukin-2 receptor alpha (IL-2Rα) expression [443]. Together, our metabolic, FoxO1, and CD44 readouts suggest that butyrate may be beneficial in maintaining stemness and persistence in CAR T cells.

We observed that butyrate treatment caused the dual upregulation of FoxO1 and T-bet in both $CD4^+$ and $CD8^+$ CAR T cells. This may suggest that butyrate disrupted the ability of FoxO1 to inhibit T-bet expression in CAR T cells, which was congruent with our observations in butyrate-treated gDT-II cells in Chapter 4. Inhibition by the transcription factor FoxO1 may be compensated by an upregulation of other transcriptional activators of T-bet. We found that butyrate upregulated *Il12rb1* and *Il12rb2* in butyrate-treated transgenic $CD8^+$ T cells (data not shown). Perhaps FoxO1-induced inhibition was bypassed through increased IL-12 signalling which is known to promote T-bet expression [444]. Additionally, the disconnect in transcriptional regulation may be attributed to butyrate-mediated mechanisms including signalling through SCFA receptors and epigenetic modifications [31, 151, 173]. As we and others have shown, butyrate is known to induce profound alterations in the transcriptome of the cell [445, 446]. These mechanisms have the potential to induce complex changes in transcriptional and epigenetic regulation of T-bet expression. Dual upregulation of FoxO1 and T-bet by butyrate is beneficial in terms of instilling both stem-like and effector-associated qualities in the CAR T cells. Of note, Gacerez *et al.* showed that T-bet overexpression in $CD4^+$ CAR T cells significantly increased *in vitro* production of proinflammatory cytokines including IFN-γ and TNF-α, and promoted the survival of lymphoma-bearing mice to a greater degree than $CD4^+$ CAR T cells that expressed CARs alone [407]. However, T-bet overexpression in their system was achieved by transduction with a CAR/T-bet construct [407], not butyrate.

To study the effects of butyrate on CAR T cell functionality, we assessed effector molecule expression. A previous study reported a butyrate-mediated increase in IFN-γ and TNF-α production by $CD8^+$ CAR T cells *in vitro* [123]. Here, we not only found that butyrate upregulated TNF-α in $CD8^+$ CAR T cells, but also promoted $CD4^+$ and $CD8^+$ CAR T cell production of other proinflammatory cytokines and cytotoxic

mediators. These phenotypic changes translated into an improved CAR T cell killing capacity induced by butyrate. We have observed a similar effect in transgenic $CD4^+$ and $CD8^+$ T cells, where butyrate significantly promoted *in vitro* direct killing of tumour cells by gDT-II cells (Section 4.2.7) and gBT-I cell killing of gB-expressing target cells *in vivo* (Lindsay Kosack; unpublished data). It is therefore likely that both $CD4^+$ and $CD8^+$ CAR T cells were able to lyse tumour cells.

One of our most striking findings was that monotherapy with butyrate-treated CAR T cells inhibited tumour growth *in vivo* similar to CAR T cell/ICB combination therapy. Our *in vitro* CAR T cell metabolic phenotyping suggests that butyrate also promoted mitochondrial activity, and potentially reduced susceptibility to exhaustion. In addition to the improved CAR T cell cytotoxicity, potential changes to stemness in both $CD4^+$ and $CD8^+$ subsets may have improved long-lived *in vivo* responses. Indeed, as other groups have also identified memory markers, fatty acid metabolism and mitochondrial metabolism to be closely associated with better anti-tumour responses [415, 447], it would not be surprising if butyrate was eliciting better tumour control through these mechanisms.

Treatment of CAR T cells with butyrate may overcome certain limitations of current strategies that are being trialled to improve treatment efficacy against solid tumours. Combination therapy with ICB, although generally effective in improving anti-cancer responses, introduces additional risks to patients [448]. ICB itself as well as CAR T cell/ICB synergy have led to potentially fatal off-target adverse events in the form of autoimmunity [448, 449]. Up to 40% of patients who received anti-PD1 reportedly suffered from fatigue or skin toxicities [450, 451], and 6% to 20% of melanoma patients who were enrolled in a phase 3 ICB clinical trial were diagnosed with thyroid dysfunction [452]. The use of butyrate in CAR T cell manufacturing processes may reduce the need for additional ICB and circumvent the associated risks.

One other study has shown that the usage of butyrate during $CD8^+$ CAR T cell manufacturing reduces the rate of tumour growth in a subcutaneous B16 melanoma model [123]. Building on these findings, we demonstrated that butyrate additionally promoted $CD4^+$ CAR T cell anti-tumour response *in vitro*, and showed that a

monotherapy consisting of both butyrate-treated $CD4^+$ and $CD8^+$ CAR T cells was as effective as CAR T cell/ICB combination therapy in an orthotopic E0771 breast cancer model. These exciting findings highlight the ability of microbiota-derived butyrate in promoting CAR T cell functionality and differentiation into anti-tumour subsets. As human CAR T cell *in vitro* phenotypes closely reflected that of murine CAR T cells, we look forward to our future studies which will aim to validate the use of human CAR T cells *in vivo*. In summary, we propose the novel concept of butyrate as a prospective avenue in improving existing CAR T cell therapy. Combined with our knowledge relating to the mechanisms of butyrate in T cells, our work presents new insights into how this compound targets selected molecules to regulate T cell fate decisions and functionality, and as such, the possible clinical relevance of this SCFA.

Chapter 6:
Final discussion and conclusions

Chapter 6 Final discussion and conclusions

6.1 Opening remarks

The appreciation of microbiota-derived SCFAs at the interface of commensals and host immune responses has grown considerably in the past few decades. SCFAs were initially understood to promote immunoregulation through Tregs, particularly in the context of autoimmunity such as ulcerative colitis [183, 201]. In recent years, their ability to induce Th1-associated factors such as IFN-γ and T-bet in Tregs [152] and IFN-γ in primary $CD8^+$ T cell responses [151, 181] has reflected a role of SCFAs that extends beyond anti-inflammatory responses. Dietary fibre consumption, SCFA-producing commensals and systemic SCFA levels have been associated with better progression-free survival of cancer patients and responses to ICB [153, 248, 249, 256]. However, our understanding of the direct contribution of SCFAs to T cell immunity during inflammation remains limited. To address this, we characterised SCFA-driven changes in effector $CD4^+$ and $CD8^+$ T cell differentiation and function, as well as their associated mechanisms and therapeutic applications.

6.2 Key findings and outlook

6.2.1 SCFA sensing through GPR41 and GPR43 promotes $CD8^+$ T cell memory potential

The majority of knowledge regarding the effects of SCFAs on $CD8^+$ T cells revolves around the upregulation of effector molecules [151, 181, 453, 454]. Although a few groups have investigated the mechanisms responsible for these effects, the importance of GPR41 and GPR43 signalling to $CD8^+$ T cell cytokine expression is still controversial [31, 151, 162, 181]. Furthermore, limited focus has been placed on how SCFA can skew $CD8^+$ T cell differentiation. Our previous work demonstrated a role for butyrate in enhancing $CD8^+$ T cell memory potential [31]. We showed that mechanistically, GPR41 and GPR43 expression was required for optimal IFN-γ production during recall responses upon the re-activation of memory T cells [31]. To understand whether this discrepancy in $CD8^+$ T cell memory function was associated with differences in priming, we compared the differentiation and function of GPR41/GPR43-deficient $CD8^+$ T cells with their competent counterparts during

primary viral infection. Given that infections with intracellular pathogens can raise SCFA levels to concentrations beyond the EC_{50} values of GPR41 and GPR43 [160, 188, 196], it was likely that cells were able to detect SCFAs through GPR41 and GPR43 in our model. Our findings suggested that GPR41 and GPR43 signalling contributed to the differentiation and optimal functionality of $CD8^+$ T cells *in vivo*. The expression of these receptors enabled increased retention of stemness, as indicated by a larger EEC population and preferential differentiation into MPECs in the spleen and skin of WT mice compared to GPR41/GPR43-deficient mice. Compared to SLECs, MPECs have been shown to preferentially seed into the skin and generate tissue-resident memory T cells, a subset of cells that confers immediate protection to local tissue upon re-infection [292, 455, 456]. This could be one important outcome of GPR41 and GPR43 signalling.

The role of SCFA receptors in T cell immunity remains unresolved with some reports showing low to undetectable mRNA transcripts encoding for these receptors in T cells [124, 174, 183, 184]. To address this, we validated that activated $CD8^+$ T cells expressed mRNA encoding GPR41 and GPR43. Secondly, to understand whether the effects on differentiation and function were due to a global deficiency in GPR41 and GPR43 or solely dependent on receptor signalling within $CD8^+$ T cells, we investigated $CD8^+$ T cell-intrinsic and extrinsic contributions of GPR41 and GPR43. By adoptively transferring WT gBT-I cells into GPR41/GPR43-deficient recipients, we discovered that optimal TNF-α production relied on $CD8^+$ T cell-intrinsic receptor signalling while memory precursor formation depended on $CD8^+$ T cell-extrinsic receptor signalling. GPR41 and GPR43 engagement activates the p38 mitogen-activated protein kinase and ERK signalling cascades that control a plethora of immune-related genes [173, 457]. For example, p38 is a key positive regulator of TNF-α in T cells [458], and ERK activation induces a memory phenotype as well as reduces the viral titres in acute and chronic LCMV infection [459]. These could be mechanisms by which SCFA signalling transcriptionally controls $CD8^+$ T cell immunity. SCFA-induced chemotaxis has been suggested to be an additional effect of GPR43 signalling in neutrophils [179], although this has not yet been demonstrated in T cells. In fact, our preliminary findings argued against a role for GPR41 and GPR43 in butyrate-induced T cell migration (data not shown).

The significant role of $CD8^+$ T cell-extrinsic receptor signalling in MPEC differentiation indicates the need to investigate the involvement of other cell types. Although there have not been prior studies describing how GPR41 and GPR43 signalling in DCs impacts $CD8^+$ T cell priming to our knowledge, SCFAs have been shown to prompt DCs to alter $CD4^+$ T cell differentiation in a GPR41- and GPR43-dependent manner [204, 234]. Taking into consideration that SCFAs can also act as metabolites [31] and induce epigenetic modifications [123], SCFA sensing through GPR41 and GPR43 is likely just one of the mechanisms by which SCFAs regulate $CD8^+$ T cell stemness and function during priming. To further distinguish the $CD8^+$ T cell-intrinsic and extrinsic effects of GPR41 and GPR43, we have generated GPR41/GPR43-deficient gBT-I mice for future experiments. We will transfer GPR41/GPR43-deficient gBT-I cells into WT recipients to confirm that MPEC differentiation and TNF-α production is driven by $CD8^+$ T cell-extrinsic and intrinsic receptor signalling respectively. Additionally, although our results indicated a correlation between GPR41- and GPR43-dependent TNF-α production by $CD8^+$ T cells and viral control, pro-inflammatory cytokine production by monocytes and epithelial cells are also known to be altered by SCFA receptors [460-462]. We next aim to validate that the attenuated viral control in receptor-deficient mice is caused by the lower TNF-α expression by $CD8^+$ T cells. To do so, we will compare the viral load in GPR41/GPR43-deficient mice that either received an adoptive transfer of TNF-α-deficient or WT gBT-I cells.

Apart from the influence of SCFAs on viral immunity, there is a growing interest in their role in cancer [153, 246, 463]. In B16 tumour-bearing mice, butyrate and pentanoate pre-treatment of $CD8^+$ T cells promoted their IFN-γ and TNF-α production [123]. Oral administration of these metabolites was also found to upregulate IFN-γ production by $CD8^+$ T cells in an MC38 mouse tumour model [154]. While it is known that agonist-induced signalling through GPR41 and GPR43 within tumour cells directly inhibits their proliferation and survival [464, 465], our results emphasise the potential of SCFA receptor signalling within $CD8^+$ T cells in aiding in anti-tumour responses. GPR41 and GPR43 enhance the following aspects of $CD8^+$ T cells which contribute to their role as central players in tumour control: their induction of cytotoxicity and ability to maintain long-term tumour surveillance. TNF-α, which is capable of inducing apoptosis and necroptosis of tumour cells [466], is elevated through GPR41 and

GPR43 signalling. Secondly, $CD8^+$ T cells are capable of long-term protection against cancer, with memory $CD8^+$ T cells associated with better patient prognosis [467, 468] and various therapies seeking to maintain a memory phenotype [469, 470]. Our observations that GPR41 and GPR43 signalling supports $CD8^+$ T cell memory potential and functionality could therefore have implications on cancer therapies. These findings add to a growing body of evidence demonstrating that SCFA sensing contributes to the $CD8^+$ T cell arm of pro-inflammatory responses. Synthetic GPR43 agonists that are currently being investigated for the treatment of inflammatory diseases such as inflammatory bowel disease [284, 471, 472] may therefore possess therapeutic potential in cancer.

6.2.2 Butyrate induces $CD4^+$ T cell cytotoxicity against tumour cells

Having shown that SCFA receptors can promote $CD8^+$ T cell stemness and functionality, we next sought to understand whether SCFAs also alter conventional $CD4^+$ T cell differentiation and function. It is well understood that SCFAs promote Treg formation and homeostasis, particularly under *in vitro* Treg polarising conditions and in autoimmune models [165, 183, 201]. However, a few studies have revealed that SCFAs can also support the enhanced expression of Th1-associated markers, such as T-bet and IFN-γ, when cells were activated under classical Th1 or even Treg polarising conditions *in vitro* [124, 152]. In a small clinical study that characterised the effects of dietary intervention on immune cell subsets, a higher number of Th1 cells were detected in healthy individuals on a high SCFA diet compared to those on a low SCFA diet [473]. Based on these studies, we hypothesised that SCFAs may enhance Th1-associated differentiation and functionality. Our study furthermore aimed to unravel the mechanisms behind this SCFA-induced phenotype and assess whether these functional changes impacted anti-tumour responses.

We cultured *in vitro* activated $CD4^+$ T cells with the SCFAs acetate, propionate or butyrate, and found that the Th1 master transcription factor, T-bet, was most strongly upregulated by butyrate. Strikingly, butyrate upregulated T-bet to a level that resembled classical Th1 cells. Butyrate promoted the expression of several other Th1-associated effector markers, such as Ly6C and IFN-γ. We additionally identified butyrate-induced increases in memory-associated and cytotoxic marker expression

that had not yet been reported by other studies. Interestingly, certain aspects of the transcriptional control induced by butyrate were non-characteristic of classical Th1 or cytotoxic $CD4^+$ T cells. For example, FoxO1 is typically downregulated in Th1 cells [304, 474] and its expression reportedly induces Treg differentiation instead [475]. However, we observed that butyrate promoted the upregulation of FoxO1 alongside T-bet. Of note, memory and terminal effector programmes are typically antagonistic. FoxO1 is a stemness marker [57, 354] while high T-bet levels are reflective of a terminal effector phenotype [305]. Butyrate appears to disrupt this inverse relationship. Although the exact mechanism for this remains unknown, inhibiting FoxO1 activity led us to pinpoint FoxO1 as a key transcriptional activator of butyrate-induced T-bet, Ly6C and IFN-γ expression. Butyrate induced significantly greater granzyme B, perforin and FasL expression – a phenotype shared with cytotoxic $CD4^+$ T cells. However, unlike cytotoxic $CD4^+$ T cells that classically upregulate Eomes, which is often recognised as their master transcription factor, butyrate did not alter Eomes expression [46, 476]. This led us to hypothesise that butyrate-treated $CD4^+$ T cells were non-classical cytotoxic Th1-like cells.

Our novel findings from this thesis highlighted the ability of butyrate to induce a pronounced increase in $CD4^+$ T cell killing of tumour cells. While many groups have shown that butyrate can directly kill tumour cells [477, 478], our data suggests that butyrate can also promote tumour cell death through $CD4^+$ T cell cytotoxicity. We identified that $CD4^+$ T cell cytotoxicity was mainly contingent on FasL. Others have likewise demonstrated that $CD4^+$ T cells can kill a range of target cells via the FasL/Fas pathway, including $CD8^+$ T cells [385] and APCs [479, 480]. Similar to untreated $CD4^+$ T cells, 65% of tumour cell death induced by butyrate-treated cells relied on FasL. This suggested that butyrate does not enhance killing through this mediator alone. Another possible contributor that can be assessed in the future is TRAIL, an inducer of programmed cell death that is known to be used by cytotoxic $CD4^+$ T cells to target FasL-resistant tumour cells [481, 482]. Most interestingly, the degree of tumour cell killing induced by butyrate even surpassed classical Th1 cells, emphasising that butyrate-treated cells were functionally distinct from classical Th1 cells. Interestingly, while other groups have identified that butyrate upregulated the immunoregulatory cytokine IL-10 in Th1 cells [203, 483] which could blunt anti-tumour immunity, our results suggest that the anti-tumour function remains intact in this model. Moreover,

butyrate-mediated cytotoxicity was strikingly similar to that induced by TSA-mediated histone acetylation. It has been shown that the deletion of HDAC3 increased the killing capacity $CD8^+$ T cells against B16 tumour cells, suggesting that histone acetylation indeed supports T cell cytotoxicity [484]. In line with previous reports of various cell types including Tregs [165, 167, 370], we showed that butyrate induced histone H3 acetylation in $CD4^+$ T cells. In this model, metabolic alterations, cytokine and cytotoxic mediator expression appeared to depend on histone acetylation. Butyrate is known to promote this epigenetic modification through HAT stimulation and HDAC inhibition [342]. HAT and HDAC activities can be assayed to understand the contributions of both pathways in butyrate-induced histone acetylation in the model tested. The potential effects of butyrate on HATs and HDACs coincides with reports that Sp1 promoter sites of various butyrate-responsive genes in tumour cells recruit HDACs and HATs which regulate histone acetylation, as summarised by Davie *et al.* [339]. Sp1 is a ubiquitous transcription factor that regulates the expression of a wide range of genes. In $CD8^+$ T cells, we established that Sp1 potentially regulated almost 60% of butyrate-responsive genes (unpublished data). Although the relationship between butyrate, Sp1, and the regulation of histone acetylation has not been studied in T cells, ChIP sequencing may shed some light on such associations in $CD4^+$ T cells. As such, another relevant question in the field is whether this transcription factor is required for butyrate-mediated epigenetic effects on target genes in $CD4^+$ T cells. As histone acetylation confers a better killing capacity to $CD4^+$ T cells, uncovering these epigenetic and transcriptional regulators could inform us about the mechanisms of butyrate-induced cytotoxicity.

Together, these results highlight the ability of butyrate to promote $CD4^+$ T cell cytotoxicity. Butyrate tunes $CD4^+$ T cell immunity, inducing stronger pro-inflammatory responses. Earlier reports about the prognostic value of cytotoxic $CD4^+$ T cells and Th1 cells in cancer have emphasised the importance of these subsets in anti-tumour responses. Upon ICB therapy, greater IFN-γ produced by Th1 cells enhanced tumour rejection, in part through the polarisation of $iNOS^+$ macrophages [485-487]. Cytotoxic $CD4^+$ T cells are particularly important as various tumours downregulate MHC-I to escape cytotoxic $CD8^+$ T cell detection, but are still susceptible to killing by $CD4^+$ T cells as they express MHC-II [488, 489]. With the ability of butyrate to enhance IFN-γ and cytotoxic mediator expression, and possibly even stemness through FoxO1

expression, butyrate may support sustained effector responses. A possible limitation of our experiments is that the concentration of butyrate which was used to treat *in vitro* cell cultures was greater than serum levels in humans but comparable to intestinal concentrations [127]. This suggests that our experimental setup may be more reflective of butyrate-mediated responses of $CD4^+$ T cells that are localised to or migrating through intestinal sites, compared to cells in distant regions. Hence, when considering the use of butyrate for therapeutic purposes, the optimal effects of butyrate on $CD4^+$ T cells are more likely to be achieved by direct SCFA administration *in vitro*. An example of how these findings may be applied in a therapeutic setting is through the use of butyrate during CAR T cell manufacturing which requires *in vitro* culturing of cells before infusion into patients.

6.2.3 $CD4^+$ and $CD8^+$ CAR T cell efficacy is improved by butyrate

CAR T cell therapy has been successful in treating haematological cancers and is currently being investigated in clinical trials for use against solid tumours [490]. Understanding the Achilles' heel of $CD4^+$ and $CD8^+$ CAR T cell subsets has informed us of potential targets to improve treatment efficacy. $CD4^+$ CAR T cells are known to be less cytotoxic than $CD8^+$ CAR T cells; while the latter are more prone to activation-induced cell death and showed reduced persistence than their $CD4^+$ counterparts [491-493]. Mechanistically, the metabolic dysfunction of CAR T cells severely limits the effectiveness of treatment resulting in reduced survival and attenuating effector functionality [494]. This is one of the key reasons for a majority of patients experiencing disease progression [495, 496]. As mentioned earlier, we detected butyrate-induced upregulation in both effector and memory-associated markers in transgenic $CD4^+$ and $CD8^+$ T cells. Additionally, in a separate experiment using chronic LCMV Docile-infected mice, we identified that butyrate significantly downregulated the exhaustion marker TOX in $CD8^+$ T cells (data not shown). We therefore hypothesised that butyrate could overcome limitations faced by conventional CAR T cells. By treating a mix of $CD4^+$ and $CD8^+$ CAR T cells with butyrate, we discovered that butyrate targeted the shortcomings of both subsets. Mitochondrial membrane potential and mitochondrial biomass were enhanced upon butyrate treatment of murine $CD4^+$ and $CD8^+$ CAR T cells. Butyrate improved the cytotoxicity and induced stemness-associated FoxO1 expression in $CD4^+$ and $CD8^+$ CAR T cells. A previous study that investigated the

effects of pentanoate on $CD8^+$ CAR T cells similarly indicated that TNF-α expression and the ability of pentanoate-treated CAR T cells to lyse K562 leukemia cells were elevated [123]. Furthermore, other studies have found that functional and dysfunctional CAR T cells possess distinct epigenetic profiles [496, 497]. As our results from Chapter 4 indicated that butyrate can induce histone hyperacetylation in $CD4^+$ T cells, it is possible that epigenetic modifications were an additional mechanism by which butyrate promoted effector- and memory-associated marker expression.

Relative to control CAR T cells, butyrate-treated murine CAR T cells showed enhanced killing of tumour cells *in vitro*. *In vivo*, we demonstrated that monotherapy using these superior CAR T cells generated with butyrate led to significantly better control of E0771-HER2 breast cancer relative to control CAR T cells or ICB monotherapy. Perhaps our most striking finding was that butyrate-treated CAR T cell monotherapy was as effective as CAR T cell/ICB combination therapy. To determine how butyrate confers an advantage to CAR T cells *in vivo*, it would be important to characterise the metabolic, cytotoxic and exhaustion marker profiles CAR T cells from mice that have received the respective therapies. The incorporation of butyrate into the CAR T cell manufacturing processes may reduce the need for combination therapy. As a result, this could serve as a potential avenue to minimise toxicities from ICB and lower treatment costs. Furthermore, our preliminary data showed that butyrate treatment of human CAR T cells led to similar changes to murine CAR T cells. The translatability of cancer immunotherapy between mouse and human immunology has also been demonstrated in a melanoma study by Gopalakrishnan *et al.* [248]. The authors showed that colonisation by microbiota from ICB patient responders led germ-free mice to control their tumours better than recipients of microbiota from patient non-responders [248]. Importantly, the bacterial families and genera associated with effector $CD4^+$ and $CD8^+$ T cells consisted of butyrate-producers. This hints at the exciting potential for butyrate-treated CAR T cells in improving treatment efficacy in humans.

As such, we sought to investigate the anti-tumour efficacy of butyrate-treated human CAR T cells. There is strong evidence for the synergy between $CD4^+$ and $CD8^+$ CAR T cells [392, 410], but we do not yet understand how butyrate alters this synergy or the contributions by the respective T cell subsets to tumour control. $CD4^+$ CAR T

cells are relatively under studied compared to their $CD8^+$ T cell counterparts. Despite this, there is evidence that $CD4^+$ CAR T cells alone improve the survival of lymphoma-bearing mice even in the absence of $CD8^+$ CAR T cells [407, 410]. This effect was even more prominent in $CD4^+$ CAR T cells that overexpressed T-bet [407]. Considering butyrate augments T-bet expression, the killing potential and stemness markers of $CD4^+$ T cells *in vitro*, we plan to further investigate the *in vivo* effects of butyrate-treated $CD4^+$ CAR T cells. This will be performed by treating LeY^+ OVCAR-3 tumour-bearing NOD SCID gamma (NSG) mice with human $CD4^+$ CAR T cells in the absence of their $CD8^+$ counterparts. Although the killing kinetics of $CD4^+$ and $CD8^+$ CAR T cells reportedly differ, they possess a similar overall effectiveness at direct killing of tumour cells [492, 498, 499]. This suggests a significant dependence of tumour control on $CD4^+$ CAR T cells that should be further investigated and harnessed. These findings can better inform us of the suitability of butyrate for therapeutic use from a translational perspective.

6.3 Concluding remarks

In summary, this thesis demonstrated that SCFAs such as butyrate are capable of complex regulation of $CD4^+$ and $CD8^+$ T cell immunity, giving rise to more efficient immune responses. Mammals are unable to digest dietary fibre, but carbohydrate-fermenting bacteria have filled this niche and co-evolved with their hosts, producing SCFAs. This commensalism suggests that SCFAs are advantageous to host biology. Our gut microbiota is known to be capable of immunomodulation [500, 501]. The disruption of this delicate ecosystem in turn creates systemic effects on our health. For example, illness, dietary changes and the use of antibiotics have the capacity to modify gut microbe composition. Dysbiosis can play a key role in cancer development, ranging from tumours in the colon to breast and laryngeal carcinomas [502, 503]. From dysbiosis stems a range of factors that are capable of tuning host immune responses and in turn, disease pathogenesis. For example, alterations in gut microbe diversity have implications on metabolic by-products generated by intestinal bacteria, such as SCFAs. Perturbances in SCFA availability in the microenvironment may change the nature of T cell responses through effects on differentiation and function, potentially resulting in sub-optimal immune responses.

From our data, not only could SCFAs enhance the production of effector molecules that possessed anti-viral and anti-tumour function, they also promoted T cell stemness which has the potential to improve memory responses to re-infection. Yet others have revealed that SCFAs also possess an immunoregulatory effect on both $CD4^+$ [210, 221, 363] and $CD8^+$ T cells [238, 504]. Perhaps an evolutionary benefit of humans housing SCFA-producing gut commensals is the homeostatic ability of SCFAs to limit excessive inflammation when self-tolerance is lost [183], but to also encourage a pro-inflammatory response in the presence of an immune threat as we have demonstrated. This dual role is also observed in the context of diet, where high fibre diets have been associated with both lower levels of inflammation in cardiovascular diseases and autoimmune conditions [505, 506], and better recovery upon viral infections or cancer [507, 508]. Exactly what tips the balance, causing SCFAs to have a pro- or anti-inflammatory effect, is not yet understood but it is likely context-dependent. Systemic SCFA concentrations may act as a rheostat in terms of determining the nature of responses induced. Infection with *Listeria monocytogenes* has been demonstrated to give rise to systemic acetate levels above baseline concentrations, thereby supporting $CD8^+$ T cell responses [160, 188]. Other factors such as the strength of antigen stimulation and type of cytokines in the microenvironment likely provide input signals in unison with SCFAs, determining the nature of the T cell response. Apart from the direct effects on T cells, the ability of SCFAs to regulate T cell responses through APCs, such as their activation, contributes an additional layer of complexity.

Our study has demonstrated that the strengthening of anti-viral and anti-tumour responses is not limited to the ability of butyrate to augment cytokine and cytotoxic mediator production, but may also be a result of improved stemness. The acquisition of effector function is generally believed to be a result of greater differentiation and a corresponding reduction in stemness. However, butyrate appears to disrupt the inverse relationship between the transcriptional regulators T-bet and FoxO1 though the potential mechanisms require further inquiry. This could nevertheless be highly advantageous, particularly in the context of potential re-infection or chronic T cell stimulation such as in cancer settings. From a translational perspective, the ability of butyrate to amplify both these qualities simultaneously can be harnessed for immunotherapy. This applies to T cell-based treatments such as CAR T cells where

the inclusion of butyrate in manufacturing processes could improve the persistence and functionality of CAR T cell products. Supporting T cell-based immunotherapies, such as ICB or CAR T cell therapy, with a higher intake of dietary fibre or butyrate supplements may also improve T cell responses. Our work invites further discussion and investigation of the clinical use of butyrate which could potentially serve as a powerful therapeutic avenue to enhance anti-cancer responses.

References

1. Haghikia, A., et al., *Dietary Fatty Acids Directly Impact Central Nervous System Autoimmunity via the Small Intestine.* Immunity, 2016. **44**(4): p. 951-953.
2. Macia, L., et al., *Microbial influences on epithelial integrity and immune function as a basis for inflammatory diseases.* Immunological Reviews, 2012. **245**(1): p. 164-176.
3. Rooks, M.G. and W.S. Garrett, *Gut microbiota, metabolites and host immunity.* Nature reviews. Immunology, 2016. **16**(6): p. 341-352.
4. Nanda, N.K., R. Apple, and E. Sercarz, *Limitations in plasticity of the T-cell receptor repertoire.* Proc Natl Acad Sci U S A, 1991. **88**(21): p. 9503-7.
5. Yang, K., et al., *The tumor suppressor Tsc1 enforces quiescence of naive T cells to promote immune homeostasis and function.* Nat Immunol, 2011. **12**(9): p. 888-97.
6. Jankovic, D., et al., *In the Absence of IL-12, CD4+ T Cell Responses to Intracellular Pathogens Fail to Default to a Th2 Pattern and Are Host Protective in an IL-10 Setting.* Immunity, 2002. **16**(3): p. 429-439.
7. Gonzalez, N.M., et al., *Schrödinger's T Cells: Molecular Insights Into Stemness and Exhaustion.* Frontiers in Immunology, 2021. **12**.
8. Gattinoni, L., et al., *T memory stem cells in health and disease.* Nature Medicine, 2017. **23**(1): p. 18-27.
9. Gattinoni, L., C.A. Klebanoff, and N.P. Restifo, *Paths to stemness: building the ultimate antitumour T cell.* Nature Reviews Cancer, 2012. **12**(10): p. 671-684.
10. Vodnala, S.K., et al., *T cell stemness and dysfunction in tumors are triggered by a common mechanism.* Science, 2019. **363**(6434).
11. Bhattacharyya, N.D. and C.G. Feng, *Regulation of T Helper Cell Fate by TCR Signal Strength.* Frontiers in Immunology, 2020. **11**.
12. Martinez-Sanchez, M.E., et al., *Role of Cytokine Combinations on CD4+ T Cell Differentiation, Partial Polarization, and Plasticity: Continuous Network Modeling Approach.* Frontiers in Physiology, 2018. **9**.
13. Buck, M.D., D. O'Sullivan, and E.L. Pearce, *T cell metabolism drives immunity.* Journal of Experimental Medicine, 2015. **212**(9): p. 1345-1360.
14. van der Windt, G.J.W. and E.L. Pearce, *Metabolic switching and fuel choice during T-cell differentiation and memory development.* Immunological reviews, 2012. **249**(1): p. 27-42.
15. Chapman, N.M., M.R. Boothby, and H. Chi, *Metabolic coordination of T cell quiescence and activation.* Nature Reviews Immunology, 2020. **20**(1): p. 55-70.
16. Plumlee, C.R., et al., *Early Effector CD8 T Cells Display Plasticity in Populating the Short-Lived Effector and Memory-Precursor Pools Following Bacterial or Viral Infection.* Scientific Reports, 2015. **5**(1): p. 12264.
17. Zimmermann, C., et al., *Kinetics of the response of naive and memory CD8 T cells to antigen: similarities and differences.* Eur J Immunol, 1999. **29**(1): p. 284-90.
18. Fazle Akbar, S.M., K. Inaba, and M. Onji, *Upregulation of MHC class II antigen on dendritic cells from hepatitis B virus transgenic mice by interferon-γ: abrogation of immune response defect to a T-cell-dependent antigen.* Immunology, 1996. **87**(4): p. 519-527.

19. Martini, M., et al., *IFN-gamma-mediated upmodulation of MHC class I expression activates tumor-specific immune response in a mouse model of prostate cancer.* Vaccine, 2010. **28**(20): p. 3548-57.
20. Jorgovanovic, D., et al., *Roles of IFN-γ in tumor progression and regression: a review.* Biomarker Research, 2020. **8**(1): p. 49.
21. Bhat, P., et al., *Interferon-γ derived from cytotoxic lymphocytes directly enhances their motility and cytotoxicity.* Cell Death & Disease, 2017. **8**(6): p. e2836-e2836.
22. Liu, Z.-g., *Molecular mechanism of TNF signaling and beyond.* Cell Research, 2005. **15**(1): p. 24-27.
23. Carswell, E.A., et al., *An endotoxin-induced serum factor that causes necrosis of tumors.* Proc Natl Acad Sci U S A, 1975. **72**(9): p. 3666-70.
24. Boivin, W.A., et al., *Intracellular versus extracellular granzyme B in immunity and disease: challenging the dogma.* Laboratory Investigation, 2009. **89**(11): p. 1195-1220.
25. Shrestha, B. and M.S. Diamond, *Fas ligand interactions contribute to CD8+ T-cell-mediated control of West Nile virus infection in the central nervous system.* J Virol, 2007. **81**(21): p. 11749-57.
26. Brincks, E.L., et al., *CD8 T cells utilize TRAIL to control influenza virus infection.* J Immunol, 2008. **181**(7): p. 4918-25.
27. Kaech, S.M. and W. Cui, *Transcriptional control of effector and memory CD8+ T cell differentiation.* Nature Reviews Immunology, 2012. **12**(11): p. 749-761.
28. Ahmed, R., et al., *The precursors of memory: models and controversies.* Nature Reviews Immunology, 2009. **9**(9): p. 662-668.
29. Joshi, N.S., et al., *Inflammation Directs Memory Precursor and Short-Lived Effector CD8+ T Cell Fates via the Graded Expression of T-bet Transcription Factor.* Immunity, 2007. **27**(2): p. 281-295.
30. Obar, J.J., et al., *Pathogen-induced inflammatory environment controls effector and memory CD8+ T cell differentiation.* J Immunol, 2011. **187**(10): p. 4967-78.
31. Bachem, A., et al., *Microbiota-Derived Short-Chain Fatty Acids Promote the Memory Potential of Antigen-Activated CD8+ T Cells.* Immunity, 2019.
32. Mescher, M.F., et al., *Signals required for programming effector and memory development by CD8+ T cells.* Immunological Reviews, 2006. **211**(1): p. 81-92.
33. Kolumam, G.A., et al., *Type I interferons act directly on CD8 T cells to allow clonal expansion and memory formation in response to viral infection.* Journal of Experimental Medicine, 2005. **202**(5): p. 637-650.
34. Khanolkar, A., M.J. Fuller, and A.J. Zajac, *CD4 T Cell-Dependent CD8 T Cell Maturation1.* The Journal of Immunology, 2004. **172**(5): p. 2834-2844.
35. Tejera, M.M., et al., *FoxO1 Controls Effector-to-Memory Transition and Maintenance of Functional CD8 T Cell Memory.* The Journal of Immunology, 2013. **191**(1): p. 187.
36. Zhang, L., et al., *Mammalian Target of Rapamycin Complex 2 Controls CD8 T Cell Memory Differentiation in a Foxo1-Dependent Manner.* Cell Rep, 2016. **14**(5): p. 1206-1217.
37. Veldhoen, M., et al., *Transforming growth factor-beta 'reprograms' the differentiation of T helper 2 cells and promotes an interleukin 9-producing subset.* Nat Immunol, 2008. **9**(12): p. 1341-6.
38. Duhen, T., et al., *Production of interleukin 22 but not interleukin 17 by a subset of human skin-homing memory T cells.* Nat Immunol, 2009. **10**(8): p. 857-63.

39. Crotty, S., *T follicular helper cell differentiation, function, and roles in disease.* Immunity, 2014. **41**(4): p. 529-42.
40. Nurieva, R.I., et al., *STAT5 Protein Negatively Regulates T Follicular Helper (Tfh) Cell Generation and Function *.* Journal of Biological Chemistry, 2012. **287**(14): p. 11234-11239.
41. Hernandez-Pando, R. and G.A. Rook, *The role of TNF-alpha in T-cell-mediated inflammation depends on the Th1/Th2 cytokine balance.* Immunology, 1994. **82**(4): p. 591-5.
42. Singh, V.K., S. Mehrotra, and S.S. Agarwal, *The paradigm of Th1 and Th2 cytokines.* Immunologic Research, 1999. **20**(3): p. 147-161.
43. Zhu, J., et al., *GATA-3 promotes Th2 responses through three different mechanisms: induction of Th2 cytokine production, selective growth of Th2 cells and inhibition of Th1 cell-specific factors.* Cell Res, 2006. **16**(1): p. 3-10.
44. Ivanov, I.I., et al., *The Orphan Nuclear Receptor RORγt Directs the Differentiation Program of Proinflammatory IL-17⁺ T Helper Cells.* Cell, 2006. **126**(6): p. 1121-1133.
45. Liang, S.C., et al., *Interleukin (IL)-22 and IL-17 are coexpressed by Th17 cells and cooperatively enhance expression of antimicrobial peptides.* Journal of Experimental Medicine, 2006. **203**(10): p. 2271-2279.
46. Takeuchi, A. and T. Saito, *CD4 CTL, a Cytotoxic Subset of CD4(+) T Cells, Their Differentiation and Function.* Frontiers in immunology, 2017. **8**: p. 194-194.
47. Brown, D.M., et al., *IL-2 and antigen dose differentially regulate perforin- and FasL-mediated cytolytic activity in antigen specific CD4+ T cells.* Cell Immunol, 2009. **257**(1-2): p. 69-79.
48. Hou, L. and K. Yuki, *CCR6 and CXCR6 Identify the Th17 Cells With Cytotoxicity in Experimental Autoimmune Encephalomyelitis.* Frontiers in Immunology, 2022. **13**.
49. Sujino, T., et al., *Tissue adaptation of regulatory and intraepithelial CD4+ T cells controls gut inflammation.* Science, 2016. **352**(6293): p. 1581-1586.
50. O'Garra, A. and N. Arai, *The molecular basis of T helper 1 and T helper 2 cell differentiation.* Trends in Cell Biology, 2000. **10**(12): p. 542-550.
51. Wan, Y.Y. and R.A. Flavell, *'Yin-Yang' functions of transforming growth factor-beta and T regulatory cells in immune regulation.* Immunol Rev, 2007. **220**: p. 199-213.
52. Newton, R.H., et al., *Maintenance of CD4 T cell fitness through regulation of Foxo1.* Nature Immunology, 2018. **19**(8): p. 838-848.
53. Dimeloe, S., et al., *The Immune-Metabolic Basis of Effector Memory CD4+ T Cell Function under Hypoxic Conditions.* The Journal of Immunology, 2016. **196**(1): p. 106-114.
54. Miggelbrink, A.M., et al., *CD4 T-Cell Exhaustion: Does It Exist and What Are Its Roles in Cancer?* Clin Cancer Res, 2021. **27**(21): p. 5742-5752.
55. MacLeod, M.K., et al., *CD4 memory T cells: what are they and what can they do?* Semin Immunol, 2009. **21**(2): p. 53-61.
56. Duhen, R., et al., *PD-1 and ICOS coexpression identifies tumor-reactive CD4+ T cells in human solid tumors.* The Journal of Clinical Investigation, 2022. **132**(12).
57. Rao, R.R., et al., *Transcription factor Foxo1 represses T-bet-mediated effector functions and promotes memory CD8(+) T cell differentiation.* Immunity, 2012. **36**(3): p. 374-387.

58. Szabo, S.J., et al., *Distinct effects of T-bet in TH1 lineage commitment and IFN-γ production in CD4 and CD8 T cells.* Science, 2002. **295**(5553): p. 338-342.
59. Mohamed Khalil, S., et al., *Protein Phosphatase 2A Activation Dependent Down Regulation of PGC1-Alpha and FOXO1 Phosphorylation with OSU-2S in Human Lymphoma Cells.* Blood, 2019. **134**(Supplement_1): p. 3977-3977.
60. Lettieri-Barbato, D., et al., *FoxO1 localizes to mitochondria of adipose tissue and is affected by nutrient stress.* Metabolism, 2019. **95**: p. 84-92.
61. van der Windt, Gerritje J.W., et al., *Mitochondrial Respiratory Capacity Is a Critical Regulator of CD8+ T Cell Memory Development.* Immunity, 2012. **36**(1): p. 68-78.
62. Prince, H.E., J. York, and E.R. Jensen, *Phenotypic comparison of the three populations of human lymphocytes defined by CD45RO and CD45RA expression.* Cellular Immunology, 1992. **145**(2): p. 254-262.
63. Gerberick, G.F., et al., *Selective modulation of T cell memory markers CD62L and CD44 on murine draining lymph node cells following allergen and irritant treatment.* Toxicol Appl Pharmacol, 1997. **146**(1): p. 1-10.
64. Baaten, B.J., C.R. Li, and L.M. Bradley, *Multifaceted regulation of T cells by CD44.* Commun Integr Biol, 2010. **3**(6): p. 508-12.
65. Ahn, E., et al., *Role of PD-1 during effector CD8 T cell differentiation.* Proceedings of the National Academy of Sciences, 2018. **115**(18): p. 4749-4754.
66. Gibney, E.R. and C.M. Nolan, *Epigenetics and gene expression.* Heredity, 2010. **105**(1): p. 4-13.
67. Tough, D.F., et al., *Epigenetic Regulation of T Cell Memory: Recalling Therapeutic Implications.* Trends in Immunology, 2020. **41**(1): p. 29-45.
68. Struhl, K., *Histone acetylation and transcriptional regulatory mechanisms.* Genes Dev, 1998. **12**(5): p. 599-606.
69. Barnes, C.E., D.M. English, and S.M. Cowley, *Acetylation & Co: an expanding repertoire of histone acylations regulates chromatin and transcription.* Essays Biochem, 2019. **63**(1): p. 97-107.
70. Gallinari, P., et al., *HDACs, histone deacetylation and gene transcription: from molecular biology to cancer therapeutics.* Cell Research, 2007. **17**(3): p. 195-211.
71. Schauder, D.M., et al., *E2A-regulated epigenetic landscape promotes memory CD8 T cell differentiation.* Proceedings of the National Academy of Sciences, 2021. **118**(16): p. e2013452118.
72. Scott-Browne, J.P., et al., *Dynamic Changes in Chromatin Accessibility Occur in CD8+ T Cells Responding to Viral Infection.* Immunity, 2016. **45**(6): p. 1327-1340.
73. Sanders, V.M., *Epigenetic regulation of Th1 and Th2 cell development.* Brain Behav Immun, 2006. **20**(4): p. 317-24.
74. Le Menn, G., A. Jabłońska, and Z. Chen, *The effects of post-translational modifications on Th17/Treg cell differentiation.* Biochimica et Biophysica Acta (BBA) - Molecular Cell Research, 2022. **1869**(6): p. 119223.
75. Fields, P.E., S.T. Kim, and R.A. Flavell, *Cutting edge: changes in histone acetylation at the IL-4 and IFN-gamma loci accompany Th1/Th2 differentiation.* J Immunol, 2002. **169**(2): p. 647-50.
76. Bandyopadhyay, S., H.Z. Qui, and A.J. Adler, *In vitro and in vivo differentiated effector CD8 T cells display divergent histone acetylation patterns within the Ifng locus.* Immunol Lett, 2009. **122**(2): p. 214-8.

77. Fields, P.E., S.T. Kim, and R.A. Flavell, *Cutting Edge: Changes in Histone Acetylation at the IL-4 and IFN-γ Loci Accompany Th1/Th2 Differentiation.* The Journal of Immunology, 2002. **169**(2): p. 647.
78. Fann, M., et al., *Histone acetylation is associated with differential gene expression in the rapid and robust memory CD8+ T-cell response.* Blood, 2006. **108**(10): p. 3363-3370.
79. Araki, Y., et al., *Genome-wide Analysis of Histone Methylation Reveals Chromatin State-Based Regulation of Gene Transcription and Function of Memory CD8+ T Cells.* Immunity, 2009. **30**(6): p. 912-925.
80. Denton, A.E., et al., *Differentiation-dependent functional and epigenetic landscapes for cytokine genes in virus-specific CD8+ T cells.* Proceedings of the National Academy of Sciences, 2011. **108**(37): p. 15306.
81. Araki, Y., et al., *Histone Acetylation Facilitates Rapid and Robust Memory CD8 T Cell Response through Differential Expression of Effector Molecules (Eomesodermin and Its Targets: Perforin and Granzyme B).* The Journal of Immunology, 2008. **180**(12): p. 8102.
82. Barski, A., et al., *Rapid Recall Ability of Memory T cells is Encoded in their Epigenome.* Scientific Reports, 2017. **7**(1): p. 39785.
83. Chisolm, D.A. and A.S. Weinmann, *TCR-Signaling Events in Cellular Metabolism and Specialization.* Frontiers in Immunology, 2015. **6**.
84. Shyer, J.A., R.A. Flavell, and W. Bailis, *Metabolic signaling in T cells.* Cell Research, 2020. **30**(8): p. 649-659.
85. Gerriets, V.A. and J.C. Rathmell, *Metabolic pathways in T cell fate and function.* Trends Immunol, 2012. **33**(4): p. 168-73.
86. Pearce, Erika L. and Edward J. Pearce, *Metabolic Pathways in Immune Cell Activation and Quiescence.* Immunity, 2013. **38**(4): p. 633-643.
87. Nicoli, F., et al., *Naïve CD8+ T-Cells Engage a Versatile Metabolic Program Upon Activation in Humans and Differ Energetically From Memory CD8+ T-Cells.* Frontiers in Immunology, 2018. **9**: p. 2736.
88. MacIver, N.J., R.D. Michalek, and J.C. Rathmell, *Metabolic Regulation of T Lymphocytes.* Annual Review of Immunology, 2013. **31**(1): p. 259-283.
89. Chang, C.-H., et al., *Posttranscriptional control of T cell effector function by aerobic glycolysis.* Cell, 2013. **153**(6): p. 1239-1251.
90. Stojan, G. and L. Christopher-Stine, *151 - Metabolic, drug-induced, and other noninflammatory myopathies*, in *Rheumatology (Sixth Edition)*, M.C. Hochberg, et al., Editors. 2015, Mosby: Philadelphia. p. 1255-1263.
91. Hume, D.A. and M.J. Weidemann, *Role and Regulation of Glucose Metabolism in Proliferating Cells.* JNCI: Journal of the National Cancer Institute, 1979. **62**(1): p. 3-8.
92. Rathmell, J.C., et al., *In the absence of extrinsic signals, nutrient utilization by lymphocytes is insufficient to maintain either cell size or viability.* Mol Cell, 2000. **6**(3): p. 683-92.
93. Buck, Michael D., et al., *Mitochondrial Dynamics Controls T Cell Fate through Metabolic Programming.* Cell, 2016. **166**(1): p. 63-76.
94. McKinney, E.F. and K.G.C. Smith, *Metabolic exhaustion in infection, cancer and autoimmunity.* Nature Immunology, 2018. **19**(3): p. 213-221.
95. Pearce, E.L., et al., *Enhancing CD8 T-cell memory by modulating fatty acid metabolism.* Nature, 2009. **460**(7251): p. 103-107.

96. O'Sullivan, D., et al., *Memory CD8(+) T cells use cell-intrinsic lipolysis to support the metabolic programming necessary for development.* 2014(1097-4180 (Electronic)).
97. van der Windt, G.J.W., et al., *CD8 memory T cells have a bioenergetic advantage that underlies their rapid recall ability.* Proceedings of the National Academy of Sciences, 2013. **110**(35): p. 14336.
98. Zhang, L., et al., *Mammalian Target of Rapamycin Complex 2 Controls CD8 T Cell Memory Differentiation in a Foxo1-Dependent Manner.* Cell Reports, 2016. **14**(5): p. 1206-1217.
99. Principe, N., et al., *Tumor Infiltrating Effector Memory Antigen-Specific CD8+ T Cells Predict Response to Immune Checkpoint Therapy.* Frontiers in Immunology, 2020. **11**.
100. Kilinc, M.O., et al., *Central Role of Tumor-Associated CD8+ T Effector/Memory Cells in Restoring Systemic Antitumor Immunity1.* The Journal of Immunology, 2009. **182**(7): p. 4217-4225.
101. Park, S.L., et al., *Tissue-resident memory CD8+ T cells promote melanoma–immune equilibrium in skin.* Nature, 2019. **565**(7739): p. 366-371.
102. Jin, Y., et al., *Prognostic Impact of Memory CD8(+) T Cells on Immunotherapy in Human Cancers: A Systematic Review and Meta-Analysis.* Frontiers in Oncology, 2021. **11**.
103. Webb, J.R., et al., *Tumor-Infiltrating Lymphocytes Expressing the Tissue Resident Memory Marker CD103 Are Associated with Increased Survival in High-Grade Serous Ovarian Cancer.* Clinical Cancer Research, 2014. **20**(2): p. 434-444.
104. Tosolini, M., et al., *Clinical Impact of Different Classes of Infiltrating T Cytotoxic and Helper Cells (Th1, Th2, Treg, Th17) in Patients with Colorectal Cancer.* Cancer Research, 2011. **71**(4): p. 1263-1271.
105. She, Y., et al., *Immune-related gene signature for predicting the prognosis of head and neck squamous cell carcinoma.* Cancer Cell International, 2020. **20**(1): p. 22.
106. He, Q.-F., et al., *CD8+ T-cell exhaustion in cancer: mechanisms and new area for cancer immunotherapy.* Briefings in Functional Genomics, 2019. **18**(2): p. 99-106.
107. Hartmann, J., et al., *Clinical development of CAR T cells—challenges and opportunities in translating innovative treatment concepts.* EMBO Molecular Medicine, 2017. **9**(9): p. 1183-1197.
108. Cai, Q., M. Zhang, and Z. Li, *Potential strategies against resistance to CAR T-cell therapy in haematological malignancies.* Therapeutic Advances in Medical Oncology, 2020. **12**: p. 1758835920962963.
109. Gattinoni, L., et al., *Acquisition of full effector function in vitro paradoxically impairs the in vivo antitumor efficacy of adoptively transferred CD8+ T cells.* The Journal of Clinical Investigation, 2005. **115**(6): p. 1616-1626.
110. Xu, Y., et al., *Closely related T-memory stem cells correlate with in vivo expansion of CAR.CD19-T cells and are preserved by IL-7 and IL-15.* Blood, 2014. **123**(24): p. 3750-9.
111. Konduri, V., et al., *A subset of cytotoxic effector memory T cells enhances CAR T cell efficacy in a model of pancreatic ductal adenocarcinoma.* Science Translational Medicine, 2021. **13**(592): p. eabc3196.

112. Xu, J. and J.I. Gordon, *Honor thy symbionts.* Proceedings of the National Academy of Sciences of the United States of America, 2003. **100**(18): p. 10452-10459.
113. Sender, R., S. Fuchs, and R. Milo, *Revised Estimates for the Number of Human and Bacteria Cells in the Body.* PLoS biology, 2016. **14**(8): p. e1002533-e1002533.
114. Gill Steven, R., et al., *Metagenomic Analysis of the Human Distal Gut Microbiome.* Science, 2006. **312**(5778): p. 1355-1359.
115. Qin, J., et al., *A human gut microbial gene catalogue established by metagenomic sequencing.* Nature, 2010. **464**(7285): p. 59-65.
116. Miller, T.L. and M.J. Wolin, *Pathways of acetate, propionate, and butyrate formation by the human fecal microbial flora.* Applied and Environmental Microbiology, 1996. **62**(5): p. 1589-1592.
117. Zhao, C., et al., *Discovery of potential genes contributing to the biosynthesis of short-chain fatty acids and lactate in gut microbiota from systematic investigation in E. coli.* npj Biofilms and Microbiomes, 2019. **5**(1): p. 19.
118. Schujman, G.E., et al., *FapR, a Bacterial Transcription Factor Involved in Global Regulation of Membrane Lipid Biosynthesis.* Developmental Cell, 2003. **4**(5): p. 663-672.
119. Chambers, E.S., et al., *Role of Gut Microbiota-Generated Short-Chain Fatty Acids in Metabolic and Cardiovascular Health.* (2161-3311 (Electronic)).
120. Sivan, A., et al., *Commensal Bifidobacterium promotes antitumor immunity and facilitates anti–PD-L1 efficacy.* Science, 2015. **350**(6264): p. 1084-1089.
121. Vetizou, M., et al., *Anticancer immunotherapy by CTLA-4 blockade relies on the gut microbiota.* 2015(1095-9203 (Electronic)).
122. Agus, A., K. Clément, and H. Sokol, *Gut microbiota-derived metabolites as central regulators in metabolic disorders.* Gut, 2021. **70**(6): p. 1174.
123. Luu, M., et al., *Microbial short-chain fatty acids modulate CD8+ T cell responses and improve adoptive immunotherapy for cancer.* Nature Communications, 2021. **12**(1): p. 4077.
124. Park, J., et al., *Short-chain fatty acids induce both effector and regulatory T cells by suppression of histone deacetylases and regulation of the mTOR–S6K pathway.* Mucosal Immunology, 2014. **8**: p. 80.
125. Knowles, S.E., et al., *Production and utilization of acetate in mammals.* Biochemical Journal, 1974. **142**(2): p. 401-411.
126. den Besten, G., et al., *The role of short-chain fatty acids in the interplay between diet, gut microbiota, and host energy metabolism.* Journal of Lipid Research, 2013. **54**(9): p. 2325-2340.
127. Cummings, J.H., et al., *Short chain fatty acids in human large intestine, portal, hepatic and venous blood.* Gut, 1987. **28**(10): p. 1221.
128. Macfarlane, G.T. and S. Macfarlane, *Bacteria, Colonic Fermentation, and Gastrointestinal Health.* Journal of AOAC INTERNATIONAL, 2012. **95**(1): p. 50-60.
129. Louis, P., et al., *Organization of butyrate synthetic genes in human colonic bacteria: phylogenetic conservation and horizontal gene transfer.* FEMS Microbiology Letters, 2007. **269**(2): p. 240-247.
130. Louis, P. and H.J. Flint, *Diversity, metabolism and microbial ecology of butyrate-producing bacteria from the human large intestine.* FEMS Microbiology Letters, 2009. **294**(1): p. 1-8.

131. Louis, P. and H.J. Flint, *Formation of propionate and butyrate by the human colonic microbiota.* Environmental Microbiology, 2017. **19**(1): p. 29-41.
132. Henson, M.A. and P. Phalak, *Suboptimal community growth mediated through metabolite crossfeeding promotes species diversity in the gut microbiota.* PLOS Computational Biology, 2018. **14**(10): p. e1006558.
133. Abdallah Ismail, N., et al., *Frequency of Firmicutes and Bacteroidetes in gut microbiota in obese and normal weight Egyptian children and adults.* Archives of medical science : AMS, 2011. **7**(3): p. 501-507.
134. Arumugam, M., et al., *Enterotypes of the human gut microbiome.* Nature, 2011. **473**(7346): p. 174-180.
135. Reichardt, N., et al., *Phylogenetic distribution of three pathways for propionate production within the human gut microbiota.* The ISME Journal, 2014. **8**(6): p. 1323-1335.
136. El Hage, R., et al., *Propionate-Producing Consortium Restores Antibiotic-Induced Dysbiosis in a Dynamic in vitro Model of the Human Intestinal Microbial Ecosystem.* Frontiers in Microbiology, 2019. **10**: p. 1206.
137. Louis, P., et al., *Diversity of human colonic butyrate-producing bacteria revealed by analysis of the butyryl-CoA:acetate CoA-transferase gene.* Environmental Microbiology, 2010. **12**(2): p. 304-314.
138. Aminov, R.I., et al., *Molecular Diversity, Cultivation, and Improved Detection by Fluorescent In Situ Hybridization of a Dominant Group of Human Gut Bacteria Related to Roseburia spp. or Eubacterium rectale.* Applied and Environmental Microbiology, 2006. **72**(9): p. 6371.
139. Louis, P., et al., *Diversity of human colonic butyrate-producing bacteria revealed by analysis of the butyryl-CoA:acetate CoA-transferase gene.* 2010(1462-2920 (Electronic)).
140. Lukovac, S., et al., *Differential Modulation by Akkermansia muciniphila and Faecalibacterium prausnitzii of Host Peripheral Lipid Metabolism and Histone Acetylation in Mouse Gut Organoids.* mBio. **5**(4): p. e01438-14.
141. Teichmann, J. and D.W. Cockburn, *In vitro Fermentation Reveals Changes in Butyrate Production Dependent on Resistant Starch Source and Microbiome Composition.* Frontiers in Microbiology, 2021. **12**: p. 976.
142. El-Salhy, M., et al., *Changes in fecal short-chain fatty acids following fecal microbiota transplantation in patients with irritable bowel syndrome.* Neurogastroenterology & Motility, 2021. **33**(2): p. e13983.
143. Puddu, A., et al., *Evidence for the Gut Microbiota Short-Chain Fatty Acids as Key Pathophysiological Molecules Improving Diabetes.* Mediators of Inflammation, 2014. **2014**: p. 162021.
144. Gomes, S.D., et al., *The Role of Diet Related Short-Chain Fatty Acids in Colorectal Cancer Metabolism and Survival: Prevention and Therapeutic Implications.* Curr Med Chem, 2020. **27**(24): p. 4087-4108.
145. Donohoe, D.R., et al., *A gnotobiotic mouse model demonstrates that dietary fiber protects against colorectal tumorigenesis in a microbiota- and butyrate-dependent manner.* Cancer discovery, 2014. **4**(12): p. 1387-1397.
146. Roediger, W.E.W., *THE COLONIC EPITHELIUM IN ULCERATIVE COLITIS: AN ENERGY-DEFICIENCY DISEASE?* The Lancet, 1980. **316**(8197): p. 712-715.
147. Dou, X., et al., *Sodium Butyrate Alleviates Mouse Colitis by Regulating Gut Microbiota Dysbiosis.* Animals : an open access journal from MDPI, 2020. **10**(7): p. 1154.

148. Tian, Y., et al., *Short-chain fatty acids administration is protective in colitis-associated colorectal cancer development.* The Journal of Nutritional Biochemistry, 2018. **57**: p. 103-109.
149. Mariño, E., et al., *Gut microbial metabolites limit the frequency of autoimmune T cells and protect against type 1 diabetes.* Nature Immunology, 2017. **18**(5): p. 552-562.
150. Li, L., et al., *Gut microbiota from colorectal cancer patients enhances the progression of intestinal adenoma in Apc(min/+) mice.* EBioMedicine, 2019. **48**: p. 301-315.
151. Luu, M., et al., *Regulation of the effector function of CD8+ T cells by gut microbiota-derived metabolite butyrate.* Scientific Reports, 2018. **8**(1): p. 14430.
152. Kespohl, M., et al., *The Microbial Metabolite Butyrate Induces Expression of Th1-Associated Factors in CD4+ T Cells.* Frontiers in Immunology, 2017. **8**: p. 1036.
153. Nomura, M., et al., *Association of Short-Chain Fatty Acids in the Gut Microbiome With Clinical Response to Treatment With Nivolumab or Pembrolizumab in Patients With Solid Cancer Tumors.* JAMA Network Open, 2020. **3**(4): p. e202895-e202895.
154. He, Y., et al., *Gut microbial metabolites facilitate anticancer therapy efficacy by modulating cytotoxic CD8+ T cell immunity.* Cell Metabolism, 2021. **33**(5): p. 988-1000.e7.
155. Kim, C.H., J. Park, and M. Kim, *Gut microbiota-derived short-chain Fatty acids, T cells, and inflammation.* Immune network, 2014. **14**(6): p. 277-288.
156. Gurav, A., et al., *Slc5a8, a Na+-coupled high-affinity transporter for short-chain fatty acids, is a conditional tumour suppressor in colon that protects against colitis and colon cancer under low-fibre dietary conditions.* The Biochemical journal, 2015. **469**(2): p. 267-278.
157. Miyauchi, S., et al., *Functional Identification of SLC5A8, a Tumor Suppressor Down-regulated in Colon Cancer, as a Na⁺-coupled Transporter for Short-chain Fatty Acids *.* Journal of Biological Chemistry, 2004. **279**(14): p. 13293-13296.
158. Poole, R.C. and A.P. Halestrap, *Transport of lactate and other monocarboxylates across mammalian plasma membranes.* American Journal of Physiology-Cell Physiology, 1993. **264**(4): p. C761-C782.
159. Halestrap, A.P., *The monocarboxylate transporter family—Structure and functional characterization.* IUBMB Life, 2012. **64**(1): p. 1-9.
160. Balmer, Maria L., et al., *Memory CD8+ T Cells Require Increased Concentrations of Acetate Induced by Stress for Optimal Function.* Immunity, 2016. **44**(6): p. 1312-1324.
161. Dennis Patrick, B., et al., *Mammalian TOR: A Homeostatic ATP Sensor.* Science, 2001. **294**(5544): p. 1102-1105.
162. Luu, M., et al., *The short-chain fatty acid pentanoate suppresses autoimmunity by modulating the metabolic-epigenetic crosstalk in lymphocytes.* Nature Communications, 2019. **10**(1): p. 760.
163. Sanchez, H.N., et al., *B cell-intrinsic epigenetic modulation of antibody responses by dietary fiber-derived short-chain fatty acids.* Nature Communications, 2020. **11**(1): p. 60.
164. Schulthess, J., et al., *The Short Chain Fatty Acid Butyrate Imprints an Antimicrobial Program in Macrophages.* Immunity, 2019. **50**(2): p. 432-445.

165. Arpaia, N., et al., *Metabolites produced by commensal bacteria promote peripheral regulatory T-cell generation.* Nature, 2013. **504**: p. 451.
166. Thomas, S.P. and J.M. Denu, *Short-chain fatty acids activate acetyltransferase p300.* eLife, 2021. **10**: p. e72171.
167. Vidali, G., et al., *Butyrate suppression of histone deacetylation leads to accumulation of multiacetylated forms of histones H3 and H4 and increased DNase I sensitivity of the associated DNA sequences.* Proceedings of the National Academy of Sciences of the United States of America, 1978. **75**(5): p. 2239-2243.
168. Magnusson, M.K., et al., *Impaired Butyrate Induced Regulation of T Cell Surface Expression of CTLA-4 in Patients with Ulcerative Colitis.* International Journal of Molecular Sciences, 2021. **22**(6).
169. Brown, A.J., et al., *The Orphan G protein-coupled receptors GPR41 and GPR43 are activated by propionate and other short chain carboxylic acids.* (0021-9258 (Print)).
170. Le Poul, E., et al., *Functional Characterization of Human Receptors for Short Chain Fatty Acids and Their Role in Polymorphonuclear Cell Activation.* Journal of Biological Chemistry, 2003. **278**(28): p. 25481-25489.
171. Nilsson, N.E., et al., *Identification of a free fatty acid receptor, FFA2R, expressed on leukocytes and activated by short-chain fatty acids.* Biochemical and Biophysical Research Communications, 2003. **303**(4): p. 1047-1052.
172. Pluznick, J.L., et al., *Olfactory receptor responding to gut microbiota-derived signals plays a role in renin secretion and blood pressure regulation.* Proceedings of the National Academy of Sciences of the United States of America, 2013. **110**(11): p. 4410-4415.
173. Kim, M.H., et al., *Short-chain fatty acids activate GPR41 and GPR43 on intestinal epithelial cells to promote inflammatory responses in mice.* Gastroenterology, 2013. **145**(1528-0012 (Electronic)).
174. Shi, Y., et al., *Induction of the apoptosis, degranulation and IL-13 production of human basophils by butyrate and propionate via suppression of histone deacetylation.* Immunology, 2021. **164**(2): p. 292-304.
175. Thangaraju, M., et al., *GPR109A Is a G-protein–Coupled Receptor for the Bacterial Fermentation Product Butyrate and Functions as a Tumor Suppressor in Colon.* Cancer Research, 2009. **69**(7): p. 2826.
176. Ulven, T., *Short-chain free fatty acid receptors FFA2/GPR43 and FFA3/GPR41 as new potential therapeutic targets.* Frontiers in Endocrinology, 2012. **3**: p. 111.
177. Bindels, L.B., E.M. Dewulf, and N.M. Delzenne, *GPR43/FFA2: physiopathological relevance and therapeutic prospects.* Trends in Pharmacological Sciences, 2013. **34**(4): p. 226-232.
178. Singh, N., et al., *Activation of Gpr109a, receptor for niacin and the commensal metabolite butyrate, suppresses colonic inflammation and carcinogenesis.* Immunity, 2014. **40**(1): p. 128-139.
179. Vinolo, M.A., et al., *Short-chain fatty acids stimulate the migration of neutrophils to inflammatory sites.* Clinical Science, 2009. **117**(1470-8736 (Electronic)).
180. Vinolo, M.A., et al., *SCFAs induce mouse neutrophil chemotaxis through the GPR43 receptor.* PLOS ONE, 2011. **6**(1932-6203 (Electronic)).
181. Trompette, A., et al., *Dietary Fiber Confers Protection against Flu by Shaping Ly6c(-) Patrolling Monocyte Hematopoiesis and CD8(+) T Cell Metabolism.* Immunity, 2018. **48**(1097-4180 (Electronic)).

182. Docampo, M.D., et al., *Expression of the Butyrate/niacin Receptor, GPR109a on T cells Plays an Important Role in a Mouse Model of Graft Versus Host Disease.* The Journal of Immunology, 2019. **202**(1 Supplement): p. 69.34.
183. Smith, P.M., et al., *The microbial metabolites, short-chain fatty acids, regulate colonic Treg cell homeostasis.* Science, 2013. **341**(1095-9203 (Electronic)).
184. Maslowski, K.M., et al., *Regulation of inflammatory responses by gut microbiota and chemoattractant receptor GPR43.* Nature, 2009. **461**(7268): p. 1282-1286.
185. Lavoie, S., et al., *Expression of Free Fatty Acid Receptor 2 by Dendritic Cells Prevents Their Expression of Interleukin 27 and Is Required for Maintenance of Mucosal Barrier and Immune Response Against Colorectal Tumors in Mice.* Gastroenterology, 2020. **158**(5): p. 1359-1372.e9.
186. Kim, C.H., *Control of lymphocyte functions by gut microbiota-derived short-chain fatty acids.* Cellular & Molecular Immunology, 2021. **18**(5): p. 1161-1171.
187. Qiu, J., et al., *Acetate Promotes T Cell Effector Function during Glucose Restriction.* Cell reports, 2019. **27**(7): p. 2063-2074.e5.
188. Balmer, M.L., et al., *Memory CD8+ T Cells Balance Pro- and Anti-inflammatory Activity by Reprogramming Cellular Acetate Handling at Sites of Infection.* Cell Metabolism, 2020. **32**(3): p. 457-467.e5.
189. Pan, Y., et al., *Survival of tissue-resident memory T cells requires exogenous lipid uptake and metabolism.* Nature, 2017. **543**(7644): p. 252-256.
190. van der Windt, G.J.W., et al., *CD8 memory T cells have a bioenergetic advantage that underlies their rapid recall ability.* Proceedings of the National Academy of Sciences, 2013. **110**(35): p. 14336-14341.
191. Kalia, V., et al., *Prolonged Interleukin-2Ralpha Expression on Virus-Specific CD8+ T Cells Favors Terminal-Effector Differentiation In Vivo.* Immunity, 2010. **32**(1): p. 91-103.
192. Sarkar, S., et al., *Functional and genomic profiling of effector CD8 T cell subsets with distinct memory fates.* (1540-9538 (Electronic)).
193. Buchholz Veit, R., et al., *Disparate Individual Fates Compose Robust CD8+ T Cell Immunity.* Science, 2013. **340**(6132): p. 630-635.
194. Gray, S.M., et al., *Polycomb Repressive Complex 2-Mediated Chromatin Repression Guides Effector CD8+ T Cell Terminal Differentiation and Loss of Multipotency.* Immunity, 2017. **46**(4): p. 596-608.
195. Pan, P., et al., *Loss of free fatty acid receptor 2 enhances colonic adenoma development and reduces the chemopreventive effects of black raspberries in ApcMin/+ mice.* Carcinogenesis, 2017. **38**(1): p. 86-93.
196. Brown, A.J., et al., *The Orphan G protein-coupled receptors GPR41 and GPR43 are activated by propionate and other short chain carboxylic acids.* 2003(0021-9258 (Print)).
197. Zhang, Y., A. Scoumanne, and X. Chen, *G Protein-Coupled Receptor 87: a Promising Opportunity for Cancer Drug Discovery.* Molecular and cellular pharmacology, 2010. **2**: p. 111-116.
198. Opferman, J.T., P.G. Ober Bt Fau - Ashton-Rickardt, and P.G. Ashton-Rickardt, *Linear differentiation of cytotoxic effectors into memory T lymphocytes.* 1999(0036-8075 (Print)).
199. Huleatt, J.W., et al., *P27kip1 regulates the cell cycle arrest and survival of activated T lymphocytes in response to interleukin-2 withdrawal.* Immunology, 2003. **108**(4): p. 493-501.
200. Reiner, S.L. and R.A. Seder, *Dealing from the evolutionary pawnshop: how lymphocytes make decisions.* (1074-7613 (Print)).

201. Furusawa, Y., et al., *Commensal microbe-derived butyrate induces the differentiation of colonic regulatory T cells.* Nature, 2013. **504**(7480): p. 446-450.
202. Zhang, M., et al., *Faecalibacterium prausnitzii produces butyrate to decrease c-Myc-related metabolism and Th17 differentiation by inhibiting histone deacetylase 3.* International Immunology, 2019. **31**(8): p. 499-514.
203. Chen, L., et al., *Microbiota Metabolite Butyrate Differentially Regulates Th1 and Th17 Cells' Differentiation and Function in Induction of Colitis.* Inflammatory bowel diseases, 2019. **25**(9): p. 1450-1461.
204. Trompette, A., et al., *Gut microbiota metabolism of dietary fiber influences allergic airway disease and hematopoiesis.* Nature Medicine, 2014. **20**(2): p. 159-166.
205. Endo, Y., et al., *ACC1 determines memory potential of individual CD4+ T cells by regulating de novo fatty acid biosynthesis.* Nature Metabolism, 2019. **1**(2): p. 261-275.
206. Michalek, R.D., et al., *Cutting Edge: Distinct Glycolytic and Lipid Oxidative Metabolic Programs Are Essential for Effector and Regulatory CD4+ T Cell Subsets.* The Journal of Immunology, 2011. **186**(6): p. 3299.
207. Zeng, H., et al., *mTORC1 and mTORC2 Kinase Signaling and Glucose Metabolism Drive Follicular Helper T Cell Differentiation.* Immunity, 2016. **45**(3): p. 540-554.
208. Beier, U.H., et al., *Essential role of mitochondrial energy metabolism in Foxp3+ T-regulatory cell function and allograft survival.* The FASEB Journal, 2015. **29**(6): p. 2315-2326.
209. Bhaskaran, N., et al., *Role of Short Chain Fatty Acids in Controlling T(regs) and Immunopathology During Mucosal Infection.* Frontiers in microbiology, 2018. **9**: p. 1995-1995.
210. Hao, F., et al., *Butyrate enhances CPT1A activity to promote fatty acid oxidation and iTreg differentiation.* Proceedings of the National Academy of Sciences, 2021. **118**(22): p. e2014681118.
211. Linke, M., et al., *mTORC1 and mTORC2 as regulators of cell metabolism in immunity.* FEBS letters, 2017. **591**(19): p. 3089-3103.
212. Delgoffe, G.M., et al., *The mTOR Kinase Differentially Regulates Effector and Regulatory T Cell Lineage Commitment.* Immunity, 2009. **30**(6): p. 832-844.
213. Araki, K., et al., *mTOR regulates memory CD8 T-cell differentiation.* Nature, 2009. **460**: p. 108.
214. Rao, R.R., et al., *The mTOR Kinase Determines Effector versus Memory CD8+ T Cell Fate by Regulating the Expression of Transcription Factors T-bet and Eomesodermin.* Immunity, 2010. **32**(1): p. 67-78.
215. Park, J., et al., *Chronically Elevated Levels of Short-Chain Fatty Acids Induce T Cell–Mediated Ureteritis and Hydronephrosis.* The Journal of Immunology, 2016. **196**(5): p. 2388.
216. Hu, H., et al., *4-Phenylbutyric Acid Increases GLUT4 Gene Expression through Suppression of HDAC5 but not Endoplasmic Reticulum Stress.* Cellular Physiology and Biochemistry, 2014. **33**(6): p. 1899-1910.
217. Chen, Y., et al., *Histone deacetylase (HDAC) inhibition improves myocardial function and prevents cardiac remodeling in diabetic mice.* Cardiovascular Diabetology, 2015. **14**(1): p. 99.

218. Brown, A.F., et al., *Memory Th1 Cells Are Protective in Invasive Staphylococcus aureus Infection.* PLOS Pathogens, 2015. **11**(11): p. e1005226.
219. Benoun, J.M., et al., *Optimal protection against Salmonella infection requires noncirculating memory.* Proceedings of the National Academy of Sciences, 2018. **115**(41): p. 10416-10421.
220. Laheurte, C., et al., *Distinct prognostic value of circulating anti-telomerase CD4+ Th1 immunity and exhausted PD-1+/TIM-3+ T cells in lung cancer.* British Journal of Cancer, 2019. **121**(5): p. 405-416.
221. Yang, W., et al., *Intestinal microbiota-derived short-chain fatty acids regulation of immune cell IL-22 production and gut immunity.* Nature Communications, 2020. **11**(1): p. 4457.
222. Preglej, T., et al., *Histone deacetylases 1 and 2 restrain CD4+ cytotoxic T lymphocyte differentiation.* JCI Insight, 2020. **5**(4).
223. Serefidou, M., A.V. Venkatasubramani, and A. Imhof, *The Impact of One Carbon Metabolism on Histone Methylation.* Frontiers in Genetics, 2019. **10**: p. 764.
224. Alegría-Torres, J.A., A. Baccarelli, and V. Bollati, *Epigenetics and lifestyle.* Epigenomics, 2011. **3**(3): p. 267-277.
225. Sharavanan, V.J., et al., *Pollutants inducing epigenetic changes and diseases.* Environmental Chemistry Letters, 2020. **18**(2): p. 325-343.
226. Tanoue, T., K. Atarashi, and K. Honda, *Development and maintenance of intestinal regulatory T cells.* 2016(1474-1741 (Electronic)).
227. Greyer, M., et al., *T Cell Help Amplifies Innate Signals in CD8+ DCs for Optimal CD8+ T Cell Priming.* Cell Reports, 2016. **14**(3): p. 586-597.
228. Lanzavecchia, A. and F. Sallusto, *Regulation of T Cell Immunity by Dendritic Cells.* Cell, 2001. **106**(3): p. 263-266.
229. Embgenbroich, M. and S. Burgdorf, *Current Concepts of Antigen Cross-Presentation.* Front Immunol, 2018. **9**: p. 1643.
230. Desch, A.N., et al., *CD103+ pulmonary dendritic cells preferentially acquire and present apoptotic cell-associated antigen.* J Exp Med, 2011. **208**(9): p. 1789-97.
231. Bedoui, S., et al., *Cross-presentation of viral and self antigens by skin-derived CD103+ dendritic cells.* Nature Immunology, 2009. **10**(5): p. 488-495.
232. Gao, Y., et al., *Control of T Helper 2 Responses by Transcription Factor IRF4-Dependent Dendritic Cells.* Immunity, 2013. **39**(4): p. 722-732.
233. Saito, Y., et al., *The Role of Type-2 Conventional Dendritic Cells in the Regulation of Tumor Immunity.* Cancers (Basel), 2022. **14**(8).
234. Tan, J., et al., *Dietary Fiber and Bacterial SCFA Enhance Oral Tolerance and Protect against Food Allergy through Diverse Cellular Pathways.* Cell Reports, 2016. **15**(12): p. 2809-2824.
235. Coutzac, C., et al., *Systemic short chain fatty acids limit antitumor effect of CTLA-4 blockade in hosts with cancer.* Nature Communications, 2020. **11**(1): p. 2168.
236. Liu, L., et al., *Butyrate interferes with the differentiation and function of human monocyte-derived dendritic cells.* Cellular Immunology, 2012. **277**(1): p. 66-73.
237. Säemann, M.D., et al., *Bacterial metabolite interference with maturation of human monocyte-derived dendritic cells.* Journal of Leukocyte Biology, 2002. **71**(2): p. 238-246.

238. Zimmerman, M.A., et al., *Butyrate suppresses colonic inflammation through HDAC1-dependent Fas upregulation and Fas-mediated apoptosis of T cells.* American Journal of Physiology-Gastrointestinal and Liver Physiology, 2012. **302**(12): p. G1405-G1415.
239. Haabeth, O.A., et al., *Inflammation driven by tumour-specific Th1 cells protects against B-cell cancer.* Nat Commun, 2011. **2**: p. 240.
240. Raskov, H., et al., *Cytotoxic CD8+ T cells in cancer and cancer immunotherapy.* British Journal of Cancer, 2021. **124**(2): p. 359-367.
241. Ling, A., et al., *The infiltration, and prognostic importance, of Th1 lymphocytes vary in molecular subgroups of colorectal cancer.* J Pathol Clin Res, 2016. **2**(1): p. 21-31.
242. Li, F., et al., *The association between CD8+ tumor-infiltrating lymphocytes and the clinical outcome of cancer immunotherapy: A systematic review and meta-analysis.* eClinicalMedicine, 2021. **41**.
243. Youn, B., et al., *Real-world use and survival outcomes of immune checkpoint inhibitors in older adults with non-small cell lung cancer.* Cancer, 2020. **126**(5): p. 978-985.
244. Graham, C., et al., *Cancer immunotherapy with CAR-T cells - behold the future.* Clinical medicine (London, England), 2018. **18**(4): p. 324-328.
245. Tanoue, T., et al., *A defined commensal consortium elicits CD8 T cells and anti-cancer immunity.* Nature, 2019. **565**(7741): p. 600-605.
246. Mirzaei, R., et al., *Role of microbiota-derived short-chain fatty acids in cancer development and prevention.* Biomedicine & Pharmacotherapy, 2021. **139**: p. 111619.
247. Helmink, B.A., et al., *The microbiome, cancer, and cancer therapy.* Nature Medicine, 2019. **25**(3): p. 377-388.
248. Gopalakrishnan, V., et al., *Gut microbiome modulates response to anti–PD-1 immunotherapy in melanoma patients.* Science, 2018. **359**(6371): p. 97.
249. Routy, B., et al., *Gut microbiome influences efficacy of PD-1–based immunotherapy against epithelial tumors.* Science, 2018. **359**(6371): p. 91.
250. Frankel, A.E., et al., *Metagenomic Shotgun Sequencing and Unbiased Metabolomic Profiling Identify Specific Human Gut Microbiota and Metabolites Associated with Immune Checkpoint Therapy Efficacy in Melanoma Patients.* Neoplasia, 2017. **19**(10): p. 848-855.
251. Lee, K.A., et al., *Cross-cohort gut microbiome associations with immune checkpoint inhibitor response in advanced melanoma.* Nature Medicine, 2022. **28**(3): p. 535-544.
252. Zhou, K., *Strategies to promote abundance of Akkermansia muciniphila, an emerging probiotics in the gut, evidence from dietary intervention studies.* J Funct Foods, 2017. **33**: p. 194-201.
253. Duncan, S.H., et al., *Contribution of acetate to butyrate formation by human faecal bacteria.* Br J Nutr, 2004. **91**(6): p. 915-23.
254. Chia, L.W., et al., *Bacteroides thetaiotaomicron Fosters the Growth of Butyrate-Producing Anaerostipes caccae in the Presence of Lactose and Total Human Milk Carbohydrates.* Microorganisms, 2020. **8**(10): p. 1513.
255. Simpson, R.C., et al., *Diet-driven microbial ecology underpins associations between cancer immunotherapy outcomes and the gut microbiome.* Nature Medicine, 2022. **28**(11): p. 2344-2352.

256. Spencer, C.N., et al., *Dietary fiber and probiotics influence the gut microbiome and melanoma immunotherapy response.* Science, 2021. **374**(6575): p. 1632-1640.
257. Lee, S.H., et al., *Bifidobacterium bifidum strains synergize with immune checkpoint inhibitors to reduce tumour burden in mice.* Nat Microbiol, 2021. **6**(3): p. 277-288.
258. Usta-Gorgun, B. and L. Yilmaz-Ersan, *Short-chain fatty acids production by Bifidobacterium species in the presence of salep.* Electronic Journal of Biotechnology, 2020. **47**: p. 29-35.
259. Matson, V., et al., *The commensal microbiome is associated with anti–PD-1 efficacy in metastatic melanoma patients.* Science, 2018. **359**(6371): p. 104-108.
260. Rios-Covian, D., et al., *Enhanced butyrate formation by cross-feeding between Faecalibacterium prausnitzii and Bifidobacterium adolescentis.* FEMS Microbiology Letters, 2015. **362**(21).
261. Valdes, A.M., et al., *Role of the gut microbiota in nutrition and health.* Bmj, 2018. **361**: p. k2179.
262. Leeming, E.R., et al., *Effect of Diet on the Gut Microbiota: Rethinking Intervention Duration.* Nutrients, 2019. **11**(12).
263. Ramirez, J., et al., *Antibiotics as Major Disruptors of Gut Microbiota.* Frontiers in Cellular and Infection Microbiology, 2020. **10**.
264. Sullivan, A., C. Edlund, and C.E. Nord, *Effect of antimicrobial agents on the ecological balance of human microflora.* Lancet Infect Dis, 2001. **1**(2): p. 101-14.
265. Gogoi, M., et al., *Dual role of arginine metabolism in establishing pathogenesis.* Curr Opin Microbiol, 2016. **29**: p. 43-8.
266. Godlewska, U., E. Bulanda, and T.P. Wypych, *Bile acids in immunity: Bidirectional mediators between the host and the microbiota.* Frontiers in Immunology, 2022. **13**.
267. Hou, H., et al., *Gut microbiota-derived short-chain fatty acids and colorectal cancer: Ready for clinical translation?* Cancer Letters, 2022. **526**: p. 225-235.
268. Lee, J.B., S.-J. Ha, and H.R. Kim, *Clinical Insights Into Novel Immune Checkpoint Inhibitors.* Frontiers in Pharmacology, 2021. **12**.
269. Taylor, B.A., *Genetic Relationships Between Inbred Strains of Mice.* Journal of Heredity, 1972. **63**(2): p. 83-86.
270. Mueller, S.N., et al., *Characterization of two TCR transgenic mouse lines specific for herpes simplex virus.* Immunology & Cell Biology, 2002. **80**(2): p. 156-163.
271. Tang, C., et al., *Loss of FFA2 and FFA3 increases insulin secretion and improves glucose tolerance in type 2 diabetes.* Nat Med, 2015. **21**(2): p. 173-7.
272. Piechocki, M.P., et al., *Human ErbB-2 (Her-2) transgenic mice: a model system for testing Her-2 based vaccines.* J Immunol, 2003. **171**(11): p. 5787-94.
273. Kershaw, M.H., et al., *Gene-Engineered T Cells as a Superior Adjuvant Therapy for Metastatic Cancer.* The Journal of Immunology, 2004. **173**(3): p. 2143.
274. Wang, S.H., et al., *Characterization of a Novel Transgenic Mouse Tumor Model for Targeting HER2+ Cancer Stem Cells.* International Journal of Biological Sciences, 2014. **10**(1): p. 25-32.

275. Lyons, M.J. and J. Heyduk, *Aspects of the developmental morphology of California encephalitis virus in cultured vertebrae and arthropod cells and in mouse brain.* Virology, 1973. **54**(1): p. 37-52.
276. Markowitz, D., S. Goff, and A. Bank, *A safe packaging line for gene transfer: separating viral genes on two different plasmids.* Journal of Virology, 1988. **62**(4): p. 1120-1124.
277. Westwood, J.A., et al., *Adoptive transfer of T cells modified with a humanized chimeric receptor gene inhibits growth of Lewis-Y-expressing tumors in mice.* Proc Natl Acad Sci U S A, 2005. **102**(52): p. 19051-6.
278. Miller, A.D., et al., *Construction and properties of retrovirus packaging cells based on gibbon ape leukemia virus.* Journal of Virology, 1991. **65**(5): p. 2220-2224.
279. Wylie, B., et al., *Cross-presentation of cutaneous melanoma antigen by migratory XCR1+CD103− and XCR1+CD103+ dendritic cells.* OncoImmunology, 2015. **4**(8): p. e1019198.
280. Rawls, W.E., et al., *A search for viruses in smegma, premalignant and early malignant cervical tissues. The isolation of Herpesviruses with distinct antigenic properties.* Am J Epidemiol, 1968. **87**(3): p. 647-55.
281. Isaaz, S., et al., *Serial killing by cytotoxic T lymphocytes: T cell receptor triggers degranulation, re-filling of the lytic granules and secretion of lytic proteins via a non-granule pathway.* Eur J Immunol, 1995. **25**(4): p. 1071-9.
282. Wojciech, L., K.S.W. Tan, and N.R.J. Gascoigne *Taming the Sentinels: Microbiome-Derived Metabolites and Polarization of T Cells*. International Journal of Molecular Sciences, 2020. **21**, DOI: 10.3390/ijms21207740.
283. Nakajima, A., et al., *The short chain fatty acid receptor GPR43 regulates inflammatory signals in adipose tissue M2-type macrophages.* (1932-6203 (Electronic)).
284. Park, B.-O., et al., *Novel GPR43 Agonists Exert an Anti-Inflammatory Effect in a Colitis Model.* Biomolecules & Therapeutics, 2022. **30**(1): p. 48-54.
285. Halnes, I., et al., *Soluble Fibre Meal Challenge Reduces Airway Inflammation and Expression of GPR43 and GPR41 in Asthma. LID - 10.3390/nu9010057 [doi] LID - 57.* (2072-6643 (Electronic)).
286. Park, J., et al., *Bidirectional regulatory potentials of short-chain fatty acids and their G-protein-coupled receptors in autoimmune neuroinflammation.* 2019(2045-2322 (Electronic)).
287. Chmielarczyk, W., et al., *Injection of anti-thy-1.2 serum breaks genetic resistance of mice against herpes simplex virus.* J Gen Virol, 1985. **66 (Pt 5)**: p. 1087-94.
288. van Lint, A., et al., *Herpes Simplex Virus-Specific CD8+ T Cells Can Clear Established Lytic Infections from Skin and Nerves and Can Partially Limit the Early Spread of Virus after Cutaneous Inoculation.* The Journal of Immunology, 2004. **172**(1): p. 392.
289. Wakim, L.M., et al., *CD8(+) T-cell attenuation of cutaneous herpes simplex virus infection reduces the average viral copy number of the ensuing latent infection.* Immunol Cell Biol, 2008. **86**(8): p. 666-75.
290. Huster, K.M., et al., *Selective expression of IL-7 receptor on memory T cells identifies early CD40L-dependent generation of distinct CD8+ memory T cell subsets.* Proc Natl Acad Sci U S A, 2004. **101**(15): p. 5610-5.
291. Heng, T.S.P., et al., *The Immunological Genome Project: networks of gene expression in immune cells.* Nature Immunology, 2008. **9**(10): p. 1091-1094.

292. Hochheiser, K., et al., *Ptpn2 and KLRG1 regulate the generation and function of tissue-resident memory CD8+ T cells in skin.* J Exp Med, 2021. **218**(6).
293. Pipkin, M.E., et al., *Interleukin-2 and inflammation induce distinct transcriptional programs that promote the differentiation of effector cytolytic T cells.* Immunity, 2010. **32**(1): p. 79-90.
294. Cui, W., et al., *Effects of Signal 3 during CD8 T cell priming: Bystander production of IL-12 enhances effector T cell expansion but promotes terminal differentiation.* Vaccine, 2009. **27**(15): p. 2177-87.
295. Justice, E.A., et al., *Disseminated cutaneous Herpes Simplex Virus-1 in a woman with rheumatoid arthritis receiving infliximab: a case report.* J Med Case Rep, 2008. **2**: p. 282.
296. Strangfeld, A., et al., *Risk of herpes zoster in patients with rheumatoid arthritis treated with anti-TNF-alpha agents.* Jama, 2009. **301**(7): p. 737-44.
297. Xiu, W., et al., *Microbiota-derived short chain fatty acid promotion of Amphiregulin expression by dendritic cells is regulated by GPR43 and Blimp-1.* Biochem Biophys Res Commun, 2020. **533**(3): p. 282-288.
298. Wu, W., et al., *Microbiota metabolite short-chain fatty acid acetate promotes intestinal IgA response to microbiota which is mediated by GPR43.* Mucosal Immunology, 2017. **10**(4): p. 946-956.
299. Ahrends, T., et al., *CD4+ T cell help creates memory CD8+ T cells with innate and help-independent recall capacities.* Nature Communications, 2019. **10**(1): p. 5531.
300. Minami, M., et al., *Role of IFN-γ and Tumor Necrosis Factor-α in Herpes Simplex Virus Type 1 Infection.* Journal of Interferon & Cytokine Research, 2002. **22**(6): p. 671-676.
301. Sergerie, Y., S. Rivest, and G. Boivin, *Tumor necrosis factor-alpha and interleukin-1 beta play a critical role in the resistance against lethal herpes simplex virus encephalitis.* J Infect Dis, 2007. **196**(6): p. 853-60.
302. Yap, Y.A., et al., *An acetate-yielding diet imprints an immune and anti-microbial programme against enteric infection.* Clinical & Translational Immunology, 2021. **10**(1): p. e1233.
303. Rangan, P. and A. Mondino, *Microbial short-chain fatty acids: a strategy to tune adoptive T cell therapy.* Journal for ImmunoTherapy of Cancer, 2022. **10**(7): p. e004147.
304. Kerdiles, Y.M., et al., *Foxo Transcription Factors Control Regulatory T Cell Development and Function.* Immunity, 2010. **33**(6): p. 890-904.
305. Marshall, Heather D., et al., *Differential Expression of Ly6C and T-bet Distinguish Effector and Memory Th1 CD4+ Cell Properties during Viral Infection.* Immunity, 2011. **35**(4): p. 633-646.
306. Renaude, E., et al., *Epigenetic Reprogramming of CD4+ Helper T Cells as a Strategy to Improve Anticancer Immunotherapy.* Frontiers in Immunology, 2021. **12**.
307. Bradbury, K.E., N. Murphy, and T.J. Key, *Diet and colorectal cancer in UK Biobank: a prospective study.* International Journal of Epidemiology, 2019. **49**(1): p. 246-258.
308. Yu, E.Y.W., et al., *Grain and dietary fiber intake and bladder cancer risk: a pooled analysis of prospective cohort studies.* The American Journal of Clinical Nutrition, 2020. **112**(5): p. 1252-1266.

309. Hester, C.M., et al., *Fecal microbes, short chain fatty acids, and colorectal cancer across racial/ethnic groups.* World J Gastroenterol, 2015. **21**(9): p. 2759-69.
310. Pichler, M.J., et al., *Butyrate producing colonic Clostridiales metabolise human milk oligosaccharides and cross feed on mucin via conserved pathways.* Nature Communications, 2020. **11**(1): p. 3285.
311. Vital, M., A. Karch, and D.H. Pieper, *Colonic Butyrate-Producing Communities in Humans: an Overview Using Omics Data.* mSystems, 2017. **2**(6).
312. Geirnaert, A., et al., *Butyrate-producing bacteria supplemented in vitro to Crohn's disease patient microbiota increased butyrate production and enhanced intestinal epithelial barrier integrity.* Scientific Reports, 2017. **7**(1): p. 11450.
313. Zhou, L., et al., *Faecalibacterium prausnitzii Produces Butyrate to Maintain Th17/Treg Balance and to Ameliorate Colorectal Colitis by Inhibiting Histone Deacetylase 1.* Inflammatory Bowel Diseases, 2018. **24**(9): p. 1926-1940.
314. Chen, X., et al., *Sodium butyrate regulates Th17/Treg cell balance to ameliorate uveitis via the Nrf2/HO-1 pathway.* Biochemical Pharmacology, 2017. **142**: p. 111-119.
315. Nishimura, T., et al., *Distinct Role of Antigen-Specific T Helper Type 1 (Th1) and Th2 Cells in Tumor Eradication in Vivo.* Journal of Experimental Medicine, 1999. **190**(5): p. 617-628.
316. Brown, D.M., A.T. Lampe, and A.M. Workman, *The Differentiation and Protective Function of Cytolytic CD4 T Cells in Influenza Infection.* Front Immunol, 2016. **7**: p. 93.
317. Nagasaki, J., et al., *The critical role of CD4+ T cells in PD-1 blockade against MHC-II–expressing tumors such as classic Hodgkin lymphoma.* Blood Advances, 2020. **4**(17): p. 4069-4082.
318. De Monte, L., et al., *Intratumor T helper type 2 cell infiltrate correlates with cancer-associated fibroblast thymic stromal lymphopoietin production and reduced survival in pancreatic cancer.* Journal of Experimental Medicine, 2011. **208**(3): p. 469-478.
319. Mucida, D., et al., *Transcriptional reprogramming of mature CD4+ helper T cells generates distinct MHC class II–restricted cytotoxic T lymphocytes.* Nature Immunology, 2013. **14**(3): p. 281-289.
320. Knudson, C.J., et al., *Mechanisms of Antiviral Cytotoxic CD4 T Cell Differentiation.* Journal of Virology, 2021. **95**(19): p. e00566-21.
321. Kim, H.-J. and H. Cantor, *CD4 T-cell Subsets and Tumor Immunity: The Helpful and the Not-so-Helpful.* Cancer Immunology Research, 2014. **2**(2): p. 91-98.
322. Liu, L., et al., *Enhanced CAR-T activity against established tumors by polarizing human T cells to secrete interleukin-9.* Nature Communications, 2020. **11**(1): p. 5902.
323. Tay, R.E., E.K. Richardson, and H.C. Toh, *Revisiting the role of CD4+ T cells in cancer immunotherapy—new insights into old paradigms.* Cancer Gene Therapy, 2021. **28**(1): p. 5-17.
324. Heinzel, F.P., et al., *Reciprocal expression of interferon gamma or interleukin 4 during the resolution or progression of murine leishmaniasis. Evidence for expansion of distinct helper T cell subsets.* J Exp Med, 1989. **169**(1): p. 59-72.
325. Mills, C.D., et al., *M-1/M-2 macrophages and the Th1/Th2 paradigm.* J Immunol, 2000. **164**(12): p. 6166-73.

326. Rogers, P.R., G. Huston, and S.L. Swain, *High antigen density and IL-2 are required for generation of CD4 effectors secreting Th1 rather than Th0 cytokines.* J Immunol, 1998. **161**(8): p. 3844-52.
327. Harms Pritchard, G., et al., *Diverse Roles for T-bet in the Effector Responses Required for Resistance to Infection.* The Journal of Immunology, 2015. **194**(3): p. 1131-1140.
328. Koch, M.A., et al., *The transcription factor T-bet controls regulatory T cell homeostasis and function during type 1 inflammation.* Nat Immunol, 2009. **10**(6): p. 595-602.
329. Groom, J.R. and A.D. Luster, *CXCR3 in T cell function.* Experimental cell research, 2011. **317**(5): p. 620-631.
330. Cabrera-Ortega, A.A., et al., *The Role of Forkhead Box 1 (FOXO1) in the Immune System: Dendritic Cells, T Cells, B Cells, and Hematopoietic Stem Cells.* Crit Rev Immunol, 2017. **37**(1): p. 1-13.
331. Brown, D.M., et al., *Multifunctional CD4 Cells Expressing Gamma Interferon and Perforin Mediate Protection against Lethal Influenza Virus Infection.* Journal of Virology, 2012. **86**(12): p. 6792-6803.
332. Marshall, N.B., et al., *NKG2C/E Marks the Unique Cytotoxic CD4 T Cell Subset, ThCTL, Generated by Influenza Infection.* J Immunol, 2017. **198**(3): p. 1142-1155.
333. Hua, L., et al., *Cytokine-Dependent Induction of CD4+ T cells with Cytotoxic Potential during Influenza Virus Infection.* Journal of Virology, 2013. **87**(21): p. 11884-11893.
334. van der Hee, B. and J.M. Wells, *Microbial Regulation of Host Physiology by Short-chain Fatty Acids.* Trends Microbiol, 2021. **29**(8): p. 700-712.
335. Yao, Y., et al., *The role of short-chain fatty acids in immunity, inflammation and metabolism.* Crit Rev Food Sci Nutr, 2022. **62**(1): p. 1-12.
336. Yonezawa, T., Y. Kobayashi, and Y. Obara, *Short-chain fatty acids induce acute phosphorylation of the p38 mitogen-activated protein kinase/heat shock protein 27 pathway via GPR43 in the MCF-7 human breast cancer cell line.* Cell Signal, 2007. **19**(1): p. 185-93.
337. Chang, C.-F., et al., *Polar Opposites: Erk Direction of CD4 T Cell Subsets.* The Journal of Immunology, 2012. **189**(2): p. 721-731.
338. Badou, A., et al., *Weak TCR stimulation induces a calcium signal that triggers IL-4 synthesis, stronger TCR stimulation induces MAP kinases that control IFN-γ production.* European Journal of Immunology, 2001. **31**(8): p. 2487-2496.
339. Davie, J.R., *Inhibition of Histone Deacetylase Activity by Butyrate.* The Journal of Nutrition, 2003. **133**(7): p. 2485S-2493S.
340. Chang, S. and T.M. Aune, *Histone hyperacetylated domains across the Ifng gene region in natural killer cells and T cells.* Proceedings of the National Academy of Sciences, 2005. **102**(47): p. 17095-17100.
341. Morinobu, A., Y. Kanno, and J.J. O'Shea, *Discrete Roles for Histone Acetylation in Human T Helper 1 Cell-specific Gene Expression *.* Journal of Biological Chemistry, 2004. **279**(39): p. 40640-40646.
342. Donohoe, Dallas R., et al., *The Warburg Effect Dictates the Mechanism of Butyrate-Mediated Histone Acetylation and Cell Proliferation.* Molecular Cell, 2012. **48**(4): p. 612-626.
343. Tay, R.E., et al., *Hdac3 is an epigenetic inhibitor of the cytotoxicity program in CD8 T cells.* Journal of Experimental Medicine, 2020. **217**(7).

344. Doñas, C., et al., *Trichostatin A Promotes the Generation and Suppressive Functions of Regulatory T Cells.* Clinical & developmental immunology, 2013. **2013**: p. 679804.
345. Kratchmarov, R., et al., *IRF4 Couples Anabolic Metabolism to Th1 Cell Fate Determination.* Immunohorizons, 2017. **1**(7): p. 156-161.
346. Macintyre, Andrew N., et al., *The Glucose Transporter Glut1 Is Selectively Essential for CD4+ T Cell Activation and Effector Function.* Cell Metabolism, 2014. **20**(1): p. 61-72.
347. Chang, C.-H., et al., *Posttranscriptional Control of T Cell Effector Function by Aerobic Glycolysis.* Cell, 2013. **153**(6): p. 1239-1251.
348. Michalek, R.D., et al., *Cutting edge: distinct glycolytic and lipid oxidative metabolic programs are essential for effector and regulatory CD4+ T cell subsets.* 2011(1550-6606 (Electronic)).
349. Trefely, S., M.T. Doan, and N.W. Snyder, *Chapter One - Crosstalk between cellular metabolism and histone acetylation*, in *Methods in Enzymology*, B.A. Garcia, Editor. 2019, Academic Press. p. 1-21.
350. Huo, M., et al., *Interplay Among Metabolism, Epigenetic Modifications, and Gene Expression in Cancer.* Front Cell Dev Biol, 2021. **9**: p. 793428.
351. Shen, Y., W. Wei, and D.X. Zhou, *Histone Acetylation Enzymes Coordinate Metabolism and Gene Expression.* Trends Plant Sci, 2015. **20**(10): p. 614-621.
352. Bailis, W., et al., *Distinct modes of mitochondrial metabolism uncouple T cell differentiation and function.* Nature, 2019. **571**(7765): p. 403-407.
353. Ouyang, W., et al., *An Essential Role of the Forkhead-Box Transcription Factor Foxo1 in Control of T Cell Homeostasis and Tolerance.* Immunity, 2009. **30**(3): p. 358-371.
354. Kraus, E.E., et al., *Regulation of autoreactive CD4 T cells by FoxO1 signaling in CNS autoimmunity.* Journal of Neuroimmunology, 2021. **359**.
355. Townsend, P.A., et al., *STAT-1 Interacts with p53 to Enhance DNA Damage-induced Apoptosis*.* Journal of Biological Chemistry, 2004. **279**(7): p. 5811-5820.
356. Xu, X., et al., *IFN-gamma induces cell growth inhibition by Fas-mediated apoptosis: requirement of STAT1 protein for up-regulation of Fas and FasL expression.* Cancer Res, 1998. **58**(13): p. 2832-7.
357. Goping, I.S., et al., *Granzyme B-induced apoptosis requires both direct caspase activation and relief of caspase inhibition.* Immunity, 2003. **18**(3): p. 355-65.
358. Waring, P. and A. Müllbacher, *Cell death induced by the Fas/Fas ligand pathway and its role in pathology.* Immunology & Cell Biology, 1999. **77**(4): p. 312-317.
359. Gui, Q., et al., *The association between gut butyrate-producing bacteria and non-small-cell lung cancer.* J Clin Lab Anal, 2020. **34**(8): p. e23318.
360. Haak, B.W., et al., *Impact of gut colonization with butyrate-producing microbiota on respiratory viral infection following allo-HCT.* Blood, 2018. **131**(26): p. 2978-2986.
361. Worby, C.J., et al., *Gut-bladder axis syndrome associated with recurrent UTIs in humans.* medRxiv, 2021: p. 2021.11.15.21266268.
362. Chen, H.-M., et al., *Decreased dietary fiber intake and structural alteration of gut microbiota in patients with advanced colorectal adenoma.* The American Journal of Clinical Nutrition, 2013. **97**(5): p. 1044-1052.

363. Jacob, N., et al., *Butyrate induced Tregs are capable of migration from the GALT to the pancreas to restore immunological tolerance during type-1 diabetes.* Scientific Reports, 2020. **10**(1): p. 19120.
364. Gil-Etayo, F.J., et al., *An Early Th1 Response Is a Key Factor for a Favorable COVID-19 Evolution.* Biomedicines, 2022. **10**(2): p. 296.
365. Oh, D.Y. and L. Fong, *Cytotoxic CD4(+) T cells in cancer: Expanding the immune effector toolbox.* Immunity, 2021. **54**(12): p. 2701-2711.
366. Delpoux, A., et al., *FOXO1 constrains activation and regulates senescence in CD8 T cells.* Cell Rep, 2021. **34**(4): p. 108674.
367. Michelini, R.H., et al., *Differentiation of CD8 memory T cells depends on Foxo1.* Journal of Experimental Medicine, 2013. **210**(6): p. 1189-1200.
368. Berger, S.L., *Histone modifications in transcriptional regulation.* Current Opinion in Genetics & Development, 2002. **12**(2): p. 142-148.
369. Halley, F., et al., *A Bioluminogenic HDAC Activity Assay:Validation and Screening.* Journal of Biomolecular Screening, 2011. **16**(10): p. 1227-1235.
370. Chriett, S., et al., *Prominent action of butyrate over β-hydroxybutyrate as histone deacetylase inhibitor, transcriptional modulator and anti-inflammatory molecule.* Scientific Reports, 2019. **9**(1): p. 742.
371. Li, X., et al., *HDAC inhibition potentiates anti-tumor activity of macrophages and enhances anti-PD-L1-mediated tumor suppression.* Oncogene, 2021. **40**(10): p. 1836-1850.
372. Nakayama, A., et al., *Transcriptional regulation of interferon γ gene by p300 co-activator.* Nucleic Acids Symposium Series, 2001. **1**(1): p. 89-90.
373. Chen, Z., et al., *Aspirin cooperates with p300 to activate the acetylation of H3K9 and promote FasL-mediated apoptosis of cancer stem-like cells in colorectal cancer.* Theranostics, 2018. **8**(16): p. 4447-4461.
374. Marchetti, P., et al., *Mitochondrial spare respiratory capacity: Mechanisms, regulation, and significance in non-transformed and cancer cells.* Faseb j, 2020. **34**(10): p. 13106-13124.
375. Gubser, P.M., et al., *Rapid effector function of memory CD8+ T cells requires an immediate-early glycolytic switch.* Nat Immunol, 2013. **14**(10): p. 1064-72.
376. Kannan, K. and S.K. Jain, *Oxidative stress and apoptosis.* Pathophysiology, 2000. **7**(3): p. 153-163.
377. Desler, C., et al., *Is There a Link between Mitochondrial Reserve Respiratory Capacity and Aging?* J Aging Res, 2012. **2012**: p. 192503.
378. Peng, M., et al., *Aerobic glycolysis promotes T helper 1 cell differentiation through an epigenetic mechanism.* Science, 2016. **354**(6311): p. 481.
379. Patsoukis, N., et al., *The role of metabolic reprogramming in T cell fate and function.* Curr Trends Immunol, 2016. **17**: p. 1-12.
380. Anderson, K.A. and M.D. Hirschey, *Mitochondrial protein acetylation regulates metabolism.* Essays Biochem, 2012. **52**: p. 23-35.
381. Reardon, S.D. and T.V. Mishanina, *Phosphorylation and acetylation of mitochondrial transcription factor A promote transcription processivity without compromising initiation or DNA compaction.* Journal of Biological Chemistry, 2022. **298**(4): p. 101815.
382. Guo, X., et al., *Global characterization of T cells in non-small-cell lung cancer by single-cell sequencing.* Nature Medicine, 2018. **24**(7): p. 978-985.
383. Oh, D.Y., et al., *Intratumoral CD4+ T Cells Mediate Anti-tumor Cytotoxicity in Human Bladder Cancer.* Cell, 2020. **181**(7): p. 1612-1625.e13.

384. Cachot, A., et al., *Tumor-specific cytolytic CD4 T cells mediate immunity against human cancer.* Science Advances, 2021. **7**(9): p. eabe3348.
385. Tateyama, M., et al., *CD4 T lymphocytes are primed to express Fas ligand by CD4 cross-linking and to contribute to CD8 T-cell apoptosis via Fas/FasL death signaling pathway: Presented in part at the 12th World AIDS Conference, Geneva, Switzerland, 1998.* Blood, 2000. **96**(1): p. 195-202.
386. Medana, I.M., et al., *MHC class I-restricted killing of neurons by virus-specific CD8+ T lymphocytes is effected through the Fas/FasL, but not the perforin pathway.* Eur J Immunol, 2000. **30**(12): p. 3623-33.
387. Kotov, D.I., et al., *Many Th Cell Subsets Have Fas Ligand-Dependent Cytotoxic Potential.* J Immunol, 2018. **200**(6): p. 2004-2012.
388. Ghare, S.S., et al., *Coordinated Histone H3 Methylation and Acetylation Regulate Physiologic and Pathologic Fas Ligand Gene Expression in Human CD4+ T Cells.* The Journal of Immunology, 2014. **193**(1): p. 412-421.
389. Michalek, R.D. and J.C. Rathmell, *The metabolic life and times of a T-cell.* Immunol Rev, 2010. **236**: p. 190-202.
390. McOrist, A.L., et al., *Fecal Butyrate Levels Vary Widely among Individuals but Are Usually Increased by a Diet High in Resistant Starch.* The Journal of Nutrition, 2011. **141**(5): p. 883-889.
391. Zhang, X., et al., *CAR-T Cell Therapy in Hematological Malignancies: Current Opportunities and Challenges.* Frontiers in Immunology, 2022. **13**.
392. Turtle, C.J., et al., *CD19 CAR-T cells of defined CD4+:CD8+ composition in adult B cell ALL patients.* J Clin Invest, 2016. **126**(6): p. 2123-38.
393. Zhang, C., et al., *Phase I Escalating-Dose Trial of CAR-T Therapy Targeting CEA+ Metastatic Colorectal Cancers.* Molecular Therapy, 2017. **25**(5): p. 1248-1258.
394. Marofi, F., et al., *CAR T cells in solid tumors: challenges and opportunities.* Stem Cell Research & Therapy, 2021. **12**(1): p. 81.
395. Bubeník, J., *Tumour MHC class I downregulation and immunotherapy (Review).* Oncol Rep, 2003. **10**(6): p. 2005-8.
396. Dhatchinamoorthy, K., J.D. Colbert, and K.L. Rock, *Cancer Immune Evasion Through Loss of MHC Class I Antigen Presentation.* Frontiers in Immunology, 2021. **12**.
397. Watson, N.F.S., et al., *Immunosurveillance is active in colorectal cancer as downregulation but not complete loss of MHC class I expression correlates with a poor prognosis.* International Journal of Cancer, 2006. **118**(1): p. 6-10.
398. Alizadeh, D., et al., *IFNγ Is Critical for CAR T Cell-Mediated Myeloid Activation and Induction of Endogenous Immunity.* Cancer Discov, 2021. **11**(9): p. 2248-2265.
399. Song, E.Z., et al., *The IAP antagonist birinapant enhances chimeric antigen receptor T cell therapy for glioblastoma by overcoming antigen heterogeneity.* Molecular Therapy - Oncolytics, 2022. **27**: p. 288-304.
400. Zhou, Z., et al., *Granzyme A from cytotoxic lymphocytes cleaves GSDMB to trigger pyroptosis in target cells.* Science, 2020. **368**(6494): p. eaaz7548.
401. Xiao, X., et al., *Mechanisms of cytokine release syndrome and neurotoxicity of CAR T-cell therapy and associated prevention and management strategies.* Journal of Experimental & Clinical Cancer Research, 2021. **40**(1): p. 367.
402. Lee, D.H., et al., *Improved Expansion and Function of CAR T Cell Products from Cultures Initiated at Defined CD4:CD8 Ratios.* Blood, 2018. **132**: p. 3334.

403. Melenhorst, J.J., et al., *Decade-long leukaemia remissions with persistence of CD4+ CAR T cells.* Nature, 2022. **602**(7897): p. 503-509.
404. Jiao, S., et al., *Differences in Tumor Microenvironment Dictate T Helper Lineage Polarization and Response to Immune Checkpoint Therapy.* Cell, 2019. **179**(5): p. 1177-1190.e13.
405. Chraa, D., et al., *T lymphocyte subsets in cancer immunity: Friends or foes.* Journal of Leukocyte Biology, 2019. **105**(2): p. 243-255.
406. Dai, M., et al., *Tumor Regression and Cure Depends on Sustained Th1 Responses.* Journal of Immunotherapy, 2018. **41**(8).
407. Gacerez, A.T. and C.L. Sentman, *T-bet promotes potent antitumor activity of CD4+ CAR T cells.* Cancer Gene Therapy, 2018. **25**(5): p. 117-128.
408. Deng, Q., et al., *Characteristics of anti-CD19 CAR T cell infusion products associated with efficacy and toxicity in patients with large B cell lymphomas.* Nature Medicine, 2020. **26**(12): p. 1878-1887.
409. Fraietta, J.A., et al., *Determinants of response and resistance to CD19 chimeric antigen receptor (CAR) T cell therapy of chronic lymphocytic leukemia.* Nature Medicine, 2018. **24**(5): p. 563-571.
410. Sommermeyer, D., et al., *Chimeric antigen receptor-modified T cells derived from defined CD8+ and CD4+ subsets confer superior antitumor reactivity in vivo.* Leukemia, 2016. **30**(2): p. 492-500.
411. Mastelic-Gavillet, B., et al., *Adenosine mediates functional and metabolic suppression of peripheral and tumor-infiltrating CD8(+) T cells.* J Immunother Cancer, 2019. **7**(1): p. 257.
412. Chang, C.-H., et al., *Metabolic Competition in the Tumor Microenvironment Is a Driver of Cancer Progression.* Cell, 2015. **162**(6): p. 1229-1241.
413. Vardhana, S.A., et al., *Impaired mitochondrial oxidative phosphorylation limits the self-renewal of T cells exposed to persistent antigen.* Nature Immunology, 2020. **21**(9): p. 1022-1033.
414. Kumar, A., et al., *Tumors attenuating the mitochondrial activity in T cells escape from PD-1 blockade therapy.* eLife, 2020. **9**: p. e52330.
415. Scharping, N.E., et al., *The Tumor Microenvironment Represses T Cell Mitochondrial Biogenesis to Drive Intratumoral T Cell Metabolic Insufficiency and Dysfunction.* Immunity, 2016. **45**(2): p. 374-388.
416. Yu, Y.-R., et al., *Disturbed mitochondrial dynamics in CD8+ TILs reinforce T cell exhaustion.* Nature Immunology, 2020. **21**(12): p. 1540-1551.
417. Hirabayashi, K., et al., *Dual-targeting CAR-T cells with optimal co-stimulation and metabolic fitness enhance antitumor activity and prevent escape in solid tumors.* Nature Cancer, 2021. **2**(9): p. 904-918.
418. Zhang, M., et al., *Optimization of metabolism to improve efficacy during CAR-T cell manufacturing.* Journal of Translational Medicine, 2021. **19**(1): p. 499.
419. Zhou, J., et al., *Chimeric antigen receptor T (CAR-T) cells expanded with IL-7/IL-15 mediate superior antitumor effects.* Protein & Cell, 2019. **10**(10): p. 764-769.
420. Sabatino, M., et al., *Generation of clinical-grade CD19-specific CAR-modified CD8+ memory stem cells for the treatment of human B-cell malignancies.* Blood, 2016. **128**(4): p. 519-28.
421. Cherkassky, L., et al., *Human CAR T cells with cell-intrinsic PD-1 checkpoint blockade resist tumor-mediated inhibition.* The Journal of Clinical Investigation, 2016. **126**(8): p. 3130-3144.

422. John, L.B., et al., *Anti-PD-1 Antibody Therapy Potently Enhances the Eradication of Established Tumors By Gene-Modified T Cells.* Clinical Cancer Research, 2013. **19**(20): p. 5636-5646.
423. Patsoukis, N., et al., *PD-1 alters T-cell metabolic reprogramming by inhibiting glycolysis and promoting lipolysis and fatty acid oxidation.* Nature Communications, 2015. **6**(1): p. 6692.
424. Chamoto, K., et al., *Mitochondrial activation chemicals synergize with surface receptor PD-1 blockade for T cell-dependent antitumor activity.* Proc Natl Acad Sci U S A, 2017. **114**(5): p. E761-e770.
425. Kiesgen, S., et al., *Comparative analysis of assays to measure CAR T-cell-mediated cytotoxicity.* Nat Protoc, 2021. **16**(3): p. 1331-1342.
426. Huang, Y., et al., *Rewiring mitochondrial metabolism to counteract exhaustion of CAR-T cells.* Journal of Hematology & Oncology, 2022. **15**(1): p. 38.
427. Rad S. M., A.H., et al., *Metabolic and Mitochondrial Functioning in Chimeric Antigen Receptor (CAR)—T Cells.* Cancers, 2021. **13**(6): p. 1229.
428. Krug, L.M., et al., *Targeting Lewis Y (LeY) in Small Cell Lung Cancer with a Humanized Monoclonal Antibody, hu3S193: A Pilot Trial Testing Two Dose Levels.* Journal of Thoracic Oncology, 2007. **2**(10): p. 947-952.
429. Souhami, R.L., et al., *Antigens of lung cancer: results of the second international workshop on lung cancer antigens.* J Natl Cancer Inst, 1991. **83**(9): p. 609-12.
430. Yang, S., et al., *The shedding of CD62L (L-selectin) regulates the acquisition of lytic activity in human tumor reactive T lymphocytes.* PLoS One, 2011. **6**(7): p. e22560.
431. Saule, P., et al., *Accumulation of memory T cells from childhood to old age: Central and effector memory cells in CD4+ versus effector memory and terminally differentiated memory cells in CD8+ compartment.* Mechanisms of Ageing and Development, 2006. **127**(3): p. 274-281.
432. Carrasco, J., et al., *CD45RA on human CD8 T cells is sensitive to the time elapsed since the last antigenic stimulation.* Blood, 2006. **108**(9): p. 2897-2905.
433. Mestas, J. and C.C.W. Hughes, *Of Mice and Not Men: Differences between Mouse and Human Immunology.* The Journal of Immunology, 2004. **172**(5): p. 2731.
434. Henderson, S., et al., *The Th1 cell regulatory circuitry is largely conserved between human and mouse.* bioRxiv, 2021: p. 2021.01.11.426266.
435. Webb, A.E., A. Kundaje, and A. Brunet, *Characterization of the direct targets of FOXO transcription factors throughout evolution.* Aging Cell, 2016. **15**(4): p. 673-85.
436. Hupperetz, C., et al., *CAR T Cell Immunotherapy Beyond Haematological Malignancy.* Immune Netw, 2022. **22**(1): p. e6.
437. Sterner, R.C. and R.M. Sterner, *CAR-T cell therapy: current limitations and potential strategies.* Blood Cancer Journal, 2021. **11**(4): p. 69.
438. Bengsch, B., et al., *Bioenergetic Insufficiencies Due to Metabolic Alterations Regulated by the Inhibitory Receptor PD-1 Are an Early Driver of CD8(+) T Cell Exhaustion.* Immunity, 2016. **45**(2): p. 358-73.
439. Sukumar, M., et al., *Mitochondrial Membrane Potential Identifies Cells with Enhanced Stemness for Cellular Therapy.* Cell Metab, 2016. **23**(1): p. 63-76.
440. Ouyang, W., et al., *An essential role of the Forkhead-box transcription factor Foxo1 in control of T cell homeostasis and tolerance.* Immunity, 2009. **30**(3): p. 358-71.

441. Dudek, M., et al., *IL-6-induced FOXO1 activity determines the dynamics of metabolism in CD8 T cells cross-primed by liver sinusoidal endothelial cells.* Cell Rep, 2022. **38**(7): p. 110389.
442. Baaten, B.J.G., et al., *CD44 Regulates Survival and Memory Development in Th1 Cells.* Immunity, 2010. **32**(1): p. 104-115.
443. Zhang, X., et al., *Potent and Selective Stimulation of Memory-Phenotype CD8+ T Cells In Vivo by IL-15.* Immunity, 1998. **8**(5): p. 591-599.
444. Takemoto, N., et al., *Cutting Edge: IL-12 inversely regulates T-bet and eomesodermin expression during pathogen-induced CD8+ T cell differentiation.* J Immunol, 2006. **177**(11): p. 7515-9.
445. Li, R.W. and C. Li, *Butyrate induces profound changes in gene expression related to multiple signal pathways in bovine kidney epithelial cells.* BMC Genomics, 2006. **7**: p. 234.
446. Vanhoutvin, S.A., et al., *Butyrate-induced transcriptional changes in human colonic mucosa.* PLoS One, 2009. **4**(8): p. e6759.
447. Miller, B.C., et al., *Subsets of exhausted CD8+ T cells differentially mediate tumor control and respond to checkpoint blockade.* Nature Immunology, 2019. **20**(3): p. 326-336.
448. Kambhampati, S., et al., *Immune-related Adverse Events Associated With Checkpoint Inhibition in the Setting of CAR T Cell Therapy: A Case Series.* Clinical Lymphoma, Myeloma and Leukemia, 2020. **20**(3): p. e118-e123.
449. Palmieri, D.J. and M.S. Carlino, *Immune Checkpoint Inhibitor Toxicity.* Current Oncology Reports, 2018. **20**(9): p. 72.
450. Naidoo, J., et al., *Toxicities of the anti-PD-1 and anti-PD-L1 immune checkpoint antibodies.* Ann Oncol, 2016. **27**(7): p. 1362.
451. Belum, V.R., et al., *Characterisation and management of dermatologic adverse events to agents targeting the PD-1 receptor.* Eur J Cancer, 2016. **60**: p. 12-25.
452. Morganstein, D.L., et al., *Thyroid abnormalities following the use of cytotoxic T-lymphocyte antigen-4 and programmed death receptor protein-1 inhibitors in the treatment of melanoma.* Clinical Endocrinology, 2017. **86**(4): p. 614-620.
453. Zhang, Y., et al., *Cord Blood CD8+ T Cells Have a Natural Propensity to Express IL-4 in a Fatty Acid Metabolism and Caspase Activation-Dependent Manner.* Frontiers in Immunology, 2018. **9**.
454. Uribe-Herranz, M., et al., *Gut microbiota modulate dendritic cell antigen presentation and radiotherapy-induced antitumor immune response.* The Journal of Clinical Investigation, 2020. **130**(1): p. 466-479.
455. Mackay, L.K., et al., *Long-lived epithelial immunity by tissue-resident memory T (TRM) cells in the absence of persisting local antigen presentation.* Proceedings of the National Academy of Sciences, 2012. **109**(18): p. 7037-7042.
456. Perdomo, C., et al., *Mucosal BCG Vaccination Induces Protective Lung-Resident Memory T Cell Populations against Tuberculosis.* mBio, 2016. **7**(6): p. e01686-16.
457. Kobayashi, M., et al., *Short-chain fatty acids, GPR41 and GPR43 ligands, inhibit TNF-α-induced MCP-1 expression by modulating p38 and JNK signaling pathways in human renal cortical epithelial cells.* Biochem Biophys Res Commun, 2017. **486**(2): p. 499-505.
458. Dodeller, F. and H. Schulze-Koops, *The p38 mitogen-activated protein kinase signaling cascade in CD4 T cells.* Arthritis Research & Therapy, 2006. **8**(2): p. 205.

459. Harabuchi, S., et al., *Manipulation of diacylglycerol and ERK-mediated signaling differentially controls CD8+ T cell responses during chronic viral infection.* Frontiers in Immunology, 2022. **13**.
460. Nastasi, C., et al., *The effect of short-chain fatty acids on human monocyte-derived dendritic cells.* 2015(2045-2322 (Electronic)).
461. Ang, Z., et al., *Human and mouse monocytes display distinct signalling and cytokine profiles upon stimulation with FFAR2/FFAR3 short-chain fatty acid receptor agonists.* Scientific Reports, 2016. **6**(1): p. 34145.
462. Macia, L., et al., *Metabolite-sensing receptors GPR43 and GPR109A facilitate dietary fibre-induced gut homeostasis through regulation of the inflammasome.* Nature Communications, 2015. **6**(1): p. 6734.
463. Ubachs, J., et al., *Gut microbiota and short-chain fatty acid alterations in cachectic cancer patients.* Journal of Cachexia, Sarcopenia and Muscle, 2021. **12**(6): p. 2007-2021.
464. Kobayashi, M., et al., *A short-chain fatty acid, propionate, enhances the cytotoxic effect of cisplatin by modulating GPR41 signaling pathways in HepG2 cells.* Oncotarget, 2018. **9**(59): p. 31342-31354.
465. Thirunavukkarasan, M., et al., *Short-chain fatty acid receptors inhibit invasive phenotypes in breast cancer cells.* PLOS ONE, 2017. **12**(10): p. e0186334.
466. Wang, X. and Y. Lin, *Tumor necrosis factor and cancer, buddies or foes?* Acta Pharmacol Sin, 2008. **29**(11): p. 1275-88.
467. Han, J., et al., *Memory CD8+ T cell responses to cancer.* Seminars in Immunology, 2020. **49**: p. 101435.
468. Jin, Y., et al., *Prognostic Impact of Memory CD8(+) T Cells on Immunotherapy in Human Cancers: A Systematic Review and Meta-Analysis.* Front Oncol, 2021. **11**: p. 698076.
469. Wang, B., et al., *Combination cancer immunotherapy targeting PD-1 and GITR can rescue CD8+ T cell dysfunction and maintain memory phenotype.* Science Immunology, 2018. **3**(29): p. eaat7061.
470. Viaud, S., et al., *The intestinal microbiota modulates the anticancer immune effects of cyclophosphamide.* Science, 2013. **342**(6161): p. 971-6.
471. Taeweon, L., et al., *Identification and Functional Characterization of Allosteric Agonists for the G Protein-Coupled Receptor FFA2.* Molecular Pharmacology, 2008. **74**(6): p. 1599.
472. Wang, Y., et al., *The first synthetic agonists of FFA2: Discovery and SAR of phenylacetamides as allosteric modulators.* Bioorganic & Medicinal Chemistry Letters, 2010. **20**(2): p. 493-498.
473. Gill, P.A., et al., *A randomized dietary intervention to increase colonic and peripheral blood SCFAs modulates the blood B- and T-cell compartments in healthy humans.* The American Journal of Clinical Nutrition, 2022. **116**(5): p. 1354-1367.
474. Buttrick, T.S., et al., *Foxo1 Promotes Th9 Cell Differentiation and Airway Allergy.* Scientific Reports, 2018. **8**(1): p. 818.
475. Harada, Y., et al., *Transcription factors Foxo3a and Foxo1 couple the E3 ligase Cbl-b to the induction of Foxp3 expression in induced regulatory T cells.* Journal of Experimental Medicine, 2010. **207**(7): p. 1381-1391.
476. Raveney, B.J.E., et al., *Eomesodermin-expressing T-helper cells are essential for chronic neuroinflammation.* Nature Communications, 2015. **6**(1): p. 8437.

477. Wang, W., et al., *Sodium Butyrate Selectively Kills Cancer Cells and Inhibits Migration in Colorectal Cancer by Targeting Thioredoxin-1.* Onco Targets Ther, 2020. **13**: p. 4691-4704.
478. Hague, A., et al., *Apoptosis in colorectal tumour cells: induction by the short chain fatty acids butyrate, propionate and acetate and by the bile salt deoxycholate.* Int J Cancer, 1995. **60**(3): p. 400-6.
479. Delgado, M. and D. Ganea, *VIP and PACAP inhibit Fas ligand-mediated bystander lysis by CD4(+) T cells.* J Neuroimmunol, 2001. **112**(1-2): p. 78-88.
480. Gorbachev, A.V. and R.L. Fairchild, *CD4+CD25+ regulatory T cells utilize FasL as a mechanism to restrict DC priming functions in cutaneous immune responses.* Eur J Immunol, 2010. **40**(7): p. 2006-15.
481. Thomas, W.D. and P. Hersey, *TNF-related apoptosis-inducing ligand (TRAIL) induces apoptosis in Fas ligand-resistant melanoma cells and mediates CD4 T cell killing of target cells.* J Immunol, 1998. **161**(5): p. 2195-200.
482. Nieda, M., et al., *TRAIL expression by activated human CD4(+)V alpha 24NKT cells induces in vitro and in vivo apoptosis of human acute myeloid leukemia cells.* Blood, 2001. **97**(7): p. 2067-74.
483. Sun, M., et al., *Microbiota-derived short-chain fatty acids promote Th1 cell IL-10 production to maintain intestinal homeostasis.* Nature Communications, 2018. **9**(1): p. 3555.
484. Tay, R.E., et al., *Hdac3 is an epigenetic inhibitor of the cytotoxicity program in CD8 T cells.* Journal of Experimental Medicine, 2020. **217**(7): p. e20191453.
485. Curran, M.A., et al., *PD-1 and CTLA-4 combination blockade expands infiltrating T cells and reduces regulatory T and myeloid cells within B16 melanoma tumors.* Proc Natl Acad Sci U S A, 2010. **107**(9): p. 4275-80.
486. Gubin, M.M., et al., *High-Dimensional Analysis Delineates Myeloid and Lymphoid Compartment Remodeling during Successful Immune-Checkpoint Cancer Therapy.* Cell, 2018. **175**(4): p. 1014-1030.e19.
487. Beavis, P.A., et al., *Dual PD-1 and CTLA-4 Checkpoint Blockade Promotes Antitumor Immune Responses through CD4+Foxp3− Cell–Mediated Modulation of CD103+ Dendritic Cells.* Cancer Immunology Research, 2018. **6**(9): p. 1069-1081.
488. Garrido, F., et al., *The urgent need to recover MHC class I in cancers for effective immunotherapy.* Curr Opin Immunol, 2016. **39**: p. 44-51.
489. Huang, Y., S. Shah, and L. Qiao, *Tumor resistance to CD8+ T cell-based therapeutic vaccination.* Arch Immunol Ther Exp (Warsz), 2007. **55**(4): p. 205-17.
490. Patel, U., et al., *CAR T cell therapy in solid tumors: A review of current clinical trials.* eJHaem, 2022. **3**(S1): p. 24-31.
491. Wang, D., et al., *Glioblastoma-targeted CD4+ CAR T cells mediate superior antitumor activity.* JCI Insight, 2018. **3**(10).
492. Agarwal, S., et al., *In Vivo Generation of CAR T Cells Selectively in Human CD4+ Lymphocytes.* Molecular Therapy, 2020. **28**(8): p. 1783-1794.
493. Liadi, I., et al., *Defining potency of CAR(+) T cells: Fast and furious or slow and steady.* Oncoimmunology, 2019. **8**(10): p. e1051298.
494. Poorebrahim, M., et al., *Counteracting CAR T cell dysfunction.* Oncogene, 2021. **40**(2): p. 421-435.
495. Kasakovski, D., L. Xu, and Y. Li, *T cell senescence and CAR-T cell exhaustion in hematological malignancies.* Journal of Hematology & Oncology, 2018. **11**(1): p. 91.

496. Shah, N.N. and T.J. Fry, *Mechanisms of resistance to CAR T cell therapy.* Nat Rev Clin Oncol, 2019. **16**(6): p. 372-385.
497. Gennert, D.G., et al., *Dynamic chromatin regulatory landscape of human CAR T cell exhaustion.* Proceedings of the National Academy of Sciences, 2021. **118**(30): p. e2104758118.
498. Yang, Y., et al., *TCR engagement negatively affects CD8 but not CD4 CAR T cell expansion and leukemic clearance.* Science Translational Medicine, 2017. **9**(417): p. eaag1209.
499. Xhangolli, I., et al., *Single-cell Analysis of CAR-T Cell Activation Reveals A Mixed TH1/TH2 Response Independent of Differentiation.* Genomics, Proteomics & Bioinformatics, 2019. **17**(2): p. 129-139.
500. Zheng, D., T. Liwinski, and E. Elinav, *Interaction between microbiota and immunity in health and disease.* Cell Research, 2020. **30**(6): p. 492-506.
501. Di Gangi, A., et al., *Go With Your Gut: The Shaping of T-Cell Response by Gut Microbiota in Allergic Asthma.* Frontiers in Immunology, 2020. **11**.
502. Fan, X., et al., *Gut Microbiota Dysbiosis Drives the Development of Colorectal Cancer.* Digestion, 2021. **102**(4): p. 508-515.
503. Sheflin, A.M., A.K. Whitney, and T.L. Weir, *Cancer-promoting effects of microbial dysbiosis.* Curr Oncol Rep, 2014. **16**(10): p. 406.
504. Nastasi, C., et al., *Butyrate and propionate inhibit antigen-specific CD8+ T cell activation by suppressing IL-12 production by antigen-presenting cells.* Scientific Reports, 2017. **7**(1): p. 14516.
505. Shivakoti, R., et al., *Intake and Sources of Dietary Fiber, Inflammation, and Cardiovascular Disease in Older US Adults.* JAMA Network Open, 2022. **5**(3): p. e225012-e225012.
506. Berer, K., et al., *Dietary non-fermentable fiber prevents autoimmune neurological disease by changing gut metabolic and immune status.* Scientific Reports, 2018. **8**(1): p. 10431.
507. Hajipour, A., et al., *The effects of dietary fiber on common complications in critically ill patients; with a special focus on viral infections; a systematic reveiw.* Immun Inflamm Dis, 2022. **10**(5): p. e613.
508. Song, M., et al., *Fiber Intake and Survival After Colorectal Cancer Diagnosis.* JAMA Oncol, 2018. **4**(1): p. 71-79.